PERCEPTION, INTEGRATION AND RESPONSE OF THE SALMONID EPITHELIAL CELL LINE RTgill-W1 TO INFECTIOUS AND PRO-INFLAMMATORY AGENTS *IN VITRO*

THESIS SUBMITTED TO THE UNIVERSITY OF STIRLING FOR THE DEGREE OF DOCTOR OF PHILOSOPHY

IN

AQUACULTURE

by

SHANKAR CHANDRA MANDAL

BS and MS in Fisheries

EMERGING AQUATIC INFECTIOUS DISEASE
&
FISH BEHAVIOUR and WELFARE
RESEARCH GROUP

INSTITUTE OF AQUACULTURE, FACULTY OF NATURAL SCIENCES
UNIVERSITY OF STIRLING
UNITED KINGDOM

March 2019

Supervisors' certificate

This is to certify that this thesis entitled "Perception, integration and response of the salmonid epithelial cell line RTgill-W1 to infectious and pro-inflammatory agents *in vitro*" submitted to the University of Stirling, UK by Shankar Chandra Mandal, has been carried out under our supervision. This is further to certify that it is an original work carried out by the candidate and suitable for the degree of Philosophy.

Professor Manfred Weidmann
Institute of Aquaculture, University of Stirling. Stirling, Scotland, UK

Professor Simon MacKenzie
Institute of Aquaculture, University of Stirling. Stirling, Scotland, UK

DECLARATION

I, the undersigned, hereby declare that this thesis has been composed entirely by me and has not been submitted for any other degree. The work presented in this thesis, except where specifically acknowledged, is the result of my own investigations which have been done by me independently.

Shankar Chandra Mandal
Stirling, UK
March 2019

Acknowledgements

I am delighted to express my wholehearted feelings of thankfulness and gratefulness to Prof Manfred Weidmann and Prof Simon MacKenzie, my supervisors and mentors, for all of their help, support, freedom, inspiration, advice and guidance throughout my PhD journey; and for giving me access to their office for a quick discussion about the experiment anytime when I needed it. I could not have wished for better supervisors. I am also indebted to them for their ceaseless endurance for careful reading and reviewing the write-up and also for teaching me fish Immunology and Virology. I would like to express my all sense of gratitude to Dr. Amaya Albalat, who is more than an official supervisor, supervising a part of my PhD project and always worked as a stimulant throughout my PhD journey. Thank you very much also for teaching me phosphoproteomics. I would also like to thank Dr Emma Carrick from Institute of Cardiovascular and Medical Sciences, University of Glasgow, UK for her help in LC MS/MS analysis.

I also express my heartfelt feelings for Dr Tharangani Herath, who was one of my supervisors, presently a faculty in the Herper Adams University in the UK, for helping and guiding me since my application for funding and admission in the University of Stirling. Also thank you for initial supervising transwell experiments and primary cell culture. I am also thankful to Dr Nilantha Jayasuriaya for his encouragement and suggestions. I am also grateful to Dr Sonia Ray for her support, encouragement, guidance and help in statistical analysis. I would like to convey my deepest appreciation to Katherine Fiona Muir for her patience in teaching cell culture and virus culture. She has a significant role in this journey from the very first day of my PhD study.

I am also beholden to Graham Harrold, past research technician in Virology, for his help in molecular works. I am also grateful to Bernat Morro, PhD student here in the Institute of Aquaculture, for his help in phosphoproteomics experiment and data analysis. A special thank goes to Dr. Benjamín López Jimena for his help in molecular work, suggestions and inspiration during his post-doctoral period in the Virology laboratory. I am also thankful to Jacquie Ireland and Dr. John Taggart for their unconditional help and suggestion in molecular work. I would like to thank Dr Mags Crumlish for her help in the bacterial invasion experiment.

I am very gratefully to all the past and present staff in the Virology and Behaviour and Welfare research groups: Dr Gilta Jackel, Debbie Faichney, Dr. Kristina Ulrich, Rona Warner, Jin Xingkun, Dr. Michael McGowan, Maureen, David, Irene and Wouter Mes. I would like to thank my friend Dr Abdullah Al Mamun for his initial help and support in application for the scholarship and for getting accommodation here in Stirling and some suggestion about how to get maximum benefits from the PhD study.

I am also thankful to Melanie Cruickshank, Anda Wright, Sandra Tulloch, Charlie Harrower and Jane Lewis from the Institute of Aquaculture for their assistance throughout my PhD journey. I am grateful to my past and present office mates and friends Savitree, Chris, Francis, Ahmed Ahmed, Ahmed, Siri, Min, Khalid, Elizabeth, Angella and Simao without whom life would be boring. I always appreciate their inspiration, suggestion and help in different aspects. I will never forget their company.

I am also grateful to the University of Dhaka, my affiliation for which I will always feel grateful, to give me the opportunity to study abroad. I would like to express my appreciation to the University of Stirling for partial sponsorship and all the supports I got during my study. I would also like to gratefully acknowledge the Doctoral Bursaries from Charles Wallace Bangladesh trust, UK. I appreciate the support from Marine Alliance for Science and Technology Scotland (MASTS) for a small grant for the method development of the phosphoproteomics work. I am also grateful to the University of Glasgow for LC-MS support.

I am wholeheartedly grateful to my sponsor the Commonwealth Scholarship Commission in the UK, without their financial support this study would not have been possible.

I am beholden to my parents, my mother in law, my brother, sister and sister in law and other relatives for their support and inspiration throughout this long journey. Finally, I would like to thank my beloved wife, JOYA who sacrificed her career and stayed with me all the time, inspired me always, helped me in writing, in understanding some complex pharmacological terms and for making the home a sweet home where I forgot all the tiredness after a long busy day in the lab.

Scientific conferences and meetings attended

1. S.C. Mandal, M. Weidmann and S. MacKenzie. Effects of stimulants on trans epithelial resistance and gene expression of RTgill-W1 cells. EAFP UK and Ireland branches, 2nd Meeting, 15-16 September 2016, Stirling, UK (Oral presentation).
2. S.C. Mandal, M. Weidmann and S. MacKenzie. Assessing virulence of fish pathogens in host cells in vitro. Lunch time seminar, 5 April 2017, Institute of Aquaculture, University of Stirling (Oral presentation).
3. S.C. Mandal, M. Weidmann and S. MacKenzie. The response of the trout epithelial cell line RTgill-W1, to viral and bacterial pathogen associated molecular patterns (PAMPS). Fish Immunology and Vaccination Workshop, Wageningen, the Netherlands, 30 April-4 May 2017 (Poster presentation).
4. S.C. Mandal, M. Weidmann and S. MacKenzie. Recognition of bacterial MDP and LPS by trout epithelial cells RTgill-W1. WGC Advanced Course: Immunophenotyping: Generation and Analysis of Immunological Datasets, Wellcome Genome Campus, Hinxton, Cambridge, UK, 9-25 February 2017 (Poster presentation).
5. S.C. Mandal, M. Weidmann and S. MacKenzie. Impacts of PhD study on national development. Development Module Workshop, 26-28 May 2017, Cumberland, UK (Poster presentation).
6. S.C. Mandal, M. Weidmann and S. MacKenzie. Response of the trout epithelial cells RTgill-W1 to salmonid alpha virus subtype 2 (SAV-2): cellular and molecular interaction, PhD research conference, 17 April 2018, Institute of Aquaculture, University of Stirling (Oral presentation).
7. S.C. Mandal, M. Weidmann and S. MacKenzie and A. Albalat. Defence tactics in rainbow trout. 3MT, 5 June 2018, University of Stirling, UK (Oral presentation).
8. S.C. Mandal, E. Carrick, M. Weidmann, B. Moro, S. MacKenzie and A. Albalat. Triggering of protein phosphorylation in rainbow trout *Oncorhynchus mykiss* epithelial cell line RTgill-W1 by viral and bacterial PAMPS. AQUA 2018. August 25-29, 2018, in Montpellier, France (Oral presentation).
9. S.C. Mandal, E. Carrick, M. Weidmann, B. Moro, S. MacKenzie and A. Albalat. Antiviral response of rainbow trout (*Oncorhynchus mykiss*) gill epithelial cell RTgill-W1. Marine Alliance for Science and Technology Scotland (MASTS) Annual Science Meeting, 30 October – 2 November 2018, Glasgow, UK (Oral presentation).

10. S.C. Mandal, M. Weidmann and S. MacKenzie. Response of the trout epithelial cells RTgill-W1 to SAV-2: cellular and molecular interactions. Fish Veterinary Society, 25-26 March 2019, Uphall, Edinburgh, UK (Poster and oral).

Trainings and workshops attended

1. Development Module Road Map Training, 11-13 March 2016. Cumberland, UK, organized by Commonwealth Scholarship Commission in the UK.
2. EMBL Course: Next Generation Sequencing: Whole Genome Sequencing Library Preparation, 4-5 July 2016. EMBL Heidelberg, Germany.
3. 22nd Glasgow Virology Workshop, 11 February 2017, Glasgow, UK
4. Fish Immunology and Vaccination Workshop, 30 April-4 May 2017, Wageningen, the Netherlands,
5. Workshop on Flow Cytometry, 17 May 2017, University of Aberdeen, UK
6. Development Module Training, 26-28 May 2017, Cumberland, UK
7. WGC Advanced Course: Immunophenotyping: Generation and Analysis of Immunological Datasets, 18-24 February 2018, Wellcome Genome Campus, Hinxton, Cambridge, UK.
8. Training on qPCR, 26-27 March 2018, Southampton, UK.
9. Early career researcher Grant workshop, 2 November 2018, Glasgow, UK.

Awards

1. Santander Travel award for attending a training at EMBL in Heidelberg Germany
2. Gold Studentship from Primer Design, UK
3. People's Choice Award, 3MT, University of Stirling, UK
4. Doctoral Bursaries from Charles Wallace Bangladesh trust, UK

Dedication

To my parents and my wife

List of abbreviations

%	Percentage
Ω	Ohm
+ssRN	Positive sense single stranded RNA
µl	Microliter
µm	Micrometre/micron
µM	Micromolar
Abbreviations	Elaboration
AKT1	AKT serine/threonine kinase 1
AMP	Antimicrobial peptide
ATM	Ataxia-telangiectasia mutated (serine/threonine kinase)
AURKA	Aurora kinase A
AURKB	Aurora kinase B
bp	Base pair
BSA	bovine serum albumin
CARDIF	CARD Adaptor Inducing Interferon-β
CD14	Cluster of differentiation 14
CDK1	Cyclin dependent kinase 1
CDK11A	Cyclin dependent kinase 11A
CDK14	Cyclin dependent kinase 14
CDK15	Cyclin dependent kinase 15
CDK18	Cyclin dependent kinase 18
CDK2	Cyclin dependent kinase 2
cDNA	complementary DNA
CHEK1	Cell cycle checkpoint kinase
CHH-1	Chum salmon heart -1 cells
CHIKV	Chikungunya virus
CHSE-214	Chinook salmon embryo 214 cells
cm	Centimetre
CPE	Cytopathic effect
CSNK1E	Casein kinase I isoform epsilon
CSNK2A1	Casein kinase II subunit alpha 1
CSNK2A2	Casein kinase II subunit alpha 2
Ct	Cycle threshold
CyD	Cytochalasin D
DAPK1	death-associated protein kinase-1
DMSO	Dimethyl sulphoxide
DPBS	Dulbecco's phosphate buffered saline without Ca and Mg
dsRNA	Double stranded RNA

E	Efficiency of qPCR
e.g.	Exempli gratia (example)
EMEM	Eagle’s Minimal Essential Medium Epithelioma
ER	Endoplasmic reticulum
FAO	Food and Agriculture Organization foetal
g	gram
GCRV	Grass carp reovirus
GSK3B	Glycogen synthase kinase 3 beta
h	h
HBEC	Human bronchial epithelial cells
IFN	Interferon
IFNR	Interferon receptor
IHNV	Infectious hematopoietic necrosis virus
IKK	I kappa B kinase
IL	Interleukin
IPEC-J2	Porcine intestinal epithelial cell clone J2
IPS1	Interferon-b promoter stimulator 1
IRF	Interferon regulatory factor
ISAV	Infectious salmon anaemia virus interferon
ISG	Interferon stimulated gene
IU	International unit
Kb	Kilo base
L	Litre
L-15	Leibovitz-15
LC-MS	Liquid chromatography -mass spectrometry
LGP2	Laboratory of genetics and physiology 2
LPS	Lipopolysaccharides
MAPK	Mitogen activated protein kinase
MAPK1	Mitogen activated protein kinase 1
MAPK10	Mitogen activated protein kinase 10
MAPK14	Mitogen activated protein kinase 14
MAPK3	Mitogen activated protein kinase 3
MAPK8	Mitogen activated protein kinase 8
MAPK9	Mitogen activated protein kinase 9
MAVS	Mitochondrial antiviral signaling
MDA5	Melanoma differentiation-associated gene 5
MDCK	Madin-Derby Canine Kidney cell line
MDP	Muramyl dipeptide
MOI	Multiplicity of infection
mRNA	Multiplicity of infection

MTOR	Mammalian Target of rapamycin (Serine/threonine kinase)
Mx	Myxovirus resistance gene
NCBI	National Center for Biotechnology Information
NFκ-β	Nuclear factor kappa-β
nm	Nanometre
nsP	Non-structural protein
OIE	Office International des Epizooties (World Organization for Animal Health)
PAMP	Pathogen associated molecular pattern phosphate
PaSRB2a	*Plecoglossus altivelis* scavenger receptor class B 2a
PBS	Phosphate buffered saline pancreas
PD	Pancreas disease
PEDV	Porcine epidemic diarrhoea virus
PGN	Peptidoglycan
PI3K	Phosphoinositide 3-kinase
Poly(I:C)	Polyinosinic and polycytidylic acid; Poly(I:C)
PKR	Double-stranded RNA-activated protein kinase
PKR	Protein kinase R
PLK3	Polo like kinase (Cytokine-Inducible Serine/Threonine-Protein Kinase)
PRKACA	cAMP-dependent protein kinase catalytic subunit alpha
PRKACB	cAMP-dependent protein kinase catalytic subunit beta
PRKCA	Protein kinase C alpha
PRKCB	Protein kinase C beta
PRKDC	DNA-dependent protein kinase catalytic subunit
qPCR	Quantitative polymerase chain reaction
qRT-PCR	Quantitative reverse transcription polymerase chain reaction
r^2	coefficient of determination
RFLP	Restriction fragment length polymerisation analysis
RIG-I	Retinoic acid-inducible gene I
RLR	RIG-like receptor
RNA	Ribonucleic acid
RPS6KA1	Ribosomal protein S6 kinase 1
RPS6KA3	Ribosomal protein S6 kinase alpha 3
RPS6KA6	Ribosomal protein S6 kinase 6
RPS6KC1	Ribosomal protein S6 kinase delta-1
RPS6KL1	Ribosomal protein S6 kinase-like 1
RSV	Respiratory syncytial virus
RT	Reverse transcription
rtCATH2	Rainbow trout cathilicidin
RTG-2	Rainbow trout gonad cells
RTgill-W1	Rainbow trout gill cell

RT-PCR	Reverse transcription polymerase chain reaction
SAV	Salmonid alphavirus
SGK1	Serum/glucocorticoid regulated kinase 1
SHK-1	Salmon head kidney -1 cells s
SRC	Proto-oncogene tyrosine-protein kinase
-ssRNA	Negative strand RNA
STAT	signal transducer and activator of transcription
SVCV	Spring viraemia of carp virus
TAE	Tris acetate EDTA
TBK1	Tank-binding kinase protein 1
$TCID_{50}$	50% tissues culture infective dose
THP-1	Human monocytic cell line
TLR	Toll like receptors
TO	A salmonid cell line
Trypsin /EDTA	Trypsin in 0.01 % ethylenediaminetetraacetic acid
TYK	Tyrosine kinase
Trypsin /EDTA	Trypsin in 0.01 % ethylenediaminetetraacetic acid
UK	United Kingdom
USA	United States of America
UV	Ultraviolet
V	Volt
v/v	volume/volume
Vero E6	African green monkey kidney epithelial cells
VHSV	Viral haemorrhagic septicaemia virus
VHSV	Viral haemorrhagic septicaemia virus
VIPERIN	Virus inhibitory protein, endoplasmic reticulum-associated, IFN-inducible
VISA	Virus-induced signaling adaptor
VNNV	Viral nervous necrosis virus
w/v	weight/volume
ZO-1	Zonula occludin-1

Abstract

Graphical abstract

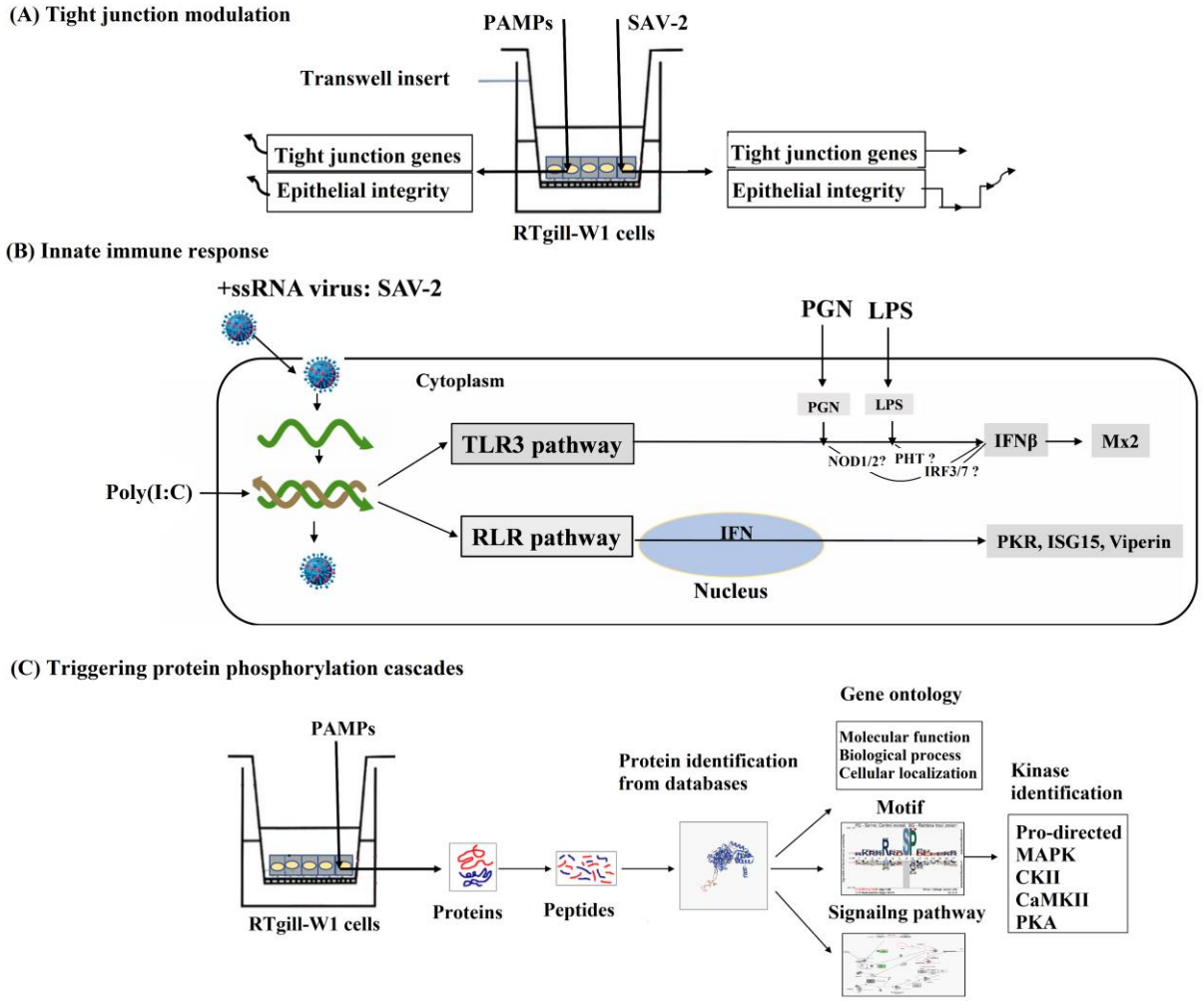

Textual abstract

The burden of disease is a major issue in aquaculture production. The fish gill is a significant portal of entry for pathogens in fish. To investigate epithelial integrity and innate immune responses in gill epithelia the salmonid gill cell line RTgill-W1 was stimulated with diverse pro-inflammatory and infectious agents. Epithelial integrity in polarised cells expressed as transepithelial electrical resistance (TER) immediately increased after stimulation with different PAMPs (pathogen associated molecular patterns). In parallel tight junction and innate immune gene expression was modulated with bacterial PAMPs, LPS and MDP, internalized through actin dependent and independent endocytic pathways.

The salmonid alphavirus subtype 2 (SAV-2) was used as an infectious agent in RTgill-W1 cells and was found to multiply at a low level. TER was found to be disturbed at an early stage of infection although tight junction related gene expression was not modulated. However, a strong PAMP-driven antiviral response was observed including upregulation of the expression of Rig-like receptor (RLRs) and several interferon stimulated genes (ISGs). Barrier function of trout gill epithelium against infection was also investigated. A bacterial invasion assay using *A. salmonicida* highlighted the capacity of PAMP pre-treatment to reduce bacterial invasion.

At the level of signal transduction of the phosphoproteome of RTgill-W1 cells in steady state and under poly(I:C) and MDP stimulation was conducted where poly(I:C) stimulated cells presented a higher number of phosphoproteins (360 unique phosphoproteins). These results provide an untargeted view of the key signaling pathways that are rapidly activated in response to PAMP stimulation.

The findings of the present study highlight an integrated response to viral infection and PAMP challenge in fish epithelia that could facilitate the development of novel therapeutic avenues for fish health management in aquaculture.

Table of contents

List of tables

List of figures

Preface

This PhD project was designed to characterize rainbow trout gill epithelial cell RTgill-W1which has included the barrier function and innate immune responses of trout gill cells to viral and bacterial PAMPs (Chapter 2) and viral infection agent (salmonid alpha virus subtype 2 which causes sleeping disease in trout) and bacterial infection agent (*A. salmonicida* which causes furunculosis in trout) (Chapter 4). The mechanisms of recognition of viral and bacterial PAMPs by the gill epithelial cells have also been studied. Further to study the cellular mechanisms involved in the barrier functions including cellular integrity and tight junction properties, and antiviral responses of RTgill-W1cells, global phosphoproteome approach has been applied (Chapter 3). The phosphoproteome study has included the identification of phosphoproteins, different kinases involved in the phosphorylation events and different signaling pathways involved in cellular integrity and antiviral responses in steady state and viral and bacterial PAMP stimulated RTgill-W1 cells.

Thus, in this thesis, the author has outlined the importance of studying fish-pathogen interactions highlighting the use of *in vitro* cell culture model. The use of different PAMPs as immune-stimulants has also been described. The interferon system and its role in innate immunity in fish have also been highlighted. The importance of antimicrobial peptides in immunomodulation has been placed. SAV-2, one of the aquatic viruses that reasons huge loss in the trout aquaculture causing sleeping disease, has been prioritized in the introductory dialogue. A bit explanation on *Aeromonas salmonicida* and its pathogenicity has also been in place in the introduction. Finally, different aspects of protein phosphorylation including its importance in phosphoproteomics including its development, has been emphasized.

Author
March 2019

Chapter 1

General introduction

1.1 General background

Aquaculture has grown steadily in the last few decades playing an increasing role in meeting the demand of fish for a growing world population (FAO, 2018). The rate of increment of fish production is double the world population growth rate (FAO, 2014). Aquaculture food fish contributed a record over 40% of the total 158 million tonnes of fish produced by capture fisheries and aquaculture in 2012 contributing the increment of per capita fish consumption over the last several decades where the average consumption has increased from nearly ten kilograms in 1960s to nearly nineteen kilograms in 2012 (FAO, 2014). This sector has great potential to expand and to meet the growing protein demand of an increasing global population. The production of aquaculture food products including fish, crustaceans, and mollusks has been recorded at 60 million tonnes in 2010 with a projected total value of US$119.4 billion (FAO, 2012) that is anticipated to increase to US$202.96 billion by 2020 (Grand View Research, 2015). Aquaculture contribution has been projected to rise to 62% of the total by 2030 (FAO, 2014).

Among aquaculture species, finfish contributes the highest production volume and values (FAO, 2014) where of 567 aquaculture species, 359 are finfishes. Among the finfish production, salmonid species as a single commodity share the highest by value (67.7%) and by quantity (80%) (FAO, 2016). Since the beginning of 1990s, more than half of the world production of diadromous fishes has come from salmonids, and the share peaked at 70.4 percent in 2001 where the production of salmonid has increased dramatically from 299 000 tonnes in 1990 to 1.9 million tonnes in 2010, at an average annual rate exceeding 9.5 percent (FAO, 2012).

Aquaculture intensification creates substantial animal stress, facilitating the emergence of infectious diseases causing huge aquaculture loss. The disease challenge in aquaculture is unlike to the disease challenge in other animal production systems as all the aquatic animals growing in the same water column have the potentiality of infection with the same pathogens (Jones et al., 2015). A rapid and dynamic development of aquaculture worldwide, epidemiological changes are leading to increase in the disease burden of aquaculture

(Kennedy et al., 2016). Evolution of virulence of pathogens also playing role in emerging of some of the fish diseases which is unavoidable due to the intensification of aquaculture (Walker & Winton, 2010).

In general, aquatic organisms have evolved specialized gas-exchange structure which is gill in fish accomplished by four pairs of vascularized gill arches composed of hundreds of gill filaments, which increase their contact surface by folding into the secondary lamella (Xu et al., 2016). Gills are in direct contact with the water and therefore are continuously exposed to environmental insults. Thus, the gill act as an important organ of entry for different pathogens including intracellular bacteria and viruses (Pratte, 2018). Thus, there is an evident need for the fish to defend such a large and delicate surface from pathogenic attack (Xu et al., 2016). How fish gill defends against pathogenic attack is little studied even a significant number of innate and adaptive immune molecules including cytokines, caspases, immunoglobulins, major histocompatibility complex (MHC), and pathways such as apoptosis, metabolic etc. operate in fish gill have been reported (Aquilino et al., 2014; Valenzuela-Miranda et al., 2015). Thus, knowledge on gill properties is important to understand gill-pathogen interaction as well as the immunological functions of gill and gill cells.

1.2 Teleost fish gill and gill properties

Many functions are carried out by the teleost fish gill which is composed of epithelial cells, chloride cells and mucous cells. The teleost gill is structurally complex (Part et al., 1993; Wilson & Laurent, 2002). A large surface area of the gill facilitates the exchange of gas, keeps balance between ion and acid/base and eliminates nitrogenous waste (Chasiotis et al. 2012a). Due to the continuous exposure to the surrounding water, fish gills are prone to contact with various pathogens, parasites and pollutants. For the study of fish gill diseases, gill cells especially primary gill cells have been widely used. Secondary cell lines however allow for more consistent and reproducible *in vitro* studies. The only available secondary fish gill epithelial cell line RTgill-W1 might therefore be a suitable alternative to study gill physiology and infection pathogenesis and immunology.

The RTgill-W1 cell line has been developed from the primary culture of rainbow trout gill *Oncorhynchus mykiss* (Walbaum) by Bols et al. (1994). This cell line offers a great potential

to study viral and bacterial gill disease *in vitro*. For example, Al-Hussinee et al. (2016) has investigated the antiviral responses of RTgill-W1 cell line upon induction with VHSV and viral and bacterial PAMPs while Trubitt et al. (2015) studied the effects of osmoregulatory hormones in RTgill-W1 cells. Previously, the pharmaceutical ecotoxicology has been investigated in RTgill-W1 and primary gill cells where double seeded and single seeded inserts (DSI and SSI) have been used to grow the cells (Claire, 2016). Cytotoxic and genotoxic responses of RTgill-W1 have also been reported (Amaeze et al., 2015). Moreover, RTgill-W1 cell have been used for the study of ichthyotoxicity by Dorantes-Aranda et al. (2011).

The fish gill epithelium covering the gill filaments and lamellae separates the external environment from extracellular fluids thus playing a critical role in gill function. Epithelial cells form intercellular junctions which result in a tight cellular barrier that separates the serosal from the basal side. The so-called tight junctions control the diffusion of different chemical components along the paracellular compartments.

1.3 Tight junction proteins

The gill plays the central role in maintaining homeostasis of the fish body (Evans et al., 2005). This homeostasis is regulated partially by tight junctions (Chasiotis et al. 2012b). The membranes of two closely associated epithelial cells are joined together by tight junctions which form a virtually impermeable barrier that controls the movement of fluids. Tight junctions are also known as occludin junctions or zonulae occludin. The tight junction paracellular space is formed and regulated by the claudin and occludin proteins (Whitehead et al., 2011) which are associated with intracellular protein ZO-1, and plays important roles in actin cytoskeleton regulation. Tight junction proteins play a vital role in the formation and development of epithelia, maintaining tissue integrity, tight junction permeability regulation and maintaining cell polarity. These tight junction proteins can be modulated by different environmental factors. Selected tight junction proteins have been shown to be sensitive to environmental changes. Moreover, endogenous factors have also been reported to mediate gill's response to the changes in environmental conditions (Chasiotis et al., 2012b). Different tight junction genes have been studied and their responses have been examined in the gill upon changing external environmental conditions. Bui et al. (2010) profiled 12 claudin genes in cultured puffer fish gill epithelia using specific primers where 9 genes were expressed in response to sea water acclimation. However, the role of gill

epithelial tight junctions in maintaining the paracellular permeability properties is not well studied.

1.3.1 Zonula occludin-1 (ZO-1)

ZO-1 is the first proteins among the tight junction proteins identified in animals (Stevenson et al., 1986). This protein resides on the inner cytosolic surface of tight junction, is composed of several binding domains targeting occludin and claudin as well as signaling molecules including transcription factors and actin cytoskeleton (Bauer et al., 2010). This protein is one of the most multipurpose tight junction components identified, and has been shown to respond to different environmental factors (Chasiotis et al., 2012b). Thus ZO-1 can be regarded as a dual activator providing important role in tight junction regulation associating claudin and occludin with actin cytoskeleton and transducing signals for the expression of different genes, cell cycle progression etc. (Bauer et al., 2010).

1.3.2 Occludin

The first transmembrane tight junction protein identified in vertebrate epithelia was occludin (Furuse et al. 1993) and extensively characterised using MDCK cells (Balda et al., 1996). McCarthy et al. (1996) demonstrated that ccludin localizes solely to tight junction fibrils at cell-cell contact sites. A wide variety of epithelial and endothelial tissues contain occludin (Gonzalez-Mariscal et al., 2003).

Occludin is the most extensively studied, well characterized and best understood tight junction protein in teleosts. Chasiotis et al. (2010) reported constitutive expression of occludin mRNA in gill tissue of rainbow trout, which indicates an important role for occludin in the regulation of branchial permeability. Compared to mammalian occludin, rainbow trout protein has 46–48% amino acid sequence similarity, 50% similarity with frog occludin while zebrafish occludin shares about 63% amino acid sequences (Chasiotis et al., ood & Kelly, 2010). Tight junction barrier formation and augmentation has been reported in mammalian models to “occlude” the paracellular movement of solutes (Cummins, 2012).

1.3.3 Tight junction protein and transepithelial electrical resistance (TER)

Epithelial and endothelial cells form intercellular tight junctions when cultured to a monolayer. Tight junctions are found in several places in the body such as; kidneys, intestine, lung epithelia in human while in fish tight junctions are found in gill epithelium.

Not only they are also found in the gill, but also in a wide range of tissues including intestine, skin, muscle, brain, blood-brain barrier, vascular system, swim bladder, lateral line, gall bladder, kidney, head kidney and spleen in different teleost fishes (McKee et al., 2014; reviewed in Kolosov et al., 2013)

Tight junctions are important components of the epithelial junctional complex and form a circumferential, belt-like structure at the luminal end of the intercellular space acting as a gatekeeper of the paracellular pathway (Farquhar and Palade, 1963). Transepithelial electrical resistance (TER) is the electrical resistance between the apical and basal side of the epithelial (or endothelial) cells. In *in vitro* studies the TER of an epithelial monolayer can be measured in transwell systems. There is a positive correlation between the development of a tight junction between the adjacent cells and TER. TER measurement is widely used and a very reliable, convenient and non-destructive method. The TER value is a strong indicator of cell integrity. This quantitative expression of the barrier integrity is expressed as ohms-cm^2 (Ω-cm^2) (Benson et al., 2013).

The complexity of the tight junction network, has an effect on TER and Claude & Goodenough (1973) demonstrated a direct relationship between TER and the number of parallel strands between cells. Epithelial gill cells have the ability to differentiate and to retain their polarised properties when the primary cultures of gill epithelial cells are grown onto permeable inserts (Moore et al., 1998). Primary gill cultures grown on to glass discs or in wells might lose the differentiation and polarisation properties while grown onto transwells the gill cells are more likely to build their epithelial properties. Thus in the transwells the cellular integrity is retained and a tight gill epithelium mimicking in vivo integrity is formed (Fijan et al., 1983; Srinivasan et al., 2016).

1.3.4 Transwell system to study cellular integrity

A typical transwell system has several components where the main component is the transwell insert carrying a microporous membrane of varying pore size. Other components are cell culture companion where the insert is placed forming serosal and basal compartments (Figure 1.1A). The integral part of the system is the cell monolayer cultured onto the microporous insert. Growth medium is used in the apical side and the basal side.

To measure the electrical resistance, different volt-ohm meters are used. The measurements are taken by using two electrodes where one electrode is placed in the serosal compartment and another in the basal compartment.

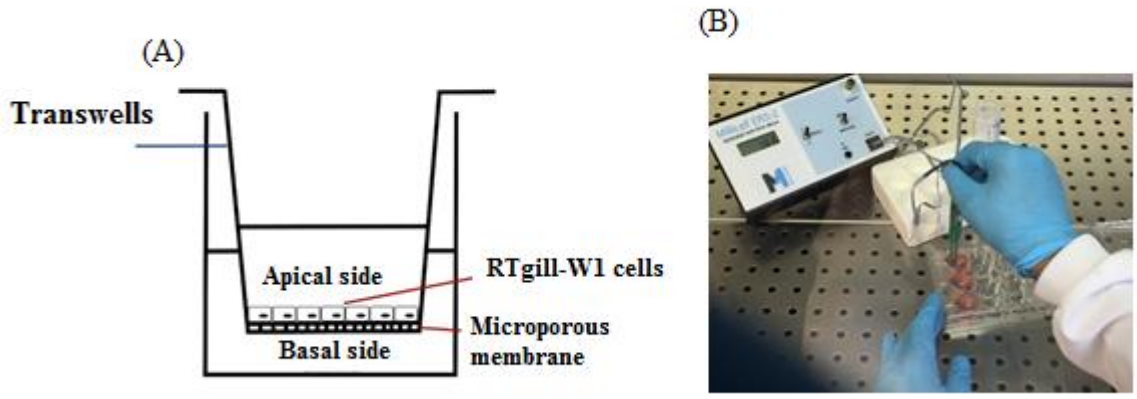

Figure 1.1: Transwell system (A) and its application in measuring transepithelial electrical resistance measurement (B).

TER measurements have been done for various cell types using different commercially available measurement systems. The Milicell ERS-2 device is widely used for measuring cellular integrity (Figure 1.1B).

Transepithelial resistance has been measured in primary and secondary fish cell lines. An overview on the literature is presented in the Appendix 3, Supplementary Table S3. The use of transwell system in mammalian models to study the barrier function is also reviewed.

1.4 Bacterial and viral fish diseases

Bacterial and viral diseases are among the most dominant causes for losses to aquaculture production which affect the economic growth of the aquaculture sector in many countries worldwide accounting total loss over 6 billion USD per year (The World Bank, 2013). Disease is not a simple interaction between pathogens and host, rather a complex interaction among host, pathogens and the environment involving infectious and non-infectious processes which are triggered by external factors (Francis-Floyd, 2013). Aquaculture intensification creates substantial animal stress, facilitating the emergence of infectious diseases causing huge aquaculture loss. Although a significant advancement has been made in diagnosis, treatment and management of disease in certain aquaculture sectors, resistance

issues still a barrier for the expansion of aquaculture. The lack of historic background of microbial diversity in aquatic system leads to the emergence of previously unknown diseases (Stentiford et al., 2017). Thus, the control of diseases of aquatic organisms is complicated because of the complexity and the nature of the aquatic environment (Assefa & Abunna, 2018). A proper and quick diagnostic technique and right therapeutic agents are required to control infectious diseases as well as proper aquaculture management and biosecurity are needed to be emphasized (FAO, 2016).

According to the Office International des Epizooties (OIE, 2018), of the listed ten fish diseases as notifiable, eight are viral (Table 1.1). These are mostly members of the Rhabdoviridae and Iridoviridae family and they have caused tremendous socio-economic losses worldwide (Aoki et al., 2011). Other viruses are erythrocytic necrosis virus (ENV), channel catfish virus (CCV), tilapia lake virus (TiLV) and largemouth bass cirus (LMBV) causing huge loss to aquaculture production. Bacteria, on the otherhand can also cause huge aquaculture loss (Dalsgaard & Danish, 2000). Among different bacterial diseases in fishes caused by various species of bacteria furunculosis, columnaris, vibriosis, dropsy, bacterial gill disease and mycobacteriosis (tuberculosis) are the most prominent (Table 1.1).

TiLV, an OIE listed but not notifiable virus, is an emerging RNA virus causes huge mortalities of tilapia of all life stages in Asia, Africa and South America (Jansen et al., 2018) where the economic loss is un-estimated. Hounmanou et al. (2018) have reported 90% mortalities of tilapia in Africa due to TiLV infection. Wallace et al. (2017) have reported six key pathogens causing diseases in wild and farmed fishes in Scotland which include *Renibacterium salmoninarum* causing bacterial kidney disease in wild salmon, *A. salmonicida* causing furunculosis in salmonid, IPNV causing Infectious pancreatic necrosis in salmonid, ISAV causing infectious salmon anaemia, SAV causing pancreas and sleeping diseases in salmonids and VHSV causing haemorrhagic septicaemia in trout. As an example, salmonid aquaculture in the UK is hampered by infectious diseases however, particularly those caused by viral pathogens where salmonid alphavirus (SAV) causes considerable loss of growth and can kill up to 60 % of a population contributing 47% of total mortality losses and the highest biomass losses (86 %) associated with infectious diseases in cultured salmon in Scotland (McLoughlin & Graham, 2007). In Japan, according to Inouye (1996), the damage caused by disease in finfish and shrimp aquaculture in 1992 was estimated to be 18 269 mt worthing US$ 264 million where the total production was 356 154 mt, worthing US$

4 376 million which was about 5% of the total production of finfish and shrimp in 1992. Disease in rainbow trout caused the total production loss of more than 600 mt Worthing more than 6 million USD (Inouye, 1996). Another study reported the loss of channel catfish aquaculture of over 100 million fish worth nearly $11 million while the trout industry reported losses of over 20 million fish worth over $2.5 million in 1988 (Meyer, 1991). This clearly demonstrates the impacts of diseases on aquaculture production.

Fish RNA viruses, and the pathology they cause relatively well characterised, however, the understanding of how these viruses and in particular SAV manipulate host machinery during their replication cycle is extremely limited. Improving knowledge in this area can thus be considered highly relevant, particularly given that improved understanding of such interactions in birds and mammals is assisting the development of new therapeutic approaches in these animal groups. Moreover, bacterial disease pathogenesis in fish is not well studied which is also important to understand to develop new therapeutics against bacterial diseases.

Table 1.1: List of important fish diseases with causative agents.

Disease	Causative agent(s)	Host	Affected organs	Comments	Reference
Viral diseases					
Channel catfish virus disease (CCVD)	Channel catfish virus (CCV)	Mainly channel catfish, also other closely related catfish	Trunk kidney and other organs including skin	-	(Camus, 2004)
Epizootic haematopoietic necrosis	Epizootic haematopoietic necrosis virus (EHNV)	Salmonids and non-salmonids	Gill, fin base, spleen and kidney	OIE listed	(OIE, 2018)
Erythrocytic necrosis	Erythrocytic necrosis virus (ENV)	More than 20 fish species including salmonids	Erythrocytes	-	(Emmenegger et al., 2014)
Infectious Haematopoietic Necrosis	Infectious haematopoietic necrosis virus (IHNV)	Salmonids and some non-salmonid fish species	Gill, fin base, spleen and kidney	OIE listed	(OIE, 2018)
Infectious salmon anaemia (ISA)	infectious salmon anaemia virus (ISAV)	Salmonids	Gill, heart, liver, kidney, spleen and others	OIE listed	(OIE, 2018)
Koi herpesvirus (KHV) disease	Koi herpesvirus (KHV)	Mainly common carp	Gill, kidney and spleen	OIE listed	(OIE, 2018)
Pancreas disease and sleeping disease	Salmonid alphavirus (SAV)	salmonids	Brain, gill, heart, pancreas etc.	OIE listed	(OIE, 2018)
Red sea bream iridovirus disease	Red sea bream iridovirus	Wide range of species including sea bass, bream, perch etc.	Gill, kidney, spleen, intestine and heart	OIE listed	(OIE, 2018)
Spring viraemia of carp (SVC)	Spring viraemia of carp virus (SVCV)	Mainly carps	Mainly liver and kidney, also gill, brain and spleen	OIE listed	(OIE, 2018)
Tilapia lake virus (TiLV) disease	Tilapia lake virus (TiLV)	Tilapia	Eyes, brain and liver	OIE listed	(Eyngor et al., 2014)
Viral haemorrhagic septicaemia (VHS)	Viral haemorrhagic septicaemia virus (VHSV)	Wide range of host species including salmonids	Mainly kidney, heart and spleen	OIE listed	(OIE, 2018)
Largemouth bass virus disease (LMBVD)	Largemouth bass virus disease (LMBV)	Largemouth bass (*Micropterus salmoides*)	Swim bladder, gill and trunk kidney	-	(Beck et al., 2006)
Bacterial diseases					
Enteric red mouth disease	*Yersinia ruckeri*	Salmonids	Skin around the mouth and throat, liver, pancreas, swim bladder and pyloric caeca		(Kumar et al., 2015)
Bacterial gill disease (BGD)	*Flavobacterium branchiophylum*	Salmonids	Gill	-	(Schachte, 1983)
Bacterial kidney disease	*Renibacterium salmoninarum*	Salmonids	Externally skin, fin base; internally kidney	-	(Wallace et al., 2017)

Furunculosis	*A. salmonicida*	Salmonids	Skin, mouth, gill	-	(Wallace et al., 2017)
Columnaris	*Flavobacterium columnare*	Carp and salmonids	Skin, gill	-	(Declerc et al., 2013)
Vibriosis	*V. anguillarum, V. ordalii and V. salmonicida*	Wide range of fish species including salmonid	Externally lateral line, vent; internally kidney and spleen	-	(Idowu et al., 2017)
Mycobacteriosis	*M. tuberculosis*	Wide range of fish species including salmonid	Skin, kidney and liver	-	(Puttinaowarat et al., 2000)

1.4.1 Salmonid alpha virus (SAV)

Salmonid alpha virus is one of the viruses cause huge losses to salmon and trout aquaculture. The most common diseases in salmonids are pancreas disease (PD) and sleeping disease (SD) where PD is associated with Atlantic salmon (*Salmon salar*) and SD is associated with rainbow trout (*Onhorhynchus mykiss)* (McLoughlin & Graham, 2007). These diseases are mainly prevalent in European countries. Like other alphaviruses, salmonid alphavirus (SAV) is a +ssRNA virus. Six subtypes of salmonid alphavirus have been reported by the recent molecular taxonomic studies (Table 1.2).

Salmonid alphavirus subtype 1, 4, 5 and 6 cause PD in salmon. Salmonid alphavirus subtype 3 (SAV-3) has been found to cause PD in salmon in Norway. SD is caused by subtype 2 (SAV-2) which has similar structural properties as SAV-1. SAV-2 causes SD in freshwater rainbow trout in several European countries.

Table 1.2: Salmonid alphavirus subtypes and the diseases, host specificity and distribution (Fringuelli et al., 2008; McLoughlin & Graham, 2007; Hjortaas et al., 2013; Smrzlic et al. 2013; Schmidt-Posthaus et al., 2014).

Virus subtype	Location	Species and environment	Disease	Expt. infections
SAV1 (PD)	Ireland (Northern Ireland), Scotland, UK	Atlantic salmon (SW) Rainbow trout (FW)	PD	Atlantic salmon, rainbow and brown trout
SAV2 (SD)	France, England, Scotland, Spain, Italy, Germany, Switzerland, Croatia	Rainbow trout (FW) Atlantic salmon (SW)	SD	Atlantic salmon, rainbow and brown trout
SAV2 Marine (PD)	Norway, UK (Scotland)	Atlantic salmon (SW)	PD	ND
SAV3 (PD)	Norway	Rainbow trout (SW) Atlantic salmon (SW)	PD	Atlantic salmon and rainbow trout
SAV 4 (PD)	Ireland, UK (Northern Ireland, Scotland)	Atlantic salmon (SW)	PD	ND
SAV 5 (PD)	UK (Scotland)	Atlantic salmon (SW)	PD	ND
SAV 6 (PD)	Ireland	Atlantic salmon (SW)	PD	ND

In freshwater aquaculture in Europe, sleeping disease (SD) is a serious infectious disease (McLoughlin & Graham, 2007). The viral aetiology of SD has been confirmed by the isolation of sleeping disease virus (SDV) in France. This virus has been characterized extensively and considered as an atypical alphavirus of the family Togaviridae which is now well known as SAV-2 (Boucher and Laurencin, 1996). SAV 2 has also been isolated from diseased rainbow trout in England, Scotland and Germany (Bergmann et al., 2008). SAV-2 was first reported in the United Kingdom in 2003 where the virus was isolated and identified from a rainbow trout (Graham et al., 2003). Infection with SAV-2 has also been shown to be present in fresh water trout in Italy and Spain (Graham et al., 2007). SAV-2 has also been isolated recently from rainbow trout in Switzerland, Croatia and from Atlantic salmon in Norway (Hjortaas et al., 2013; Smrzlic et al., 2013; Schmidt-Posthaus et al., 2014; Table 1.2). However, very few SAV 2 isolates are available (Table 1.3).

Table 1. 3: SAV2 isolates with related information

Virus isolate	Country of origin	Species	Cell line for isolation	References
SDV S49P	France	rainbow trout	CHSE-214 and RTG-2	(Castric et al., 1997)
SDV G 1 (DF 11/03)	Germany	rainbow trout	CHSE-214 and RTG-2	(Bergmann et al., 2008)
SDV G 2 (DF 18/03)	Germany	rainbow trout	CHSE-214 and RTG-2	(Bergmann et al., 2008)

1.4.1.1 Alpha virus genome

Alphavirus is a small virus 65-70nm in diameter with a genome size of 11.7 kb, coding for two open reading frames (ORFs) (Jose et al., 2009). The nucleocapsid of alphavirus is composed of 240 copies of capsid protein arranging in a T=4 icosahedral shell (Figure 1.2). Two viral glycoproteins E1 and E2 enclose the nucleocapsid. Eighty trimers of E1/E2 heterodimers arranged in a T=4 icosahedral lattice comprise the surface of the virion (Guo, 2015).

One ORF encodes the replicase polyprotein and the other one encodes viral structural proteins (Figure 1A). There is a 5’ cap and poly(A) at the 3’ end. Two thirds of the alphavirus genome (RNA) at the 5’end encodes non-structural proteins (nsP1-nsp4). The remaining third at the 3’ end encodes structural proteins. Structural proteins include the capsid protein, two glycoproteins (E1 and E2), and two small peptides 6k and E3. The alphavirus genome also contains two untranslated regions (5’UTR and 3’UTR residing between ORF1 and (Frolov et al., 2001; Levis et al., 1990).

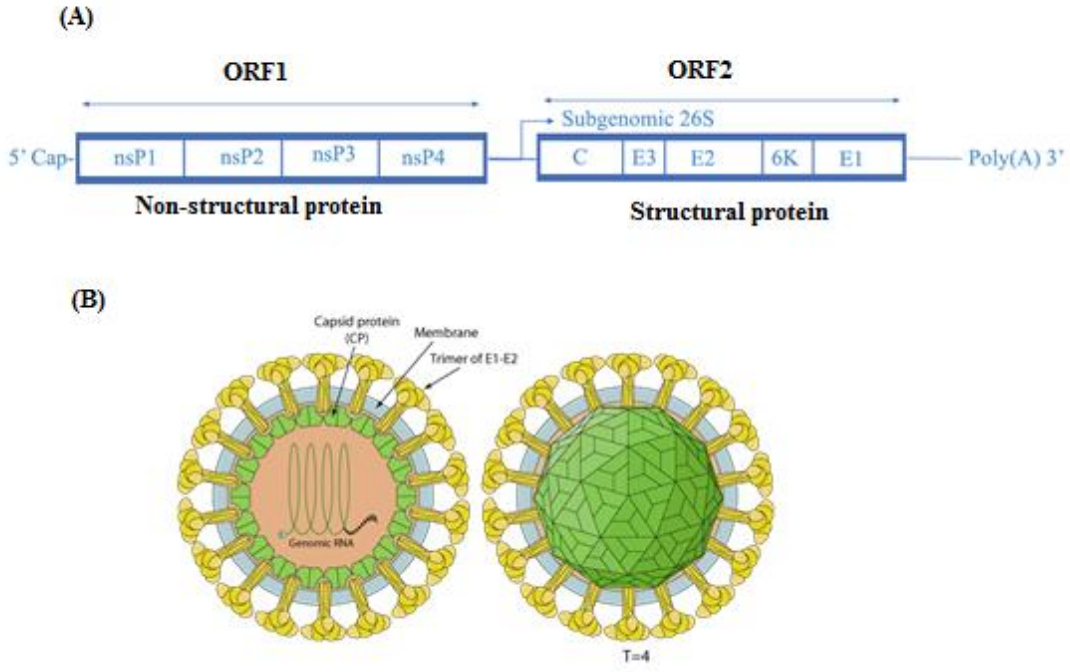

Figure 1.2: Structure of alpha virus. (A) Alpha virus genome showing the arrangement of structural and non-structural protein. (B) Alpha virus virion (taken from viralZone; https://viralzone.expasy.org/625?outline=all_by_species).

E1 triggers viral and cellular membrane fusion (Roussel et al., 2006) whereas E3 is a small cysteine-rich glycoprotein carrying the signal for the translocation of E2 into the lumen of the ER (Lobigs et al., 1990), and E2 stabilizes the interaction between the virus and the receptor thus contributing to greater virulence (Lee et al., 2002). Among the 4 non-structural proteins (nsp1-nsp4), nsp1 plays a role in capping of viral RNA at the 5' end (Ahola et al., 1997), nsp2 has an enzymatic RNA binding activity associated with ATPase and GTPase activity, which is implicated in the unwinding of intermediate double-stranded RNA during replication at N-terminal whereas C-terminal functions as a non-structural proteinase (Mayuri et al., 2008), nsP3 is associated with the synthesis of negative strand RNA and sub-genomic RNA. Function of replication complex is associated with the interaction of nsp2/nsp3 (LaStarza et al., 1994). RNA dependent RNA polymerase (RdRp) activity is performed by nsp4. Excessive concentration of nsp4 is rapidly degraded which is strictly regulated inside cells (de Groot et al., 1991).

Alphavirus capsid protein has several functions where the C-terminal end has autoproteolytic activity and N-terminal peptide plays role in down-regulating cellular

transcription and developing CPE (Garmashova et al., 2007). The capsid of SFV has been shown to act as translational enhancer (Yamanaka & Xanthopoulos, 2004). 6K is another important alphavirus protein which is highly hydrophobic and small in size and has been found to act at late stage of infection in SFV or SINV (Sanz et al., 1994).

1.4.1.2 Alphavirus life cycle

Upon attachment on the host cells, alphavirus enters the host cells through receptor-mediated endocytosis. As alphavirus receptors or attachment factors several cell surface molecules have been suggested which include laminin receptor, MHC class 1 antigen, integrin beta 1 or alpha 1, cell surface heparin sulfate (HS) and DC-SIGN (Kielian et al., 2010). However, the receptors for salmonid alphavirus has not been identified.

The pH of the endosome plays an important role in the initiation of viral fusion. Low pH is required for this initiation. The viral nucleocapsid needs to be disassembled where ribosome facilitates the disassembly by interacting with capsid protein before the replication begins. Upon disassembly of the viral RNA genome in the cytoplasm replication takes place. Replication of viral genome and transcription of RNA involve the non-structural viral proteins that make a membrane-bound replication complex together with host factors. The last step of viral replication is the budding where the newly synthesized nucleocapsid cores are assembled in the cytoplasm and act together with the envelope glycoproteins at the plasma membrane and form the virions (Figure 1.3).

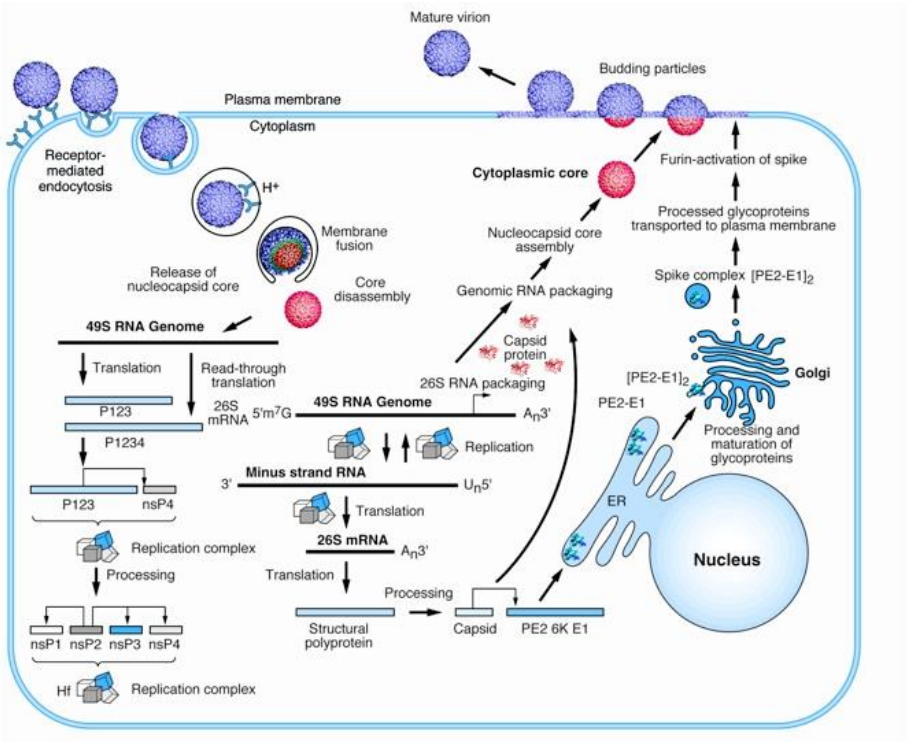

Figure 1.3: Alphavirus replication cycle. Figure has been taken from Jose et al., 2009.

1.4.1.3 Virus isolation and identification

Isolation and identification of aquatic viruses is possible using several developed fish cell lines (Essbauer & Ahne, 2001). Primary cells are also used for virus isolation and identification. PCR or RT-PCR is used for the detection of specific viral gene material from the cells or cell supernatant. Thus, cell culture is regarded as the gold-standard test for the isolation and identification of viruses though it is costly and time consuming. Generally, virus identification from cell culture is done by the observation of formation of cytopathic effects (CPE) which present as changes in morphology of cells due to viral infection. Virus lyse the host cells and cause CPE. Virus can also kill the host cell without forming CPE. The common symptoms of CPE include rounding and dying of the infected cell, forming syncytia which is the fusion of infected cells with adjacent cells (also known as polykaryocytes), and the formation of inclusion bodies which might be nuclear or cytoplasmic origin or may be viral components. Most common cell lines used for SAV isolation and growing are CHSE-214, CHH-1 and SHK-1 (OIE, 2017). Several other methods are applied for virus identification which include immunostaining, ELISA, immuno-electron microscopy, etc.

1.4.2 *Aeromonas salmonicida* as a fish pathogen

A. salmonicida is a facultative anaerobic, gram-negative, non-encapsulated, non-motile coccobacilli which is catalase and oxidase positive and whose optimum growth temperature is between 22 and 25 °C (Popoff, 1984). On the basis of biochemical properties, *A. salmonicida* has been classified into typical and atypical *A. salmonicida* pathogroups where the typical group includes *A. salmonicida* subsp. *salmonicida* and the atypical group includes *A. salmonicida* subsp. *achromogenes*, *masoucida*, *smithia*, and *pectinolytica* (Wiklund & Dalsgaard, 1998). Typical isolates are responsible for causing furuculosis in salmon and trout which appears to infect fish cultured usually in a polluted environment. The first indication of the disease is the appearance of boil like lesions followed by haemorrhagic muscles, kidney necrosis, blood-spattered fins and vent. The atypical group have been found to cause ulcerative diseases in salmonid and non-salmonid fishes (Wiklund & Dalsgaard, 1998). Both groups have worldwide distribution, including North America, Europe, and Japan (Kim et al., 2011).

Furunculosis caused by *A. salmonicida* was first reported in Germany 1894 in brown trout from a hatchery by Emmerich & Weibel (1894). Later, this disease was diagnosed in other salmonids in different countries. Salmonid species including Atlantic salmon, rainbow trout, brown trout and non-salmonid fish species including atlantic cod (*Gadus morhua*), halibut (*Hippoglossus hippoglossus*), sea bream (*Sparus aurata*), turbot (*Psetta maxima*), sea lamprey (*Petromyzon marinus*) etc. are susceptible to furunculosis (Department of Agriculture, 2009). Among salmonids, *A. salmonicida* has been isolated from Atlantic salmon in Canada, Finland, Iceland, Norway and Sweden, rainbow trout in Canada, Finland and Sweden but also from many other non-salmonid fish species (Cited by Wiklund and Dalsgaard, 1998). Furunculosis has been reported to cause huge salmonid aquaculture loss in Scotland costing 20 million USD in 1989 (Wallace et al., 2017). Furunculosis has also been reported to cause severe problem in rainbow trout aquaculture in Denmark (Dalsgaard & Madsen, 2000). In Norway, salmonid aquaculture faces serious challenges due to furunculosis (Bornø et al., 2017). In Japan, furunculosis has been reported to cause the largest salmonid aquaculture loss (95.6 mt) in 1992 (Inouye, 1996).

A. salmonicida transmission mechanism is not well reported despite the disease having been studied for over hundred years (Munro & Hastings 1993). Infected fish, contaminated water or farm materials can transmit the pathogen while the vertical transmission has not been reported for furunculosis (McCarthy, 1977). Among different organs, gills and skin have been reported as the main routes of entry of *A. slmonicida* (Svendsen et al., 1999). A recent *in vivo* study using fluorescent tagged *A. salmonicida* reported gills as one of the important colonization sites for *A. salmonicida* in rainbow trout (Bartkova et al., 2016). Thus, fish gill epithelial cell lines might be an ideal model for studying pathogenesis of *A. salmonicida* and developing possible therapeutic agents.

1.5 Fish immune system

The immune system protects animals from foreign substances like pathogens, toxins or malignant cells. Like the mammalian immune system, the fish immune system can be divided into an innate and an adaptive immune system. The innate immunity, phylogenetically, is the oldest system originating in the most primitive diploblastic metazoans during the evolutionary period (Lieschke & Trede, 2009). The innate immune system includes all the components present before the entry of pathogens and acts as a first line of defense. This includes skin (acts as physical barrier), the complement system, the interferons, various defence cells (granulocytes, monocytes, macrophages, natural killer cells), antimicrobial molecules and cytokines (Biller-Takahashi & Urbinati, 2014). For cellular defence, teleosts have been shown to use phagocytic cells similar to macrophages, neutrophils and natural killer (NK) cells, as well as T and B lymphocytes while presence of cytokines including interferon, interleukins, macrophage activating factors have been reported in many different fishes (Detail in section 1.9.1 and 1.10) (Zou et al., 1999; Zou et al., 2004; Zou et al., 2014; Change et al., 2009; Reyes-Cerpa et al., 2012; Stachura et al., 2013; Wang et al., 2008; Liongue & Ward, 2007; Yamaguchi et al., 2015; Lutfalla et al., 2003; Sangrador-Vegas et al., 2012; Najakshin et al., 1999; Secombes et al., 1996).

1.6 Pathogen associated molecular patterns (PAMPs) as immuno-stimulants

To protect against infection, it is essential to detect the presence of microorganisms. Microbial molecules distinctive for associated microorganisms with specific molecular structures, so called pathogen-associated molecular patterns or PAMPs can be detected by host defence molecules. Danger-associated molecular patterns or DAMPs of infected, injured or even transformed host cells can also be sensed by host receptors.

There are many examples of PAMPs. Lipopolysaccharides (LPS) are present on the outer membrane of the cell wall of gram-negative bacteria also containing peptidoglycans (PGN), which predominately functions as a signifying component of the cell wall of gram-positive bacteria. Lipoteichoic acids are also a component of the cell wall of gram-positive bacteria. Flagellin is a structural protein of bacterial flagella. Bacterial and in particular viral nucleic acids including dsRNA and ssRNA are also recognized as PAMPs. Finally, zymosan from the cell wall of yeast is detected as a PAMP.

PAMPs can be used as immune-stimulants which can be defined as the elements that trigger the immune system through Pattern recognition receptors (PRRs) and Toll like receptors (TLRs) and increase overall resistance to various diseases (Magnadottir, 2010). Immuno-stimulants may be viral or bacterial derivatives or chemically synthetic. Immuno-stimulants are mostly used as dietary supplements in aquaculture to improve the innate defence of animals providing resistance to pathogens during periods of high stress, such as grading, reproduction, transportation (Bricknell & Dalmo, 2005). The most commonly experimentally used PAMPs are poly(I:C) a viral dsRNA analogue, LPS and PGN.

1.6.1 Polyinosinic-polycytidylic acid (poly(I:C))

Poly(I:C)) is a synthetic chemical compound structurally similar to dsRNA viral gene material. It acts as a ligand of TLR3, thus poly(I:C) is sensed by TLR3 (Alexopoulou et al., 2001; Matsumoto et al., 2002). In human and mice poly(I:C) has been shown to act against viral diseases (Zhou et al., 2014). Poly(I:C) is known to induce type I interferons (IFN) and to enhance cytokine production and innate and adaptive immunity. It is one of the promising immuno-stimulants used in aquaculture which is believed to enhance antiviral defences upon binding to TLR3 in fish (Jensen et al., 2002; Lockhart et al., 2004; Bricknell & Dalmo, 2005; Fernandez-Trujillo et al., 2008). Zhou et al. (2014) found poly(I:C) to induce antiviral activity and to boost the activation of head kidney macrophages. Antiviral effects of poly(I:C) have been reported against several aquatic viruses. However, the mechanism of antiviral activity of poly(I:C) in fish gill epithelia is not clear.

Upon recognition of poly(I:C), IRF3, a transcription factor, is activated by TLR3 (Yamamoto et al., 2003). Subsequent production of type one interferon especially IFN-β is

initiated by the activation of IRF3. Another pathway is also suggested where the transcription factors NF-κB and AP-1 are activated by poly(I:C) (Kawai & Akira, 2008a). The production of inflammatory cytokines and chemokines such as TNF-α, IL-6 and CXCL10 are triggered by poly(I:C) (Ritter et al., 2005). Poly(I:C) has also been reported to be sensed by the cytosolic pattern recognition receptors RIG-I and MDA5 (Kato et al., 2006).

Ortholog of mammalian TLR3 has been reported in a wide range of fish species which include Japanese flounder (*Paralichthys olivaceus*) (Shahsavarani et al., 2006), catfish (*Ictalurus punctatus*) (Baoprasertkul et al., 2006), fugu (*Takifugu rubripes*) (Oshiumi et al., 2003), rainbow trout (*Oncorhynchus mykiss*) (Rodriguez et al., 2005), zebrafish (*Danio rerio*) (Phelan et al., 2005), and Atlantic salmon (*Salmo salar*) (Svingerud et al., 2012). Poly(I:C) has been found to induce antiviral responses through TLR3 signaling upon infection by haemorrhagic septicaemia virus (Takami et al., 2010), infectious hematopoietic necrosis (Hyoung et al., 2009), infectious salmon anaemia virus (Jensen et al., 2002), haematopoietic necrosis virus (Purcell et al., 2004), infectious pancreatic necrosis virus (Lockhart et al., 2004), and channel catfish virus (Plant et al., 2005).

1.6.2 Lipopolysaccharide (LPS)

Lipopolysaccharide is associated with LPS binding protein (LBP). LBP is a protein that is found in the bloodstream in the acute- phase of infection (reviewed in Akira et al. 2006). This protein then binds to CD14 which is expressed on the cell surface of phagocytes (Poltorak et al., 1998; Shimazu et al. 1999). In Atlantic salmon macrophages, LPS has been shown to stimulate phagocytosis and the subsequent production of superoxide (Solem et al., 1995). Moreover, in goldfish lymphocytes, LPS has been found to stimulate macrophage activating factor production (Neumann et al., 1995) and interleukin 1 like molecules production in catfish monocytes (Clem et al., 1985).

1.6.3 Peptidoglycan (PGN)

Peptidoglycan, on the other hand, is one of the important components of the cell wall of Gram-positive bacteria. Gram-positive bacterial cell walls may contain up to 40 layers of peptidoglycan providing rigidity and mechanical strength to the cell wall. PGN in gram-positive bacterial cell wall makes up about 20% of the cell wall dry weight compare to 10%

in Gram negative bacteria. PGN has been shown to be a powerful biological effector with different immuno-stimulatory activities such as activation of macrophages, cytokine production, induced autoimmunity, induction of antimicrobial peptide production (Boneca, 2005). PGN is efficiently recognised by the eukaryotic innate immune system (Dziarski, 2004).

1.7 Recognition of PAMPs by host receptors

Viral and bacterial PAMPs play significant roles in immunomodulation of host cells by activating different antiviral and antibacterial responses. Different PAMPs bind to different intracellular and extracellular receptors on host cells. Extracellular receptors are present on the cell surface and upon binding to the PAMPs, activate distinct downstream signalling pathways. On the other hand, to bind to the intracellular receptors, PAMPs must firstly be internalized. Different endocytic mechanisms, both actin-dependent and independent may be employed to internalise molecules.

As mentioned before, the first condition of initiation of immunity is the recognition of pathogens by PRRs which are key elements of the innate immune system. Mainly antigen-presenting cells such as dendritic cells and macrophages express these PRRs. However, they can also be expressed by other immune cells and even non-immune cells like epithelial cells. These receptors are localised at different subcellular location of the cells. Receptors present on the cell surface recognize extracellular pathogens like bacteria or fungi whereas receptors in the endosome recognize intracellular pathogens like viruses. Different groups of PRRs are distinct in their ligand specificity, signal transduction and sub-cellular localisation.

The PRRs are divided into four families, there are Toll-like receptors (TLR), Nucleotide-binding oligomerization domain (NOD)-like receptors (NLR), C-type lectin receptors (CLR) and RIG-1 like receptors (RLR). Toll-like receptors (TLRs) are a family of transmembrane proteins first discovered in *Drosophila* for their role in dorsal-ventral patterning (Belvin & Anderson, 1996). TLRs are perhaps the most exclusively studied and one of the important PRRs sensing conserved microbial products, triggering a series of immune responses against invading pathogens. In vertebrates, to date 27 different TLRs have been identified where fish specific or non-mammalian TLRs include TLR18-27 (Palti,

2011). TLR22 has been shown to be induced by viral PAMP poly(I:C) and bacterial infection in common carp (Li et al., 2017). TLR22 has also been shown to recognize poly(I:C) in fugu and subsequent induction of interferon and protection from birnaviruses (Matsuo et al., 2008).

1.7.1 Recognition and signaling through TLRs

TLR3, an intracellular recognition receptor localized in the endosomal compartment, is ubiquitously expressed in innate immune cells as well as non-immune cells (Hayashi et al., 2003). Poly(I:C), an analogue of dsRNA, has been found to activate TLR3 signaling that initiates or stimulates the production of type I IFN, especially IFN-β and different cytokines in macrophages (Edelmann et al., 2004). In the same study, wild type splenocytes have been found to be activated by genomic dsRNA of reovirus while TLR3 deficient splenocytes were unable to be activated by the same agent. Thus, it can be deduced that TLR3 could respond to poly(I:C) which would enhance innate immunity and will lead to the production of IFNβ through binding to TLR3. It was shown that IFNβ triggers antiviral response by inducing the production of interferon stimulated genes (ISGs) like for example Mx (Figure 1.4).

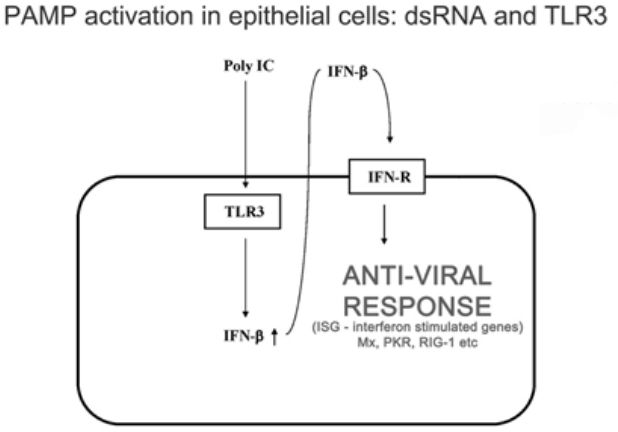

Figure 1.4: TLR3 signaling pathway activated by poly(I:C).

1.7.2 Recognition and signaling through RLRs

It is well known that most viruses produce dsRNA at some stages of their replication. As a general rule of thumb, ssRNA viruses produce dsRNA from replicative intermediates (Jacobs & Langland, 1996). DNA viruses are believed to produce dsRNA via transcription before producing complementary mRNAs, which when annealed, produce long strands of dsRNA (DeWitte-Orr & Mossman, 2010). During replication, viral dsRNA accumulates in

the cellular compartment. When viruses replicate in the cytoplasm, viral dsRNA is cytoplasmic and in the case of replication in the nucleus, viral dsRNA can be detected in both the nucleus and cytoplasm (Kumar & Carmichael, 1998).

Antiviral immunity starts upon recognition of pathogens by the host PRRs mostly TLR3 and RIG-like Receptors (RLRs) comprising MDA5 (melanoma differentiation-associated gene 5), RIG-I (retinoic acid-inducible gene I) and LGP 2 (laboratory of genetics and physiology 2) (Figure 1.5). RLRs are cytosolic pattern recognition receptors and are expressed in most of the tissues including epithelial cells and initiate innate immune responses (Loo & Gale, 2012). A varieties of viruses and the particles similar to viral molecules are detected by RIG-I and MDA5 and initiate the production of IFN and MDA5 and RIG-I signaling (Jiang et al., 2012). Studies in mammals have differentiated the roles of RIG-I and MDA5 in response to RNA viruses where RIG-I preferentially binds to short (<300 bp) or up to 1 kb dsRNAs that have blunt ends and a 5' triphosphate (5'ppp) moiety, facilitating discrimination between host and viral dsRNA or 5′-triphosphate end of single-stranded (ss) RNA. MDA5 does not have end specificity, however, it binds specially to long dsRNA usually >1,000 bp (Kato et al., 2006; Pichlmair et al., 2006).

Interaction of RIG-I and MDA5 with IPS1 (interferon-b promoter stimulator 1) helps to relocate the RLRs to IPS1-associated membranes where they along with downstream signaling molecules accumulate to form an IPS1 signalosome that drives IFN production (Hiscott et al., 2006). Upon recognition of RNA by RIG-I or MDA5, a complex signaling downstream pathway is activated where IPS1 Kawai et al., 2005), also called MAVS (mitochondrial antiviral signaling; Seth et al., 2005), VISA (virus-induced signaling adaptor; Xu et al., 2005), or CARDIF (CARD Adaptor Inducing Interferon-β; Meylan et al., 2005), serves as a critical signaling adaptor for RIG-I/MDA5. Upon activation by viral RNA, RIG-I and MDA5 act on the mitochondria via interaction of CARDs between RIG-I/MDA5 and IPS1, facilitating phosphorylation of interferon regulatory factors IRF3 and 7 which are key transcription factors involved in triggering the production of interferon (Kawai et al., 2005; Satoh et al., 2010; Xu et al., 2005). IRF3, a transcription factor, is ubiquitously expressed in eukaryotic cells while IRF7 expression is induced by IFN treatment (Yoneyama et al., 2002). Transcription factors IRF3 and IRF7 play crucial role in antiviral responses and their transcriptional activity is regulated by phosphorylation (Yoneyama et al., 2002). IRF3 has

been shown to be involved at immediate early phase of gene activation while IRF7 at late phase (Au et al., 1998; Weaver et al., 1998).

Tank-binding kinase protein 1, TBK1 has serine-threonine protein kinase activity and has been identified as one of the kinases that phosphorylate IRF3 and 7 (Hiscott et al., 2003; Yoneyama et al., 2002). TBK1 integrates multiple signals induced by receptor- mediated pathogen detection and thus modulating interferon levels (Ma et al., 2012).

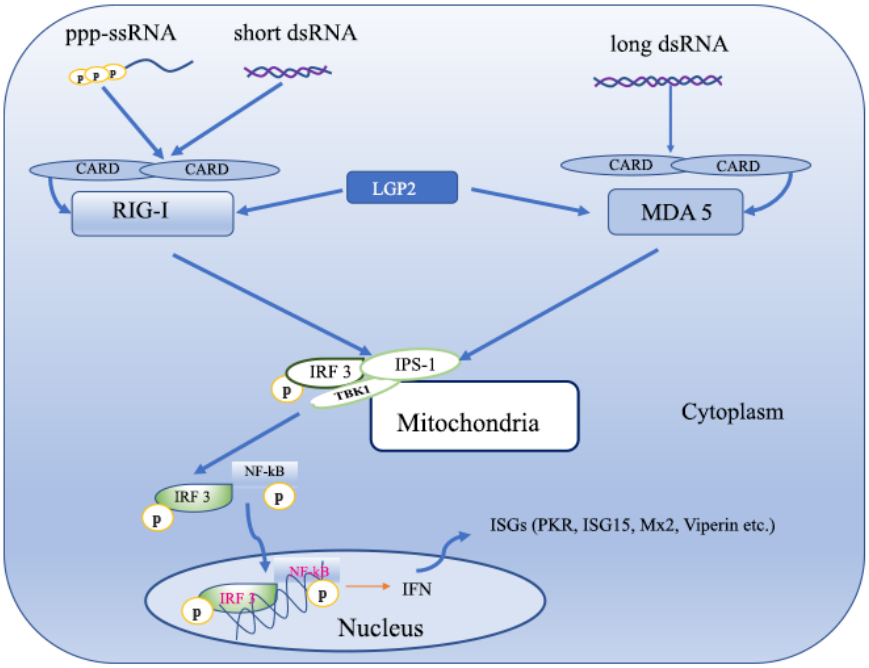

Figure 1.5: RLR signalling pathway. Viral dsRNA are sensed by RIG-I and MDA5 and their activation is strongly regulated by the phosphorylation of LGP2. RIG-I and MDA5 signal to IPS1, which consequently initiates interferon signalling by interacting with TBK1 and IRF 3. IRF 3 is phosphorylated (shown by **P** in the cytoplasm and moves to the nucleus where it initiates the production of interferon and interferon stimulated genes (ISGs). ISGs are then translated in the cytoplasm and interfere with viral replication. The figure contains the elements detected in this study and adapted from Reikine et al. (2014), Shrivastav & Niewold (2013).

1.7.2.1 RIG-Like Receptors (RLRs) and associated molecules in fish

In the last decade, studies identifying and characterizing fish RLRs and RLR signaling molecules has increased. However, the studies on the RLR identification and antiviral characterization is bottleneck. The list of RLRs and related signaling molecules identified in fish until 2018, is presented in Table 1.4. Main findings of the works cited in Table 1.4, has been demonstrated in Chapter 5, general discussion, Table 5.1.

Table 1.4: List of RLRs and other signaling molecules identified in fish until 2018

RLR Molecules	Fish species	Reference
RIG-I	Crucian carp (*Carassius auratus*)	(Sun et al., 2011)
	Grass carp (*Ctenopharyngodon idella*	(Yang et al., 2011)
	Common carp (*Cyorinus carpio*)	(Feng et al., 2011; Kitao et al., 2009)
	Zebra fish (*Danio rerio*)	(Nie et al., 2015)
	Channel catfish (*Ichtalurus punctatus*)	(Rajendran et al., 2012)
	Atlantic salmon (*Salmo salar*)	(Biacchesi et al., 2009)
	Rainbow trout (*Onchorhynchus mykiss*)	Gene Bank Acc. XM_021593781
MDA5	Zebra fish (*Danio rerio*)	(Zou et al., 2014, 2015)
	Rainbow trout (*Onchorhynchus mykiss*)	(Chang et al., 2011)
	Crucian carp (*Carassius auratus*)	(Sun et al., 2011)
	Grass carp (*Ctenopharyngodon idella*	(Su et al., 2010)
	Channel catfish (*Ichtalurus punctatus*)	(Rajendran et al., 2012)
	Japanese flounder (*Paralichthys olivaceus*)	(Ohtani et al., 2011)
	Sea perch (*Lateolabrax japonicsu*)	(Jia et al., 2016)
	Sea bream (*Sparus aurata*)	(Valero et al., 2015)
LGP2	Crucian carp (*Carassius auratus*)	(Sun et al., 2011)
	Channel catfish (*Ichtalurus punctatus*)	(Rajendran et al., 2012)
	Rainbow trout (*Onchorhynchus mykiss*)	(Chang et al., 2011)
	Zebra fish (*Danio rerio*)	(Sun et al., 2011)
	Black carp (*Mylopharyngodon piceus*)	(Xiao et al., 2016)
	European sea bass (*Dicentrarchus labrax*)	(Valero et al., 2015)
IPS1	Common carp (*Cyprinus carpio*)	(Feng et al., 2011).
	Rainbow trout (*Onchorhynchus mykiss*)	Gene Bank Acc. NM_001195181
	Zebra fish (*Danio rerio*)	(Lu et al., 2015)
TBK1	Crucian carp (*Carassius auratus*)	(Sun et al., 2011)
	Black carp (*Mylopharyngodon piceus*)	(Yan et al., 2017)
	Grass carp (*Ctenopharyngodon idella*	(Feng et al., 2014)
	Zebra fish (*Danio rerio*)	(Zhang et al., 2016),
	Common carp (*Cyorinus carpio*)	(Feng et al., 2011),
	Atlantic salmon (*Salmo salar*)	Gene Bank Accession no. AEA42006
	gilt-head sea bream (*Sparus aurata*)	(Valero et al., 2015)
	Atlantic cod (*Gadus morhua*)	(Chi et al., 2011)
	Rainbow trout (Onchorhynchus mykiss)	Gene Bank Acc. XM_021592888
IRF3	Common carp (*Cyorinus carpio*)	(Feng et al., 2011).
	European seabass (*Dicentrarchus labrax*)	(Valero et al., 2015)
	Rainbow trout (Onchorhynchus mykiss)	(Holland et al., 2008)
	Zebra fish (*Danio rerio*)	(Feng et al., 2016)
PKR	European seabass (*Dicentrarchus labrax*)	(Valero et al., 2015)
	Zebra fish (*Danio rerio*)	(Rothenburg et al., 2005)
	Atlantic salmon (*Salmo salar*)	(Bergan et al., 2008)
	rare minnow (*Gobiocypris rarus*)	(Su et al., 2008)
	grass carp (*Ctenopharyngodon idella*	(Hu et al., 2013)
	Japanese flounder (*Paralichthys olivaceus*)	(Zhu et al., 2008)
	Fugu (*Xenopus tropicalis*)	(del Castillo et al., 2012)
	Rock bream (*Oplegnathus fasciatus*)	(Zenke et al., 2010)
	Rainbow trout (*Onchorhynchus mykiss*)	Gene Bank Acc. NM_001145891
ISG15	Atlantic salmon (*Salmo salar*)	(Røkenes et al., 2007)
	grass carp and crucian carp	(Zhang et al., 2007)
	Atlantic cod (*Gadus morhua*)	(Seppola et al., 2007; Furnes et al., 2009)
	Japanese flounder (*Paralichthys olivaceus*)	(Yasuike et al., 2011)
	Rainbow trout (*Onchorhynchus mykiss*)	Gene Bank Acc. NM_001124609
	Zebra fish (*Danio rerio*)	(Langevin et al., 2013)
Viperin	Rainbow trout (*Onchorhynchus mykiss*)	(Boudinot et al., 1999).
	Crucian carp (*Carassius auratus*)	(Wang et al., 2014).
	Mandarin fish (*Siniperca chuatsi*)	(Sun & Nie, 2004).

	Grass carp (*Ctenopharyngodon idella*	Wang et al., 2014)
	Tilapia (*Oreochromis niloticus*)	(Lee et al., 2013)
	Rock bream (*Oplegnathus fasciatus*)	(Zhang et al., 2014).
	Large yellow croaker (*Larimichthys crocea*)	(Zhang et al., 2018)
	TO cell line (*Atlantic salmon*)	(Sun et al., 2011).
	Fathead minnow (FHM) cell (*Pimephales promelas*	(Wang et al., 2019a)
	Zebra fish (*Danio rerio*)	(Thwaite et al., 2018)
Mx	Perch (*Perca fluviatilis*)	(Staeheli et al., 1989)
	Rainbow trout (*Onchorhynchus mykiss*)	(Trobridge et al., 1997)
	Atlantic salmon (*Salmo salar*)	(Robertsen et al., 1997)
	Atlantic halibut (*Hippoglossus hippoglossus*)	(Jensen & Robertsen, 2000)
	Japanese flounder (*Paralichthys olivaceus*)	(Lee, 2000)
	Fugu (*Xenopus tropicalis*)	(Yap et al., 2003)
	Channel catfish (*Ichtalurus punctatus*)	(Plant & Thune, 2004)
	Zebra fish (*Danio rerio*)	(Thwaite et al., 2018)

1.8 Other intracellular receptors

Among intracellular receptors, NOD-like receptor (NLR) is one of the intracellular cytosolic receptors that detects bacterial molecules including PGN and MDP (Meylan et al., 2006). NLRs involve in immune response against bacterial and viral infection, apoptosis and autoimmunity (reviewed in (Reviewed by Boltaña et al., 2011). Among intracellular receptors, NOD1 and NOD2 are the first receptors that have been identified (Reviewed by Meylan et al., 2006). Different members of NLR family have been identified in several fish species which include zebrafish, Atlantic salmon, Japanese puffer (*Takifugu rubripres*), grass carp, medaka and channel catfish (Reviewed by Boltaña et al., 2011).

In mammals PGN has been reported to be recognized by several PGN recognition molecules including CD14, TLR2, NOD1/2 and PGN-lytic enzymes (Dziarski, 2003). PGN recognition protein (PGRP) has also been identified in several fish species including grass carp (Li et al., 2013, 2014), rockfish (Kim et al., 2010), rainbow trout (Jang et al., 2013), yellow croaker (Mao et al., 2010) and zebrafish (Chang, 2007).

Apart from TLR3 and TLR22, several other TLRs have also been reported to recognize microbial nucleic acids which include TLR7, TLR8 and TLR9 which are expressed exclusively intracellularly in vesicles including the endoplasmic reticulum, endosomes, lysosomes and endolysosomes. TLR4, another intracellular receptor molecule that has been reported to recognize bacterial LPS in mammals (reviewed in Kawai & Akira, 2010) is not present in rainbow trout.

TLR7, TLR8 and TLR9 have been identified in different fish species including rainbow trout where TLR7 and TLR8 were not induced by poly(I:C) (Palti et al., 2010). However, in large yellow croacker, TLR7 and TLR8 have been shown to be induced by poly(I:C) stimulation in different organs including gill (Qian et al., 2013). TLR9 on the other hand, has been shown to be induced by the intramascular injection with G protein of VHSV at the injection site suggesting the recruitment of dendritic like cells into the muscle (Ortega-Villaizan et al., 2009).

1.9 Antiviral responses

Antiviral response is important to stop or cease viral replication. Antiviral response is mostly mediated by interferon and interferon stimulated genes.

1.9.1 Interferon responses

Interferons are a family of proteins that are released in response to entry of virus or viral particles into the host cells (Sen, 2001). Interferons are generally secreted by white blood cells, natural killer cells, fibroblast cells and epithelial cells. Type I interferons (INFs) include INF-α, β, τ and Ω because of their similar amino acid sequences. Type I interferons are primarily known to induce an anti-viral state of cells while tnterferon of type II comprises only INF-γ which has a unique amino acid sequence having the ability to regulate overall immune system functions (Robertsen, 2006)..

The first line of defence against viruses is the activation of the type I interferon system (Saint-Jean & Pérez-Prieto, 2006). Interferon, upon binding to its specific receptor on the cell surface, triggers the production of antiviral proteins which can inhibit or delay viral replication (Sen, 2001). As in mammals, IFNs are also synthesized in teleost fish and activate antiviral response (Robertsen, 2006). In salmonids, three subgroups of type one interferon, IFNα, d and e and three subgroups of type two interferon , IFNβ, c and f have been demonstrated (Zou et al., 2014). The IFN genes have been identified, sequenced and characterized in Atlantic salmon (Robertsen et al., 2003), carp (Kitao et al., 2009), catfish (Long et al., 2006), pufferfish (Lutfalla et al., 2003), goldfish (Yu et al., 2010), sea bass (Casani et al., 2009), rainbow trout (Chang et al., 2009; Chang et al., 2009) and zebrafish (Altmann et al., 2003). As in mammals, the synthetic poly(I:C) has been shown to stimulate IFN production in fish (Eaton, 1990). Poly(I:C) induced IFN expression has been shown in

several fish species including Atlantic salmon, zebrafish and channel catfish (cited in Robertsen, 2006). Failure of induction of the antiviral state by poly(I:C) in CHSE-214 cell has been reported and suggested to be due to a defective interferon system in this cell line (Saint-Jean & Pérez-Prieto, 2006). However, antiviral activity of poly(I:C) has been reported in many fish cell cultures including CHSE-214 against several fish viruses including ISAV, IHNV and IPNV (Jensen et al., 2002; Jensen & Robertsen, 2002; Nygaard et al., 2000). Unlike mammals, a limited number of functional studies have been conducted with cloned fish interferons. Antiviral active recombinant IFN has been reported in Atlantic salmon and channel catfish against infectious pancreatic necrosis virus (IPNV) and channel catfish herpesvirus (CCV), respectively by Robertsen et al. (2003) and Long et al. (2004). Robertsen et al. (2003) has also shown induction of Mx expression by IFN in Atlantic salmon. Moreover, zebrafish IFN has been shown to increase resistance against snakehead rhabdovirus infection through increased expression of Mx gene (Altmann et al., 2003). These findings clearly demonstrate the role of interferon in inducing antiviral state in fish and protecting from viral infection.

1.9.2 Interferon stimulated genes

Several interferon stimulated genes have been identified in fish in response to viral infections. Interferon signaling is initiated by IPS1 upon interacting with TBK1 and IRF 3. IRF 3 is phosphorylated in the cytoplasm and is transported to the nucleus where it initiates the production of interferon and interferon stimulated genes (ISGs). ISGs then translated in the cytoplasm and interfere viral replication. The most common interferon stimulated genes are Mx, ISGs and Viperin. Moreover, PKR also acts as an ISG and is a dsRNA-dependent serine/threonine protein kinase. PKR is regarded as one of the important players in interferon response upon stimulation or viral infection. PKR is constantly expressed but inactive in the absence of IFN. IFN induction leads to auto-phosphorylation of PKR followed by interaction with dsRNA (Sen, 2001; Balachandran et al., 2000).

One of the most well studied antiviral genes is Mx which is a widely used gene marker for IFN responses. Mx is highly conserved having GTPase activity and antiviral function (Haller and Cochs, 2002). It was originally revealed in influenza virus-resistant mice where the single dominant trait was found to be responsible for the resistance which was later termed as Mx for myxovirus resistance (Lindenmann et al., 1963). In fish, the Mx gene was first

reported in perch (*Perca fluviatilis* L.) by Staeheli et al. (1989). Afterwards, the Mx gene was cloned and characterized in several fish species (Table 1.4). Even though, over fifty years have passed after the discovery of Mx protein, and antiviral activity has been studied in wide range of animals, the mechanism of antiviral function of this protein has not been established. However only recently, Verhelst et al. (2013) described the mechanisms of antiviral functions of Mx proteins in mammals. They described the inhibition of release of viral proteins of influenza virus by porcine Mx1 in the cytoplasm, inhibition of transport of viral protein of influenza virus from cytoplasm to nucleus by human MxA, inhibition of transcription of VSV by mouse and human Mx, and inhibition of translation of influenza virus by human MxA. However, in fish the mechanisms of antiviral functions of Mx protein against aquatic viruses have not yet been discovered.

In mammals, ISG15 has been identified as one of the most abundant mRNA transcripts that is expressed upon type I interferon induction (Lenschow, 2010) which was first reported in type I interferon including IFBα and β stimulated cell lysates in 1984 (Jeon, Yoo, & Chung, 2010). Viperin which has been named after virus inhibitory protein, endoplasmic reticulum-associated, IFN-inducible, has been found to be induced by RNA virus infection by interferon dependent and independent pathway through IRF-1, and has a diverse range of antiviral actions (Helbig et al., 2013). Viperin was identified and characterized for the first time in fish as a virus induced gene (vig1) where high levels of expression were detected in rainbow trout leucocytes upon infection with viral haemorrhagic septicaemia (Boudinot et al., 1999). A human homologue of viperin, cig5 (cytomegalovirus induced gene 5) was also identified and characterized (Zhu et al., 1997).

Viral multiplication and release have been shown to be prevented by viperin thus playing a crucial role in innate immunity (Helbig & Beard, 2014). Viperin has also been found to exert antiviral effects at a late stage of viral life cycle (Chin & Cresswell, 2001). Most of the cell types express viperin at a very low level which has been shown to be upregulated by dsRNA/DNA analogues and several viruses through classical interferon pathways by binding and activating TLR3 and TLR4, RLRs and cytosolic DNA sensor (Hinson et al., 2010; Seo et al., 2011; Severa et al., 2006; Boudinot et al., 2000; Helbig & Beard, 2014).

Multiple mechanisms have been developed by viruses to contest varied artillery of the host innate immune system, one of them is the evasion of antiviral host proteins (Dauber &

Wolff, 2009; Arnaud et al., 2010). Alphavirus has the ability to shutdown host transcription and translation processes without affecting viral protein and nucleic acid synthesis, which subsequently reduces the expression of IFN-α/β in the host cell, and consequently reduces the functions of the hosts' innate immune system to attenuate the infection (Jose et al., 2009). Non-structural protein, nsP2 of Chikungunya virus (CHIKV), has been found to induce cellular shutoff and promote viral replication by interacting with several host proteins (Bourai et al., 2012). However, overexpression of viperin has been found strongly related to decreased CHIKV nsP2 expression levels (Teng et al., 2012).

Since first identification of viperin in trout leucocytes, very little works has been conducted on the identification and characterization of viperin in fish, thus little is known on the expression pattern of viperin in fish. Among fish, apart from trout, the viperin gene has been identified and characterized in crucian carp (Yibing et al., 2003), mandarin fish (Sun & Nie, 2004). Overexpression of crucian carp viperin has been found to protect culture cells against grass carp reovirus (B. Wang et al., 2014). Viperin has also been identified and characterized in tilapia and rock bream where viperin expression has been found to be upregulated upon induction with LPS and poly(I:C) (Lee et al., 2013) in tilapia and by infection with megalocytivirus in rock bream (Zhang et al., 2014). Recently, Zhang et al. (2018) identified and characterized viperin in large yellow croaker where they detected ubiquitous expression in different tissues and significant upregulation with *in vivo* poly(I:C) stimulation. In TO cell line (an Atlantic salmon cell line developed from head kidney leukocytes), viperin has been found to be overexpressed upon interferon alpha stimulation (Sun et al., 2011).

The complete RLR signaling pathway and the expression pattern of relevant genes in fish gill epithelia in response to alphavirus is still unknown. On the basis of the previous studies on fish RLRs that have been conducted up to date, the fish RLR signaling pathway can be deduced from mammalian RLR signaling pathway as shown in figure 1.5.

1.10 Cytokines and chemokines in innate immunity in fish

Cytokines are the proteins that are secreted from immune and nonimmune cells through different secretory pathways (Stanley & Lacy, 2010). Cytokines regulate the immune responses including innate immunity and cytotoxic T cell development and antibody production. Cytokine directed expression of immune related genes through different

signaling pathways can be induced by different immune-stimulants (Reyes-Cerpa et al., 2012). Cytokines are grouped as pro-inflammatory, anti-inflammatory, interferon, chemokine etc. Pro-inflammatory cytokines enable the cells to respond to non-self infectious agents and induce a cascade of events leading to the infection modulating the expression of other cytokines (Huising et al, 2004). In mammals TGF-β has been shown to act as a multifunctional cytokine playing diverse roles in the proliferation, differentiation and survival of different cell types including T cells, B cells, NK and dendritic cells, and macrophages, thus regulating the inflammatory responses (reviewed in Li et al., 2006). The function of TGF-β in fish is not well studied. However, Kohli et al. (2003) has reported the role TGF-β in reproduction in zebrafish. IL-17 on the other hand, has pro-inflammatory actions. The pro-inflammatory activity of trout IL-17 has been shown by Monte et al. (2013). Chemokines, an important group of cytokines, direct immune cells to migrate to infection sites (Reyes-Cerpa et al., 2012).

In mammals, intestinal epithelial cells have been reported to express almost every type of cytokine which include IFNγ, a wide range of interleukins, anti-inflammatory cytokines protecting intestinal barrier function, and chemokines such as IL-8. Thus, epithelial cells have an importsnt role in the orchestration of inflammation (Onyiah & Colgan, 2016). An osmoregulatory function of TNFα and IL-8 has been reported in gill epithelia of Japanase ell (*Anguila anguila*), as well as the involvement of IL-6, IL-8 and IL-9 signaling pathways in the osmotic stress response in gill epithelia (Gu et al., 2018).

1.11 Antimicrobial peptides in fish

Antimicrobial peptides (AMPs) are small antibacterial molecules comprising of 100 or less than 100 amino acid residues which are generally positively charged and evolutionary conserved playing an important role in innate immune response (Giuliani et al., 2007). AMPs were first discovered about 35 years ago by Boman's group in the Cecropia moth (Hultmark et al., 1982). AMP in teleost was reported for the first time in 1986 in Red Sea Moses sole by Lazarovici et. al. (1986). From prokaryotes to vertebrates, all life forms produce AMPs and AMPs are conserved in the genome (Hancock, 2000).

AMPs have been identified and characterized from a wide range of fish species. The most common AMPs that have been identified and characterized in fish are piscidins

(characterized in American plaice, Atlantic salmon, Atlantic cod, red seabream etc.) defensins (in Atlantic cod, common carp, gilthead seabream, Japanese pufferfish, Mandarin fish, zebra fish, rainbow trout etc.), hepcidins (in Atlantic cod, Atlantic salmon, Ayu, Barramundi, channel catfish, common carp and many other), cathilicidins (in Atlantic cod, Atlantic salmon, Ayu, brown trout, rainbow trout etc.) and histone-derived (in Channel catfish, Atlantic halibut and rainbow trout) (reviewed by Masso-Silva & Diamond, 2014).

1.11.1 Mechanism of action of AMPs

AMPs work on the pathogens in two different ways, by direct killing or by inactivating or damaging the DNA, RNA or inhibiting their protein synthesis. AMPs are cationic peptides which can directly interact with the negatively charged peptidoglycan in the cell wall of gram-positive and negative bacteria (see chapter 1.5.3). Moreover, the cell wall of gram-positive bacteria contains teichoic acids and the outer membrane of gram-negative bacteria contains lipopolysaccharides (LPS) which provide further electronegative charge to the bacterial surface (Figure 1.6). AMPs can also interact with the bacterial cell wall by trans-locating through the outer membrane via so called self-promoted uptake (Mahlapuu et al., 2016).

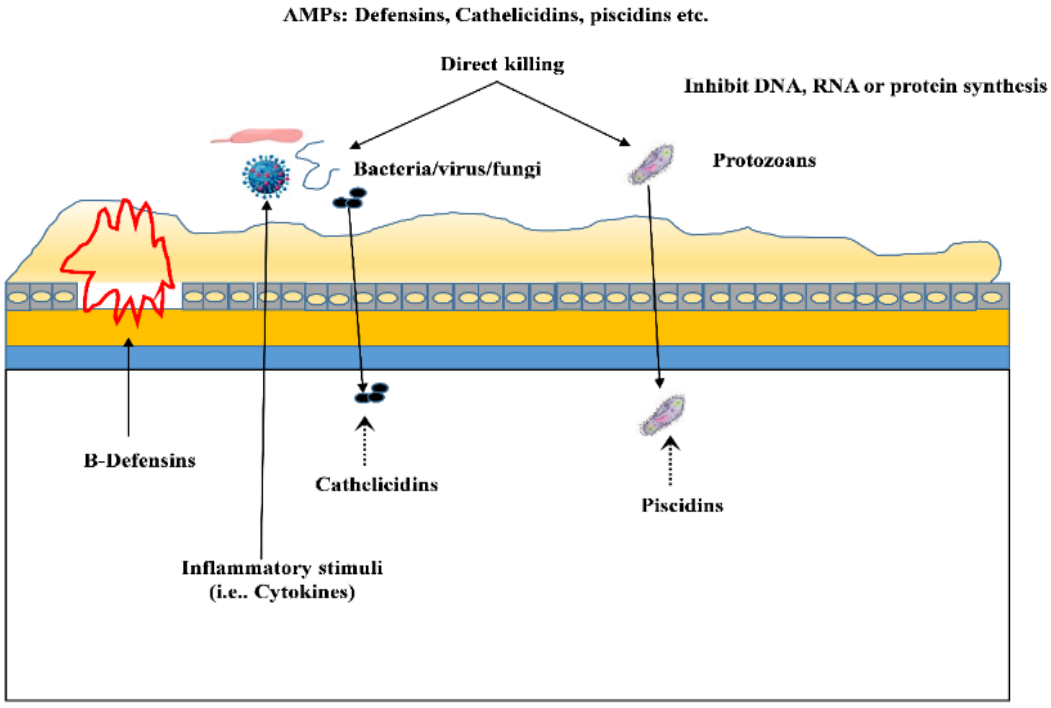

Figure 1.6: The mechanisms of antimicrobial peptides. Upon infection, cytokines or different AMPs are released from the epithelial cells. AMPs can directly kill the pathogens or can inactivate their pathogenesis. Modified from Rakers et al. (2013).

1.11.2 Immunomodulatory activities of AMPs

Cationic antimicrobial peptides play an important and significant role in modulation of host defences against microbial infection having antibacterial, antifungal, antiparasitic, antitumoural, and antiviral activities (Hancock & Diamond, 2000). Among the immunomodulatory activities employed by AMPs, immune cell differentiation modulation and induction of adaptive immunity contributes to clearance of bacteria (Figure 1.7). Moreover, suppression of certain TLR expression, and/or cytokine-mediated production of pro-inflammatory cytokines, prevents excessive and harmful pro- inflammatory cytokine responses (Mookherjee et al., 2006; Van Der Does et al., 2010; Yeung et al., 2011). LPS induced expression of TNF-α in THP-1 cells and TNF-α, IL- 1β, IL-6, and IL-8 in human primary monocytes has been found to be inhibited by LL- 37 (Mookherjee et al., 2006).

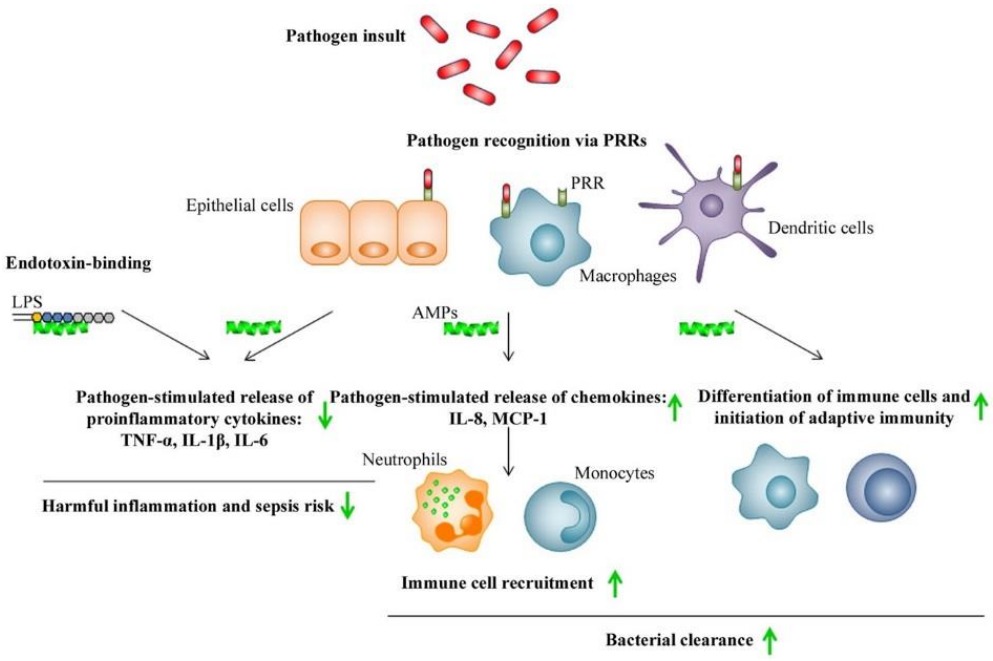

Figure 1.7: Immunomodulatory activities of AMPs. Figure has been taken from Mahlapuu et al. (2016).

1.12 Protein phosphorylation

Protein phosphorylation is a key regulatory mechanism of cell life and the most studied post-translational modification (PTMs) of proteins playing a crucial role in the regulation of signaling pathways and other cellular processes in eukaryotes, in particular, protein phosphorylation is a major coinage of signal transduction pathways (Hunter, 1995). In fact,

phosphorylation has functions in metabolism, cell cycle, and immunology etc. (Figure 1.8). It is projected that one third of proteins are phosphorylated at some points of their life cycle (Zolnierowicz & Bollen, 2000). Protein phosphorylation regulating most of the processes is a reversible mechanism controlled by protein kinases and phosphatases (Figure 1.9B) constituting about 2% of the human genome (Alonso et al., 2004; Manning et al., 2002). The most commonly phosphorylated amino acid residues are serine, threonine and tyrosine (Figure 1.9A).

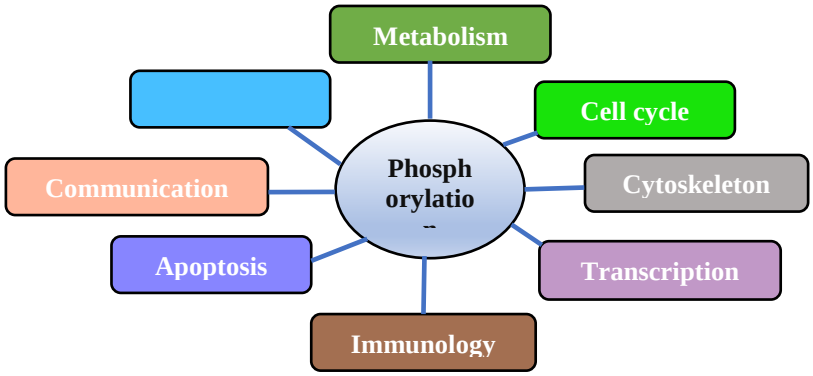

Figure 1.8: Most common functions of phosphorylation in eukaryotes.

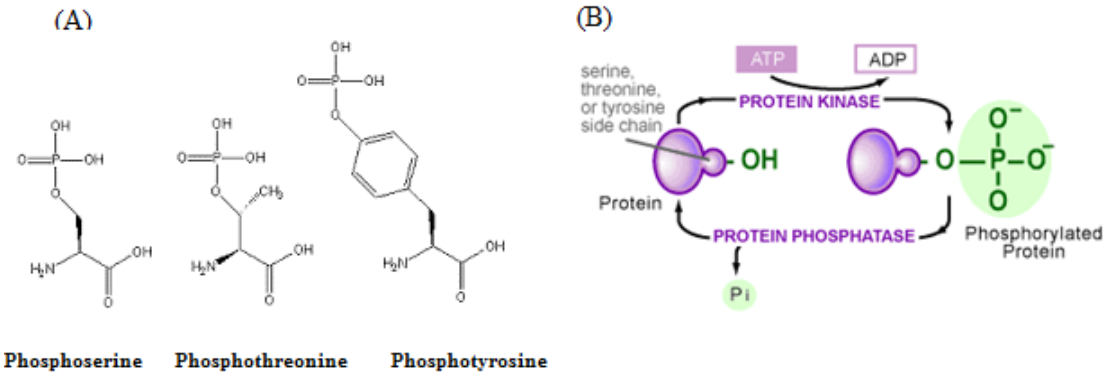

Figure 1.9: A) Main phosphorylated amino acids, B) Protein phosphorylation and dephosphorylation reaction. Protein kinases are responsible for phosphorylation where a phosphate group is added to the specific amino acid residue from ATP and protein phosphatases are responsible for dephosphorylation where a phosphate group is removed from phosphoprotein.

1.12.1 Challenges in phosphorylation studies

Studying phosphorylation events is not a straight- forward approach, facing several challenges, which should be taken into consideration before starting phosphorylation experiments. The first one is the sub stoichiometry nature of phosphorylation allowing a

fraction of the accessible protein to be analysed at a certain time upon stimulation. The Second is the variability in the phosphorylation sites on proteins which means the heterogenicity in any given phosphoprotein (Delom & Chevet, 2006). Third, low abundance of many of the signaling molecules within the cells (Yoon & Seger, 2006). Fourth, difficulty in the identification of minor Phosphosites by most used analytical techniques, which have a limited dynamic range in identification of Phosphosites. Finally, the reverse reaction dephosphorylation, which might reduce the recovery of phosphoproteins (Delom & Chevet, 2006).

The first and the third challenges can be overcome by enrichment of phosphopeptides. For example, TiO_2 based enrichment. The second challenge might be compensated by appropriate replication and verification of the results. The fourth challenge is currently being addressed by many researchers by using high throughput LC-MS/MS technique which allows the identification of all possible Phosphosites. Finally, the final challenge can be dealt with by using different phosphatase inhibitors during sample preparation.

1.12.2 Phosphoproteome separation and detection

Several techniques are employed for the identification of phosphoproteins. One of the most used techniques for phosphoprotein separation and identification is two-dimensional gel electrophoresis (2-DGE) where cell extracts are loaded onto the 2-D gels and run for a specific time at specific voltage followed by in-gel digestion and analysis by LC-MS/MS or by MALDI-TOF-MS. Another method is immunoblotting or Western blotting using specific antibodies for the detection of proteins (Magi et al., 1999). Direct staining is another way of analysing phosphoproteome of cells, tissues or organs using specific reagents in 1 or 2-DGE for the detection of selective phosphoproteins. Isotope staining with inorganic phosphate isotope (^{32}Pi) or γ-(^{32}P)-ATP is also used in *in vivo* and *in vitro* protein phosphorylation studies (Wettenhall et al., 1991).

Phosphoproteome analyses based on 2-DGE have significant limitations which include the lower loading capacity and the lower separation of certain types of proteins like acidic, alkaline and hydrophobic (Bunai & Yamane, 2005).

1.12.3 Phosphoproteome enrichment

Researchers working on phosphoproteomics have been encouraged by the limitations of in gel phosphoproteome analysis to develop the alternative techniques to identify phosphoproteins. In one of the commonly used methods, the entire cell lysates are fractionated into peptides and are identified by liquid chromatography (LC) followed by analysis on mass spectrometry (MS/MS). Phosphoprotein abundance is only a small fraction of total protein in given cell lysate which is one of the down sides of phosphoproteomics. This leads to the limited number of phosphoprotein identification in a given cell extract which directed the development of techniques to purify or enrich phosphopeptides from a complex cell extract. Several techniques like immobilized metal affinity chromatography, immunoprecipitation, a specific chemical derivation etc. are available to enrich phosphoproteins present in complex samples (Delom & Chevet, 2006).

1.12.4 Phosphoproteome identification

In the past decade, the use of mass spectrometry (MS) has become popular for phosphorylation analysis. It has become a dominant technology for phosphorylation site detection as well as phosphoprotein identification. For MS analysis, generally 2 steps are followed; the first step is the digestion of proteins into peptides and the second step is adding phosphorylation as a variable modification when analysing the MS-data. Phosphorylation at a single amino acid residue in a specific peptide adds a mass of 80 Da. Thus, by looking at the increase of masses of 80 Da of the observed peptide and comparing with expected peptide mass, phosphopeptide can be identified (Delom & Chevet, 2006). Then the MS data are used to identify proteins by searching the available database.

1.12.5 Potentials and challenges in fish phosphoproteome study

While, several proteomic analyses have been conducted in a number of fish species including zebra fish (Lucitt et al., 2008) and *Arapaima gigas* (Torati et al., 2017) the analysis of the phosphoproteome and other PTMs in fish species has rarely been addressed. Currently, only one report has analysed phosphoproteins in zebra fish (Lemeer, Jopling, et al., 2008). Currently, besides zebrafish most of the bioinformatics tools have been developed for human, rat or other mammalian species. Thus, the bioinformatics analysis for other fish species is based mainly on zebrafish if available or using underlying mammalian databases which in some cases might provide inaccurate functional information. To this end, it is

required to convert any identified fish proteins into human or zebra fish proteins or genes homologs to do some analyses missing those that do not have any human homolog. However, the advancement of different techniques and growing interest in fish proteomics will encourage to include fish proteomics data (e.g. zebra fish) which will enable researchers to get more accurate and relevant predictions on the functions, localization and properties of phosphoproteins in fish.

1.13 Hypothesis and objectives

Viral and bacterial pathogens cause huge losses to aquaculture production. However, knowledge on how aquatic viruses and in particular SAV manipulate the host machinery and in particular the innate immune response during their replication cycle is extremely limited. Moreover, bacterial disease pathogenesis in fish is also not well understood. Improving knowledge in this area could help in the development of new therapeutic approaches to prevent or treat viral and bacterial diseases in fish.

An intact gill epithelium is necessary to protect the fish from external insults but also a target organ for viral and bacterial infection. The cellular integrity of fish gill epithelial cells can be modulated by external stimuli, but this process is poorly understood. Viral and bacterial PAMP induced innate immunity in fish gill epithelia is also unclear. The mechanism by which the bacterial and viral cell components are recognized by the fish gill epithelia have not been studied before. The molecular mechanisms that are involved in innate immune response including signal transduction pathways and cellular integrity in fish gill epithelia can broadly be studied by protein phosphorylation. However, the fish phosphoproteome is not well studied.

Thus, the general hypothesis of this research thesis is that viral and bacterial pathogens and pathogen associated molecular patterns (PAMPs) interact with the fish gill epithelium resulting in a modulation of epithelial integrity in relation to barrier function and associated cell signalling.

The overall objective was to determine the effects of viral PAMP poly(I:C) and bacterial PAMPs LPS and PGN, salmonid alpha virus subtype 2 (SAV-2) and one of the fish pathogenic bacteria, *Aeromonas salmonicida* on the barrier functions and molecular response of rainbow trout gill epithelial cell RTgill-W1.

My PhD thesis addressed three specific hypotheses to meet the objectives:

(1) Viral and bacterial PAMPs can modulate the cellular integrity of RTgill-W1 through inducing the expression of tight junction genes. PAMPs can also induce the antiviral response through internalization into the gill epithelial cells (Chapter 2).

(2) Viral and bacterial PAMP stimulation can trigger the dynamics of protein phosphorylation including antiviral signaling pathways in gill epithelial cells (Chapter 3).

(3) Salmonid alphavirus subtype 2 (SAV-2), an infectious pathogen of salmonids can replicate in fish gill epithelia and induce an antiviral response which subsequently limits viral replication. Moreover, viral and bacterial PAMPs can induce the barrier function against *A. salmonicida*, a bacterial pathogen of salmonids through inducing the expression of cytokines and antimicrobial peptides (Chapter 4).

Chapter 2

Cellular response and signalling in RTgill-W1 cell upon stimulation with viral and bacterial PAMPs

2.1 Introduction

The gill is one of the most important organs in teleost fishes playing a central role in respiration and osmoregulation. As gills are continuously exposed to the surrounding environment, contact with different pathogens is very likely. An intact gill barrier is essential for normal physiological function and to combat pathogens. This barrier is not static, can be modulated by external insults like environmental stress, pathogens and toxins (Benson et al., 2013) and is regulated by the tight junctions between the cells. Tight junction proteins claudin and occludin are regulated by tight junction regulatory protein ZO-1 and other proteins (Whitehead et al., 2011). The tight junction protein barrier connects epithelial cells, thus preventing the passage of substances through the intercellular space and allowing passage only through the cell from apical to the basolateral side (Benson et al., 2013). Thus, tight junction proteins maintain the cell polarity and cellular integrity. By forming a barrier tight junction contribute to creating transepithelial electrical resistance (TER) between the apical and basolateral side. Bacteria and bacterial toxin, and viral pathogens can disrupt the epithelial integrity interacting with tight junction and render cells susceptible for infection by the pathogens (Torres-Flores & Arias, 2015; Bonazzi & Cossart, 2011). Viral and bacterial Pathogen associated molecular patterns (PAMPs) can play important role in modulating cellular integrity thus impacts on TER of epithelial cells.

Moreover, PAMPs activate the immune system through pattern recognition proteins/receptors and TLRs and enhance overall resistance to various diseases (Magnadottir, 2010). PAMPs may be viral or bacterial derivatives or chemically synthetic. Most commonly used PAMPs in fish immunology studies are poly(I:C), lipopolysaccharides and peptidoglycan. Poly(I:C), a structural analogue of dsRNA acting as a ligand of toll-like receptor 3 (TLR3), has been widely used as an immuno-stimulant in humans and mice against viral diseases based on its ability to enhance innate and adaptive immunity (Zhou et al., 2014). Both natural and synthetic dsRNAs are known to induce type I interferons (IFN) and the production of other cytokines. Lipopolysaccharide (LPS) is also used widely as a potent PAMP which can be released from gram-negative bacteria that can associate with LPS binding protein (LBP), an acute-phase protein present in the bloodstream of vertebrates

including fish (Solstad et al., 2007) and then binds to CD14, a glycosylphosphatidylinositol (GPI) linked protein expressed on the cell surface of phagocytes (Poltorak A et al. 1998; Shimazu et al. 1999). *In vitro*, LPS stimulates phagocytosis and the production of superoxide anions in Atlantic salmon macrophages (Solem et al., 1995). Similarly, LPS stimulates the production of macrophage activating factor in goldfish lymphocytes (Neumann et al., 1995) and the production of interleukin 1 like molecules in catfish monocytes (Clem et al., 1985). Peptidoglycan, on the other hand, an important component of bacterial cell walls, has been shown to be a powerful biological effector with different immuno-stimulatory activities such as activation of macrophages, cytokine production, induced autoimmunity, induction of antimicrobial peptide production (Boneca, 2005).

In humans and other mammals, TLR3 signalling pathway is well studied. Upon recognition of poly(I:C), TLR3 activates interferon regulatory factor 3 (IRF 3), through the adapter protein Toll-IL-1 receptor (TIR) domain-containing adapter inducing IFN-β (Yamamoto et al., 2003). Activation of IRF3 leads to the production of type I IFNs, especially IFN-β. In teleost, orthologs of mammalian TLR3 have been identified in a number of species, however, the working mechanism of poly(I:C) in teleost is unclear, and very little is known about the relationship between poly(I:C) -induced antiviral effects and TLR3 signalling in fish.

The type I interferon system is the first line of defence against viruses, upon binding to its receptor on the surface of other cells, it triggers the production of antiviral proteins which can inhibit or delay viral replication. As in mammals, IFNs are also synthesized in teleost fish and activate antiviral response (Børre Robertsen, 2006). Synthetic poly(I:C) stimulates IFN production in mammals and also in fish (Eaton, 1990) and fish cell cultures where antiviral activity of poly(I:C) against several fish viruses has been evaluated (Nygaard et al. 2000; Jensen et al., 2002; Jensen & Robertsen, 2002). Mx is one of the most well studied IFN-induced antiviral proteins which has been used as an indicator of IFN responses. The Mx gene in fish was first reported in the perch (*Perca fluviatilis* L.) by Staeheli et al. (1989), but has been characterised and cloned from several fish species.

Bacterial and viral PAMPs play significant roles in immunomodulation of host cells by activating different antibacterial or antiviral genes. Different PAMPs bind to different receptors of host cells where some are intracellular, and some are extracellular. Extracellular

receptors are present on the cell surface and upon binding to the PAMPs, send signal to the downstream pathways. On the other hand, to bind to the intracellular receptors, PAMPs must be internalized to the host cells. Different molecules use different mechanisms to enter the cells. Most common mechanism is the endocytosis. Endocytosis is a process by which extracellular material and plasma membrane are internalized into the cell interior. This plays an important role in proper signaling and regulation of cell surface receptors, for the delivery of nutrients into the cell, establishment and maintenance of cell polarity, and the turnover of plasma membrane proteins and lipids (Dutta & Donaldson, 2012). Moreover, endocytosis is also used by bacterial toxins and pathogens as a mode of entry to the cell interior.

Several substances have been tested to block the endocytosis pathway. Cytochalasin D (CyD) is one of the chemical components that has the property to inhibit endocytosis. It is a cell-permeable and potent inhibitor of actin polymerization which disrupts actin microfilaments (May et al., 1998). By inducing depolymerization of the actin cytoskeleton it selectively blocks endocytosis of membrane bound and fluid phase markers from the apical surface of polarized cells without affecting the uptake from the basolateral surface (Gottlieb et al., 1993). CyD has been reported to the inhibition of cell ruffling and motility, cell retraction and arborization, zeiosis, blebbing, and enucleation (Schliwa, 1982).

Several other chemical components have been tested to block or inhibit or reduce the uptake of certain viral or bacterial molecules by the host cells. Cefradin, a semi-synthetic cephalosporin, inhibits the last stage of bacterial cell wall synthesis by binding to certain penicillin-binding proteins (PBPs), such as PBP3, which results in cell lysis. Cell lysis is mediated by bacterial cell wall autolytic enzymes. It is effective against gram-positive and gram-negative bacteria. Cefradin may also interfere with the autolysin inhibitor. Lisinopril, an angiotensin converting enzyme, used to treat high blood pressure in adults and children, was also used in the study as an inhibitor of ligand internalization.

The mechanism by which the bacterial and viral cell components are recognized by the fish gill epithelia is unclear. These can be internalized by endocytosis which can be Clathrin-mediated or Clathrin-independent endocytosis. In this study, the rainbow trout gill epithelial cell line RTgill-W1 was used to investigate the effects of PAMPs on the epithelial integrity and on the expression of the tight junction and antiviral response genes as well as the mechanisms of internalization of PAMPs by trout epithelial cells.

2.2 Materials and Methods

2.2.1 Cell culture

The rainbow trout gill epithelial cell line RTgill-W1 was used as a model of fish gill epithelia. The cell line was available at the Institute of Aquaculture, University of Stirling, UK and obtained from American Type Culture Collection (ATCC, Manassas, VA, USA). The cells were maintained using protocols developed in the Virology laboratory of the Institute of Aquaculture, University of Stirling, Scotland, UK, following Bols *et al.* (1994). Briefly, cells were maintained in Leibowitz L-15 media supplemented with L-glutamax (GIBCO Life Technologies) and 10% of fetal bovine serum (FBS) (Life Technology) at 22 °C in 75 cm^2 plastic flasks (SARSTEDT, Germany). The cells were sub-cultured once a week by trypsinysing with 0.05% trypsin –EDTA (GIBCO Life Technologies).

For transepithelial electrical resistance experiment, the Madin-Derby Canine Kidney cell line MDCKII was used as a control. The cells were maintained at 37 °C with 5% CO_2 in 75 cm^2 plastic in Eagle's Minimum Essential Medium (MEM) (GIBCO Life Technologies) supplemented with 10% FBS, 2mM L-glutamine (GIBCO Life Technologies) and 2mM nonessential amino acid (GIBCO Life Technologies).

2.2.2 Pathogen associated molecular patterns (PAMPs)

Viral and bacterial PAMPs were used as immune-modulators. Poly(I:C), a structural analogue of dsRNA acting as a ligand of TLR3 and RLRs was used as viral PAMP while bacterial lipopolysaccharide (LPS) and peptidoglycan (PGN) were used as bacterial PAMPs. For internalization study fluorescein labelled poly(I:C), Alexa Fluor 488 labelled LPS and rhodamine labelled MDP were used. Poly(I:C), LPS, PGN, fluorescein labelled poly(I:C) (HMW) and Rhodamine labelled MDP were purchased from InvivoGen while Alexa Fluor 488 labelled LPS was purchased from Thermo Fisher.

2.2.3 Effects of PAMPs on the trans-epithelial electrical resistance (TER)

RTgill-W1 cells were seeded onto 12 well transwells (BD Falcon) with 0.9 cm^2 growth area, 0.4 μm pore size and a pore density of 1.6×10^6 pores per cm^2. The apical compartment contained RTgill-W1 cells in complete growth medium (L-15 medium supplemented with 10% FBS and L-Glutamax) and the basolateral compartment contained only complete growth medium. Transwells with medium only in both apical and basolateral sides were

used as background control. Before starting the final experiments, some trial experiments were conducted to optimize the seeding density onto the transwell system. MDCKII cells were used as the positive control for the transwell system. TER measurements were performed with a chopstick-type probe (STX-2) connected to a Millicell ERS-2 voltmeter (EMD Millipore Corporation, Billerica, USA), according to manufacturer instructions. The resistance measured across a culture insert with no seeded cells was used for background correction of all TER measurements. Post seeding TER was measured at different time points until TER values reached stability. When TER values stabilized, cells were stimulated with poly(I:C) and LPS at a concentration of 10 µg/mL in the first experiment. In the second experiment cells were activated with LPS and PGN at 10 µg/mL. During stimulation, medium from the apical compartments of control and blank groups were replaced with fresh medium as was done for the treatment groups. Each treatment in each experiment was run in triplicate and each experiment was performed three times.

TER was calculated according to the manufacturer`s guideline. To get the true cell resistance, resistance of the blank insert having only medium is subtracted from the reading of the cell culture insert with cells. The unit of TER measure is Ωcm^2. The unit area resistance is obtained by multiplying the meter reading by effective membrane area of the insert.

TER is calculated as**;**

$$Unit\ Area\ Resistance\ (\Omega - cm^2) = Resistance\ (\Omega) \times Effective\ membrane\ Area\ (cm^2)$$

2.2.4 Effects of PAMPs on the expression of innate immune gene markers

To evaluate the effects of PAMPS on tight junction protein expression in RTgill-W1 cells, cells were grown to around 95% confluence in triplicate onto 12-well plates and in transwells. To equilibrate inserts to the medium, insert and wells were preloaded for 2 h with 1 mL and 2 mL of cell culture medium (Section 2.2.1) respectively. Each insert and well was seeded with 1.0×10^5 and 4.0×10^5 RTgill-W1 cells respectively. Cells were treated with or without poly(I:C) (10µg/mL) LPS (10µg/mL) and PGN (10µg/mL) for 6 and 24h and then harvested for further processing.

For the short window time course response experiment, cells were stimulated with poly(I:C) at a concentration of 1µg/mL for 30 min, 1, 3, 6 and 24 h. Afterwards, cells were harvested with TRI-reagent (Sigma) for total RNA extraction.

2.2.4.1 Total RNA extraction and cDNA synthesis

2.2.4.1.1 RNA extraction

Total RNA was extracted from 12 well culture inserts and wells using TRI reagent (Sigma-Aldrich, St. Louis, MO, USA) according to the manufacturer's directions with some modifications (detailed protocol in appendix 1.1). Briefly, cells were washed twice with 1ml of PBS and cell lysate was collected in 500 µL of TRI-reagent and incubated at room temperature (RT) for 5 min, then 50 µL of 1-bromo-3-chloropropane (BCP) was added and the tube was shaken vigorously by hand for 15 seconds followed by incubation at room temperature for 15 min. Samples were then centrifuged at 16900 × g for 15 min at 4 ºC. After centrifugation, the upper aqueous phase was transferred to a new tube without disturbing the interface. Then ½ volume (half of total volume of upper phase) of RNA precipitation solution (prepared in house with 1.2 M NaCl and 0.8 M Sodium citrate sesquihydrate in nuclease free water (Ambion), 0.22 µm filter sterilized) and another ½ volume of isopropanol were added and mixed properly by inverting gently for 4-6 times followed by incubation for 10 min at room temperature. The sample was then centrifuged at 16900 × g for 15 min, at 4ºC. The RNA precipitate forms a gel like pellet on the side/bottom of the tube. The supernatant was removed carefully without disturbing the pellet by pipetting and the pellet was washed with 500 µl of 75% and then centrifuged at 16900 × g for 15 min, at room temperature. The supernatant was removed carefully by pipetting and the RNA was air dried at room temperature for 5 min and eluted in RNase free water.

Quantity and purity of RNA were assessed using Nanodrop Spectrophotometer (ND-1000, Labtech International, Uckfield, UK) through UV-light absorbance at 260 and 280 nm, where a 260/280 nm absorbance ratio of 1.8–2.0 was considered as a pure RNA sample. Low quality RNA was discarded. The quality of RNA was also checked by gel electrophoresis using 1.5% agarose gel (pure and intact RNA gives two bands 28S and 18S).

2.2.4.1.2. cDNA synthesis

The cDNA was obtained from 1µg of total RNA from each sample and cDNA was synthesised using the protocol of Superscript III First-Stand Synthesis System (Invitrogen) (detail protocol in appendix 1.2). Briefly, 1 µL of 50 µM oligo(dT) and 1 µL of 10 mM dNTP mix were added in required volume of nuclease free water (Ambion) and RNA to a final volume of 10 µL. Then the reaction mix was incubated at 65 °C for 5 min in Thermal

Cycler (Biometra) and placed on ice for at least 1 min. Then 10 µL of cDNA synthesis mix containing 2 µL of 10X RT buffer, 4 µL of 25 mM $MgCl_2$, 2 µL of 0.1 M DTT, 1 µL of RNaseOUT™ (40 U/µL) and 1 µL of SuperScript III RT enzyme (200 U/µL) was added into each RNA/primer mixture. The reaction was mixed gently and collected by brief centrifugation and then incubated for 50 min at 50 °C in Thermal Cycler (Biometra). The reaction was terminated by incubating at 85 °C for 5 min. Then the tube was chilled on ice and collected by brief centrifugation. Finally, 1 µL of RNase H was added and incubated for 20 min at 37 °C. The cDNA synthesis reaction was stored at −20 °C or used for PCR immediately.

2.2.4.1.3 PCR and PCR product purification

Primers for PCR and qPCR used in the study were for tight junction genes claudin 3a and 8d, tight junction regulatory gene ZO-1, innate immune response genes TLR 3, IFNβ and interferon induced Mx2 (Table 2.1). All the lyophilized primers were eluted in nuclease free water (Ambion) and diluted to 10 µM. RT-PCR was conducted using MyTaq HS DNA polymerase (BIOLINE) according to the manufacturer's instruction. Each PCR reaction mixture contained 12.5 µL of 2X MyTaq mastermix (1X), 1 µL of each 10 µM primer (final primer concentration 400 nM), 1 µL of template cDNA and the rest was nuclease free water (Ambion) to a final volume of 25 µL. PCR was performed in a thermal gradient thermocycler (Biometra). PCR reaction condition was: initial denaturation for 1 min at 95 °C for 1 cycle followed by 35 cycles of denaturation for 15s at 95 °C, annealing for 15s at 55-62 °C (optimum annealing temperature for each primer set), and extension for 15s at 72°C followed by final extension for 2 min at 72 °C. The PCR products were run on a 1-2% agarose gel stained with ethidium bromide. The gel was checked on a gel documentation system (Syngene InGenius).

2.2.4.1.4 Plasmid DNA standard generation

For the absolute quantification, a DNA standard for each of the target gene was generated. For this, PCR product of each target needed to be cloned into a vector. Thus, the PCR product of each target gene was purified using the PCR clean-up and Gel extraction kit (Macherey-Nagel) according to manufacturer's instructions (detailed protocol in appendix 1.3). Purified DNA was eluted in 20 µL nuclease free water (Ambion). DNA concentration was determined using Nanodrop Spectrophotometer (ND-1000, Labtech International,

Uckfield, UK). Purified PCR products were directly used for the ligation procedure or kept at -20°C until used.

In the present study, to quantify mRNA transcripts of target genes, absolute real-time qPCR was employed where each target was cloned into pGEM-T easy vector to produce a quantitative DNA standard. A standard curve from the serially diluted standards of known copy number (10^7 to 10^1 molecules/µL) was generated and the copy number of unknown samples was then calculated by extrapolating the CT (cycle threshold) into the standard curve. No reference gene or housekeeping gene was used in this study as the quantification by absolute qPCR does not depend on the reference gene or housekeeping gene since the reference is the standard curve.

Moreover, absolute quantification based real- time qPCR was preferred as for relative real-time qPCR choosing the right housekeeping gene is critical and expression of many of the housekeeping genes such as GAPHDH (glyceraldehyde-3-phosphate dehydrogenase), β-actin and 18S rRNA vary depending on the cell types and experimental conditions (Kozera & Rapacz, 2013) which supports the idea that there is no ideal reference gene (Rebouças et al., 2013). Thus, for ideal relative quantification assay requires a series of reference genes even for the investigation of expression of a single gene of interest, which is expensive and time consuming. Bearing these constraints of using housekeeping genes in real time qPCR in mind, absolute real time qPCR based on a quantitative standard was used.

2.2.4.1.5 Competent cells preparation

The chemically competent cells were prepared using two chemical solutions where solution 1 contained 1M potassium acetate (Sigma-Aldrich), 1M $RbCl_2$ (Sigma-Aldrich), 1M $CaCl_2$ (Sigma-Aldrich), 1M $MnCl_2$ (BDH Chemicals) and 80% (w/v) glycerol in a required volume of deionized water. The pH of the solution was adjusted to 5.8 using 100 mM acetic acid (Fisher Chemical); and solution 2 was prepared with 100 mM MOPS (pH 6.5) (Sigma-Aldrich), 1M $RbCl_2$, 1M $CaCl_2$, and 80% (w/v) glycerol (Sigma-Aldrich) in a required volume of deionized water. pH of the solution was adjusted to 6.5 using concentrated HCl (Sigma). The solutions were filter sterilized using 0.22 µm syringe filter (Sartorius).

One frozen aliquot of competent cell (DH5α, Thermo fisher) was retrieved by plating onto the LB agar (Merck) plate with no antibiotics and was grown overnight at 37 °C. A single colony from overnight incubated plate was picked and inoculated in 5 mL of LB broth and was grown overnight at 37 °C in s in a Maxq 2000 shaker at a speed of 200 rpm which was then sub-cultured into 2 conical flasks each with 50 mL of LB broth (Merck) and was grown by incubating at 37 °C in in a Maxq 2000 shaker at a speed of 200 rpm and optical density (OD) at 550 nm was measured periodically using spectrophotometer (Equipnet, CECIL CE 2041) until OD reaches 0.48-0.50. The flasks were then chilled on ice for 5 min. Then the cells were transferred into 50 mL falcon tubes and centrifuged at 3000 rpm for 10 min at 4 °C. The pellet was re-suspended in 20 mL of solution 1 by gentle pipetting and then chilled on ice for 5 min followed by centrifugation at 3000 rpm for 10 min at 4 °C. The pellet was finally re-suspended in 2 mL of solution 2 by gentle pipetting and chilled on ice for 15 min. The cells were then aliquoted in sterile pre-chilled 1.5 mL Eppendorf tubes in a volume of 110 µL and the ready to use competent cells were stored at -80 °C.

2.2.4.1.6 Ligation

Ligation of PCR product was done into pGEM-T easy vector system (Promega) according to the manufacturer's instruction. Briefly, 3 µL (20-30 ng) of purified PCR product was used in 10 µL of standard reaction containing 5 µL of T4 DNA ligase buffer, 1 µL (50 ng) of pGEM-T easy vector 1 µL of T4 DNA ligase enzyme. A positive (with control insert) and a negative (without PCR product or insert) controls were always set. The ligation mixture was then incubated at 4°C for 18-24 h.

2.2.4.1.7 Transformation

Following ligation, 2 µL of each ligation reaction was transferred to 50 µL *E. coli* competent cells (DH5α cells, Thermo Fisher Scientific; prepared in section 2.2.5.1) in 1.5 mL Eppendorf tube and mixed gentle by pipetting and incubated on ice for 30 min. After incubation the cells were heat shocked for 50 seconds at 42 °C in water bath following incubation on ice for 2 min. Then 250 µL of LB medium was added in each tube and incubated for an h in shaking incubator at a speed of 200 rpm. After incubation, from each transformation tube 50 µL, 100 µL and rest of the cells were spread on Luria-Bertani (LB)

agar plates containing 100 µg/mL ampicillin. The plates were then incubated overnight at 37 °C.

In the following day, plates were checked for growth of bacteria. Three single colonies were picked per transformation reaction and placed in sterile 1.5 mL eppendorf tube containing 1 mL of LB broth supplemented with 100 µg/mL ampicillin. The tubes were then incubated overnight at 37 °C in a Maxq 2000 shaker at a speed of 200 rpm. Following overnight incubation, the tubes were checked for bacterial growth by observing the cloudiness of the growth medium.

2.2.4.1.8 Plasmid purification and ligation confirmation

Plasmid DNA purification was then conducted using NucleoSpin plasmid DNA purification kit (Macherey-Nagel) following the protocol outlined in the kit (detailed in Appendix 1.4). The concentration and quality of plasmid DNA was checked using Nanodrop Spectrophotometer (ND-1000, Labtech International, Uckfield, UK). To confirm the correct insertion of the target, conventional PCR was conducted using the gene specific primers. After PCR confirmation, plasmid samples of each target were sequenced using SP6 (TAAGATATCACAGTGGATTTA) or T7 (ATTATGCTGAGTGATATCCC) primer.

For sequencing, plasmid samples were sent to GATC Biotech, using LIGHTrun sequencing. LIGHTrun sequencing was prepared in tubes containing a mixture of 5µl plasmid DNA (80-100 ng/µL) and 5 µL of SP6 or T7 primer (5 µM). When sequences were obtained, they were blasted in NCBI to check the correct insertion into the pGEM-T easy vector.

2.2.4.1.9 Copy number calculation and subsequent dilution

The copy number per microliter of plasmid DNA was calculated using the formula stated below.

Step 1: Calculation of molecular weight

$$(base\ pair\ of\ fragment + base\ pair\ of\ vector) \times 660 = 1\ mol$$

Step 2: Calculation of moles

$$(measured\ weight\ in\ g\ per\ microliter \div molecular\ weight\ in\ g) \times 1\ mol = X\ mol$$

Step 3: Calculation of molecules or copy number per microliter

$$\frac{\text{X mol}}{1\text{ mol}} \times 6.023 \times 10^{23} = \text{molecules}/\mu\text{L}$$

Where, 660 is the molecular weight of each base pair of nucleotides in plasmid DNA, 6.023×10^{23} is the Avogadro's number.

Finally, the plasmid DNA was diluted in nuclease free water to 1×10^7 copy/µL to 1×10^1 copy/µL and used as standard for absolute quantification of mRNA expression in the samples.

2.2.4.1.10 Standard curve generation

Syber green based qPCR was performed to test the DNA standard using Luminaries Color HiGreen qPCR Master Mix (Thermo Scientific) in Stratagene Mx3005P thermal cycler (Agilent Technologies, Santa Clara, US). Standard sets of each target were run in duplicate. No template control (NTC) was always performed to check contamination or false positive amplification. Three independent runs were conducted, and mean CT values were plotted against log of copy number to generate standard curve.

Table 2.1: Primer sequences used in RT-PCR and RT-qPCR for rainbow trout transcript targets

Target gene	Primer sequences (5'-3')	Amplicon size (bp)	TM (°C)	Reference sequence accession number	Application
Claudin-3a	F-TGGATCATTGCCATCGTGTC R- GCCTCGTCCTCAATACAGTTGG	139	60	BK007964	RT-PCR, RT-qPCR
Claudin-8d	F-GCAGTGTAAAGTGTACGACTCTCTG R- CACGAGGAACAGGCATCC	339	60	BK007966	RT-PCR, RT-qPCR
ZO-1	F-AAGGAAGGTCTGGAGGAAGG R- CAGCTTGCCGTTGTAGAGG	291	59	HQ656020	RT-PCR, RT-qPCR
TLR3	F- TGACAGAGCTTAACCTGGC R- AAGAACTTCCAGGCATGGACA	538	60	CA363490	RT-PCR
TLR3	F-AGCCCTTTGCTGCCTTACAGAG R-GTCTTCAGGTCATTTTTGGACACG	61	60	CA363490	RT-qPCR
Mx2	F-GATGCTGCACCTCAAGTCCT R-TAGCTGCGTGCCTTCATCAG	237	60	RBTMx2/RBTMx3	RT-PCR, RT-qPCR
IFNβ	F-GACGTCTGTCACGTGGAACAAAAT R-CCAAACACCGCCCACAACA	100	59	NP_001153974	RT-qPCR

2.2.4.11 Absolute quantification of tight junction and antiviral response genes

The mRNA expression levels of the TJ proteins claudin 3a and 8d and tight junction regulatory protein ZO-1 and antiviral response proteins TLR3, IFNβ and Mx2 were quantified using Luminaries Color HiGreen qPCR Master Mix (Thermo Scientific). SYBR green based RT-qPCR (Figure 2.1) was performed to quantify the mRNA transcripts using Stratagene Mx3005P thermal cycler (Agilent Technologies, Santa Clara, US). The following qPCR protocol was employed: pre-treatment at 50 °C for 2 mins; initial denaturation at 95°C for 10 mins, 35 cycles of denaturation 95 °C for 15s, annealing 59/60 °C (target specific) for 30s, and extension 72 °C for 30s; followed by dissociation curve temperature profile: 95 °C for 10s, 55 °C for 5s and 95 °C for 30s to confirm the generation of a single specific amplicon. Two microliters of each standard of 1×10^7 copy/ µL to 1×10^1 copy/ µL (generated in section 2.2.5) in duplicate or diluted cDNA (1:5 dilution) in triplicate or nuclease free water (Ambion) for NTC were used with 18 µL of mastermix containing 10 µL of SYBR Green, 0.5 µL of each primer (200 nM) and 7 µL of nuclease free water (Ambion).

For absolute quantification of each mRNA transcript, the copy number was extrapolated from the standard curve. The MIQE guideline (Bustin et al., 2009) was followed in all the steps from RNA extraction to qPCR data analysis.

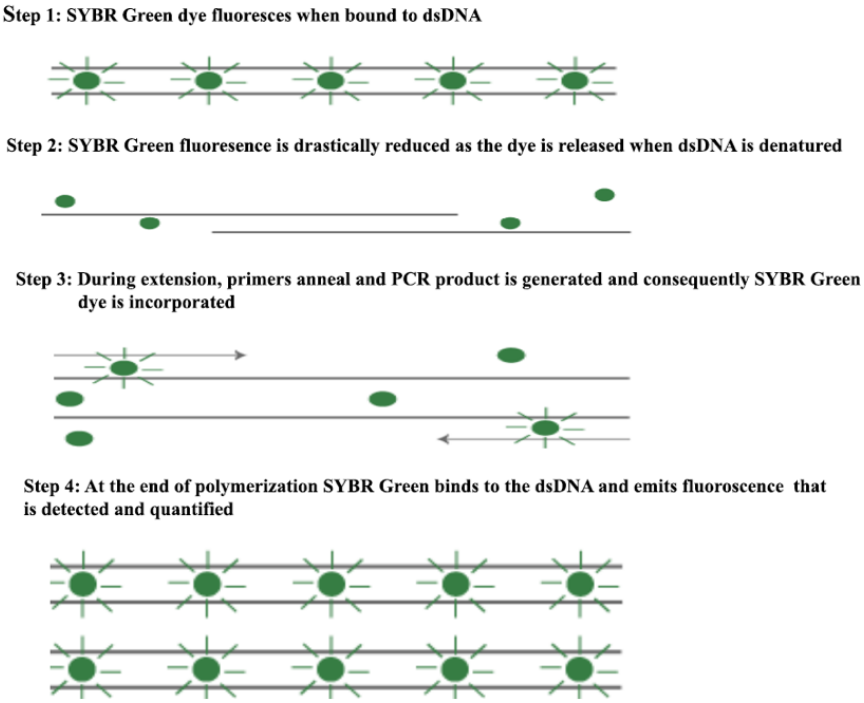

Figure 2.1: SYBR green chemistry: SYBR green dye detects polymerase PCR products by intercalating into double-stranded DNA formed during PCR. During PCR, the DNA polymerase amplifies the target sequence which creates double-stranded DNA PCR products resulting is an increase in fluorescence intensity proportional to the amount of PCR product produced.

2.2.5 Recognition of PAMPs in RTgill-W1 cells by FACS-Analysis

To investigate the mechanisms of recognition of poly(I:C), LPS and MDP by salmonid epithelial cells, a flow cytometry-based technique was applied. Regularly maintained RTgill-W1 cells were seeded onto 96 well plate or 24 well plate transwells at a seeding density of 0.04×10^6 cells per well or per insert in a volume of 100 µL. Cells were incubated at 22 °C until they formed a confluent monolayer (around 48 h). Initially, cells were stimulated with 10 µL/well or insert of poly(I:C) (InvivoGen) at 10 µg/mL (stock 100 µg/mL); 2 µL/well or insert of MDP labelled with Rhodamine (InvivoGen) at 10 µg/mL (stock 500 µg/mL); 5 µL/well or insert of LPS labelled with Alexa Fluor 488 (Thermo Fisher) at 10 µg/ml (stock 200 µg /mL) for 24 h. Cells were then washed with 200 µL of PBS (Life Technology) three times and harvested in 100 µL PBS and analysed by flow cytometer (Beckman Coulter).

The procedure of flow cytometer data analysis for the target channels is presented in Figure 2.2. Gating was performed for each channel and PAMP. The green FITC channel (excitation 494 nm and emission 520 nm) was used for both Fluorescein and Alexa Fluor 488 as both have similar excitation (495 and 492 nm respectively) and emission (519 and 518 nm

respectively) spectra while for MDP-rhodamine (excitation 546 nm and emission 576 nm) the PE channel (excitation 565 nm and emission 578 nm) was used.

Before the inhibition study, the working concentration and duration of treatment of CyD (Sigma-Aldrich) were optimized by investigating the effects of different doses and durations of treatment of CyD on the cell viability. The optimum concentration and duration of CyD treatment were found to be 2 µg/mL for 1 h pre-treatment. Cells were then treated with CyD at a concentration of 2 µg/mL in respective wells or DMSO diluted in medium in control group one h prior to stimulation with PAMPs. After one h of CyD treatment cells were stimulated with MDP labelled with Rhodamine at 10 µg/mL and LPS labelled with Alexa Fluor 488 at 10 µg/mL. Cells were incubated in dark at 22 °C for 3 h. After 3 h cells were washed with 200 µL of PBS for three times and harvested using citric saline (270 mM KCl and 30 mM sodium citrate solution in deionized water and sterilized by autoclaving) in 0.1 mL PBS and analysed by flow cytometer.

To further investigate the mechanisms of internalization of MDP in RTgill-W1 cells, several other inhibitors including L-histidine (Sigma-Aldrich), cefradine (Sigma-Aldrich) and Lisinopril (Sigma-Aldrich) were used. The dose and duration of treatment of each of the inhibitors were optimized which was 2 mM and the duration of pre-treatment was 1 h. The duration of MDP stimulation was 3 h. Each treatment was performed in triplicate and each experiment was performed at least three times.

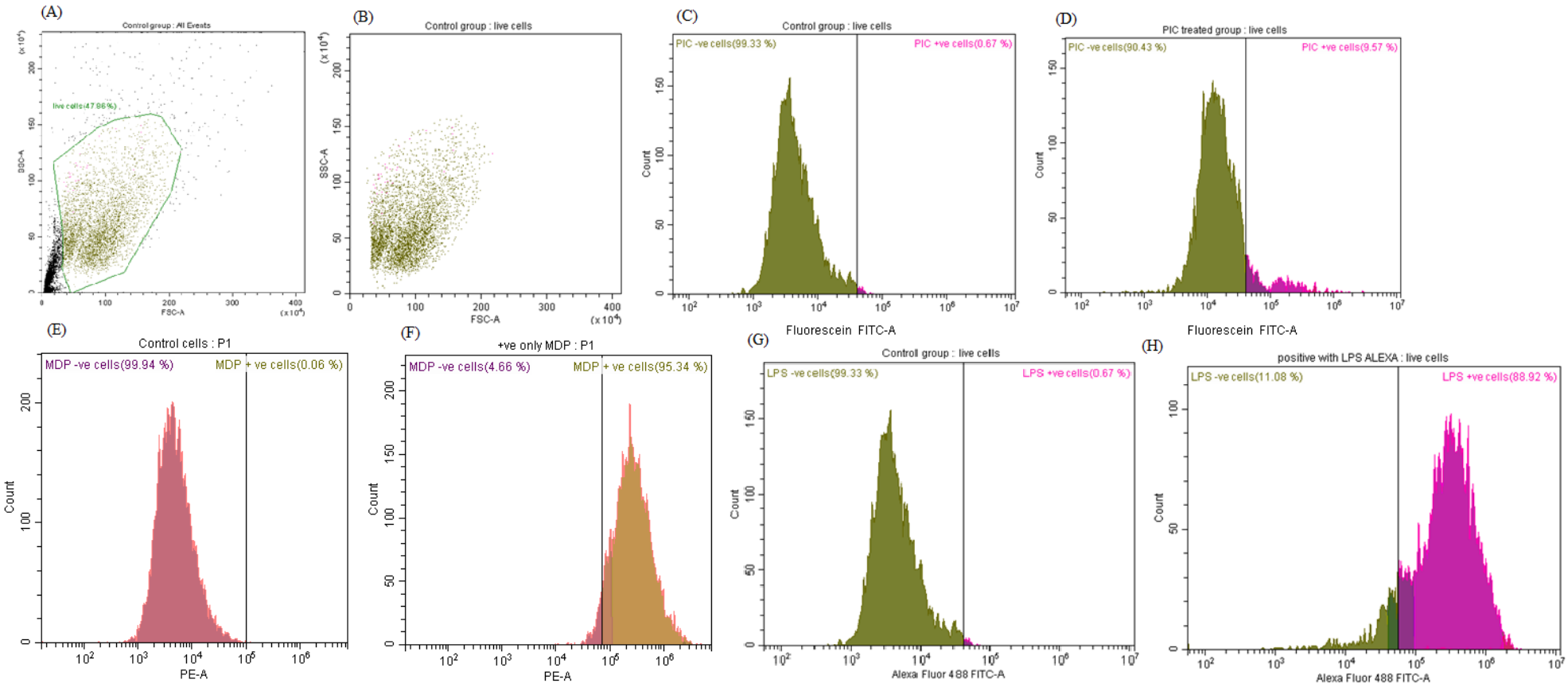

Figure 2.2: Procedure of analysing flow cytometry data for ligand internalization. RTgill-W1 cells growing on 96 well plate or 24 well transwells were stimulated with fluorescent labelled PAMPs and harvested after specified durations. Discriminating live cells (A and B), gating for control (C) and poly(I:C) stimulated (D) cells for the detection of poly(I:C) positive and negative cells using green channel for fluorescein FITC, for MDP-rhodamine detection, PE channel was used where MDP positive and negative cells in control (E) and MDP stimulated (F) group are shown, and for LPS labelled with Alexa Fluor 488 detection green channel was used for where MDP positive and negative cells in control (E) and MDP stimulated (F) group are presented.

2.2.8 Statistical analysis

TER data were analysed using two-way repeated measure ANOVA followed by Bonferoni's multiple comparison using GraphPad prism version 6.0 (San Diego, CA, USA). RT-qPCR data were analysed using one-way ANOVA followed by Bonferoni's multiple comparison, internalization data were analysed using paired sample t-test using GraphPad prism. In all analyses, differences between groups were considered statistically significant at $p<0.01$ unless mentioned otherwise.

2.3 Results

2.3.1 Changes of epithelial integrity in response to PAMPs

The integrity of the epithelial membrane depends on the correct polarization of epithelial cells. This polarization can be measured by Transepithelial Electrical Resistance (TER). TER is a non-destructive technique carried out using a volt-ohm meter in cells grown onto transwells.

TER was used to study the cellular integrity of RTgill-W1 cells in response to immune challenges with various PAMPS. Before starting the RTgill-W1 experiment, the seeding density in the 12 well transwells was optimized. A commonly used mammalian cell line MDCKII was used as a positive control to check whether the system was working. The seeding density of 0.1×10^6/per insert in both cell lines gave the highest resistance (Figure 2.3). For subsequent experiments this seeding density was chosen.

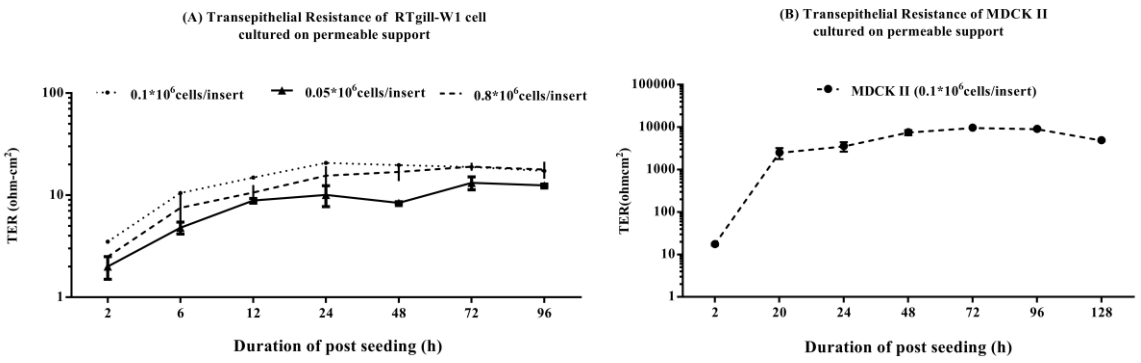

Figure 2.3: Optimization of seeding density of RTgill-W1 and MDCKII cells on transwell insert. For RTgill-W1 cells, three different seeding densities were tested to optimize the seeding density onto the transwells. Seeding density of 0.10×10^6 cells per insert was found to show the highest resistance (a). High TER value was detected in MDCK II cells at 48 h of post seeding which was around 8.5 KΩ-cm^2 (b).

To investigate the effects of PAMPs on TER, viral and bacterial PAMPs were used in two experiments to investigate their effects on cellular integrity. Cells were grown onto the transwells and post-seeding TER was measured at different time points (i.e. 2h, 6h, 12h…) until TER reached its peak and stabilized. In most cases 72 h post seeding yielded a stable TER. Cells were stimulated with poly (I:C) and lipopolysaccharide (LPS) at 10 µg/mL prior to TER measurement over time. Before stimulation, all treatment groups had similar TER. Immediately after stimulation, TER increased gradually until 24 h in stimulated cells and

then decreased slowly (Figure 2.4A). Significantly higher electrical resistance was detected in activated cells than that of control cells at 3 h of post stimulation and onwards ($p<0.001$). However, similar resistance was detected in poly(I:C) and LPS treated cells at all time points. In poly(I:C) and LPS stimulated cells, TER values reached a peak of around 40 to 46 Ωcm^2 at 24 h of stimulation which were around 1.6 and 1.9 times higher than that of control cells, respectively. Moreover, after 48 h of post activation the values were around 1.65 and 2.0 times higher in poly(I:C) and LPS treated cells than control cells, respectively.

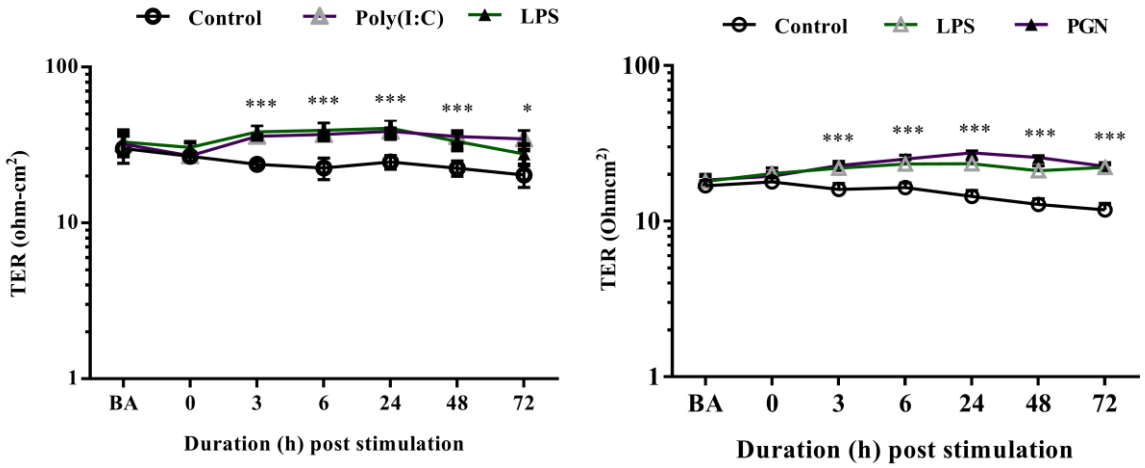

Figure 2.4: Effect of poly(I:C), lipopolysaccharide (LPS) and peptidoglycan (PGN) on transepithelial resistance (TER) across RTgill-W1 cell layers: (A) 10 µg/mL poly(I:C) and 10 µg/mL LPS were used to stimulate the cells; (B) 10 µg/mL LPS and PGN were used. The experiments were started nearly 72 h after seeding in transwells when TER was stable. Values are expressed as mean±SEM. Any course 3 independent experiments in triplicate were conducted having 3 measurements at a single time point in each insert. Values are mean ± SEM (n=3×3=9). *=$p<0.01$ and ***= $p<0.0001$ (between control and stimulated cells). No asterisk indicates lack of significant differences at a specific time point. Repeated measure one-way ANOVA followed by Bonferoni's multiple comparison was conducted using GraphPad prism v.6.0. BA denotes before activation.

Further to investigate the immunomodulatory and cellular effects of another commonly used bacterial PAMP PGN, cells were stimulated with PGN (10 µg/mL) along with LPS (10 µg/mL) stimulation where both LPS and PGN stimulation gave significantly higher resistance than that of control cells at all the time points from 3 h ($p<0.001$). However, similar resistance in LPS and PGN treated cells was found. Highest electrical resistance was found in LPS and PGN stimulated cells after 24 h of activation which were around 23 to 27 Ωcm^2, respectively being 1.62 and 1.91 times higher than that of control group (Figure 2.4B).

2.3.2 Molecular response of rainbow trout gill epithelia to viral and bacterial PAMPs

Cellular and molecular response initiate upon the recognition of antigens by host receptors. Different pathogens and pathogen associated molecular patterns (PAMPs) are recognized by various specific receptors. To investigate the molecular response upon PAMP stimulation, the expression of innate immune genes and tight junction related genes were tested upon stimulation with viral and bacterial PAMPs.

Two *in vitro* cell culture systems (conventional cell culture and transwells) were employed to investigate the innate immune response at different time points. The response was monitored using Syber green based quantitative real time PCR (qPCR). For absolute quantification of the copy numbers of mRNA transcripts of selected target genes, DNA standard were generated for each target gene (method section 2.2.6). For each quantitative standard, co-efficient of determination (R^2), efficiency (optimum value 2) and sensitivity were calculated (Table 2.1). Copy numbers of mRNA transcripts were from the quantitative standard curve.

Table 2. 2: Co-efficient of determination (r^2), efficiency and sensitivity for the target genes generated from the standard curve. Efficiency was calculated using the formula, $E = 10^{(-1/slope)}$. An E value of 2.0 is equivalent to 100% efficiency. N represents the number of qPCR repetitions for each gene to produce the standard values, while sensitivity is the lowest number of target molecule copies determined.

Target	r^2	Efficiency	N	Sensitivity
TLR3	0.99	2.03	3	10^1
IFNβ	0.97	2.24	3	10^1
Mx2	0.99	2.04	3	10^1
ZO-1	0.99	2.03	3	10^2
Claudin 3a	0.96	1.72	3	10^1
Claudin 8d	0.98	1.71	3	10^2

The standard curve of each gene is presented in Appendix 2.1, Figure 2.1.

2.3.2.1 Innate immune response

To study the innate immune response of RTgill-W1 cells upon induction of viral and bacterial PAMPs, two different culture conditions; conventional 12 well plate culture system

and transwell system were employed. Viral PAMP Poly(I:C), and bacterial PAMPs LPS and PGN were used as immune modulators.

2.3.2.1.1 Response to poly(I:C), viral PAMP

Stimulation with poly(I:C) at 1 and 10 µg/mL for 6 and 24 h yielded interferon beta and Mx2 signals in the transwells (Figure 2.5). In the traditional 12 well cell culture system, expression was observed only at 24 h of stimulation with poly(I:C) 1 and 10 µg/mL. Data for 1µg/mL concentration are not shown.

TLR 3 was found to be expressed in RTgill-W1 cells of all the groups. Poly(I:C) stimulation for 24 h induced significantly higher expression of TLR3 than in control cells ($p<0.001$). However, the expression was significantly more upregulated in transwells than in 12 well culture.

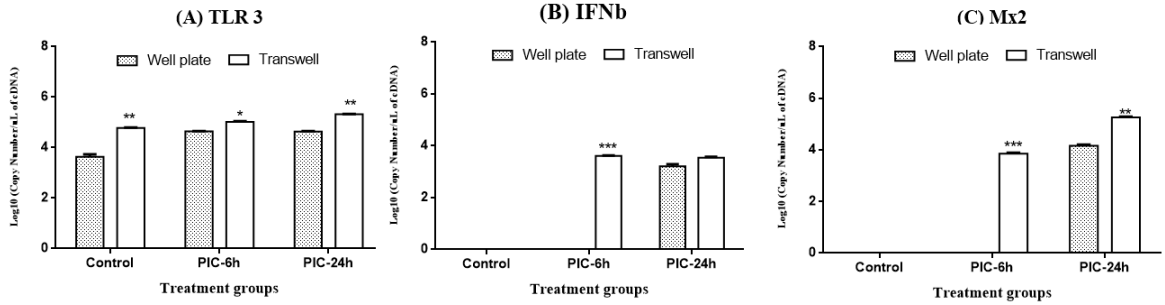

Figure 2.5: Antiviral response of RTgill-W1 cells upon stimulation with viral PAMP poly(I:C) at a concentration of 10 µg/mL for 6 and 24 h in the transwells and 12 well plate. Expression of TLR3 (A), IFNβ (B) and Mx2 (C) in RTgill-W1 cells upon stimulation was investigated. Data are mean ± SEM of three course independent experiment. Data are mean ± SEM of three course independent experiments. Two-way ANOVA followed by Bonferoni's multiple comparison was conducted to analyse the data with the level of significance of $p<0.01$ using GraphPad Prism version 6.0. *=$p<0.01$, **=$p<0.001$ and ***=$p<0.0001$ denote significantly different.

To determine the time-point of initiation of the antiviral response, a time course response experiment was conducted where cells were stimulated with poly(I:C) for 30 min, 1, 3,6 and 24 h using the lower dose (1 µg/mL). This experiment was conducted in the transwell system. In this experiment, significantly higher mRNA transcripts of TLR 3 was found in the 24 h post stimulation group while similar expression was detected in the control, at 1h and 3h post stimulation (Figure 2.6). Very low level of expression of IFNβ was detected in poly(I:C) stimulated cells while no expression was detected in control cells. However,

significantly higher mRNA transcript numbers were detected in the 6h post stimulation cells ($p<0.01$). Surprisingly, antiviral response gene Mx 2 expression initiated at 30 min of stimulation with poly(I:C) progressively and upregulated up to 24 h to a final copy number of $8.54\pm2.82\times10^7$ per µL of cDNA, which was significantly higher than at all the other time points ($p<0.0001$). In comparison control cells did not show any signal for Mx2 expression.

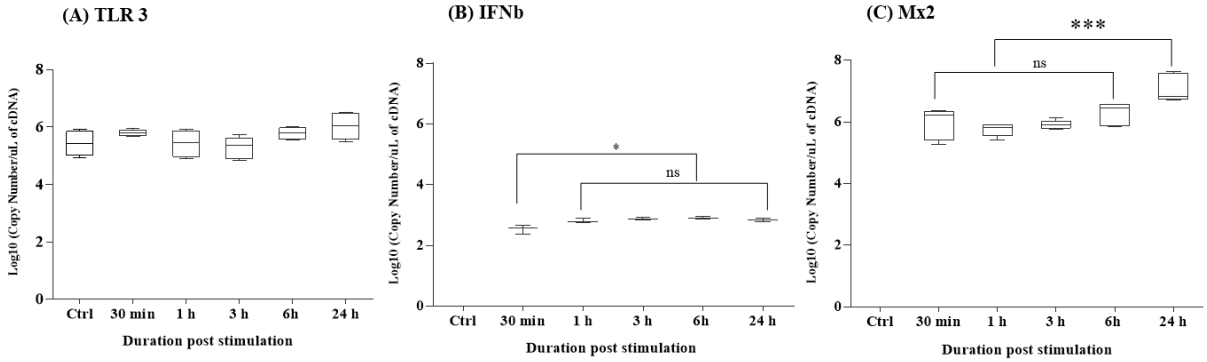

Figure 2.6: Antiviral response of RTgill-W1 cells in a time dependent manner upon stimulation with poly(I:C) at 1 µg/mL for different durations in the transwells. Expression of TLR3 (A), IFNβ (B) and Mx2 (C) in RTgill-W1 cells upon stimulation was investigated. Data are mean ± SEM of three course independent experiment. One-way ANOVA followed by Bonferoni's multiple comparison was conducted to analyse the data with the level of significance of $p<0.01$ using GraphPad Prism version 6.0. *=$p<0.01$, **=$p<0.001$, ***=$p<0.0001$.

2.3.2.1.2 Response to bacterial PAMP (LPS and PGN)

To evaluate whether bacterial PAMPs have the ability to show antiviral response, cells were stimulated with LPS and PGN at a concentration of 10 µg/mL for 24 h. As viral PAMP, TLR3 was found to be upregulated in transwells in control and LPS stimulated cells (Figure 3). However, in the 12 well culture, PGN was found to upregulate TLR3 expression compare to control cells. No expression of IFNβ and Mx2 was found in both the culture system in control and 12 well plate in LPS stimulated cells. However, LPS in transwells and PGN in both systems were found to be able to trigger the expression of IFNβ and Mx2 (Figure 2.7).

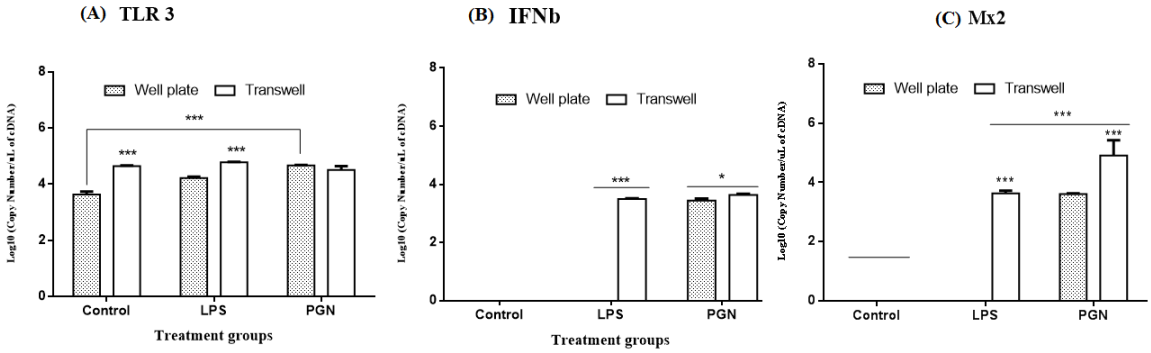

Figure 2.7: Antiviral response of RTgill-W1 cells upon stimulation with bacterial PAMPs LPS and PGN at a concentration of 10 µg/mL for 24 h in the transwells and 12 well plate. Expression of TLR3 (A), IFNβ (B) and Mx2 (C) in RTgill-W1 cells upon stimulation was investigated. Data are mean ± SEM of three course independent experiments. Two-way ANOVA followed by Bonferoni's multiple comparison was conducted to analyse the data with the level of significance of $p<0.01$ using GraphPad Prism version 6.0. *=$p<0.01$, **=$p<0.001$ and ***=$p<0.0001$.

2.3.4 Tight junction gene expression

To investigate the effects of viral and bacterial PAMPs on the epithelial integrity of RTgill-W1 cells, the expression of a set of tight junction (TJ) related gene markers were tested.

2.3.4.1 Response to viral PAMP, poly(I:C)

Poly(I:C) was not found to stimulate the expression of claudin 3a. A similar expression of claudin 3a was observed in both the culture conditions. Claudin 8d was significantly upregulated in poly(I:C) stimulated cells in the 12 well plate at 6h ($p<0.0001$) and in the transwells at 24h ($p<0.001$). ZO-1 was significantly upregulated in both culture conditions at both 6- and 24-h stimulation ($p<0.0001$) (Figure 2.8).

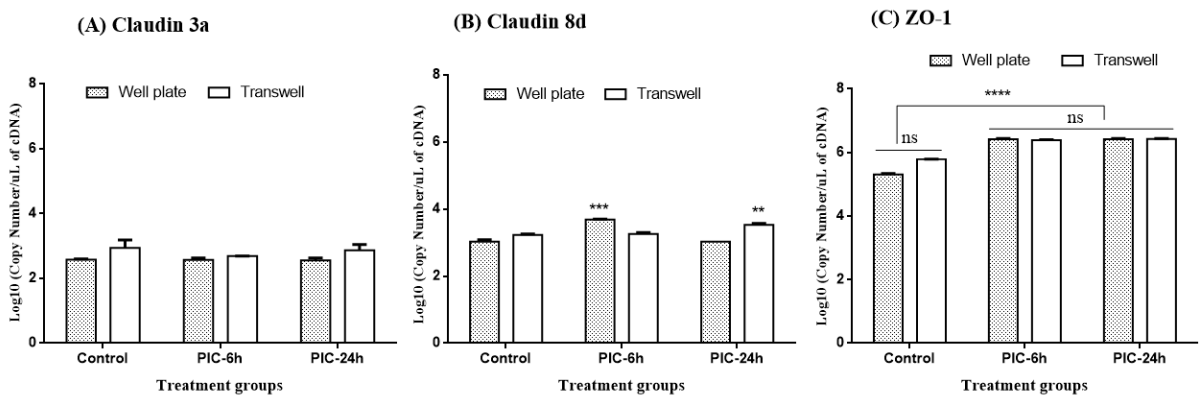

Figure 2.8: Tight junction response of RTgill-W1 cells upon stimulation with viral PAMP at a concentration of 10 µg/mL for 6 and 24 h in the transwells and 12 well plate. Expression of tight junction gene Claudin 3a (A), Claudin 8d (B) and tight junction regulatory gene ZO-1 (C) in RTgill-W1 cells upon stimulation was investigated. Data are mean ± SEM of three course independent experiments. Two-way ANOVA followed by Bonferoni's multiple comparison was conducted to analyse the data the level of significance of $p<0.01$ using GraphPad Prism version 6.0. *=$p<0.01$, **=$p<0.001$, ***=$p<0.0001$.

2.3.4.2 Response to bacterial PAMP, LPS and PGN

Bacterial PAMPs LPS and PGN were not found to induce the expression of claudin 3a and 8d which was also similar in both the culture conditions. However, ZO-1 was significantly upregulated in the transwells in all the groups compared to the counterparts in the 12 well plates. In the 12 well plate culture, LPS was found to upregulate ZO-1 expression ($p<0.001$) while in the transwells both LPS and PGN were found to upregulate ZO-1 expression ($p<0.0001$) (Figure 2.9).

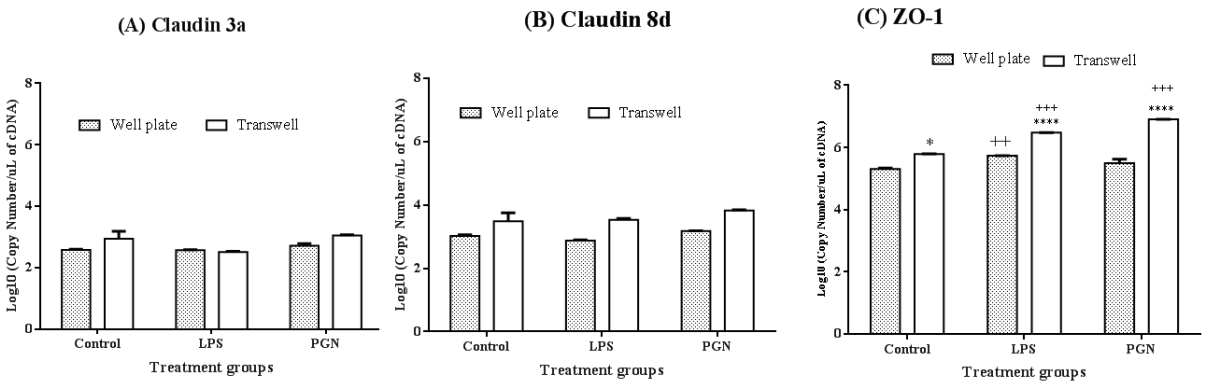

Figure 2.9: Tight junction response of RTgill-W1 cells upon stimulation with bacterial PAMPs LPS and PGN at a concentration of 10 µg/mL for 24 h in the transwells and 12 well plate. Expression of tight junction gene Claudin 3a (A), Claudin 8d (B) and tight junction regulatory gene ZO-1 (C) in RTgill-W1 cells upon stimulation was investigated. Data are mean ± SEM of three course independent experiments. Two-way ANOVA followed by Bonferoni's multiple comparison was conducted to analyse the data with the level of significance of $p<0.01$ using GraphPad Prism version 6.0. The asterisk *=$p<0.01$, **=$p<0.001$, ***=$p<0.0001$ and ****=$p<0.00001$ denote significance between culture methods within treatments while $^{++}$=$p<0.001$ and $^{+++}$=$p<0.0001$ denote significance between control and treatment within the culture methods.

2.3.5 Recognition of PAMPs in RTgill-W1 cells

Bacterial and viral PAMPs play significant roles in immunomodulation of host cells by activating different antimicrobial responses. Different PAMPs bind to different intracellular and extracellular receptors on host cells and become internalized by endocytic mechanisms either in actin-dependent or independent manner. Flow cytometry and fluorescent microscopy techniques were used to investigate the pathway of recognition of PAMPs in RTgill-W1 cells.

2.3.5.1 Observation of internalization by fluorescent microscopy

To investigate the recognition pathway of PAMPs by RTgill-W1 cells, cells were grown in 96 well plates. Cells were stimulated with poly(I:C) labelled with fluorescein isothiocyanate (FITC), LPS labelled with Alexa Fluor 488 and Muramyl dipeptide (MDP) labelled with Rhodamine. All were applied at 10µg/mL for 24 h and then cells they were observed under fluorescent microscope. MDP and LPS were found to be internalized by RTgill-W1 cells, as the cells produced a fluorescent signal. However, poly(I:C) treated cells did not give any fluorescent signal.

To inhibit actin dependent uptake cells were treated with Cytochalasin D (CyD) which led to rounding, detachment from the surface and reduced numbers of cells. MDP Rhodamine LPS-labelled Alexa Fluor 488 were internalised by CyD treated cells.

2.3.5.2 PAMPS internalization in polarized and non-polarized RTgill-W1 cells

To investigate the recognition pathway of PAMPs by RTgill-W1 cells, cells were grown onto 96 well plates and 24 well transwells system as both having similar growth area. Cells were stimulated with poly(I:C) labelled with FITC, LPS labelled with Alexa Fluor 488 and MDP labelled with Rhodamine at 1 µg/mL and 10µg/mL for 30 min, 3h, 24 h and 48 h. Cells were analysed by flow cytometry for the detection of internalization of poly(I:C), LPS and MDP. Initial data showed the internalization of MDP and LPS at 3, 24 and 48 h of stimulation at the dose of 10 µg/mL while the percentage of positive cells was very low at 30 min post stimulation at 10 µg/mL and at all the time points at 1µg/mL concentration (data not shown). However, the percentage of internalization of poly(I:C) was 1-2% (data not shown).

To further analyse the internalization of ligands cytochalasin D (CyD) was added 1 h before stimulation at a concentration of 1µg/mL to inhibit ligand internalization. Concentration of CyD and duration of pre-treatment were optimized before starting the final experiments. Cells were subsequently stimulated for 3 h with the labelled ligands at a concentration of 10 µg/mL in 96 well plate and 24 well transwells.

CyD was found to decrease the internalization of LPS significantly in both non-polarized and polarized cells ($p<0.05$ and $p<0.01$ respectively) (Figure 2.10 C, D and Figure 2.11 C, D). However, MDP internalization was not significantly inhibited by CyD in either polarized or non-polarized cells (Figure 2.10 A, B and Figure 2.11 A, B). Moreover, internalization and inhibition of both of the ligands were higher but not significant in polarized epithelial cells (transwells) than that of non-polarized cells (well plate).

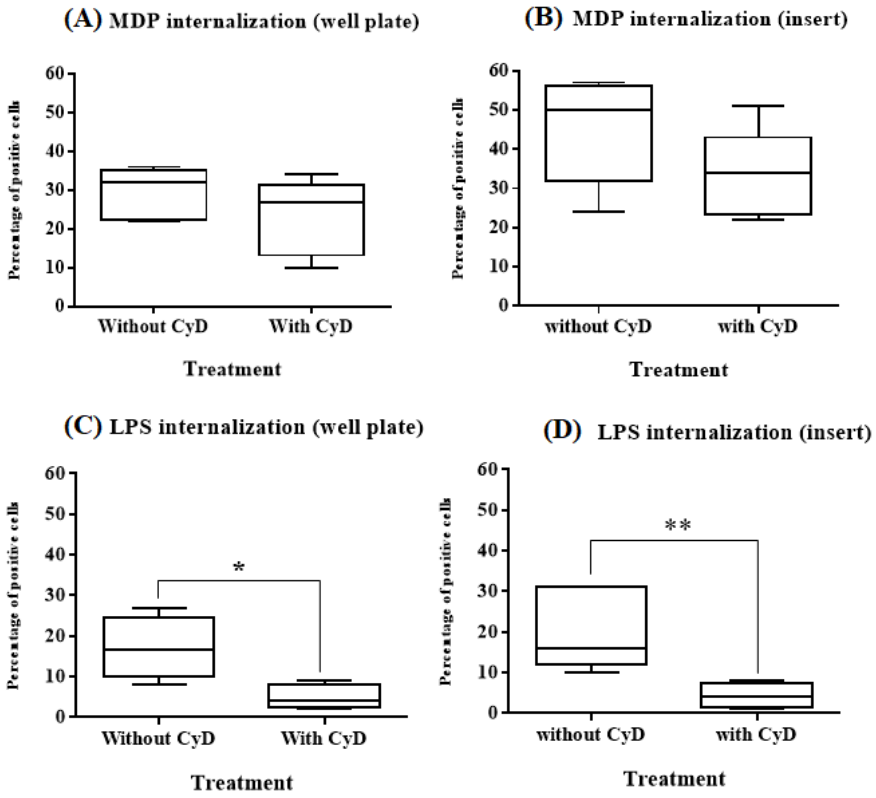

Figure 2.100: Internalization of PAMPs in RTgill-W1 cells in presence and absence of CyD. Cells were treated with CyD 1 h prior to stimulation in treated group. Percentage internalization data were obtained from FACS analysis. Four independent experiments were conducted, and data were presented as mean ± SEM. Bars represent the percentage of internalization of MDP in well plate (A) and transwells (B); and LPS in the well plate (C) and transwells (D) into RTgill-W1 cells. Data were analysed using GraphPad prism version 6.0 with the level of significance of *$p<0.005$, **$p<0.001$.

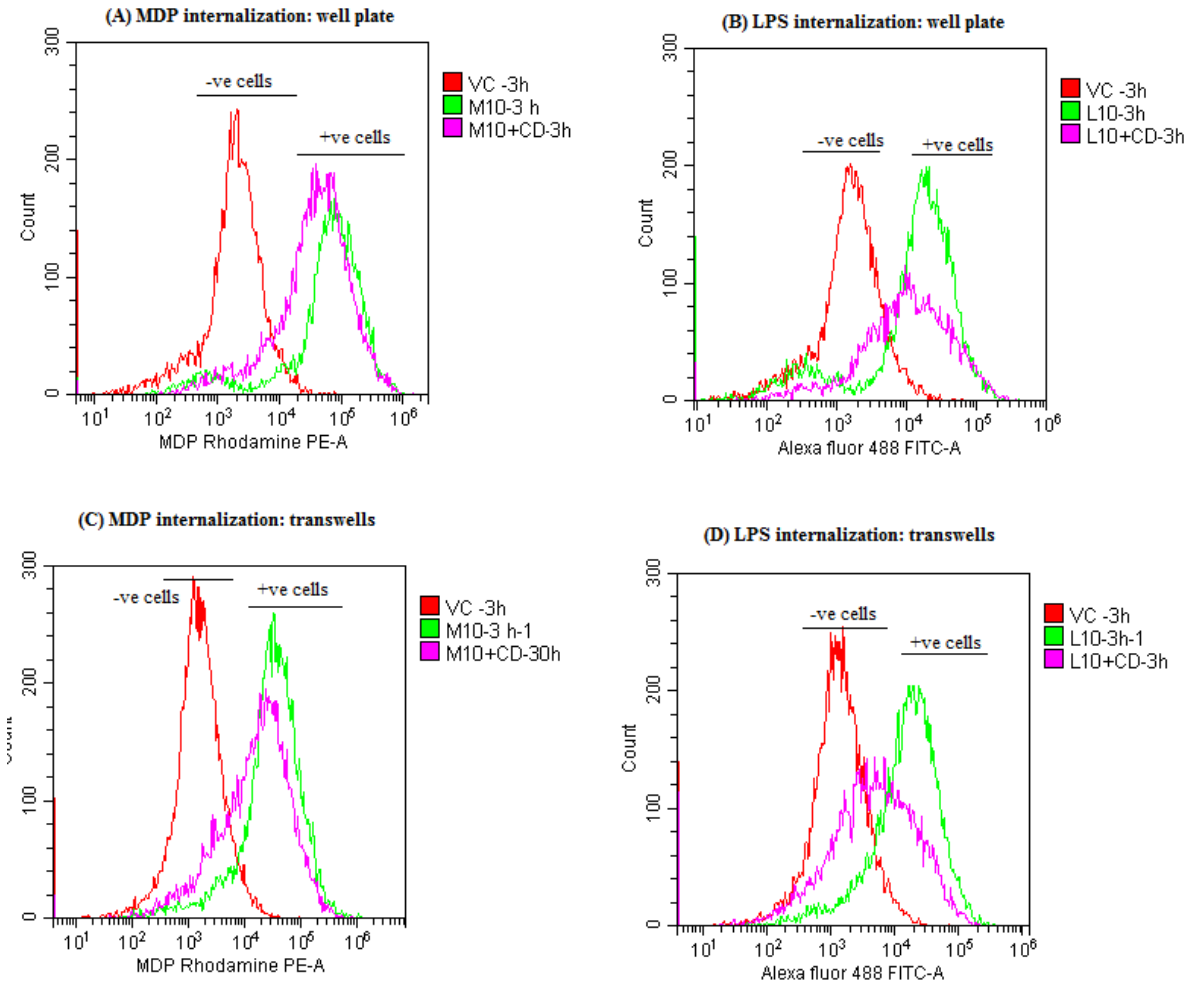

Figure 2.111: Intracellular fluorescent labelling of RTgill-W1 cells at 3 h incubation with 10 µg/mL MDP-Rhodamine and LPS-Alexa Fluor 488 in 96 well plate (A and B) and in transwells (C and D). CyD was used as the inhibitor. Cells were analysed in CytFlex flow cytometer and data were analysed using CytExpert software.

To study other uptake mechanisms, involve in MDP internalisation 3 other inhibitors including L-histidine, cefradine and lisinopril were used. Initially the dose of the inhibitors was optimized which was 2 mM. The experiment was conducted in 24 well transwells. The MDP internalization in RTgill-W1 cells was significantly inhibited by L-histidine, cefradine and lisinopril. The amino acid L-histidine was found to reduce the uptake of MDP by 17%. The antibacterial drug cefradine was able to inhibit the internalization of MDP by 24% while ACE inhibitor lisinopril was found to suppress the uptake by 30% (Figures 2.12, 2.13).

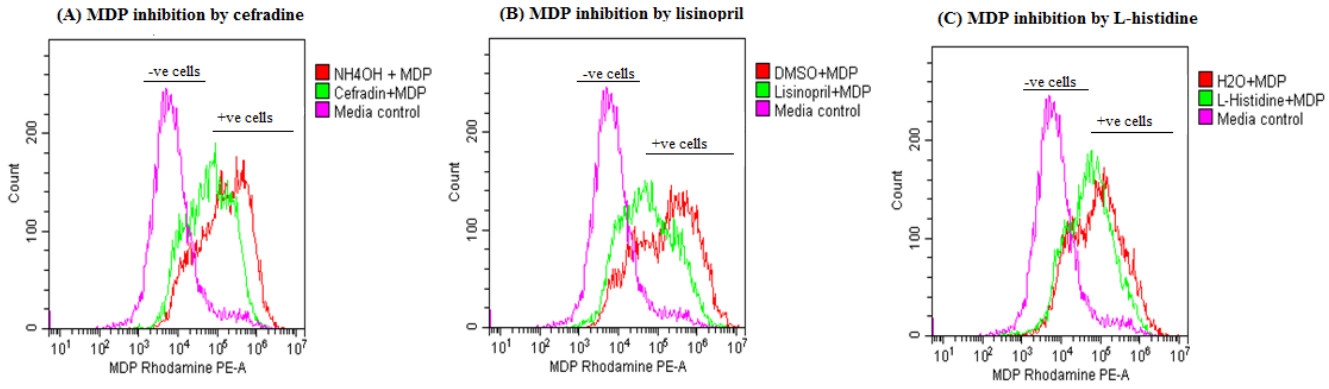

Figure 2.12: Histograms showing the flow cytometry data of positive and negative RTgill-W1 cells for MDP-Rhodamine. MDP internalization was inhibited by Cefradine (A), Lisinopril (B) and L-histidine (C). Cells were analysed in CytFlex flow cytometer and data were analysed using CytExpert software.

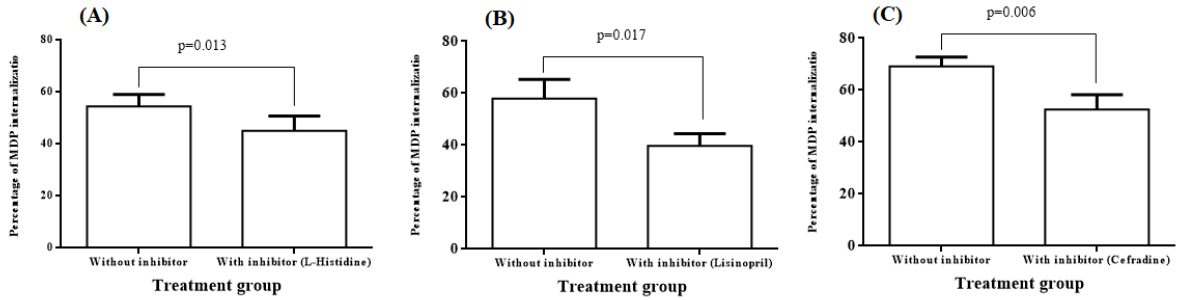

Figure 2.13: Internalization of MDP in RTgill-W1 cells in presence or absence of inhibitors. Cells were treated with inhibitors before 1 h of stimulation in treated group at a concentration of 2 mM. Percentage internalization data were obtained by FACS analysis. Four independent experiments were conducted, and data were presented as mean ± SEM. Bars represent the percentage of internalization of MDP into RTgill-W1 cells with or without L-histidine (A), lisinopril (B) and cefradine (C). Data were analysed (Paired sample t-test) using GraphPad prism version 6.0 with the level of significance of $p<0.05$.

2.4 Discussion

Gill is one of the most important organs in fish which is a point of entry for many microorganisms. The gill has a complex architecture comprising several different types of cells making it difficult to study the role of each cell in host defence. The expression pattern of certain genes in the gill in *in vivo* studies might be the cumulative effect of several cell types within the gill. As blood is continuously flowing through the gill, different nucleated blood cells also play a role in the expression of genes in the gills. This together makes it difficult to evaluate the contribution of gill epithelial cells to innate immunity. Thus, epithelial RTgill-W1 cells, have a great potential to study the contribution of gill epithelial cells in barrier function and innate immunity,

2.4.1 Modulation of epithelial integrity and tight junction function by viral and bacterial PAMPs

Epithelial barrier properties of gills play a key role in innate immunity against microbial infection. The integrity of an epithelial layer can be monitored as a function of transepithelial electrical resistance (TER) and the expression of tight junction proteins. To monitor the barrier function of RTgill-W1 cells in transwells upon stimulation with viral and bacterial PAMPs, TER measurement (method section 2.2.3), and quantification of the expression of some selected tight junction genes by absolute RT-qPCR (method section 2.2.4) was performed.

2.4.1.1 Response to viral PAMP, poly(I:C)

The epithelial integrity of RTgill-W1 as measured by TER was found to increase if exposed to viral PAMP poly(I:C) (10µg/mL). The tight junction genes Claudin 8d and ZO-1 were found to be upregulated by poly(I:C) which correlates to the observed increased epithelial resistance. Similar induction of TER by poly(I:C) (10µg/mL) has been reported in human epidermal keratinocytes (Yuki et al., 2011) while Borkowski et al. (2015) have reported dose-dependent increase of TER along with claudin and occludin mRNA expression by poly(I:C) in human epidermal keratinocytes. These findings are in accordance with the current results and could represent the response of epithelial cells to poly(I:C) stimulation while endothelial cells respond in the opposite way. Poly(I:C) has been shown to induce a decrease in TER as early as 6 h of stimulation along with decrease in claudin 5 and no change in ZO-1 gene expression in human endothelial cells (Huang, Stuart, Takeda, D'Agnillo, &

Golding, 2016). In another study, poly(I:C) has been shown to reduce TER in human polarized airway epithelial cells (Comstock et al., 2011).

2.4.1.2 Response to bacterial PAMP, LPS and PGN

Bacterial PAMPs LPS and PGN were found to increase TER (Figure 2.4) while tight junction genes claudin 3a and 8d were not regulated. ZO-1 was found to be significantly upregulated in the transwells by both LPS and PGN (Figure 2.5). Previously, both LPS and PGN have been shown to modulate the resistance of in human epidermal keratinocyte cells by increasing TER as early as 3 h post stimulation with LPS and PGN (10µg/mL). Furthermore in the same study ZO-1 mRNA abundance was induced by PGN induction (Yuki et al., 2011). In contrast, LPS has been shown to disrupt the integrity and decrease TER in rat cholangiocytes (epithelium of bile duct) and Caco-2 cells (colorectal epithelium) (Guo et al., 2013; Sheth et al., 2007).

Considering the previous findings and the results of the current study, it can be suggested that viral and bacterial PAMPs increase cellular integrity and resistance towards the exterior environment.

2.4.2 Induction of innate immunity by PAMPs

As the first line of defence, innate immune response is important for the subsequent and quick activation of adaptive immune mechanisms (Zhao et al., 2009). In the present study, the innate immune response effectors in RTgill-W1 cells was investigated in a short and long-time windows post stimulation with PAMPs (Figures 2.3-2.5 in result section). The earliest antiviral response was observed at 30 min post stimulation which suggests that, RTgill-W1 cells are able to respond to viral infection by producing interferon (IFNβ) and subsequently Mx2. The bacterial PAMPs LPS and PGN were also found to modulate innate immune responses in RTgill-W1 cells by upregulating mRNA abundance of TLR3, IFNβ and Mx2.

Kasamatsu et al. (2010) have reported the upregulation of mRNA transcripts of TLR3 upon poly(I:C) stimulation in blood cells of lamprey (*Lethenteron japonicum*). Upregulation of TLR3 and interferon has been shown in rainbow trout spleen upon stimulation with poly(I:C) (Abós et al., 2014). Al-Hussinee et al. (2016) reported no expression of interferons

or Mx1 in control RTgill-W1cells while cells stimulated with LPS or poly(I:C) or with both simultaneously upregulated interferon and Mx production. Moreover, poly(I:C) was shown to reduce viral replication of VHSV in RTgill-W1 cells while LPS was found to be less effective in delaying viral replication (Al-Hussinee et al., 2016). poly(I:C) was also shown to be an effective inducer of interferon stimulated genes (ISGs) like Mx in BF-2 cells (Saint-Jean & Pérez-Prieto, 2006), and interferon-1 and Mx-1 and -3 in RTgill-W1 cells (Poynter et al., 2015a). The upregulation of TLR3, IFNβ and Mx2 upon stimulation with poly(I:C), suggests that, the antiviral response in rainbow trout gill epithelial cells follows the TLR3 signaling pathway (Børre Robertsen, 2008) which depends on induction by viral particles.

IFNβ and innate immune response gene Mx2 were upregulated by LPS in polarized RTgill-W1 cells (Figure 2.7). The antiviral function of LPS in fish has not yet been reported. Thus, the mechanism involved in antiviral response upon LPS stimulation in RTgill-W1 cells is not clear. However, studies in mammalian cell lines demonstrated LPS induced antiviral response. For example, in mouse primary peritoneal exudates cells (PECs), LPS has been shown to induce IFNβ and NO production (Ito et al., 2005). IFN-α/β induction by LPS has also been reported in mouse macrophages (Gao et al., 1998). Tafalla et al. (2001) have reported the production of Nitric Oxide (NO) by turbot kidney macrophages in response to LPS stimulation and NO had previously been shown to inhibit the replication of VHSV (Tafalla et al., 1999). Later, NO was also shown to inhibit viral replication cycle of several mammalian viruses including SARS CoV (Akerstrom et al., 2005) and Adenovirus (Cao et al., 2003). Mehta et al. (2012) reported the role of NO as an alternative antiviral factor in primary mouse embryonic fibroblast cells.

NO and NO synthetase (NOS) have been identified in fish gill epithelium (Ebbesson et al., 2005; Hyndman et al., 2006; Mistri et a., 2018; Tipsmark & Madsen, 2003). In rainbow trout gill, inducible nitric oxide (iNOS) expression has been shown to be induced by parasitic infection (Bridle et al., 2006) and bacterial infection (Ward et al., 2003). These together suggest that, in the rainbow trout gill epithelia, LPS induced interferon induction might follow the alternative antiviral pathway where NO acts as an intermediate product. It would, therefore, be necessary to investigate the effects of LPS on NO production in RTgill-W1 cells.

In the study, PGN induced an antiviral response in RTgill-W1 cells by upregulating TLR3, IFNβ and Mx2 (Figure 2.7). PGN has been reported to induce interferon production in mammalian cells. PGN synthesized from *Lactobacillus rhamnosus* has been shown to upregulate interferon α, β and γ production in mice (Clua et al., 2017). Liu et al. (2004) have also reported interferon induction (IFN α/β production) and subsequent reduction of viral replication of vaccinia virus in RAW 264.7 cells (murine macrophage) by the stimulation of PGN synthesized from *Bacillus alcalophilus*. This study confirms that PGN stimulation of antiviral response may be through conserved activation pathways in vertebrate history.

2.4.3 Traditional cell culture vs transwells

Since the development of cell culture techniques, *in vitro* studies have become more popular than *in vivo* studies as *in vitro* studies alone allow consistent and reproducible experimentation. Cell culture also supports the 3R (replacement, refinement and reduction) agenda (https://www.nc3rs.org.uk/). However, in the case of epithelial cells *in vitro* studies do not reflect the *in vivo* situation as the epithelial cells typically develop polarization which is reduced or lost in conventional cell culture systems but can be retained in transwell culture. Epithelial cells cultured in permeable inserts (transwells) can mimic the *in vivo* condition (Srinivasan et al., 2016). Polarisation of epithelial cells can be retained in the transwell systems. In the present study, tight junction response and antiviral response of RTgill-W1 cells in conventional cell culture and in transwell system culture were compared.

Upon stimulation with poly(I:C), an immediate antiviral response in the transwell system was observed within 30 min while in conventional culture the antiviral response was detected much later at 24 h post stimulation. Moreover, a 4 to10 fold higher antiviral responses by RTgill-W1 cells upon stimulation with bacterial LPS and PGN in the transwells were also shown. A 5- to 23-fold higher expression of the tight junction mRNA ZO-1was also observed in RTgill-W1 cells cultured on transwells upon stimulation with LPS and PGN highlighting the importance of polarization. Innate immune response has also been shown in polarized epithelial cells expressing IL-6 in response to bacterial infection (Healy, Cronin, & Sheldon, 2015). Taken together it demonstrates that fully polarised epithelial cells respond significantly faster than non-polarized epithelial cells. Polarized epithelial cells grown onto the transwells can uptake molecules from both apical and basal surfaces which resembles the *in vivo* situation allowing a faster response to stimuli. Clearly cell polarity is important

in a balanced immune response as failure of the formation of apico-basal polarity has been shown to be associated with human cancer development. For example, adenovirus E4-ORF1 oncoprotein has been found to interact with several cellular proteins including ZO-1 localizing to the tight junction of epithelial cells resulting in blocking functional tight junction formation and polarization of MDCK cells (Latorre et al., 2005).

2.4.4 Perception of viral and bacterial PAMPs by RTgill-W1 cells

The first step of innate immune response is the recognition of pathogens or the molecules associated with the pathogens. Upon recognition pathogens or PAMPs are internalized into the cells. Sometimes, pathogens enter cells through the hosts' mechanisms of internalization. Thus, to block the entry of the pathogens into the cells, it is crucial to know the underlying mechanisms of internalization. In the present study, the mechanisms involved in the recognition of poly(I:C), LPS and PGN by RTgill-W1 cells was studied by using flow cytometry.

Poly(I:C) is a well-known dsRNA analogue that is recognized by TLR3 in the endosomal compartment where it plays a key role in initiating an antiviral state. In this study, a low percentage of cells was found to internalize fluorescein-labelled poly(I:C), although a strong and rapid antiviral response had been shown even at a low concentration (1µg/mL) of poly(I:C) (Figure 2.6). On the other hand, LPS was found to be internalized in polarized and non-polarized trout gill epithelial cells (18.94±1.3%). To reveal the LPS signalig pathway in trout gill epithelia, a potential inhibitor Cytochalasin (CyD) was used to selectively block actin polymerization. CyD significantly reduced (71-78%) the internalization of LPS.

CyD is cell-permeable and is a potent inhibitor of actin polymerization that disrupts actin microfilaments (May et al., 1998) by inducing the depolymerization of the actin cytoskeleton. CyD selectively blocks endocytosis of membrane bound and fluid phase markers from the apical surface of polarized cells without affecting the uptake from the basolateral surface (Gottlieb et al., 1993). CyD has also been found to inhibit infections by viruses that enter cells by apical endocytosis in polarized MDCK cells (Gottlieb et al., 1993). It therefore, appears that LPS internalization in rainbow trout gill epithelia follows the actin-dependent endocytosis pathway. In a study by Lu et al. (2018) the scavenger receptor class B 2a (PaSRB2a) mediated internalization of LPS in ayu (*Plecoglossus altivelis*)

macrophages has been reported. As Class-A scavenger receptor has been identified in RTgill-W1 cells earlier (Poynter et al., 2015b), it is tempting to speculate that this receptor might be involved in the endocytosis pathway of the observed LPS internalization in trout.

However, in mammals and some fishes with TLR4 orthologs, LPS is known to be sensed by TLR4. Suzuki et al. (2003) demonstrated that internalization of LPS in human intestinal epithelial cells may take place through TLR4 dependent and independent pathways. As TLR4 is not present in the rainbow trout genome, thus, the pathway by which LPS is recognized by trout gill epithelia remains unclear. However, a recent study demonstrated a non-canonical pathway of sensing LPS by zebra fish caspase caspy2 in zebra fish cell line ZF4 (Zhang et al., 2018).

Another bacterial PAMP, in the current study, MDP has also been found to be internalized in both polarized and non-polarized epithelial cells. However, the internalization was not significantly reduced by CyD (6-11% inhibition) indicating an actin independent uptake. For further investigation of the internalization pathway, several other inhibitors include Lisinopril (an angiotensin converting enzyme inhibitor), cefradine (antibiotic known to inhibit autolysin which breaks down PGN) (Foster et al., 2000) and L-histidine (a proteinogenic amino acid with peptide uptake inhibitory properties (Song, Hu, Wang, Smith, & Jiang, 2017)) have been used in the present study. The inhibition of MDP uptake was found to be 30%, 24% and 17% respectively (Figure 2.13). In a study, MDP uptake into MDCK cells has been shown to be reduced by around 75-85% by lisinopril and cefradine, and by 50% by histidine (Song et al., 2017) suggesting peptide/histidine transporter 1(PHT1) mediated internalization. Therefore, partial inhibition of MDP internalization in the RTgill-W1 cells by Lisinopril, cefradine and L-histidine supports PHT1 mediated internalization.

2.5 Conclusion

The findings of the current study suggest faster antiviral response of trout gill epithelial cells when cultured on transwells rather than when cultured in conventional cell culture system due to polarization. Bacterial and viral PAMPs can increase the epithelial resistance and upregulate tight junction mRNA expression in RTgill-W1 cells. Bacterial and viral PAMPs also trigger an innate immune response in RTgill-W1 cells. Bacterial LPS internalization in RTgill-W1 cells is mediated by actin dependent endocytosis whereas MDP internalization follows PHT mediated actin independent endocytosis.

Chapter 3

Cellular response and signalling in RTgill-W1 cell upon stimulation with viral and bacterial PAMPs through activation of phosphorylation cascades

3.1 Introduction

Rapid signal transduction from cell membrane receptors to the nucleus relies on different mechanisms such as the post-translational modification (PTM) of proteins. PTMs of proteins can alter the location of a protein within the cell, can trigger the specific interaction with other proteins, enzymatic activity or the stability of substrate proteins. Several PTMs have been described in cell systems being ubiquitination, acetylation and phosphorylation the best characterised molecular switches in cell signaling (Deribe et al., 2010). Protein phosphorylation is a reversible process by which a phosphate group from ATP (or other nucleoside phosphates) is esterified to specific amino acids by protein kinases. Generally, the most common sites (amino acids) of phosphorylation identified in eukaryotes are serine, threonine and tyrosine which comprise approximately 78.7-90, 10.3-18.5 and <1-2.8% of total phosphoproteome respectively (Arrington et al., 2017; Olsen et al., 2006; Bo Zhai et al., 2008; Wang et al., 2013; Zhu et al., 2017). Pphosphorylation at histidine, aspartate, cysteine, lysine and arginine residues have also been reported although at a very low percentage (Liu & Chance, 2014). The addition of a phosphoryl group adds a – 2 charge at physiological pH provoking conformational changes to proteins. Moreover, phosphorylation creates docking sites for interaction with other proteins by domains that recognise phosphorylated residues (reviewed by Deribe et al., 2010).

Phosphoproteins are regulated by a network of protein kinases, phosphatases and phospho-binding proteins that are able to modify the phosphorylation state of proteins, recognise unique phosphopeptides or target particular proteins for degradation (reviewed by Liu and Chance, 2014). Although both kinases and phosphatases have been recognised to be very important for signal transduction, it is currently understood that while kinases control the amplitude of the signal, phosphatases are key dictators of the rate and duration of the signal (Hornberg et al., 2005). In humans, more than 500 kinases have been described to control protein phosphorylation. Most characterised kinases are serine/threonine kinases. Protein kinases have a conserved structural motif, which include an activation loop, a catalytic domain and ATP binding domain. Protein kinases often catalyse the phosphorylation of

proteins and are themselves substrates for other protein kinases creating signal amplification as the activity of the first kinase is magnified by the catalytic activity of the other kinases downstream, a mechanism used by mitogen-activated protein kinases (MAPKs) (Morrison 2012). Kinases are able to recognise highly conserved regulatory motifs. However, kinase specificity varies and as result while on average in humans each protein kinase may phosphorylate a few dozen proteins some protein kinases are highly specific while others are likely to phosphorylate hundreds of distinct proteins within cells (i.e.) (Litchfield, 2003).

Traditionally, the study of phosphorylation events has been studied in a targeted manner by the use of phosphorylation-specific antibodies. However, recent advances in proteomics technology, which include phosphopeptide enrichment, high-accuracy mass spectrometry and associated bioinformatics tools make it now possible to analyse the phosphoproteome in an untargeted manner without initially relying on antibodies (Macek et al., 2009).

There are several issues that should be considered before starting phosphoproteomics experiment. Sample preparation steps prior to LC-MS analysis can have important role on the final results. The amount of protein that is used for analysis is a critical point to get reasonable number of phosphoproteins. Use of an appropriate protease for sample digestion is also important. The most commonly used enzyme is trypsin, which cleaves proteins at the carboxyl terminus of arginine and lysine residues (Beltran & Cutillas, 2012). Isolation of phosphopeptides from the mixture of more abundant unmodified peptides is also a critical step in the phosphoproteomics workflow (Montoya et al., 2011). To overcome this complexity, several enrichment techniques are used. Enrichment using TiO_2 based columns is a popular choice with showing good reproducibility (Cutillas, 2015; Zhu et al., 2017). Recently, a high select TiO_2 phosphopeptide enrichment kit has been introduced which has been shown to capture more 97% phosphopeptides (Choi et al., 2017). For the identification and functional and molecular characterization of proteins, many different bioinformatics tools are available. Uniprot (https://www.uniprot.org/) and NCBI (https://www.ncbi.nlm.nih.gov/) are the most comprehensive protein databases. For gene ontology analysis, motif and kinase enrichment analysis, subcellular localization, functional characterization based on orthologous groups, gene conversion from one species to another, protein-protein interaction, signaling pathway analysis, several tools are available. Some of the commonly used platforms are *Enrichr* (http://amp.pharm.mssm.edu/Enrichr/), cytoscape (https://cytoscape.org/) and gene ontology consortium (http://geneontology.org/), Gene

STRING (https://string-db.org/) for protein-protein interaction and pathway analysis, eXpression2Kinases (X2K) Web (http://X2K.cloud), KSEA web (https://github.com/casecpb/KSEA) and KEA2: Kinase Enrichment Analysis 2 (http://www.maayanlab.net/KEA2/) for kinase enrichment analysis, motif-X (http://motif-x.med.harvard.edu/) and pLogo algorithm (https://plogo.uconn.edu) for motif analysis. *Enrichr* is also useful for kinase and pathway analysis. However, most of these bioinformatics tools are suitable for human, rat or other mammalian species. Some tools have the possibility to work with an underlying zebrafish database. Thus, bioinformatics analysis for other fish species is mainly based on mammalian functional information which in some cases might be inappropriate to other vertebrates. To this aim, it is required to convert fish proteins or genes accession numbers to human or zebra fish proteins or genes homologs to do some of the analyses. If there is not a human homolog then the information of those proteins is lost.

Over the years, a substantial number of the gene expression studies in fish have been conducted based on the transcriptome analysis and sometimes the proteins have been deduced from the transcriptome which may be inaccurate in many cases. Few studies have analysed the phosphoproteome of zebrafish (Kwon et al., 2016; Lemeer et al., 2008; Lemeer et al., 2008) while as a non-model organism, rainbow trout has been studied focusing on the transcriptome in response to pathogens and PAMPs (Rebl et al., 2014). Very few studies have been conducted on the proteomics or phosphoproteomics of rainbow trout providing only partial information of phosphoproteomics data (Long et al., 2015).

The molecular innate immune responses and tight junction gene expression in rainbow trout gill epithelial cells have been studied and demonstrated in previous chapter (Chapter 2). The innate immune responses have been found to be modulated by viral and bacterial PAMPS. Cellular integrity of trout gill epithelia has also been found to be modulated by viral and bacterial PAMPs while tight junction gene has been partially induced by PAMPs. Thus, to investigate the molecular mechanisms that are involved in innate immune response including signal transduction pathways and cellular integrity, phosphoproteome of trout gill epithelia in steady state and PAMPs induced state was studied. The present study included the identification of phosphoproteins with their sub-cellular localization, molecular and cellular functions, identification of different motifs and associated kinases and different signaling pathways in stimulated and non-stimulated RTgill-W1 cells by applying label free

in-solution quantitative phosphoproteomics using TiO_2 enrichment-based LC-MS/MS analysis.

3.2 Materials and methods

3.2.1 Cell culture, stimulation and cell lysis

Rainbow trout gill epithelial cells RTgill-W1 were maintained in L-15 medium with 10% FBS. Cells were grown in 75 cm^2 flask. Ninety to ninety five percent sub-confluent culture was used for the experiment. The experiment was conducted in 6-well format transwell with a membrane pore size of 0.4 micron having a growth area of 4.2 cm^2. Cells were seeded at a density of 0.8×10^6 cells per insert and were maintained until they reached confluency. Then cells were stimulated with poly(I:C) and muramyl dipeptide (MDP) at a concentration of 10 µg/mL for 30 min. Control cells were treated with DMSO as a mock stimulation. Lysates from 4 inserts of each treatment were pooled together. Conditions tested were as follow: control (n=4 biological replicates), MDP (n=3 biological replicates) and poly(I:C) (n=5 biological replicates). After 30 min of stimulation, cells were washed three times with PBS followed by cell lysis with 400 µL lysis-buffer (1 % (w/v) Sodium deoxycholate in 50 mM ammonium bicarbonate and 1% phosphatase inhibitor cocktail (v/v) (Thermo Fisher Scientific, Hemel Hempstead, UK) per insert. All chemicals were from Sigma Aldrich (Dorset, UK) unless otherwise specified.

3.2.2 Protein quantification and visualisation by 1D SDS-PAGE

Protein quantification was performed using BCA assay according to the manufacturer's instructions (Interchim Uptima, France) using Bovine Serum Albumin (BSA) (stock 2mg/ml) as standard. Protein samples (25 µL) were dispensed in 96 well plates together with 100 µL of working solution. Plates were incubated for 30 min at 37°C, cooled at room temperature and the absorbance was read at 562 nm using a BioTek Synergy HT 96-well plate spectrophotometer (BioTek, USA). To check the quality and integrity of the cell protein lysates extracted proteins from each sample were visualised by 1-Dimensional Sodium Dodecyl Sulphate Polyacrilamide Gel Electrophoresis (1D SDS-PAGE gel).

1D SDS-PAGE: Ten micrograms of protein was mixed with 2 Laemmli sample buffer (Bio-Rad, UK) at a ratio 1:1, then incubated in a heat block (Thomas Scientific, USA) at 100°C for 10 min. Samples were centrifuged for 3 min at 16,000 × g, then 25 µL of each sample

and 5 µL protein standard (Precision Plus Protein™ Standards, 10-250 kDa from Bio-Rad, USA) were loaded into each well of a 4-15%, 10-well comb, 30 µL Mini- protean TGX precast gel (Bio-Rad, UK). Gels were electrophoresed in 1x Lamelli SDS electrophoresis buffer (Tris base 250 mM, Glycine 1.92 M, SDS 1% in double distilled water) at 100 v for 90 min and then stained with SimplyBlue™ Safe stain (Thermo Fisher Scientific, Hemel Hempstead, UK) overnight in mild shaking following 3 washes each wash with mili-Q water for 1 h in mild shaking. Finally, the gel was visualized and scanned using an Epson expression 1680 artist scanner (Epson, USA).

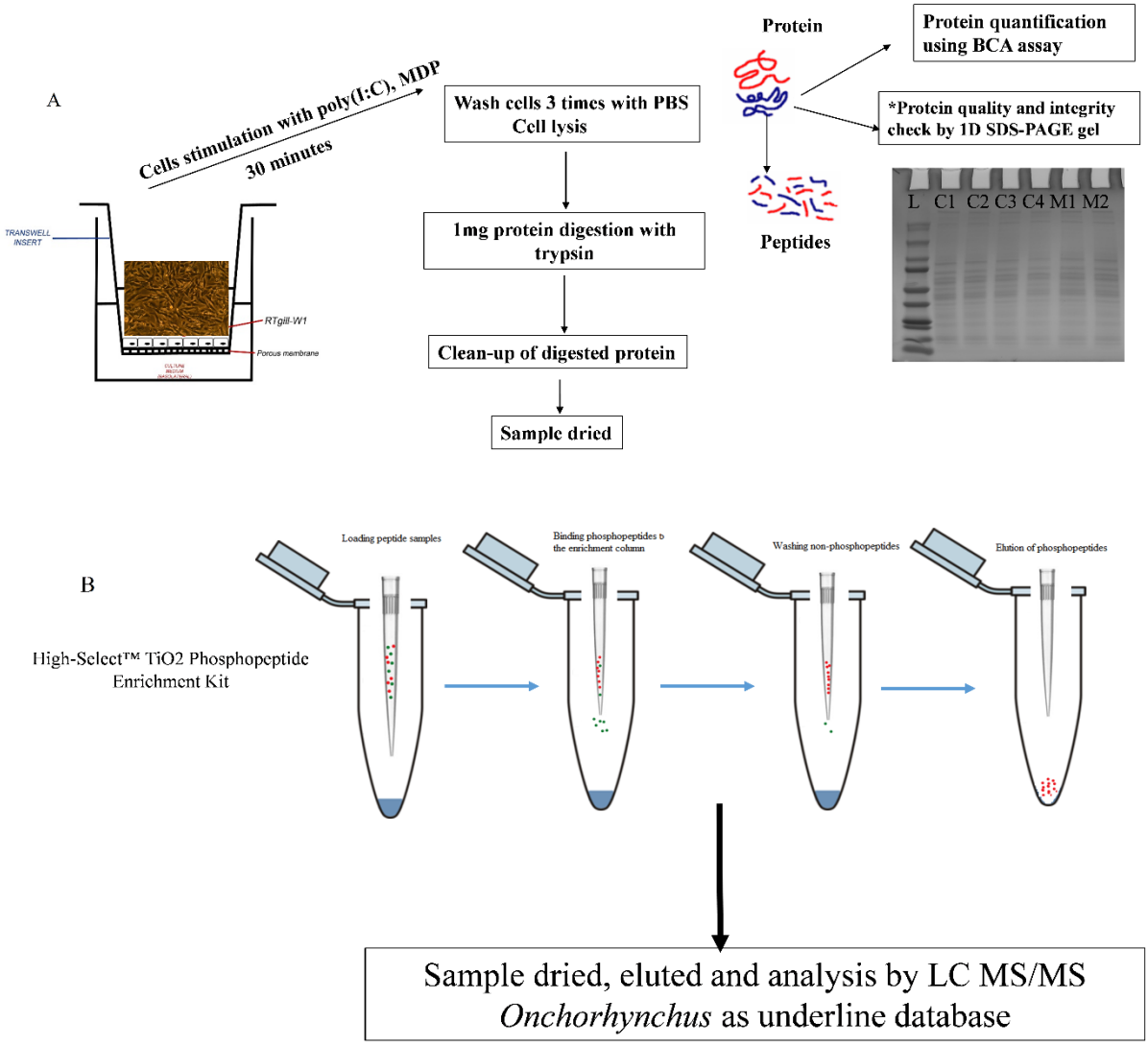

Figure 3.1: Illustration of phosphoproteomics workflow. A) Cell culture, stimulation, collection of cells using lysis buffer, protein quantification and digestion, B) enrichment of phosphopeptides using enrichment kit.

3.2.3 Trypsin digestion

One miligram of protein was used as the initial input. Protein samples were dried in Savant DNA 110 SpeedVac® Concentrator and re-suspended in 400-500 µL of 2 mM DTT (Bio-Rad, UK) in 50 mM ammonium bicarbonate (Sigma-Aldrich, UK) by vortexing until protein dissolved completely. Samples were then incubated for 60 min at 37°C followed by another incubation for 60 min at 37°C in dark after adding 200 mM freshly prepared iodoacetamide (IAA) (Fisher Scientific, Leicestershire, UK) at 5 µL/100 µL of sample. Then 10 µL of 200 mM DTT per 105 µL of sample were added followed by further incubation for 30 min at room temperature in dark. Finally, sequencing grade modified trypsin (Promega, UK) was added in a trypsin to protein ratio of 1:100 and incubated at 37°C overnight in dark. On the following day, the digestion was stopped by adding 96% formic acid (Fisher Scientific, Leicestershire, UK) to a final concentration of 1%.

3.2.4 Clean-up of the tryptic digestion

Clean-up of digested samples was performed using HyperSep™ SpinTips (Thermo Fisher Scientific, Hemel Hempstead, UK) according to the manufacturer's instruction. Briefly, first the spin tip was washed three times with 50 µL of releasing solution (40% of 0.1% formic acid (Fisher Scientific, Leicestershire, UK) in miliQ water plus 60% of acetonitrile (Fisher Scientific, Leicestershire, UK)) by pushing through with syringe, followed by washing three times with 50 µL of binding solution (1% formic acid (Fisher Scientific, Leicestershire, UK) in miliQ water) in the same way. Then the samples were loaded to the spin tips using 50 µL each time. Spin tips were washed three times with binding solution followed by elution of sample in 50 µL of releasing solution. Second elution was done during which the sample was wetted with releasing solution and incubated for 5 min and pushed through with syringe. Eluted samples were directly dried for enrichment or stored at 4°C until further usage.

3.2.5 Phosphopeptide enrichment

Phosphopeptide enrichment was done using High-Select TiO_2 Phosphopeptide enrichment kit (Thermo Scientific, Hemel Hempstead, UK). Before starting, all solutions were equilibrated at room temperature for around an h. Lyophilized peptide samples were re-suspended in 150 µL of Binding/Equilibration Buffer. The pH of re-suspended samples was verified (acidic pH, <3 is recommended for optimum binding). The TiO_2 spin tip was conditioned by washing the column in 20 µL of Wash Buffer followed by centrifugation at

3,000 × *g* for 2 min followed by another centrifugation at 3,000 × *g* for 2 min with 20 µL of Binding/Equilibration Buffer. The next step was the addition of 150 µL of peptide samples to the TiO_2 spin tip and incubation for 5 min at room temperature followed by centrifugation at 1,000 × *g* for 5 min. Samples were reapplied in the spin tip column and centrifuged at 1,000 × *g* for 5 min. The next step was wash step where the TiO_2 spin tip was washed by adding 20 µL of Binding/Equilibration Buffer and centrifuged at 3,000 × *g* for 2 min followed by washing by adding 20 µL of Wash Buffer and centrifugation at 3,000 × *g* for 2 min. These steps were repeated once. Finally, phosphopeptides were eluted in 50 µL of phosphopeptide Elution Buffer. The elution buffer was added directly to the TiO_2 spin tip and was centrifuged at 1,000 × *g* for 5 min. Elution step was repeated once. The eluted phosphopeptides were dried in Savant DNA 110 SpeedVac® Concentrator and stored at -80°C until analysis by LC-MS/MS.

3.2.6 LC MS/MS

The digested and enriched phosphopeptides were analysed using a Dionex Ultimate 3000 RSLS nano-flow system (Dionex, Camberley UK). Samples were reconstituted in 10 µL of water and a volume of 5 µL were loaded onto a Dionex 100 µm × 2 cm 5 µm C_{18} nano-trap column at a flow rate of 5 µL min^{-1}. The composition of the loading solution was 0.1% formic acid and ACN (98:2). Once loaded onto the trap column samples were washed off into an Acclaim PepMap C_{18} nano-column 75 µm × 15 cm, 2 µm 100 Å at a flowrate of 0.3 µL min^{-1}. The trap and nano-flow column were kept at 35°C in a column oven in the Ultimate 3000 RSLC. Samples were eluted with a gradient of solvent A: 0.1% formic acid and ACN (98:2) versus solvent B: 0.1% formic acid and ACN (20:80) starting at 5% B rising to 50% B over 100 min. The column was washed using 90% B before being equilibrated prior to the next sample being loaded. The eluant from the column was directed to a Proxeon nano-spray ESI source (Thermo Fisher, Hemel, UK) operating in positive ion mode then into an Orbitrap Velos Fourier Transform (FTMS). The ionisation voltage was 2.5 kV and the capillary temperature was 200°C. The mass spectrometer was operated in MS–MS mode scanning from 380 to 2000 amu. The top 20 multiply charged ions were selected from each full scan for MS/MS analysis, the fragmentation method was HCD at 30% collision energy. The ions were selected for MS2 using a data dependant method with a repeat count of 1 and repeat and exclusion time of 15s. Precursor ions with a charge state of 1 were rejected. The resolution of ions in MS1 was 60,000 and 7500 for MS2.

3.2.7 MS data processing

LC-MS/MS data were processed initially uploading the raw spectra data into Thermo Proteome Discoverer 1.4 (Thermo Scientific, Hemel Hempstead, UK). Peak picking was performed under default settings for FTMS analysis such that only peptides with signal to noise ratio higher than 1.5 and belonging to precursor peptides between 700-8,000 Da were considered. Identification of peptide and protein was performed with SEQUEST algorithm. An in house compiled database containing proteins from the latest version of the UniProt SwissProt database (2017) was compiled to include only *Oncorhynchus mykiss*. The search parameters were: Tryptic cleavage with 2 missed cleavages; static modification was carbamidomethyl of cysteines; allowed dynamic modifications were oxidation of methionine and phosphorlyation of serine, threonine and tyrosine. Precursor tolerance was set at 10 ppm and MS2 tolerance was set at 0.05 Da. Resulting peptides and protein hits were further screened by excluding peptides with an error tolerance higher than 10 ppm and by accepting only those hits listed as high and medium confidence by Proteome Discoverer software. The confidence of peptide matching was based on the false discovery rate (FDR). FDR threshold was set at 0.05, therein data was comprised by both peptides identified with high confidence (FDR<0.01) and medium confidence (FDR<0.05).

3.2.8 Protein identification

Protein identification was based on the presence of at least one unique peptide and quantification was based only on unique peptide(s). An *Oncorhynchus mykiss* uniprot database (https://www.uniprot.org) was used to match peptide sequences to protein identity (accession numbers). Sequences of uncharacterised proteins were blasted in BLASTp of NCBI (https://blast.ncbi.nlm.nih.gov/Blast.cgi) (McGinnis & Madden, 2004). The protein homologies were selected according to the criteria (identity >80%, E value <0.001) demonstrated by Pearson (2014).

After phosphoprotein identification, the number of phosphoproteins were visualised by Venn diagram using online tool BioVenn (http://www.biovenn.nl) showing the unique and shared phosphoproteins by the different groups. Shared phosphoproteins were further analysed by t-test ($p<0.05$) using Microsoft Excel and presented by volcano plot using RStudio version 1.0.153.

3.2.9 Identification of phosphoprotein localization

Predicted sub-cellular localization of phosphoproteins was obtained using WoLF PSORT algorithm (https://wolfpsort.hgc.jp) based on both known signal motifs and their amino acid sequence features having over 80% prediction accuracy (Horton et al., 2007). The protein sequences were uploaded into the algorithm and the prediction of sub-cellular localization was made based on the highest identity to the database.

3.2.10 Gene Ontology (GO) annotation and kinase enrichment analysis (KEA)

Enrichr (http://amp.pharm.mssm.edu/Enrichr; Chen et al., 2013; Kuleshov et al., 2016) tool was used to perform GO and kinase enrichment analysis (KEA). Since the tool supports only human, mouse and rat genes, best matched human counterparts of the trout genes identified in rainbow trout were used. To this end, trout protein accession numbers were blasted in NCBI against zebrafish (*Danio rerio*) and zebrafish uniprot protein IDs were exported. The gene symbols of respective proteins of zebrafish were then extracted using the biological DataBase network (https://biodbnet-abcc.ncifcrf.gov/db/db2db.php). Finally, zebrafish gene symbols were then converted to human gene symbols using OrthoRetriever tool (http://lighthouse.ucsf.edu/orthoretriever/). The procedure of extracting tentative gene list of human counterparts of relevant trout sequences has been illustrated in figure 3.2. Adjusted p-value and combined score were considered for GO annotation and kinase prediction where the combined score was described by Chen et al. (2013) as $c = \log(p) \times z$, where c = the combined score, p = Fisher exact test p-value, and z = z-score for deviation from expected rank.

For general cellular and molecular characterization of phosphoproteins identified in salmonid gill epithelia in steady state and stimulated conditions, all the phosphoproteins identified in each group were used for GO analysis. Kinase enrichment analysis was also performed using all the phosphoproteins in each group. The bigger data set was used to draw a more complete picture of phosphoproteome in fish gill epithelia for each tested condition.

3.2.11 Pathway analysis

The gene symbols of human counterparts of the identified rainbow trout proteins were used in *Enrichr* and significantly enriched ($p<0.05$) KEGG pathways were predicted. Relevant KEGG pathways for human were exported and the pathways were adopted for the genes

identified in rainbow trout using the tool Pathvisio (https://www.pathvisio.org/). Similar to GO annotation and KEA, all the phosphoproteins identified in each group were used for pathway analysis to have overall picture regarding the signaling pathways activated in steady state and stimulated RTgill-W1 cells.

3.2.12 Phosphorylation motif analysis

Phosphopeptide sequences were uploaded to pLogo algorithm (https://plogo.uconn.edu) for the identification motifs present in each data set (O'Shea et al., 2013). The whole phosphopeptide data from each treatment group were used to identify motif which would allow to identify main kinases involved in the phosphorylation events in rainbow trout gill cells at stimulated and control conditions. Sequences were centered on each phosphorylation site and extended to a total length of 15 amino acids (±7 residues). When the site was located in the N/C-terminal of the protein, the sequence was filled up to 15 amino acids with the required number of "X". The sequences of proteins from rainbow trout identified in this study were used as a background dataset. For the graphical presentation of the identified motifs, logo-like representations were generated for each motif using pLogo based on their statistical significance ($p<0.05$).

3.2.13 Kinase identification by literature search

From the motif substrates, kinases can be predicted. Motif substrates, identified in RTgill-W1 cells, were associated with literature (Schwartz and Gygi, 2005; Pearson and Kemp, 1991; Villen et al., 2007; Leighton et al., 1995; Burch et al., 2004; Pinna and Ruzzene, 1996). Then the Kinases were identified from the literature search.

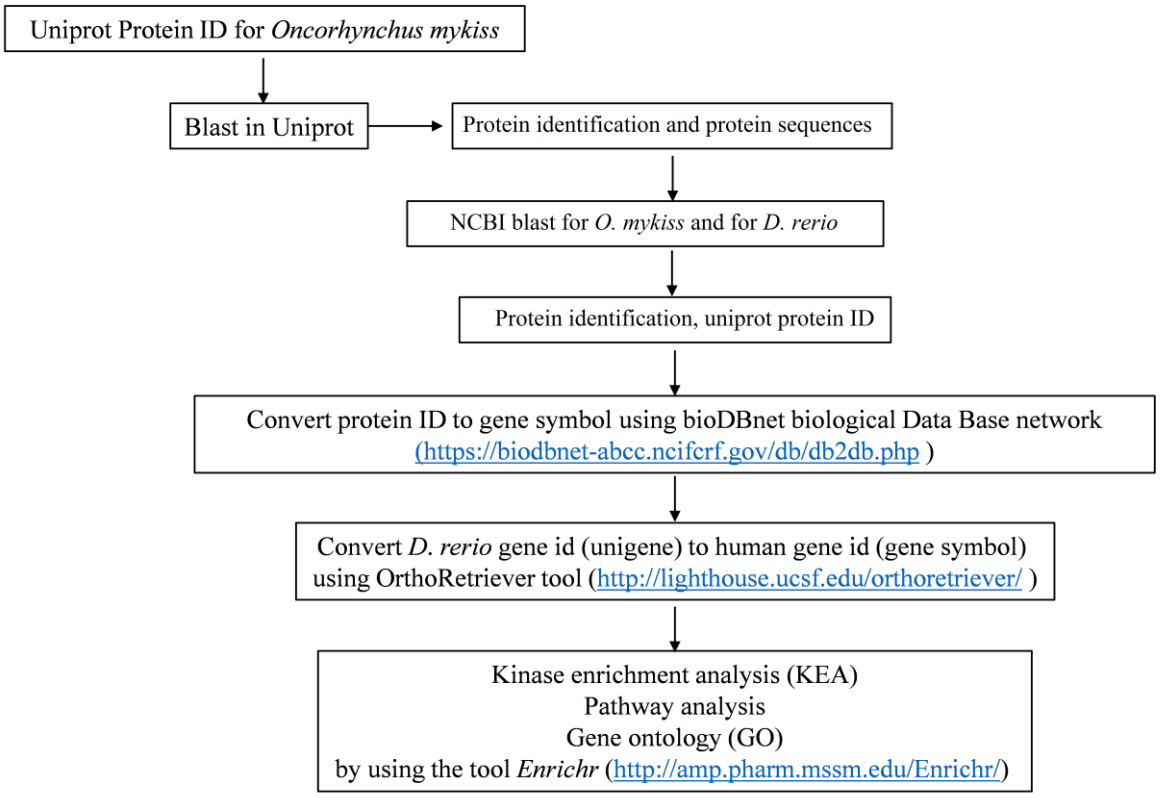

Figure 3.2: Workflow of phosphoprotein analysis for KEA, pathways and GO.

Phosphoproteins were also classified based on the functional annotation of orthologous groups. For this Discover EggNOG version 4.5.1 (http://eggnog.embl.de; Huerta-Cepas *et al.*, 2016) which utilizes the database of GO and KEGG, was used. The protein sequences of the identified phosphoproteins from the uniprot database were used to find the functional groups.

3.2.14 Statistical analysis

Phosphoprotein abundance between groups was compared by t-test using Microsoft Excel where differences between groups were considered statistically significant at $p<0.05$.

3.3 Results

3.3.1 Phosphoproteome analysis of RTgill-W1 cells

To study the signalling mechanisms involved in the molecular innate immune responses, the phosphoproteome of RTgill-W1 cells was analysed by LC-MSMS following phosphopeptide enrichment in steady state and in cell stimulated with poly(I:C) and MDP-Rhodamine independently for 30 min. Phosphopeptide enrichment, yielded similar percentage of phosphorylated peptides in all samples which was 83.23±7.58%, 78.40±2.61% and 83.30±5.33% (mean±SD) respectively in control, MDP and poly(I:C) treatment groups (Figure 3.3a). However, although the percentage of phosphopeptide enrichment was similar, the number of phosphopeptides identified was higher in poly(I:C) stimulated cells (1,388 phosphopeptides) compared to control (734 phosphopeptides) and MDP stimulated cells (666 phosphopeptides). In total, 1,789 phosphopeptides were identified, 751 peptides of which were unique in poly(I:C) stimulated cells (Figure 3.3b).

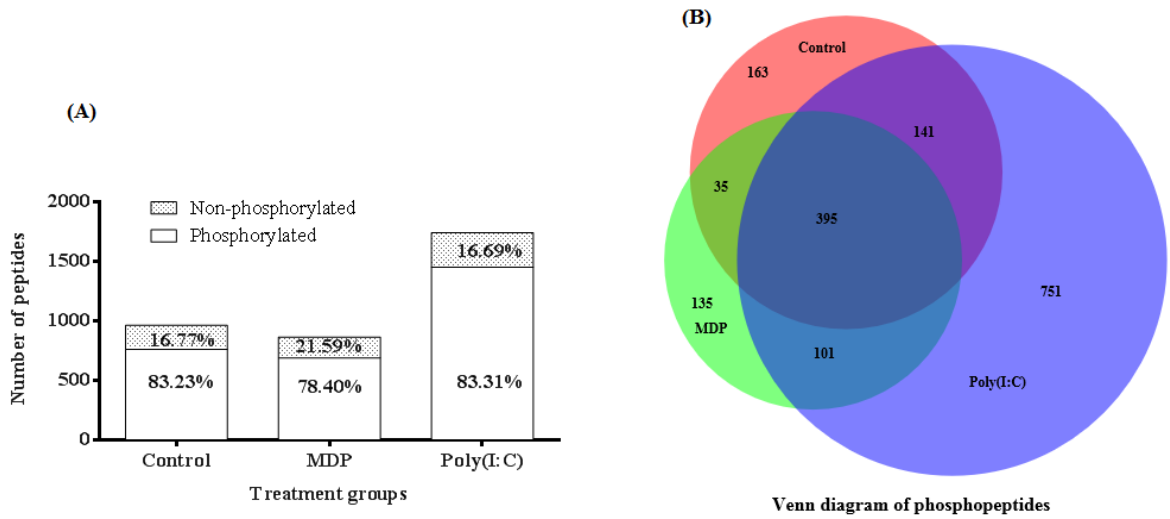

Figure 3.3: Phosphopeptides identified in RTgill-W1 cells in different treatment groups. (A) Stacked histogram showing the number and percentage of phosphopeptides and non-phosphopeptides in different groups. (B) Venn diagram showing the number of phosphopeptides shared and unique between different treatment groups.

A total of 2,612 phosphorylation sites were detected in 1,789 phosphopeptides. More than half of the phosphopeptides were monophosphopeptides (65%) whereas 30% were diphosphopeptides (Figure 3.4A). The distribution of phosphorylated amino acids was similar in all samples, ranging from 70.72-73.80% pSer, 20.05-21.55% pThre and 5.91-7.23% pTyr (Figure 3.4 B-D).

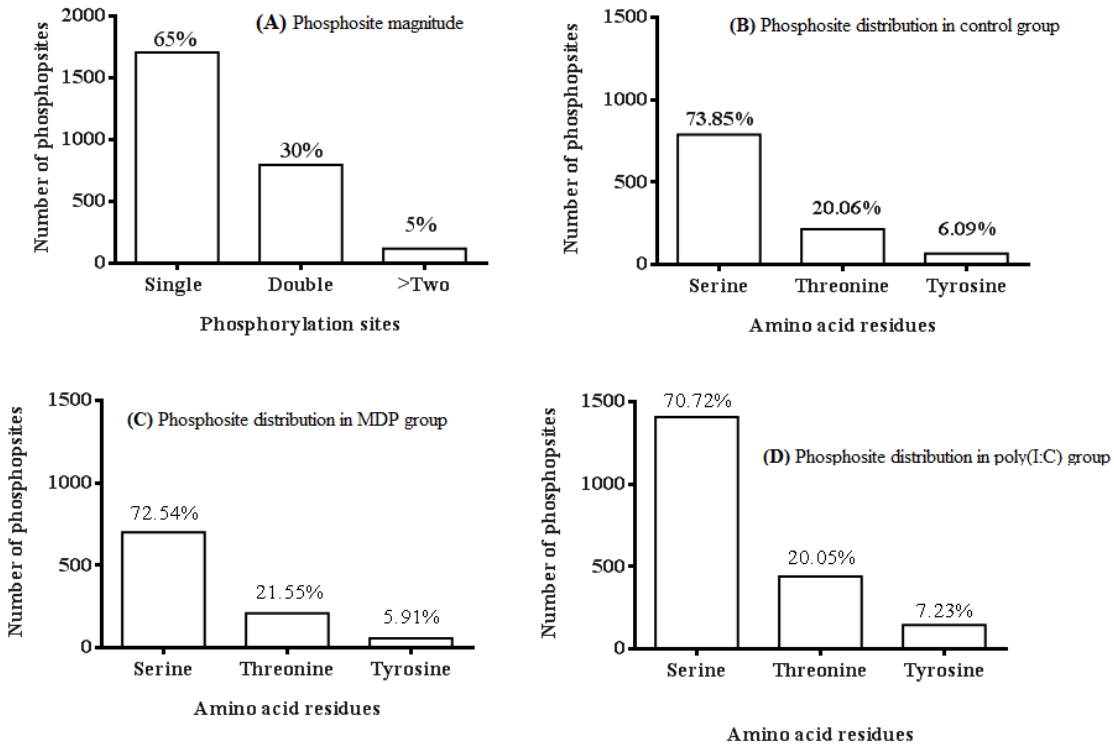

Figure 3 4: Phosphorylation sites at Serine, Threonine and Tyrosine residues. Phosphorylation sites were detected in LC-MS/MS using Proteome discoverer. (A) Phosphorylation frequency in each peptide at different residues, number and percentage of phosphosites at each residue in control (B), MDP (C) and poly(I:C) (D) stimulated cells.

Phosphopeptide identifications compiled at protein level resulted in the identification of 691 phosphoproteins in total, with poly(I:C) group comprising 597 phosphoproteins, 360 of them being unique (Figure 3.5). Information on the phosphoproteins identified available in Supplementary Table S3.2. Phosphoproteins shared in all the groups were further analysed and presented in volcano plot. Among the shared phosphoproteins, 5 phosphoproteins (Thymosin β 11, Lupus La protein homolog B-like, Sequestosome 1-like, Laminin-A-like and heat shock 70kDa protein) were significantly upregulated in poly(I:C) treated cells compared to control cells (t-test, $p<0.05$; Figure 3.5 C) while one phosphoprotein (scaffold attachment factor B2-like isoform X1) was significantly upregulated in MDP compared to the control group (Figure 3.5D). Moreover, compared to MDP treatment, 2 phosphoproteins (Thymosin β 11 and, Sequestosome 1-like) were significantly upregulated in poly(I:C) stimulated cells (Figure 3.5C).

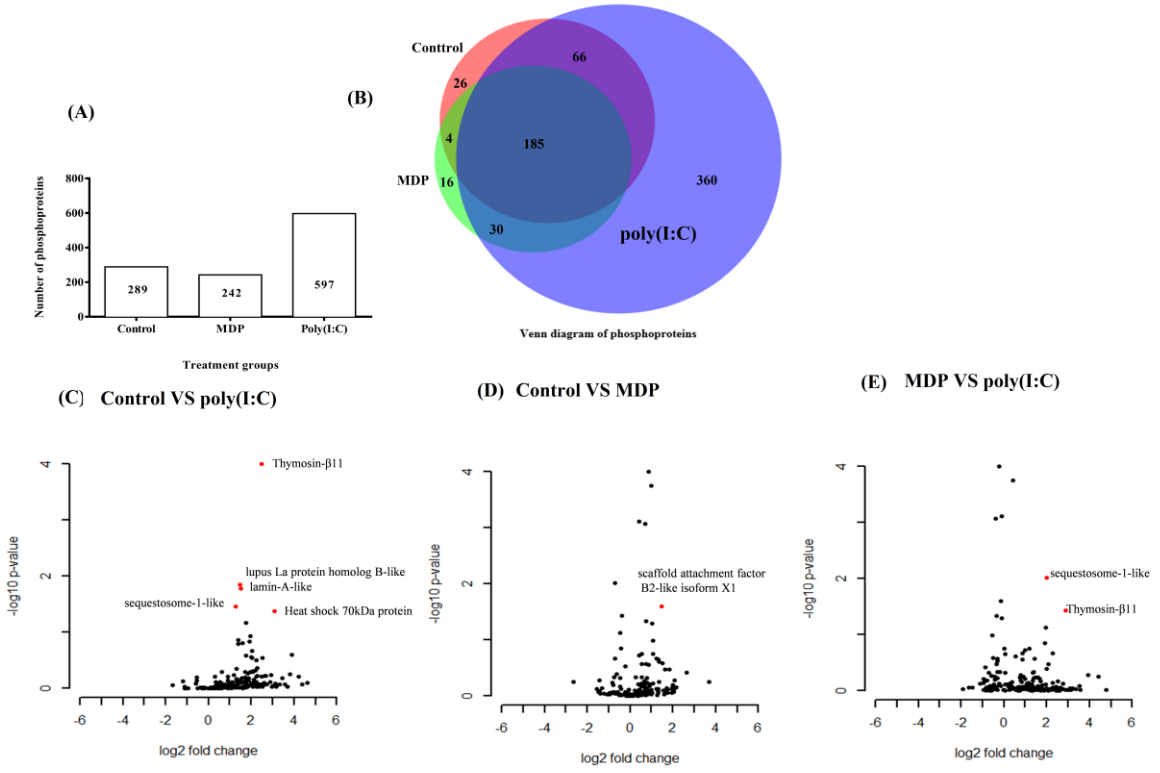

Figure 3.5: Number of phosphoproteins identified in RTgill-W1 cells in different groups. (A) Actual number of phosphoproteins in control, MDP and poly(I:C) stimulated cells. (B) Venn diagram showing the distribution of phosphoproteins in different groups. (C-E) Volcano plot of shared proteins between different treatment groups, (C) Control vs MDP, (D) Control vs poly(I:C), (E) MDP vs poly(I:C). Red dot represents significantly higher abundance of protein between groups, $p<0.05$. Phosphoprotein abundance between treatment groups was analysed by t-test using Microsoft excel and presented by volcano plot using RStudio version 1.0.153.

3.3.2 Phosphoprotein localization

Localization of the phosphoproteins was predicted using the WoLF PSORT algorithm (https://wolfpsort.hgc.jp). Most of the phosphoproteins were predicted to be localized in the nucleus and cytoplasm, which comprised around 80% of total phosphoproteins identified (Figure 3.6). Other predicted subcellular locations were mitochondria, plasma membrane, extracellular membrane and cytoskeleton. Interestingly, phosphoproteins localized in the cytoskeleton were found only in poly(I:C) stimulated cells. Similarly, the percentage of phosphoproteins residing in the extracellular and plasma membrane was higher in poly(I:C) stimulated cells compared to control cells. However, similar cellular distribution of phosphoproteins was observed in control and MDP stimulated cells except for mitochondria

where the percentage was lower for MDP stimulated cells compared to control cells and for plasma membrane where the percentage was higher in MDP stimulated cells compared to control cells. Full data are available in Supplementary Table S1.

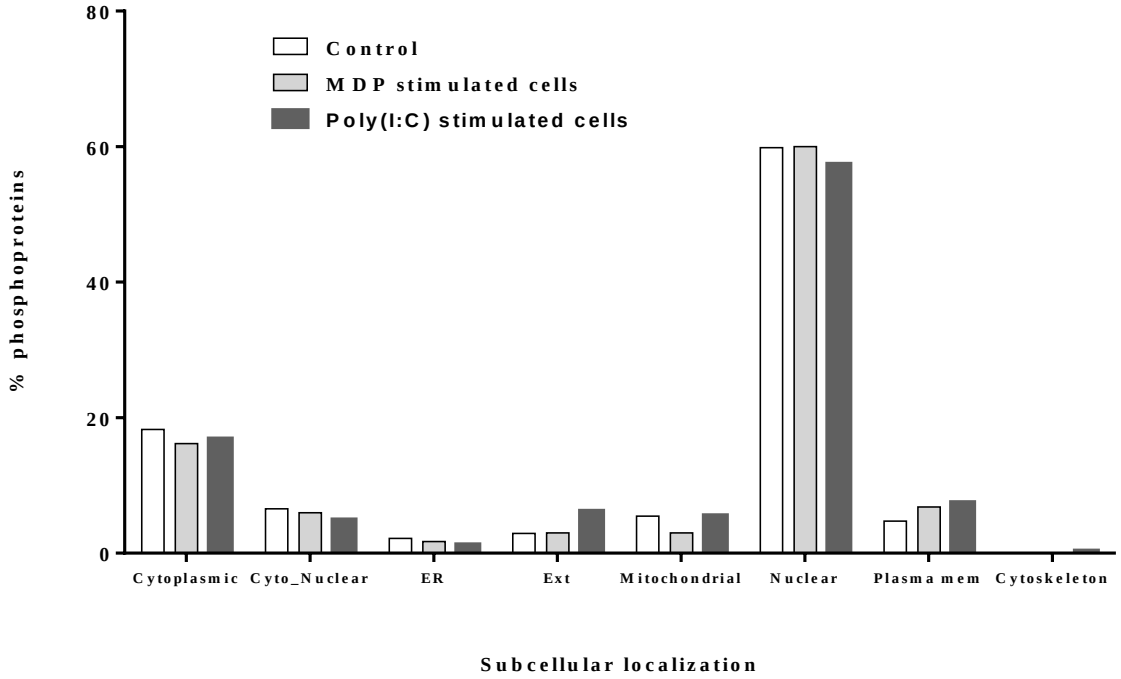

Figure 3.6 : Localization of phosphoproteins identified in different treatment groups. Bar with same colour shows the percentage of phosphoproteins in specific localization in the respective treatment group.

3.3.3 Gene ontology (GO) enrichment analysis of phosphoproteins

The *Enrichr* tool was used for GO enrichment analysis. Based on annotations obtained according to biological processes, an enrichment in phosphoproteins associated with RNA and mRNA processing, regulation and metabolism was obtained. Many of the biological processes like cytoskeleton organization, signal transduction, regulation of cytoskeleton organization and protein kinase activity were found only in the poly(I:C) stimulated cells (Figure 3.7A).

In case of molecular functions, an enrichment in binding and receptor activity including RNA binding was found. Transmembrane signalling receptor and G-protein coupled receptor activity related proteins were found only in poly(I:C) stimulated cells (Figure 3.7B). In most cases, significantly higher enrichment was found in poly(I:C) stimulated cells compared to control and MDP stimulated cells (Figure 3.7).

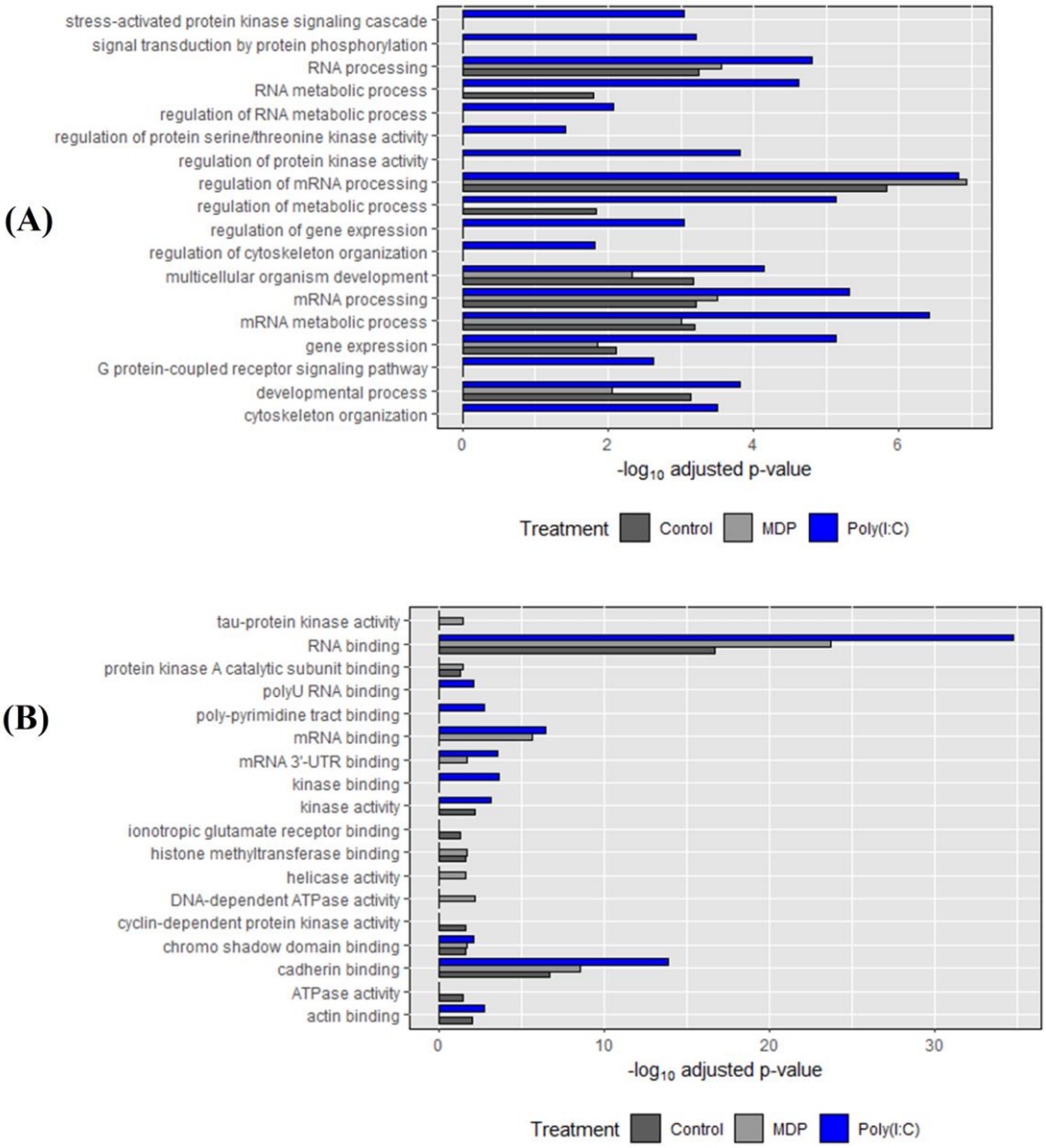

Figure 3.7: Gene ontology (GO) enrichment analysis of the identified proteins. (A) Biological processes and (B) molecular function of phosphoproteins identified in control, MDP and poly(I:C) stimulated cells sharing each component of GO. Rainbow trout protein accession numbers were converted to zebra fish protein accession number followed by conversion to zebra fish gene symbol which were further converted to human gene symbol. Human gene symbols were analysed using the tool *Enrichr* for each treatment group for gene ontology. Top 10 entries of each category (on the basis of combined score, which was described by Chen et al., 2013) were then plotted against the negative logarithm of adjusted p values ($p<0.05$).

To visualise the phosphoprotein functional groups in a different way, all the phosphoproteins were classified according to the Discover EggNOG 4.5.1 (http://eggnog.embl.de) tool which provides functional characterization for the inferred orthologous groups. All the phosphoproteins belonged to 20 different functional groups (detailed presented in the Supplementary Table S1). Based on the number of phosphoproteins in a specific function group, the top 5 molecular functions were signal transduction (K), RNA processing (A), transcription (T), post translational modifications (M) and cytoskeleton (Z). The percentage of phosphoproteins involved in signal transduction and cytoskeleton organization was higher in poly(I:C) stimulated cells whereas proteins related to RNA processing and post translational modifications was higher in the control and MDP stimulated cells (Figure 3.8).

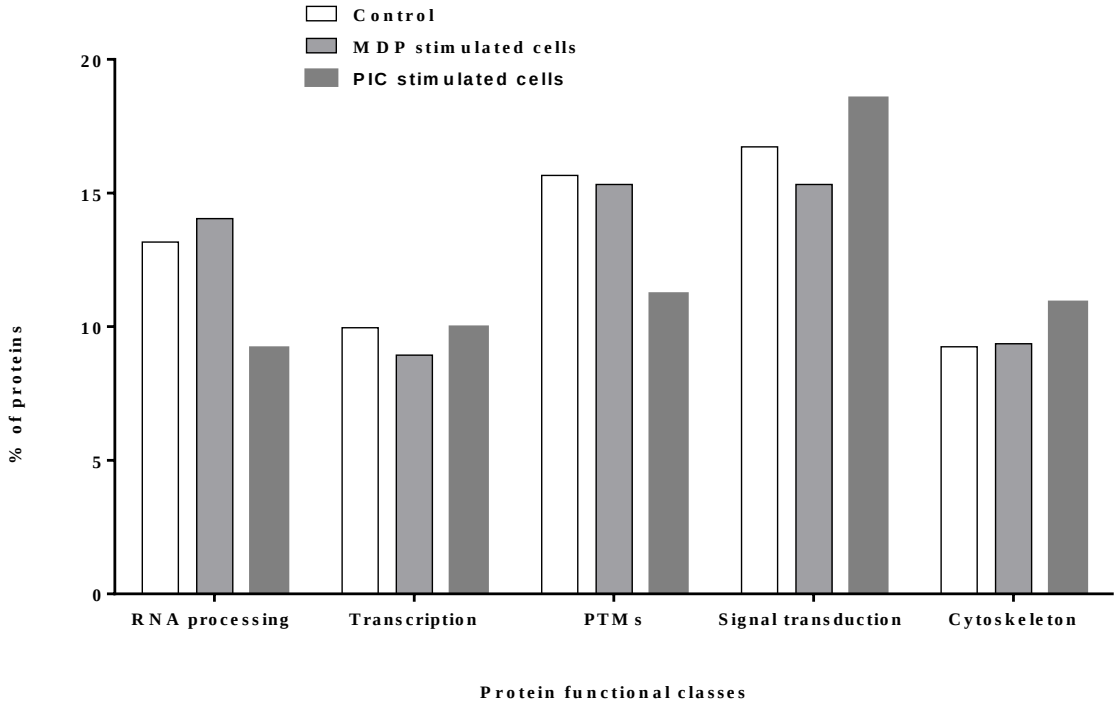

Figure 3.8: Top 5 functional groups and percentage of phosphoproteins identified in RTgill-W1 cells of different treatment groups.

3.3.4 Motif analysis and kinase prediction

Motif sequences using the phosphopeptide sequences of each treatment group were analysed using the plogo tool (https://plogo.uconn.edu/). To find the significant motifs from the phosphopeptide data, first, overall motifs were identified for each group for serine and threonine residues (Figure 3.9). Individual motifs were then extracted from the overall motifs for serine and threonine residues for each group (Supplementary Figure S1). The plogo tool provides some statistical information like foreground data (FG), background data

(BG), percentage matching of specific motif with the foreground data and values (scores). The value or score provides the strength of the prediction for the motif.

For serine residue, around 90 different motifs were detected in all three groups where 39 of them were unique in poly(I:C) treated cells. MDP treated cells had 9 unique motifs. However, phosphopeptides in control cells did not show any unique motifs. In the case of threonine residue, only 4 motifs were identified where 2 of them were unique in poly(I:C) treated cells. However, only 2 and 1 motifs were detected respectively in control and MDP treated cells at threonine residue. No significant motifs were found for phosphotyrosine residue in any of the groups.

Associated kinases for the motif substrates were identified by literature search where some of the kinases from motif sequences were identified (Table 3.2). However, the kinases were predicted based on the motif substrates of human database. For most of the motifs, associated kinases could not be found in the literature. Complete list of kinases identified from motif substrate has been presented in Appendix: 3, Supplementary Table S 3.5 and 3.6. The most enriched kinase detected in the study was proline directed MAPK kinase. However, casein kinase was the most prevalent kinase which had many substrate specificities. Several protein kinases like PKA, PKB and PKC were also identified from the motif sequences.

3.3.5 Motif and kinase in differentially expressed phosphoproteins

To identify the involvement of any specific motif and kinase in the phosphoproteins that were differentially expressed in the poly(I:C) stimulated cells, motif analysis using the phosphopeptides of the diffefentially expressed phosphoproteins were used where only one motif (…D…pS…….) and one kinase CK2 was identified (Table 3.1).

Table 3.1 Differentially expressed phosphoproteins from poly(I:C) stimulated cells along with phosphopeptides, related kinases and functions

Differentially expressed phosphoproteins	Phosphopeptides	Functions of proteins	Motif and kinase
Thymosin	KTEpTQEKNPLPTK	Actin monomer binding, actin filament organization (Litwack, 2018)	…D…pS……. CK2 (Songyang et al., 1996)
Lamin-a	EEERLRLpSPSPPPTR GGTATPLpSPTR LNDNDpSETSSLAGGAVTR LSPpSPPPTR	Structural function and transcriptional regulation in the nucleus (Andrés & González, 2009).	
Sequestosome	GGKDAGGpSGDEEWTHVTSK DAGGpSGDEEWTHVTSK EVDPSTGELQpSLR DPGGpSGDDEWTHLTSK VMpTPNPSPPGSGGPPSAR	Main role in autophagy (Pankiv et al., 2007); Also involved in translation, ribosomal structure and biogenesis (Ciani et al., 2003).	
Lupus la	FDDGDNDDAPPpSPK DSpSPPREPIIDVHR FDDGDNDDAPPpSPK KIIEDQQEpSLNK KPEDpSSTPR KTKFDDGDNDDAPPpSPK KTKFDDpSDDDAPPSPK LDFNNKVLpTDETK SQSEADLSPQSpTETQQR TLLApSSFSIR VpTGVSADQEER pYRPSEESQR	RNA processing and binding (Alfano et al., 2004).	
Heat shock 70 KDa	TSpSGDSpSQGPTIEEID	Response to heat (Rendell et al., 2006); also functions in immune responses (Tsan & Gao, 2009).	

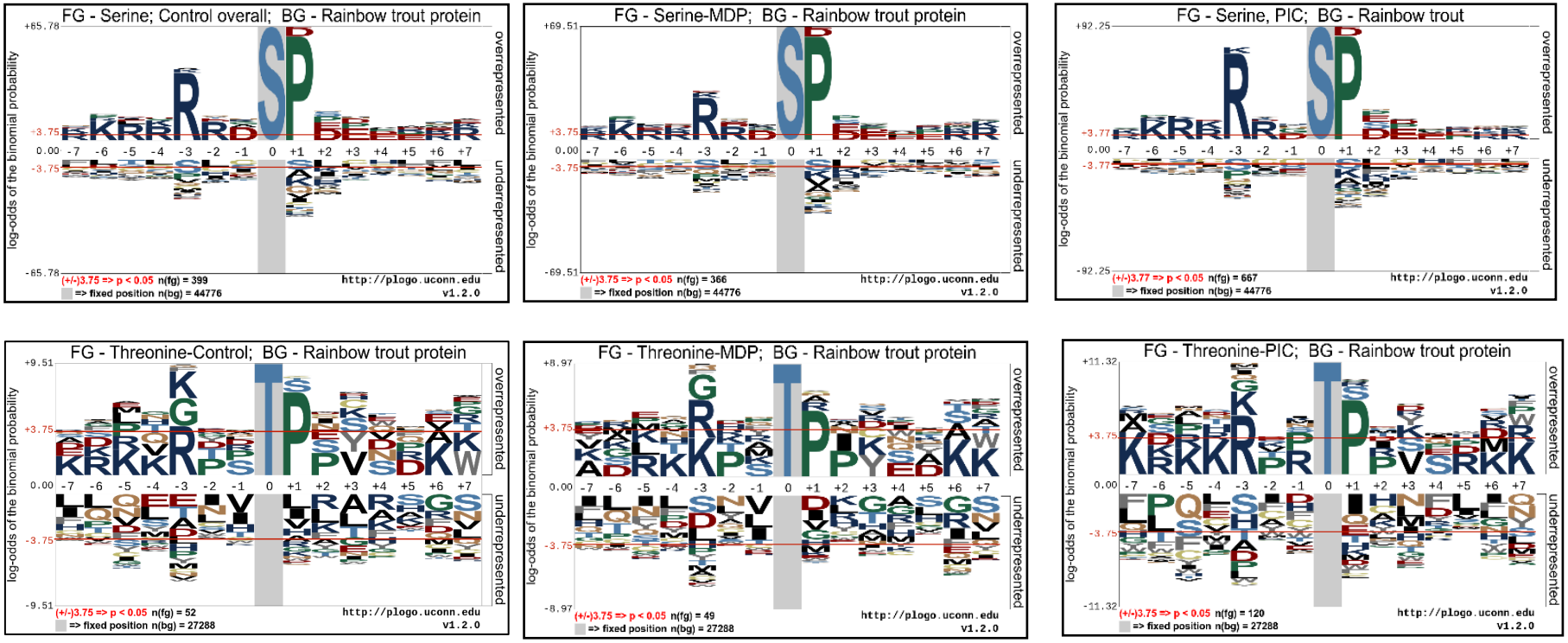

Figure 3.9: Overall pLogos for motifs of control, MDP and poly(I:C) treated cells illustrated by serine (S); top three and threonine (T); bottom three pLogos were derived from phosphorylation sites in rainbow trout (*Oncorhynchus mykiss*) phosphopeptides. In each pLogo, residue heights are proportional to their log binomial probabilities in the context of the rainbow trout protein background with residues above the x-axis indicating overrepresentation and residues below the x-axis indicating underrepresentation ($p<0.05$). The central residue in each pLogo is fixed and denotes the phosphorylation site. The n(fg) and n(bg) values at the bottom of each pLogo indicate the number of aligned foreground and background sequences respectively. The pLogos and corresponding extracted motifs have been presented in supplementary Figure S3.1 and Table S 3.5 and 3.6.

Table 3.2: List of kinases identified from the phosphorylation sites in RTgill-W1 cells in the study. Number in the parenthesis represents percentage probability.

Motif	Kinases	Foreground[a] aligned			Background[b] aligned			Reference
		Control	MDP	Poly(I:C)	Control	MDP	Poly(I:C)	
.....sP.....	Proline directed MAPK	156(60.19)	153(63.74)	242(84.78)	3910	3910	3910	(Schwartz & Gygi, 2005)
....R..s.....	CaMK II	121(39.26)	96(25.97)	210(70.53)	3455	3455	3455	(Pearson & Kemp, 1991)
.....R.s.....	Protein Kinase B kinase (PKB)	61(10.8)	52(8.21)	96(14.77)	2653	2653	2653	(Pearson & Kemp, 1991)
..R....s.....	Casein II Kinase	64(9.4)	52(6.09)	111(16.81)	3102	3102	3102	(Pinna & Ruzzene, 1996)
...R...s.....	cGMP dependent protein kinase	58(8.05)	48(5.5)	85(8.52)	2900	2900	2900	(Pearson & Kemp, 1991)
.....s.D.....	CaMK II	49(6.58)	43(5.37))	77(8.64)	2500	2500	2500	(Schwartz & Gygi, 2005)
.....s.E.....	Glucokinase	49(4.0)	48(4.64)	79(5.39)	3128	3128	3128	(Schwartz & Gygi, 2005)
....RR.s.....	Protein Kinase A kinase (PKA)	22	-	32	320	-	320	(Pearson & Kemp, 1991)
......DsD.....	CK2 like	18	17	23	256	256	256	(Schwartz & Gygi, 2005)
.....sD.E....	CK2	21	20	33	297	297	297	(Schwartz & Gygi, 2005)
.....sDE.....	CK2	-	10	16	-	2292	213	(Schwartz & Gygi, 2005)
.P..R..s.....	PKB kinase	-	20		-	290	-	(Pinna & Ruzzene, 1996)
...K...s.....	PKA kinase	-	-	77	-	-	2864	(Pearson & Kemp, 1991)
....K..s.....	PKA kinase	-	-	76	-	-	2824	(Pearson & Kemp, 1991)
..R.R..s.....	p70 S6 kinase	-	-	35	-	-	535	(Leighton et al., 1995)
...RR..s.....	ZIP kinase	-	-	29	-	-	393	(Burch et al., 2004)
...KR..s.....	PKA/PKC kinase	-	-	33	-	-	286	(Pearson & Kemp, 1991)

.....sD.....	CK2		51	40	68	2464	2372	2372	(Villen et al., 2007)
.....s..E....	CK2		63	53	97	3476	3476	3476	(Villen et al., 2007)
.....s.D..E..	CK2		15			238			(Villen et al., 2007)
.....s..E.E..	CK2			18			451		(Villen et al., 2007)
.....Ds.....	CK2			44	65		2464	2464	(Villen et al., 2007)
.....s...E...	CK2				82			3338	(Villen et al., 2007)
.....s.D.E...	CK2				21			238	(Villen et al., 2007)
.....sDEE....	CK2				12			58	(Villen et al., 2007)
.....tP.....	Proline directed MAPK	18	2252		15	2252	30	2252	(Schwartz & Gygi, 2005)
...R...t.....	cGMP dependent protein kinase	11	1427		-	-	21	1427	(Schwartz & Gygi, 2005)

[a] Foreground data set is the sequences within which a motif is searched, and the number is the total peptide sequences that are aligned to the foreground dataset.
[b] Background data set is the proteome of specific organism from where the probability of specific residue of foreground data is determined.

3.3.6 Kinase identification by kinase enrichment analysis (KEA)

To identify the kinases that are responsible for phosphorylation the human counterpart of the genes identified in rainbow trout, were used. The *Enrichr* tool as mentioned earlier was used for kinase enrichment analysis. A total of 105 significant kinases were identified. Kinases with adjusted p value of <0.05 were considered. Based on the adjusted p values, top ten kinases that were identified in all the groups were CDK2, GSK3B, MAPK14, CDK1, RSP6KA3, PRKCB, MAPK1, CHEK1, AKT1 and MAPK3. However, the kinases were more significantly enriched in poly(I:C) treated cells (Figure 3.10). In control and MDP treated cells similar enrichment was observed. Kinases having at least 4 associated genes from the identified genes in rainbow trout gill epithelia have been presented in the Supplementary Table S3.4.

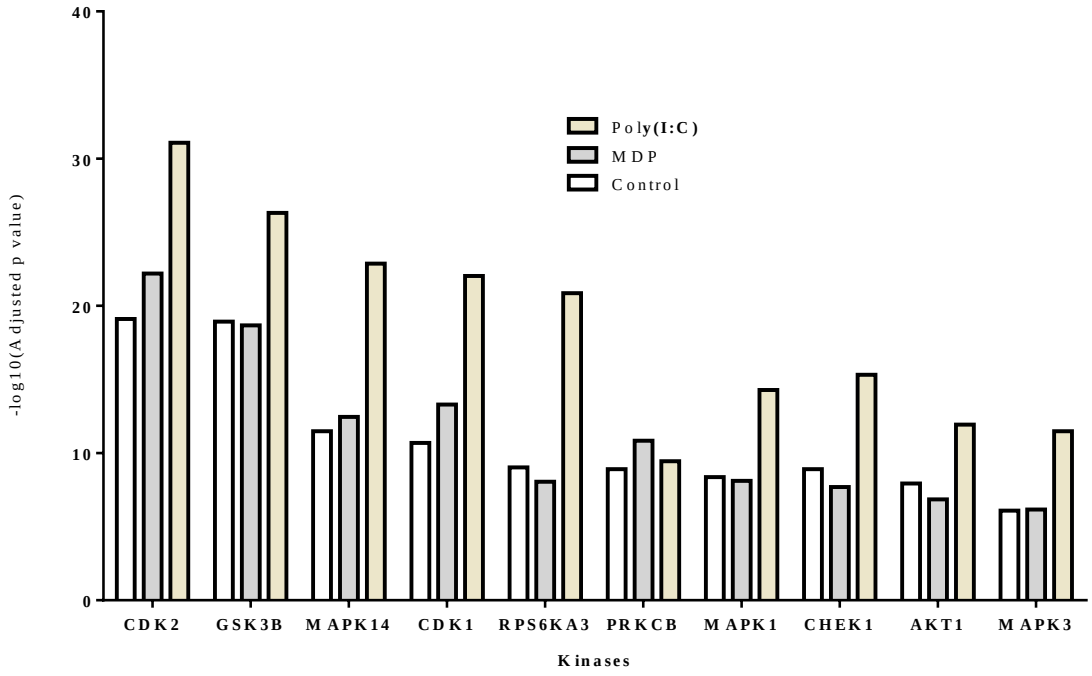

Figure 3.10: Top ten identified kinases using *Enrichr* tool. Top ten kinases were selected on the basis of the combined score given by the tool. Negative logarithm of adjusted p values was plotted in Y-axis while kinases in the X-axis.

3.3.7 Activation of signaling pathways

Pathway analysis was done using the tool *Enrichr*. Several signaling pathways were activated in steady-state and stimulated cells (complete pathway list presented in Supplementary Table S3.3). Pathways here presented were exclusively related to human

pathways as the *Enrichr* uses only the human database and therefore phosphoproteins identified in rainbow trout were converted to human counter gene symbols.

Based on the findings of previous experiment related to cellular integrity, mRNA expression including tight junction and antiviral responses upon stimulation with viral and bacterial PAMPs, several unique and common pathways were found to be activated in control and stimulated cells. Three important pathways related to the previous findings were further explored. One of the important pathways that was found to be activated in all the groups was the spliceosome pathway (Figure 3. 11). In this study, proteins related to all small nuclear ribonucleoproteins (snRNP) groups (U1, U2, U4, U5, and U6) were phosphorylated. Moreover, some other proteins were also identified (Figure 3. 11). Supporting this, in poly(I:C) stimulated cells a higher number of phosphoproteins were identified that were related to this particular pathway.

Another important pathway related to the innate immune responses was the mitogen activated protein kinase (MAPK) pathway which was found to be activated in MDP and poly(I:C) stimulated cells (Figure 3.12). In the present study, Raf and MAP2K2 (MEK), the initiators of MAPK pathway, were phosphorylated. The c-Jun N-terminal kinase (JNK) and p38 pathways were also found to be activated. Moreover, some of the intermediate proteins like MAP4K4, MAP3K1, PAK2, MAP14, MAPKAPK5 and JUN were also phosphorylated. Moreover, MAPK14 was found to phosphorylate TP53 and subsequently activated P53 signaling pathway. Furthermore, a couple of DNA damage related proteins TAOK2 and TAOK3 were also found to be phosphorylated (Figure 3.12).

The third pathway was related to cellular integrity which was regulation of the actin cytoskeleton. This pathway was found to be activated only in poly(I:C) stimulated cells (Figure 3.13). The phosphoprotein associated genes of this pathway were fibronectin binding protein integrins itga4 and itga5, RRAS2 (homology of Ras), raf1a and ARHGEF6 which participated in the activation of regulation of actin cytoskeleton signaling.

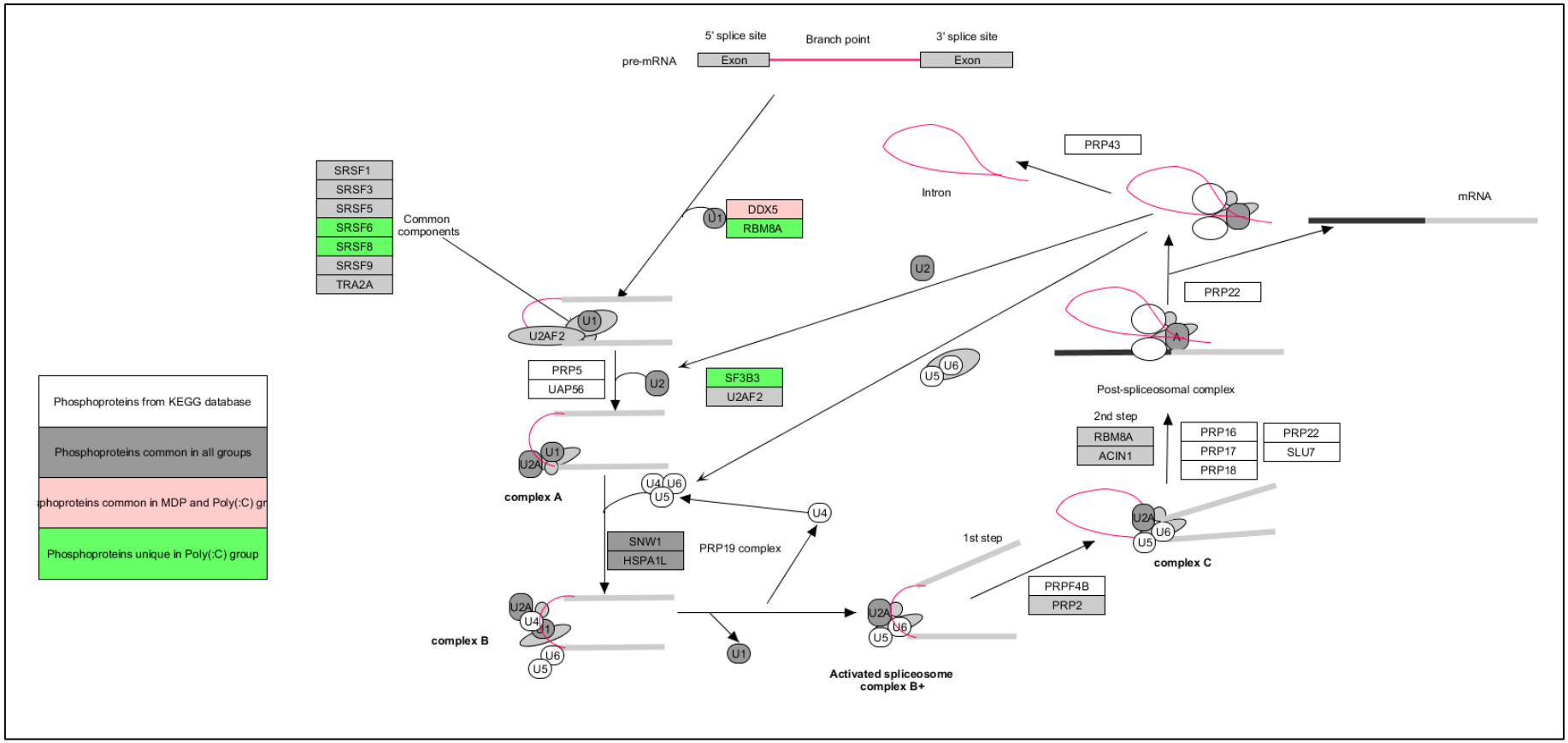

Figure 3.11: Spliceosome signaling pathway. The pathway has been adopted from the KEGG pathway database for Homo sapiens (pathway id hsa03040; https://www.genome.jp/kegg-bin/show_pathway?org_name=hsa&mapno=03040&mapscale=&show_description=hide). The pathway was activated in all the treatment groups. Phosphoproteins in green filled are associated with the phosphorylated proteins identified only in poly(I:C) stimulated RTgill-W1 cells while in pink filled are associated with the phosphoproteins identified in both poly(I:C) and MDP stimulated cells, grey filled are common in all the groups. Phosphoproteins without filled are from the KEGG database.

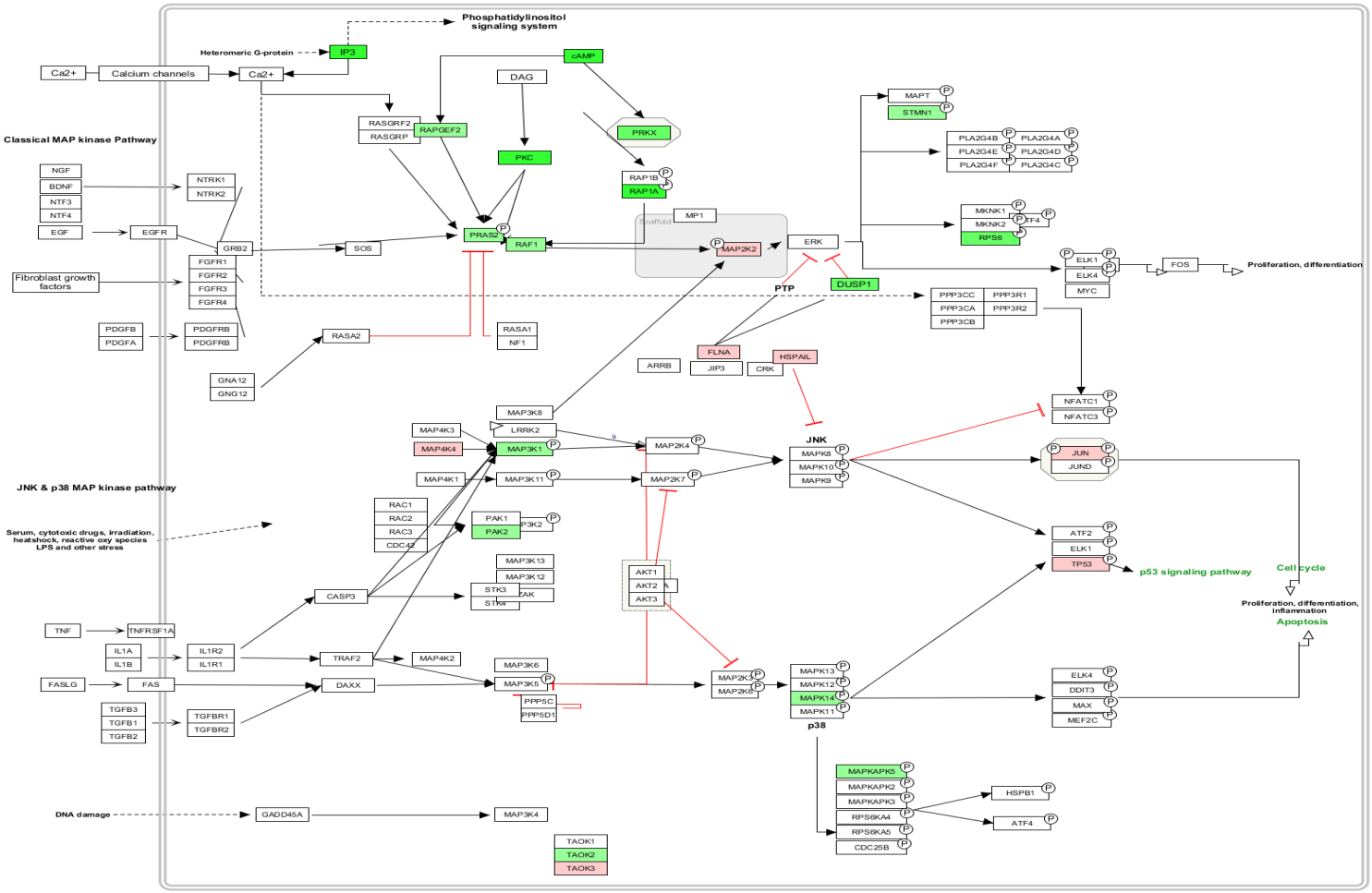

Figure 3.12: MAPK signaling pathway. The pathway has been adopted from the KEGG pathway database for Homo sapiens (pathway id hsa04010; https://www.genome.jp/kegg-bin/show_pathway?org_name=hsa&mapno=04010&mapscale=&show_description=hide). Phosphoproteins in green filled are associated with the phosphorylated proteins identified only in poly(I:C) stimulated RTgill-W1 cells while in pink filled are associated with the phosphoproteins identified in both poly(I:C) and MDP stimulated cells.

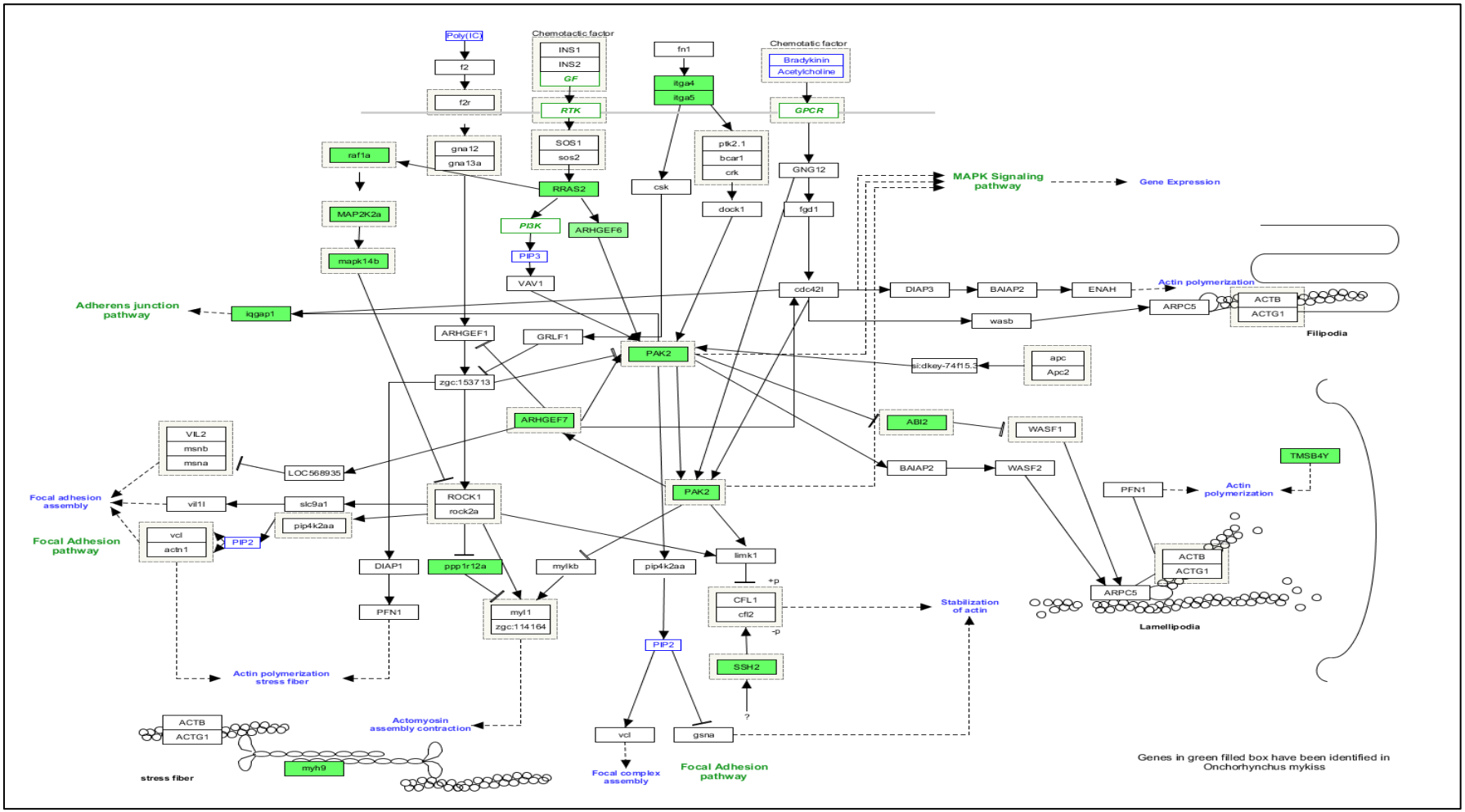

Figure 3.13: Regulation of actin cytoskeleton pathway. The pathway has been adopted from the KEGG pathway database for Homo sapiens (pathway id hsa04810; https://www.genome.jp/kegg-bin/show_pathway?org_name=hsa&mapno=04810&mapscale=&show_description=hide). Phosphoproteins in green filled are associated with the phosphorylated proteins identified in poly(I:C) stimulated RTgill-W1 cells.

3.4 Discussion

3.4.1 Phosphoproteomics method development for fish gill epithelial cells

Global phosphoproteomics using different enrichment strategies coupled to LC-MSMS has been increasingly used specially in mammalian tissue and cell studies (Koch et al., 2016; Villen et al., 2007; Zhu et al., 2017) and in plants (Reiland et al., 2009; Sugiyama et al., 2008; Wang et al., 2013b). However, very few studies on phosphoproteomics have been conducted in fish with work so far focussed on zebrafish (Kwon et al., 2016; Lemeer et al., 2008; Lemeer et al., 2008). In the present study, methods on cell lysis, trypsin digestion, phosphopeptide enrichment and finally bioinformatics for the analysis of the phosphoproteome have been developed for the first time in rainbow trout gill epithelial cells which could be applied for the study of other fish cell systems.

In the present study, TiO_2 based enrichment technique was applied. This approach yielded around 80% of the recovered peptides being actually phosphorylated independently of the treatment. Similar levels of enrichment have been reported in HeLa S3 cells using TiO_2 based enrichment technique (Choi et al., 2017) indicating the capability of this approach to enrich phosphopeptides from complex cell protein samples.

The most challenging part of phosphorylation study in fish is data analysis using current bioinformatic tools. There are a number of tools and software available for phosphoproteome analysis although unfortunately are mainly targeting mammalian organisms. Zebrafish has got attention in the research commonly because of the suitability of this fish to be used as model organism in human disease study. In the present study, different tools were used for fish phosphoproteome data analysis.

Global phosphoproteomic approach has been used to reveal protein phosphorylation in fish gill epithelial cells in the current study where thousands of phosphorylation sites and almost one thousand phosphoproteins were identified from trout gill cell line RTgill-W1. Most of the phosphoproteins were characterized and some were uncharacterized due to the unavailability of information in protein database. A single database or tool has been found unable to provide the necessary information; thus, several tools and protein databases have been tested to characterize phosphorylation events in fish gill epithelia.

3.4.3 Phosphosites in rainbow trout proteome

It is important to determine the site of phosphorylation as phosphosites determine the motif and kinases that are involved in phosphorylation, thus phosphosites provide the information about the function of phosphorylation events. In the current study around 70, 20 and 6% of phosphosites have been found at serine, threonine and tyrosine residues respectively. Similar phosphothreonine percentage have been reported in drosophila embryo by Zhai et al. (2008). However, in human the percentage is around 86, 12 and 2% respectively at serine, threonine and tyrosine residues (Olsen et al., 2006). In zebrafish embryo 88.9, 10.2, and 0.9% of serine, threonine and tyrosine phosphorylation sites have been reported (Kwon et al., 2016). The higher percentage of threonine and tyrosine phosphosites detected in the present study might have roles in cellular mechanisms that are particular in rainbow trout.

3.4.4 PAMP mediated phosphorylation

A viral PAMP poly(I:C) and a bacterial PAMP MDP were used in the study to trigger the phosphorylation events in RTgill-W1 cells. The number of phosphoproteins identified in poly(I:C) stimulated cells was more than double to control cells while MDP stimulated cells and control cells produced similar number of phosphoproteins. However, among the phosphoproteins sharaed by all groups, only 5 phosphoproteins were differentially expressed in poly(I:C) stimulated cells which involved one motif and one protein kinase CK2 (Figure 3.5 and Table 3.1). The functions of those phposphoproteins are related to actin polymerization, transcription and translation (Table 3.1). MDP stimulated cells had only one differentially expressed phosphoprotein involved in transcription. The number of Motifs identified in poly(I:C) stimulated cells were higher than control and MDP stimulated cells. Although similar number of kinases were predicted by kinase enrichment analysis, poly(I:C) showed higher enrichment with higher number of associated genes in each kinase. Moreover, poly(I:C) induced signaling pathways were activated in fish gill epithelia. Even the higher number of phosphoproteins were identified in poly(I:C) stimulated cells and activation of some signaling pathways, no core antiviral signaling pathway such as TLR3 or RLR was not identified by phosphoproteomics in gill epithelial cells as was found to be activated by transcriptomics in poly(I:C) stimulated cells by qPCR assay (chapter 2 and 4). Overall, results confirm that poly(I:C) is, off course, a potent inducer for protein phosphorylation in RTgill-W1 cells.

3.4.5 Motif analysis

Motif identification is also important to find the kinases responsible for the phosphorylation. Several online tools have been tested to identify the motifs at serine, threonine and tyrosine residues. In the present study pLogo tool (https://plogo.uconn.edu) has been used. The tool provides some statistic regarding the strength of the motif. Most of the motifs identified in the present study are at pSer residue (almost 96%) while the rest have been found at pThr residue. Even having 6% phosphotyrosine residue, no motif has been found at pTyr residue. Less than one third of the motifs associated kinases could be identified by literature while others are novel motifs that need further studies to identify related kinases.

As motif analysis depends on the protein sequences, the motif can move around within the protein sequences in evolutionary distant animals thus the position of a motif in a protein might be different between animals (Lee & Yaffe, 2016). Taken together, the novel motifs for which there have not been found any kinases may be associated with a broad spectrum of kinases that play significant role in protein phosphorylation in fish gill epithelia.

3.4.6 Protein kinases

By modifying the substrate activity, protein kinases arbitrate most of the cellular processes including signal transduction, progression of cell cycle, rearrangement of actin cytoskeleton, cell differentiation, metabolism, transcription and many more (Manning et al., 2002). For better understanding of the dynamics of protein phosphorylation networks and their regulation inside the cells, the kinases that are mediating the phosphorylation event need to be known (Newman et al., 2014). More than 500 different kinases have been identified in humans (Manning et al., 2002). In the present study, more than100 different kinases have been predicted in rainbow trout gill epithelial cells. Stimulation with poly(I:C) have been found to play a vital role in activation of different protein kinases.

In cancer biology, protein phosphorylation plays a vital role where protein kinases contribute to the advancement of cancer of nearly every cell type. Thus, the pathways mediated by kinase can be blocked with targeted treatment which have an important clinical-therapeutic application (Ardito et al., 2017). The advancement of phosphoproteomics research has enabled the researchers to identify potential inhibitors against activated tyrosine kinases involved in cancer where some of them are already in use in cancer treatment and many of

them are tested (reviewed by De Castro et al. 2013). Similarly, fish phosphoproteome might be useful in designing and developing antiviral drugs for inhibiting viral replication and infection.

From the motif analysis, the most enriched kinase family that have been identified is proline-directed MAPK which is a subclass of protein serine-threonine kinases that phosphorylate proteins on a serine or threonine residue that is immediately preceding a proline residue. Proline directed kinases include cyclin dependent kinases (CDKs), glycogen synthase kinases (GSK3) and mitogen activated protein kinases (MAPKs).

In the present study, the most prevalent and enriched kinases that have been predicted (by KEA) are cyclin dependent kinases (CDKs) including CDK1, 11A, 14, 15 and 18. CDK1, 14 and 15 have been shown to be involved in cell cycle regulation. CDK inhibitors can be used to stop cell cycle to interrupt cancer development or in the treatment of chronic inflammation (Rossi et al., 2006). However, some CDKs like CDK5, 7, 8, and 9 are involved in transcription, physiology of neuron and homeostasis of glucose (Sausville, 2002). CDK11, apart from cell cycle progression, has been found to play role in promoting pre-mRNA splicing (Hu et al., 2003) while CDK18 has been reported to be involved in signal transduction cascades. The next highly enriched kinase predicted by KEA in the present study is GSK3B which is a member of GSK3 family. GSK3 is an enzyme playing a key role in glycogen metabolism, in one hand, while act as an important component of Wnt pathway on the other hand, which is essential in forming body architecture during embryonic development (Barford, 1996). Another highly enriched and prevalent predicted kinase family is the MAPK including MAPK14, 1, 3, 9, 8 and 10. MAP kinase play a key role in the signal transduction. MAPK has been shown to regulate MAPK pathway controlling many cellular processes including cell proliferation, differentiation and death (Sundaram, 2006).

Another highly enriched kinase that has been identified by motif analysis is Ca^{2+}/calmodulin-dependent protein kinase II (CaMKII). CaMKs phosphorylate proteins in response to the increase of intracellular calcium ion and regulate many genes and transcription factors (Racioppi & Means, 2012; Wayman, Tokumitsu, Davare, & Soderling, 2011).

Casein kinase 2 (CK2) has also been identified by motif analysis and KEA. CK2 has been reported to be involved in cellular processes, such as cell cycle progression, apoptosis and transcription, as well as viral infection. CK2 has also been reported to play role in antiapoptotic mechanism which might be involved in cancer development in human. Thus development of CK2 inhibitors can be used in cancer treatment (litchfield 2003). However, Sayed et al. (2001) demonstrated the role of CK2 in p53-mediated apoptosis.

Three members of the protein kinases of AGC family, PKA (also known as cyclic AMP dependent kinase) and PKC and PKG (cGMP dependent protein kinase) have also been identified by motif substrate analysis in the present study. AGC kinases are involved in a number of cellular functions including signal transduction, which influence a collection of biological processes related to health and diseases. The dysregulation of AGC kinases have serious consequences that may cause cancer and diabetes in humans (Pearce et al., 2010).

Taking together, it can be suggested that, kinases identified in RTgill-W1 cells might play significant role in the regulation of different cellular functions including cell cycle progression, transcription, signal transduction and regulating viral infection. The development of inhibitors to cease some of the targeted kinase activities might be useful in preventing viral diseases.

3.4.7 Signaling pathways

To uncover different signaling pathways essential for innate immune responses and activated by protein phosphorylation in trout gill epithelia, the identified phosphoproteins were used as input employing the *Enrichr* tool (http://amp.pharm.mssm.edu/Enrichr). The signaling pathways are the main player in the cellular activity which is controlled by protein phosphorylation. Interaction of PAMPs and host cell receptors induces intracellular signaling pathways controlling the expression of antimicrobial genes and augmentation of other cellular functions (Mikkelsen et al., 2009). Thus, to identify the pathway that is in action in response to certain stimulus or infection agents is of prime importance. In the present study, poly(I:C) has been found to activate several unique signaling pathways including actin cytoskeleton regulation and also participated in activation of other pathways including spliceosome and MAPK by incorporating more related phosphoprotein related genes.

3.4.7.1 Activation of spliceosome signaling pathway

As mentioned earlier (section 3.3.6), spliceosome signaling pathway was activated in both control and stimulated cells. However, the number of pathway- associated phosphoproteins identified in poly(I:C) simulated cells (16 genes) were higher than that of control (12 genes) and MDP (13 genes) stimulated cells.

Spliceosome is an important signaling pathway for effective gene expression in eukaryotes, where the absence or dysregulation of splicing impairs the synthesis of functional proteins (Meyer, 2016). Spliceosome signaling pathway has been found to be activated in control and stimulated RTgill-W1 cells in the present study. This pathway initiates splicing of exons and excision of introns from transcribed precursor mRNA in a macromolecular complex. The standard spliceosome is made up of five small nuclear ribonucleoproteins (snRNPs), U1, U2, U4, U5, and U6 snRNPs, and several spliceosome-associated proteins (SAPs). In this study, proteins related to all snRNP groups were found to be phosphorylated. This suggests that spliceosome signaling pathway is spontaneously activated in trout gill epithelial cells for the translation of required proteins. Moreover, CDK11 which has been identified in trout gill epithelial cells (Appendix 3, Supplementary table S3.4), have been shown to be involved in transcription and splicing (reviewed by Loyer et al., 2005) which is in accordance with the activation of spliceosome signaling pathway.

3.4.7.2 The mitogen-activated protein kinase (MAPK) pathway activation

MAP kinases play important roles in cellular processes including cytokine signaling (Platanias, 2005) and innate immunity regulation (Arthur & Ley, 2013). MAPK pathway contributes in the induction of interferon responses. MAPK signaling cascade is the principal signaling pathway regulating a diverse cellular process including cell proliferation, differentiation, apoptosis, stress responses stimulated by external stimuli. Transcription of many of the regulatory genes are MAPK dependent (Plotnikov et al., 2011).

In the present study, MAPK signaling pathway was found to be activated in poly(I:C) and MDP stimulated cells. However, poly(I:C) stimulation has induced higher number of phosphoprotein associated genes associated with MAPK pathway compare to MDP stimulation.

The classical MAPK pathway includes the signaling molecules Ras, Raf, MEK, and ERK. In the present study, Raf has been found to be phosphorylated which further phosphorylated MAP2K2 (MEK). The c-Jun N-terminal kinase (JNK) and p38 pathway, major signalling cassettes of the MAPK pathway, have also been found to be activated as well as some of the intermediate proteins like MAP4K4, MAP3K1, PAK2, MAP14, MAPKAPK5 and JUN. Moreover, Phosphorylation of MAPK14 has been found to phosphorylate TP53 of which activation subsequently activated P53 signaling pathway (Figure 3.12). DNA damage related proteins TAOK2 and TAOK3 have also found to be phosphorylated. These together suggest the activation of classical MAPK, JNK, p38 and p53 signaling pathways. In previous study, poly(I:C) has been shown to activate MAPK cascade via the activation of TAKI and subsequent activation of MKK6 and JNK pathway (Dunlevy et al., 2010).

MAPK pathway has previously been shown to be activated in gill by bacterial infection by transcriptomic analysis (Rebl et al., 2014). Upon PAMP (flagellin peptide, flg22) stimulation three MAPKs namely MAPK3, MAPK4 and MAPK6 have been shown to be activated through phosphorylation in plant (*Arabidopsis*) (Nitta et al., 2014). In Jurkat human T lymphoma cells, JNK and p38 MAPK have been found to be activated by bacterial PAMPs LPS, PGN and flagellin and triggered the production of cytokines (Zhong & Kyriakis, 2007). Environmental stresses have also been shown to activate p38 MAPK, ERK1/2 and JNK in mammals (reviewed by Cargnello & Roux, 2011).

In rainbow trout primary macrophages, LPS induced activation of ERK, p38MAPK and JNK signaling pathways and subsequent production of cytokine TNFα have been demonstrated by western blotting (Roher et al., 2011). Moreover, PGN induced activation of p38 MAPK has been shown by inhibition study in carp macrophages (Ribeiro et al., 2010).

3.4.7.3 Regulation of actin cytoskeleton pathway activation

Regulation of actin cytoskeleton pathway has also been found to be activated only in the poly(I:C) stimulated RTgill-W1 cells. The pathway associated proteins that have been found to be phosphorylated are fibronectin binding protein integrins (associated genes are itga4 and itga5) and RRAS2 (homology of Ras). RRAS2 is a key regulator of the actin cytoskeleton which subsequently phosphorylates raf1a and ARHGEF6 which are also key

regulators of this pathway that can be activated by extracellular stimuli. Phosphorylation of these two proteins were found to phosphorylate other proteins and initiate the activation of the regulation of actin cytoskeleton pathway.

The actin cytoskeleton signaling pathway is related to cellular integrity of epithelial cell which has been found to be modulated by poly(I:C) (Chapter 2, section 2.1). Higher percentage of phosphoproteins related to cytoskeleton has also been found in the poly(I:C) stimulated cells (Figure 3.8) which is in accordance with the activation of actin cytoskeleton signaling pathway. Moreover, Rho GTPases has been shown to play critical role in the regulation of actin cytoskeleton and tight junction barrier in MDCK cells (Jou et al., 1998). In the present study, several isoforms of rho GTPase-activating protein have been found to be phosphorylated in the poly(I:C) stimulated cells (Supplementary table S3.5) which might play roles in the activation of actin cytoskeleton signaling pathway regulation.

3.4.8 Validation of findings from phosphoproteomics analysis

In the present study, it is important to note that no validation on the detected phosphoproteins was performed. Further trials using specific antibodies were not possible due to time constrains. One of the potential limitations to validate the data obtained is that commercially available antibodies are specific mostly to human, mouse, rat and a few of them are suitable for zebrafish. The generation of custom antibodies are costly, time consuming and sometimes with unsuccessful results.

Nevertheless, the functional analysis of phosphorylation mediated cell signaling identified in the present study should be validated. Phosphate-affinity polyacrylamide gel electrophoresis can be used to detect stoichiometric protein phosphorylation (Kinoshita-Kikuta et al., 2007). Phosphorylation levels of cellular proteins of interest can be assessed by subsequent Western blotting which would be useful to evaluate the obtained phosphoproteomic data when antibodies are available (Mahmood & Yang, 2012). Thus, future studies are recommended on targetted phosphoproteomics for the detection and expression of TLR and RLR members in salmonid gill epithelia by western blotting or flow cytometry. Moreover, some of the kinases such as p38 MAPK, CDK, AKT, CK2, PKA/B/C and CaMKII should be validated by antibody based western blotting or flow cytometry.

Kinase specific inhibitors could also be used to investigate the involvement of the kinase in activating specific signaling pathway.

3.5 Conclusion

The phosphoproteome in rainbow trout gill epithelial cells has been investigated using LC-MS/MS coupled with TiO_2 phosphopeptide enrichment of trypsin digested peptides to identify phosphoprotein in steady state and stimulated condition. In total 2,612 phosphorylation sites on 1,789 phosphopeptides in 691 different phosphoproteins have been identified in the present study. The majority of the phosphorylation events in the trout gill epithelia might be occurred by the proline-directed motifs such as glycogen synthase kinase, CDK2 and MAPK which have been found to be dominating in the identified kinase.

Moreover, in the present study, poly(I:C) has been found to trigger the phosphorylation in trout gill epithelial cells to a greater extent in all aspects of phosphorylation event which include higher number of phosphopeptides and subsequent phosphoprotein, higher number and highly enriched motifs and associated kinases, signaling pathways and highly enriched GO. As poly(I:C) is believed to play roles in innate antiviral response, activation of antiviral signaling pathways such as TLR3 and RLR is expected. Many of the pathways were related to human viral diseases including cancer, information of which might be useful in studing fish diseases. Apart from the viral diseases, some bacterial diseases related to human have also been activated which will be usefull to study bacterial pathogenesis in fish and to develop potential therapeutics against bacterial pathogenesis.

The dynamic phosphorylation, for the first time, in rainbow trout gill cells, has been reported in the present study which can be used for the future studies to elucidate further functional characterization of phosphoproteins, motifs and kinases, investigation of signaling pathways and development of potential inhibitors.

Chapter 4

RTgill-W1 cells -pathogens interactions

4.1 Introduction

To understand disease pathogenesis, it is important to understand host-pathogen interactions. As an aquatic organism, the fish body including the gill, is subjected to continuous contact with many different types of microorganisms (Tort et al., 2003). The first barrier against pathogens is the integumentary surface which is equipped with mechanisms protecting against pathogen entry (Secombes & Oliver, 1997). Some microorganisms can evade the barriers and can cause diseases to host while some hosts have evolved the mechanisms to kill or eradicate the pathogens. Mucus secretion, and production of diverse groups of antimicrobial molecules are some of the important protective mechanisms (Tort et al., 2003).

Viral and bacterial pathogens are the predominant agents causing huge loss to aquaculture production. Among them, salmonid alphavirus (SAV) is one of the viruses causing pancreas disease and sleeping disease in farmed Atlantic salmon and rainbow trout in Europe (Graham et al., 2011). Recent molecular taxonomic studies demonstrate six salmonid alphavirus subtypes where subtype 2 (SAV-2) is associated with sleeping disease which is a serious infectious disease of rainbow trout in freshwater aquaculture in several European countries (McLoughlin & Graham, 2007). Several organs of fish are infected with virus, where gill is the most vulnerable to viral infections. However, the interactions between fish gill epithelia and viruses are still unclear. In the present study, the infectivity of SAV-2 was tested in a trout epithelial cell line RTgill-W1.

Bacterial pathogens also contribute to the huge aquaculture loss. In case of rainbow trout, several bacterial species have been reported to cause different diseases like furunculosis caused by *A. salmonicida*, enteric red mouth disease (ERM) by *Yersinia ruckeri*; and infections with *Flavobacterium psychrophilum* called cold water disease or rainbow trout fry syndrome (RTFS) depending on the size of the diseased fish (Bernardet et al. 1996).

Hosts' responses against viral and bacterial infections depend on the recognition of pathogens by the host receptors. Antiviral immunity starts upon recognition of pathogens by the host pattern recognition receptors mostly Toll-Like Receptor 3 (TLR3) and RIG- like

Receptor (RLRs) comprising MDA5 (melanoma differentiation-associated gene 5), RIG-I (retinoic acid-inducible gene I) and LGP2 (laboratory of genetics and physiology 2). RLRs are cytosolic pattern recognition receptors and are broadly expressed in most tissues where they signal innate immune activation in a variety of cell types including epithelial cells (Loo & Gale, 2012). RIG-I and MDA5 detect a variety of viruses and signal the production of IFN and induction of an antiviral response while LGP2 regulates MDA5 and RIG-I signaling (Jiang et al., 2012). Studies in mammals differentiated the roles of RIG-I and MDA5 in response to RNA viruses where RIG-I preferentially binds to short (<300 bp) or up to 1 kb dsRNAs that have blunt ends and a 5' triphosphate (5'ppp) moiety, facilitating discrimination between host and viral dsRNA or 5′-triphosphate end of single-stranded (ss)RNA while MDA5 preferentially binds to long dsRNA (>1,000 bp) without end specificity (Kato et al., 2006; Pichlmair et al., 2006).

Interaction of RIG-I and MDA5 with IPS1 helps to relocate the RLRs to IPS1-associated membranes where they and downstream signaling molecules accumulate to form an IPS1 signalosome that drives IFN production (Hiscott et al., 2006). Upon recognition of RNA by RIG-I or MDA5, a complex signaling downstream pathway is activated where IPS1 (interferon-b promoter stimulator 1; Kawai et al., 2005) serves as a critical signaling adaptor for RIG-I/MDA5.

Tank-binding kinase protein 1, TBK1 has serine-threonine protein kinase activity and has been identified as one of the kinases that phosphorylate IRF3 and 7 (Hiscott et al., 2003; Yoneyama et al., 2002). TBK1 integrates multiple signals induced by receptor- mediated pathogen detection and thus modulating interferon levels (Ma et al., 2012). IRF3 is a unique member of the IRF family whose transcriptional activity is regulated solely by phosphorylation, a posttranslational modification (Yoneyama et al., 2002). On the other hand, IRF7 (the closest relative of IRF-3) has several common with and distinct features from IRF3.

Several interferon stimulated genes have been identified in response to viral infections. Interferon signaling is initiated by IPS1 upon interacting with TBK1 and IRF 3. IRF 3 is phosphorylated in the cytoplasm and is transported to the nucleus where it initiates the production of interferon and interferon stimulated genes (ISGs). ISGs then translated in the

cytoplasm and interfere viral replication. The most common interferon stimulated genes are Mx, ISGs, PKR, and Viperin.

Research on fish immunology has progressed significantly over the last few decades, where mammalian gene markers have been based and many of them have been identified in fish, and their function has been investigated in a range of fish species such as RIG-I, TBK1 and PKR have been identified and characterized in a range of fishes. However, complete RLR signaling pathway and the expression pattern of relevent genes in fish gill epithelia in response to alpha virus is still unknown. Present study was thus designed to investigate the host response to SAV-2 at cellular level by transepithelia electrical resistance and molecular level by investigating the expression of different antiviral response gens.

Antibacterial response, on the other hand, can be explained as inflammatory response and the expression and production of antimicrobial peptides (AMPs). A significant number of inflammatory cytokines have been studied and found functionally active in teleost. Several cytokines and regulatory molecules reported in fish include a number of interleukins (IL-6, IL-8, IL-10, IL- 12) and Tumour Growth Factor (TGF)-β, and interferon regulatory factor (IRF)-1 and Tumour Necrosis Factor alpha, TNF-α (Tort et al., 2003). Antimicrobial molecules are peptide-based molecules commonly known as antimicrobial peptides (AMPs) that act both directly and indirectly on components of the bacterial cell wall resulting in lysis of the cell (Tort et al., 2003).

As part of the innate immune system, animals including fish produce a range of cationic antimicrobial peptides (AMPs) as a first line of defence (De Bruijn et al., 2012). Several AMPs have been identified in different fishes having antimicrobial properties against bacterial infection. Most common AMPs are defensin, cathelicidins, hepcidins, piscidins, etc. which have been shown as effective antibacterial agents (Rakers et al., 2013). Several other innate immune genes like c-type lectin CD209a and b, COX-2, MMP9/13 and LECT2 have also been shown to be upregulated upon parasitic infection in rainbow trout (De Bruijn et al., 2012). However, antibacterial properties of fish gill epithelia are not well studied.

Expression of selected AMPs, cytokines and innate immune genes in rainbow trout gill epithelial cells RTgill-W1 in response to fish pathogenic bacteria *A. salmonicida* and viral and bacterial PAMPs were also investigated in the present study.

4.2 Materials and Methods

4.2.1 Cellular and molecular response of RTgill-W1 cells upon SAV-2 infection

To investigate the response of RTgill-W1 cells to viral infection, the cells were infected with salmonid alphavirus subtype 2 (SAV-2). Cellular integrity in terms of Transepithelial Electrical Resistance (TER) and tight junction gene expression, and antiviral responses were investigated using absolute RT-qPCR technique. Initially, SAV-2 was grown and the infectivity titer was determined by $TCID_{50}$.

4.2.1.1 Culture and titration of SAV2

Three fish cell lines CHSE-214, CHH-1 and TO were initially tested for growing SAV-2 (Isolate V0702, Passage 1, cell line: CHH-1). Two different inoculation methods; adsorption inoculation where virus was inoculated on preformed cell monolayer, and simultaneous inoculation where cell seeding and virus inoculation were done simultaneously, were used. For adsorption inoculation, virus was adsorbed on the preformed cells for 3 h. Five different dilutions of the virus (10^{-1} to 10^{-5}) each in duplicate were used. Cells were monitored every day under the inverted microscope to check for CPE. Cells were grown at 15 °C with 1% CO_2. Upon CPE formation and development, virus was harvested from each dilution at day 18 following the standard protocol developed in the laboratory. Briefly, cells were scrapped with a cell scraper and collected in 4 mL growth medium, centrifuged at 4700 rpm for 15 min at 10 ºC and stocked at -70 ºC until further use. Viral copy number was quantified by RT-q PCR (methods described in 4.2.4). The highest viral RNA copy number was found in CHSE-214 cell inoculated with a virus dilution of 10^{-3} which was further used for mass production in 25 cm^2 TC flasks for both adsorption and simultaneous inoculation methods. At day 20, almost all the cells were infected with virus. Virus was harvested at this point following the method above and was stocked at -70 ºC until further use.

4.2.1.2 Titration of virus for infectivity study ($TCID_{50}$)

The tissue culture infective dose indicates the quantity of a virus cytopathogenic to 50 % of the cells inoculated. To determine the titer, several dilutions of virus stock were prepared, in a 10-fold dilution from 10^{-1}, to 10^{-11} and 5-fold dilution from neat to 2×10^{-1}, 4×10^{-2} and so forth until 2×10^{-6}. Both adsorption and simultaneous inoculation methods were used for virus titration (detailed method in Appendix 1.5). Viral titre was calculated using the following formula:

Mean log TCID50(m) = x + 1/2 d - d Σ(r/n);

$$Mean \log TCID50 = \text{x} + ½d\sum \frac{r}{\text{n}}$$

Where x = log of highest reciprocal dilution that has no positive wells, d = log of dilution interval, r = number of test subjects not infected at any dilution and n = number of test subjects inoculated at any dilution (last number will always be 1).

$$Mean\ titre\ (m) = \frac{10^{mean \log TCID50}}{volume\ innoculated}$$

4.2.1.3 Generating SAV-2 quantitative RNA standard

To generate SAV-2 quantitative RNA standard, the target fragment of SAV-2 genome was amplified, ligated into pCRII vector, transformed into *E. coli* competent cells and plasmid DNA was extracted. To transcribe +strand RNA fragment from the plasmid DNA, M13 PCR was employed and RNA was transcribed from the purified PCR product following the steps in 4.2.3.5 to 4.2.3.10.

4.2.1.3.1 Viral RNA extraction, RT-PCR and clean-up of PCR product

Viral RNA was extracted from the virus supernatant using Roche High Pure Viral RNA extraction Kit (version 18) following the manufacturer's instructions. Briefly, 400 µL of binding buffer supplemented with poly(A) was added into 200 µL of virus supernatant and mixed well and transferred to the filter tube assembly. Then the tube with filter was centrifuged for 15s at 8000*g*. The flow through and the collection tube was discarded, and the filter was placed into another collection tube. Then, 500 µL of inhibitor removal buffer was added into the filter and centrifuged for 1 min at 8000*g*. The flow through and the collection tube was discarded, and the filter was placed into another collection tube. Then, 450 µL of wash buffer was added into the filter and centrifuged for 1 min at 8000*g*. The wash step was repeated once followed by another centrifugation for 10s at maximum speed and the flow through and the collection tube was discarded. Finally, 50 µL elution buffer was added into the filter and centrifuged for 1 min at 8000*g*. The supernatant (purified viral RNA) was used for subsequent application.

Viral RNA was then reverse transcribed using Transcriptor Onestep RT-PCR kit (Roche). Primers used for RT-PCR were SD STD UP 5'-AAGAAATGCACCAGGTTYTCCAC-3'

and SD STD DP 5'-CACCTCTTTGCCTCCGCTG-3'. The RT-PCR was conducted in 50 µL reaction volume containing 1 µL of viral RNA (around 250 ng), 2 µL of each primer (800 nM), 10 µL of 5X RT buffer, 1 µL RT enzyme mix and 34 µL of PCR grade water. The temperature profile was: 1 cycle of reverse transcription at 50 ºC for 30 mins, 1 cycle of activation at 94 ºC for 7 mins, followed by 35 cycles of denaturation for 10s at 94 °C, annealing for 30s at 60 °C and extension for 2.5 mins at 68 °C followed by final extension for 5 min at 68 °C. The RT-PCR product was then run on 1% agarose gel to check the correct amplification of the product. The target PCR product was then purified using the DNA Clean & Concentrator (Zymo Research), according to manufacturer's instructions (Appendix 1.6). Purified PCR product was eluted in 20 µL DNA nuclease free water. Concentration of PCR product was determined using Nanodrop Spectrophotometer (ND-1000, Labtech International, Uckfield, UK). Purified PCR products were directly used for the ligation procedure, and the rest of the product was then kept at -20 °C for long-term storage.

4.2.1.3.2 Ligation and transformation

a) Calculation of ligation ratios for vector and insert

$$\frac{size\ of\ PCR\ fragment\ (bp) \times 50\ ng\ pCRII\ (vector)}{Size\ of\ pCRII\ vector\ (3900\ bp)}\ X\ ng\ of\ PCR\ product\ for\ 1{:}1\ insert{:}vector$$

The preferred insert and vector ratio was 3:1.

Thus, the amount of product = $\frac{315\times50}{3900}$×3= 12.1 ng; product size was 315 bp

Then 12.1 ng of PCR product was used in 10 µL of reaction volume containing 2 µL of 5X buffer, 2 µL of vector (50ng) pCRII, restriction enzyme, and nuclease free water. The reaction mix was then incubated for 1 h at room temperature.

After incubation, 2 µL of ligation mix was transferred to 100 µL of TOP 10 F' *Escherichia coli* competent cells (Invitrogen) and incubated on ice for 30 min. The subsequent steps were performed according to section 2.2.4.1.7 of Chapter 2.

4.2.1. 3.3 Plasmid purification and ligation confirmation

Plasmid DNA was extracted using High Pure Plasmid Isolation Kit (Roche) according to the manufacturer's instruction (Appendix 1.8). The concentration and quality of plasmid DNA was checked using Nanodrop Spectrophotometer (ND-1000, Labtech International, Uckfield, UK). To confirm the correct insertion into the vector, PCR was performed using SAV-2 SD STD UP/DP primers and also M13-FP (5'-GTAAAACGACGGCCAG-3') and M13-RP (5'-CAGGAAACAGCTATGAC-3') primers (as described in 4.2.3.5).

4.2.1.3.4 Recombinant plasmid analysis

Recombinant plasmid was analysed by restriction fragment length polymorphism (RFLP) and sequencing. RFLP was performed using the restriction enzyme KpnI-HF (New England BioLabs) using 10X NEBuffer (CutSmart) in a reaction volume of 50 µL containing 500 ng of plasmid DNA, 5 µL of buffer, 1 µL of restriction enzyme and nuclease free water. The reaction mix was incubated for 15 min at 37 ºC in a thermocycler and after incubation, the reaction was stopped by adding 10 ºC of 6X dye to 50 µL reaction. The reaction was then run onto a 1% agarose gel. The pattern of bands on gel was analysed on the basis of the figure 4.1. Plasmid DNA was also sent for sequencing to GATC Biotech, using LIGHTrun sequencing using M13 forward primer to further check the correct orientation of the insert into the vector (sample was prepared for sequencing according to section 2.2.5.2, Chapter 2). When sequences were obtained, they were checked for the correct orientation into the pCRII vector using SAV-2 specific primer sequences.

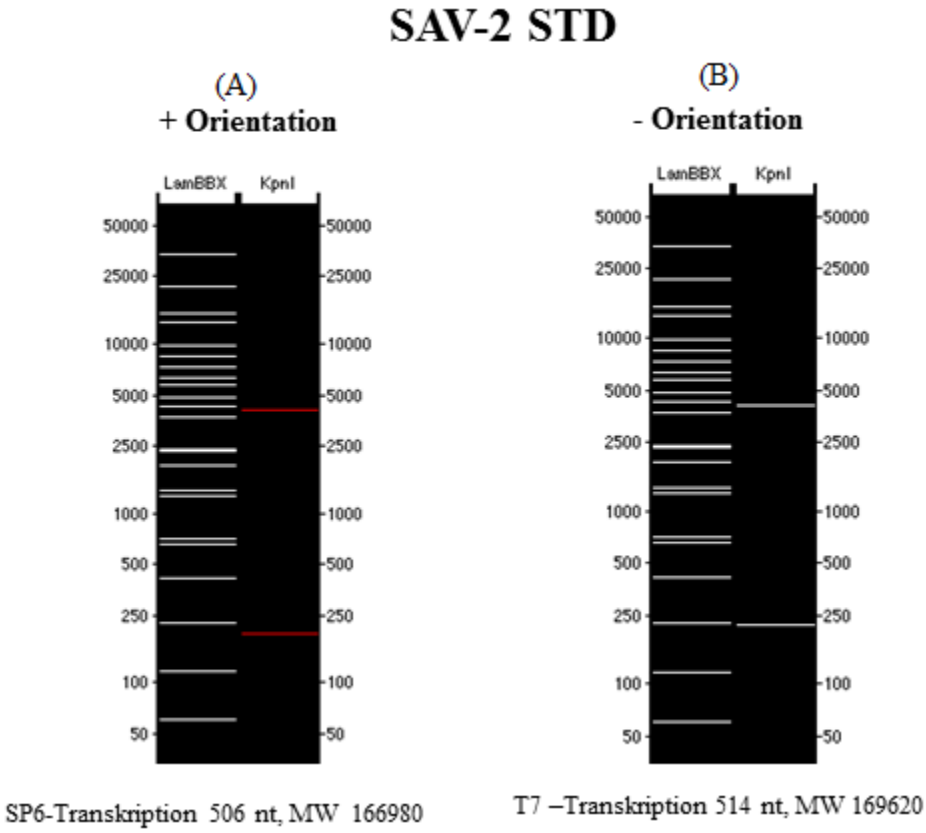

Figure 4.1: Calculated expected RFLP pattern of KpnI digested plasmid DNA on agarose gel simulation. Positive (A) or negative (B) orientation of the SAV-2 fragment into pCRII vector was determined based on the size of the band.

4.2.1.3.5 PCR using M13 FP-RP primers and purification of PCR product

M13 PCR was conducted in 50 µL reaction volume containing 1 µL of diluted plasmid (1:10 to 1: 10000), 2 µL of each primer (800 nM), 25 µL of 2X MyTaq HS Mix (Bioline) and 20 µL of PCR grade water. The reaction condition was: 1 cycle of activation at 95 ºC for 3 mins, followed by 35 cycles of denaturation for 15s at 95 °C, annealing for 15s at 60 °C and extension for 15s at 72 °C. The PCR product was then run on 1% agarose gel to check the correct amplification of the product. The target PCR product was then purified using the DNA Clean & Concentrator (Zymo Research), according to manufacturer's instructions (Appendix 1.6). Purified DNA was eluted into 20 µL nuclease free water. DNA concentration was determined using Nanodrop Spectrophotometer (ND-1000, Labtech International, Uckfield, UK). Purified PCR product was directly used for *in vitro* transcription, and the rest of the product was then kept at -20 °C for long-term storage.

4.2.1.3.6 *In vitro* transcription

Based on the RFLP and sequence analysis, the insert into the vector was found to be positively oriented. So, the transcription was performed using SP6 RNA polymerase (Roche) in a 40µL reaction volume containing 150 ng of purified PCR product, 4 µL of 25 mM of rNTPs, 4 µL of 10X transcription buffer, 2 µL of SP6 polymerase (stock 20U/µL) and nuclease free water. The reaction was incubated at 37 °C for 2 h followed by inactivation at 65 °C for 2 min in a thermocycler.

4.2.1.3.7 RNA clean-up and DNase treatment

RNA was then purified using Clean ALL DNA/RNA clean up and concentration kit (Norgen Biotek Corp.) according to manufacturer's instruction. Briefly, RNA sample was adjusted to 100 µL by adding RNase-free water. Then 250 µL of Binding Buffer H (working buffer was prepared by adding β-mercaptoethanol at a concentration of 10 µL per mL) was added followed by an addition of 200 µL of absolute ethanol. Then the mixture was vortexed for 10s and transferred into the binding column assembled in the provided collection tube and centrifuged for 1 min at 14000*g*. The flowthrough was discarded and the column was washed with 500 µL of Wash Solution K by centrifuging for 1 min at the same speed followed by another was by adding another 500 µL of Wash Solution K by centrifuging for 2 min at 14000g. An additional centrifugation for 1 min was done at the same speed. The column was then transferred into a 1.5 mL eppendorf tube and 40 µL of elution buffer was added and centrifuged for 2 min at 200*g* followed by an additional centrifugation for 1 min at 14000*g*. The purified RNA was then collected in the eppendorf tube. In the next step, the purified RNA was then treated with DNase enzyme to remove DNA, using DNA free kit (Ambion) in a 50 µL reaction containing all the purified RNA, 5 µL of DNase buffer (10X), 1 µL of DNase enzyme (2U/ µL) and nuclease free water. The reaction mix was then incubated for 30 min at 37 °C in a thermocycler. After 30 min, 1 µL of DNase enzyme was added and incubated for another 15 min at 37 °C. After incubation, the reaction was inactivated by adding 5 µL DNase inactivation agent followed by incubation for 2 min at room temperature. Finally, the supernatant (containing RNA) was collected by centrifuging for 1.5 min at 10000*g* avoiding the pellet. After DNase treatment, the RNA clean-up step was repeated to remove all traces of buffer and enzymes containing salts. In this RNA clean-up step, RNA was eluted in 20 µL of elution buffer.

4.2.1.3.8 RT-qPCR testing for residual plasmid DNA

The DNase treated purified RNA was analysed by real time one-step RT-PCR using QuantiTect Probe RT-PCR kit (Qiagen) to check for any residual plasmid DNA and their respective CT value. The reactions were set up in LightCycler capillary tubes (Roche) in a 20 µL reaction volume. Two reactions were set; one with RT-enzyme (RT+), for PCR amplification of RNA and another without RT enzyme (RT-) for PCR amplification from residual DNA.

The reaction contained 10 µL of RT-PCR mastermix, 1 µL of each primer (SAV-2 specific), 0.4 µL of probe (200 nM), 1 µL of transcribed RNA and 1 µL of RT (for RT+ reaction) or 1 µL of nuclease free water (for RT- reaction). The reactions were run in a LightCycler 2.0 thermocycler (Roche). The temperature profile for RT-qPCR was: reverse transcription for 20 min at 50 °C, activation for 15 min at 95 °C, followed by 45 cycles of amplification for 1s at 95 °C and 1 min at 60 °C, and a final cooling stage for 40s at 40 °C. Analysis was conducted using LightCycler software version 4.1.1.21 (Roche), with the CT values obtained for both the RT+ and RT- reactions. Based on the difference of the CT values between the RT+ and RT- reactions, a decision was made on whether further DNase treatments were required to remove any residual plasmid DNA. A good separation (>10 CT) between RT+ and RT- is required for RNA standard.

4.2.1.3.9 Quantification of transcribed RNA

Quantification of transcribed RNA sample was conducted using the Quant-iT RiboGreen RNA Reagent Kit (Invitrogen), according to manufacturer's instructions. The transcribed RNA was diluted in 1:10 and 1:100. RNA standard was diluted from 1 µg/mL to 20ng/mL. Each sample was used in triplicate. The samples were prepared in a black 96 well plate. The analysis was performed in a Synergy HT Multi-Mode Microplate Reader (BioTek) and Gen5 2.04 software. Calculations were then made between the samples and negative control to determine the concentration of RNA in transcribed RNA sample. The number of molecules per microliter of RNA was calculated according to the section 2.2.5.3 of chapter 2 with some modifications. Transcribed RNA solution was then diluted in tRNA (100ng/µL) from neat until 10^1. RNA of 10^7 to 10^1 molecules/µL were used as standard for viral quantification.

4.2.1.3.10 Test run for SAV-2 standard

TaqMan probe based real time RT-qPCR (Figure 4.2) was performed to quantify the viral RNA copy number using hydrolysis kit (Roche) and Roche LightCycler 2.0. Primer and probe used for RT-qPCR were as SAVSDUP 5'-TCCACCACCCCGAAGAAGTC-3', SAVSDDP 5'-ATGTCACCACGGTGCTGATCTC-3' and probe SAVSDLNAP 5'-ATCTCGTTGATGTGTATGA-3'. The reaction contained 1 µL of each primer (400 nM), 0.4 µL of probe (200 nM), 1.3 µL of activator (3.25 mM Mn(OAc)), 7.5 µL of buffer, 7.8 µL of nuclease free water (to make up 19 µL) and 1 µL of each standard or 1 µL of nuclease free water (for NTC) to make 20 µL of reaction volume. Each standard was run in duplicate. The reactions were run in a LightCycler 2.0 thermocycler (Roche). The temperature profile for RT-qPCR was: reverse transcription for 3 min at 63 °C, activation for 30s at 95 °C, followed by 45 cycles of amplification for 5s at 95 °C and 15s at 60 °C, and a final cooling stage for 40s at 40 °C. Analysis was conducted using LightCycler software version 4.1.1.21 (Roche). Three runs in duplicate of each dilution was performed and the mean CT value of each dilution was used to generate the standard curve.

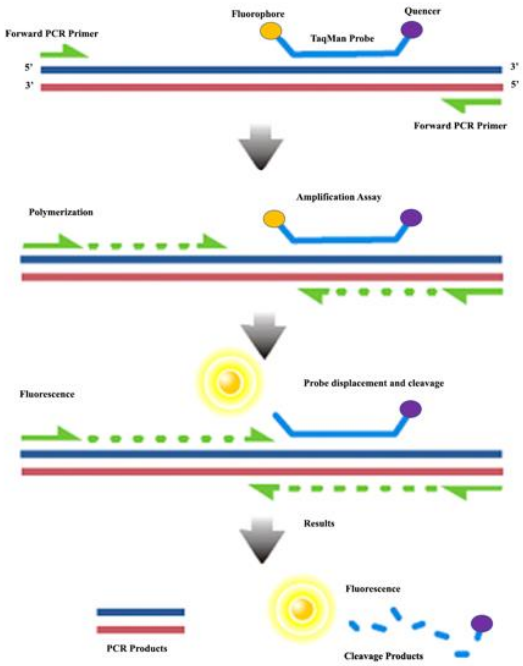

Figure 4.2: TaqMan chemistry: An oligonucleotide probe, containing a fluorescent reporter dye on the 5' end and a quencher dye on the 3' end is used. When the target sequence is present, the probe anneals downstream from one of the primer sites and is cleaved by the 5' nuclease activity of Taq DNA polymerase as this primer is extended. This cleavage of the probe separates the reporter dye from the quencher dye, increasing the reporter dye signal and removes the probe from the target strand, allowing primer extension to continue to the end of the template strand.

4.2.1.4 RTgill-W1 cell culture

RTgill-W1 cells were maintained in accordance with protocols developed in the Virology laboratory in the Institute of Aquaculture, University of Stirling, Scotland, UK. Briefly, cells were maintained in Leibowitz L-15 media (GIBCO Life Technologies) supplemented with L-glutamax and 10% of fetal bovine serum (FBS) at 22 °C in 75 cm^2 plastic flasks (SARSTEDT, Germany).

4.2.1.5 Growth of SAV-2 in RTgill-W1 cells

RTgill-W1 cells were grown onto the 12 well transwells and the cells were allowed to grow until confluency. Cells were then infected with SAV2 at MOI 10, 1 and 0.1 and let for 6, 12, 18, 24 and 96 h. Uninfected cells were used as a control. Each treatment in both infected and uninfected groups was conducted in triplicate and cells in triplicates were pooled together for cytoplasmic extraction. For cytoplasmic RNA extraction, 0.2% octylphenoxypolyethoxyethanol (NP-40) was used to lyse cytoplasmic fraction and cytoplasmic fraction was collected by centrifuging for 1 min at 14000 rpm at 4 °C. Cytoplasmic RNA was then extracted following TRI-Reagent extraction protocol (detail in Appendix 1.1). RNA purity and quantity were also checked. RNA integrity was assessed by agarose gel electrophoresis. TaqMan probe based real time RT-qPCR (Figure 4.2) was performed to quantify the viral RNA copy number at defined time points and virus concentration using hydrolysis kit (Roche) and Roche LightCycler 2.0. Primer and probe used for RT-qPCR were as SAVSDUP 5'-TCCACCACCCCGAAGAAGTC-3', SAVSDDP 5'-ATGTCACCACGGTGCTGATCTC-3' and probe SAVSDLNAP 5'-ATCTCGTTGATGTGTATGA-3'. RT-qPCR was performed according to section 4.2.3.10.

4.2.1.6 Replication of SAV-2 in RTgill-W1 cells

To detect the replicative strand in RTgill-W1 cells, cytosolic RNA extracted in section 4.2.4 was used for strand specific RT-qPCR. For the detection of replicative viral genome, a SAV-2 specific tag was used for cDNA synthesis using superscript III kit (Invitrogen) following the manufacturer's instruction (detail in Appendix 1.2) using a tailed SAVFPtag primer (5'-ggccgtcatggtggcgaattccaccaccccgaagaagtc-3'). For the qPCR detection of SAV-2 replicative strand the SSTag primer ((5'-ggccgtcatggtggcgaat-3') complementary to the sequence introduced by the tailed primer (Figure 4.3) was used. The PCR temperature profile was initial denaturation at 95 °C for 10 mins followed by 55 cycles of denaturation

95 °C for 10s, annealing 58 °C for 20s, and extension 72 °C for 15s and cooling 40 °C for 30s.

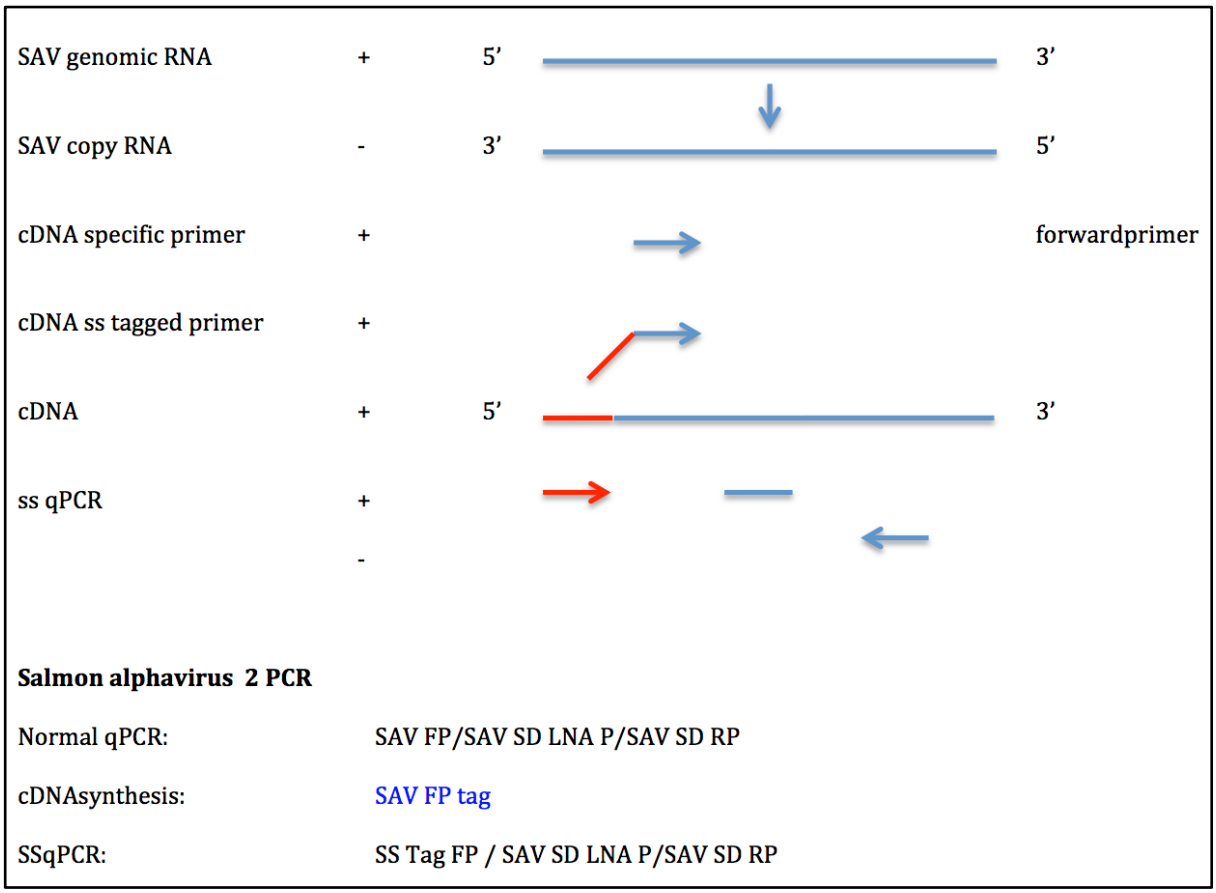

Figure 4.3: Strand specific PCR for the detection of replicative strand of SAV 2. A replicative strand specific primer, SSTag primer is used for the synthesis of first strand which further is detected by qPCR where another primer, SStagFP was used as complementary to the SSTag primer.

4.2.1.7 Effects of SAV-2 on TER of RTgill-W1 cells

RTgill-W1 cells were seeded onto the 12 well transwells with a growth area of 0.9 cm^2 and 0.4-micron pore size. Each transwell insert (Corning) was seeded with 0.12×10^6 cells. Post seeding TER was measured over time. When TER values were found to be stable, cells were infected with SAV-2 at the multiplicity of infection (MOI)10, 1 and 0.1 and a control group with no virus but diluent was added in the control wells at the time of infection. TER was measured at ½, 1, 3, 6, 24, 48, 72 and 96 h of post infection. Three independent experiments were conducted where each treatment was conducted in triplicate and TER in each well at each time point was measured three times. Blank wells without cells in triplicate was always used as a background control. TER in blank was subtracted from TER of each treatment to

have the true resistance in each treatment. TER was calculated following the method explained in chapter 2, section 2.2.3.

4.2.1.8 Expression of tight junction gene and TLR 3 and RLR mediated antiviral response in RTgill-W1 cells upon SAV-2 infection

4.2.1.8.1 Conducting experiment, extraction of RNA and cDNA synthesis

RTgill-W1 cells were grown onto the 12 well transwells and the cells were allowed to grow until confluency. Cells were then infected with SAV2 at MOI (10) and incubated for 6, 12, 18, 24 and 30 h. Uninfected control groups for each time point were maintained. Each treatment in both infected and uninfected groups was conducted in triplicate and cells in triplicates were pooled together for cytoplasmic and total RNA extraction. For cytoplasmic RNA extraction, cell lysate was collected in 100 µL of 0.2% NP-40 (Thermo Fisher Scientific). Then the cytoplasmic fraction was collected by centrifuging for 1 min at 14000 rpm at 4 °C. Cytoplasmic RNA was then extracted following TRI-Reagent extraction protocol explained in section 2.2.4.1.1 of chapter 2. For total RNA extraction cells were lysed with TRI-Reagent followed by RNA extraction following the same RNA extraction protocol. RNA was quantified using Nanodrop Spectrophotometer (ND-1000, Labtech International, Uckfield, UK). RNA purity and quantity were also checked. RNA integrity was assessed by agarose gel electrophoresis. The experiment was repeated twice for reproducibility.

The cDNA was synthesized from 500 ng of cytoplasmic or total RNA using Maxima H Minus First Strand cDNA Synthesis Kit with dsDNase (Invitrogen) (detail in Appendix 1.7). Briefly, 1 µL of 10X dsDNase, and 1 µL of 10X dsDNase buffer were added in required volume of nuclease free water and RNA to a final volume of 10 µL. Then the reaction mix was incubated at 37 °C for 2 min in a thermal cycler (Biometra) and placed on ice for at least 1 min. Then 10 µL of cDNA synthesis mix containing 4 µL of 5X Maxima cDNA H Minus Synthesis Master Mix and 6 µL of nuclease free water and the reaction was then incubated for 10 min at 25 °C followed by another incubation for 15 min at 50 °C in Thermal Cycler (Biometra). The reaction was terminated by incubating at 85 °C for 5 min. The cDNA synthesis reaction was stored at −20 °C or used for PCR immediately.

Each RLR primer pair (Table 4.1) was checked by conventional RT-PCR. Primers that yielded a single and specific band on the agarose gel, were used for qPCR.

4.2.1.8.2 DNA standard generation for absolute quantification of mRNA transcript

For absolute quantification of mRNA transcripts of each gene, a plasmid DNA standard was generated. Plasmid standards for tight junction genes (claudin 3a, 8d and ZO-1), TLR3, IFNβ and Mx2 generated in Chapter 2, section 2.2.5 were used. DNA standards for RLR molecules were generated following the protocols described in Chapter 2, section 2.2.5.

Table 4. 1: Primer for RLRs and RLR associated molecules for RT-qPCR (S and T before the name of each primer represents salmon and trout respectably)

Name of the gene	Sequence (5'-3')	Ann. Tmp. (°C)	Product size (bp)	Reference sequence Acc. No.
S-RIGI	F1- ACTGATCGGGAGAGGACACAA R1- CTTGACCACATTGCCAACGTAT	59	202	XM_021593781
T-MDA5	F1- AGAGCCCGTCCAAAGTGAAGT R1- GTTCAGCATAGTCAAAGGCAGGTA	59	357	NM_001195179
T-LGP2b	F1- GTGGCAGGCAATGGGGAATG R1-CCTCCAGTGTAATAGCGTATCAATCC	59	212	FN396358
T-IPS1	F1- AGCCAGCCATACTCAGGAGA R1- CGTCCTCAGACACGTGAACA	59	268	NM_001195181
S-TBK1	F1- GACCTGTATGCGGTGAAGGT R1- CAGACTCCCACAGGGACAAT	59	161	XM_021592888
T-IRF3	F1- TGTATACACAGCGGAGGGGA R1- CACCCACAGCATCCTCCATT	59	209	NM_001257262
T-PKR	F1- GGAAAGCTAAGCGGGAGGTT R1- TCCTCTCGTCGATCCACACT	59	219	NM_001145891
S-ISG15	F1- AAGTGATGGTGCTGATTACGG R1- TTGGCTTTGAACTGGGTTACA	56	118	NM_001124609
T-VIG-1	F1- CTCCAGCTCCCAAGTGTCAG R1- TTGTACTTCCGGCACCAGTC	60	206	NM_001124253

4.2.1.8.3 Absolute quantification of mRNA transcripts

To investigate TLR3 and RLR mediate antiviral response and tight junction response in RTgill-W1 cells upon SAV-2 infection, TLR 3, IFNβ, Mx2, claudin 3a, 8d and ZO-1 primers were used (listed in Table 2.1). Moreover, RLRs and RLR associated gene markers (listed in Table 4.1) were used to investigate RLR mediated antiviral responses.

SYBR green based RT-qPCR (Chapter 2, Figure 2.1) was performed to quantify the mRNA transcripts of each gene using Roche LightCycler 480 instrument and Luminaries Color HiGreen qPCR Master Mix (Thermo Scientific). The following qPCR temperature profile was used: pre-treatment to 50 °C for 2 min; initial denaturation at 95 °C for 10 min, 40 cycles of denaturation 95 °C for 15s, annealing variable temperature depending on primer sets for 30s, and extension 72 °C for 30s; followed by dissociation curve: 95 °C for 10s, 55 °C for 5s and 95 °C for 30s to confirm the generation of a single specific amplicon. 2 µL of diluted cDNA (1:5) was used in18 µL of mastermix which includes 10 µL of SYBR Green (2x), 0.5 µL of each primer (400 nM) and 7 µL of molecular grade water to make final volume of 20 µL.

MIQE guidelines (Bustin et al., 2009) were followed in all the steps from RNA extraction to qPCR data analysis.

4.2.1.9 RLR mediated antiviral response in RTgill-W1 cells upon poly(I:C) induction

Similar experiment as described in section 4.2.8 was conducted in triplicate, where cells were stimulated with poly(I:C) at a concentration of 10 µg/mL. RNA extraction and cDNA synthesis were conducted using the protocol described before. Standards of RLR molecules were used for absolute quantification of mRNA transcripts where Syber Green based RT-qPCR was conducted in Roche LightCycler 480 instrument (Roche).

4.2.2 *A. salmonicida* invasion model for RTgill-W1 cells

4.2.2.1 Bacterial isolates and bacterial cell preparation for experiment

A. salmonicida subsp. *salmonicida* (NCIBM1102) was used in the study. The isolate is in place in the Institute of Aquaculture, University of Stirling, UK. The bacterium was revived from the frozen stock using Tryptic Soya Agar (TSA) (Oxoid). A single colony of bacterial culture of no more than 48 h was grown in 20 mL of Tryptic soya broth (TSB) (Oxoid) in

50 mL sterile falcon tube and incubated at 22 °C in static for 48. After 48 h of incubation, bacterial cells were harvested by centrifugation at 4°C for 15 min. Cells were then re-suspended in 5 mL 0.85% NaCl solution. An aliquot of cell suspension was used for flow cytometry analysis to enumerate the number of bacterial cells per microliter of cell suspension. Cells were always kept on ice to cease bacterial multiplication.

4.2.2.2 RTgill-W1 Cell culture

RTgill-W1 cells were maintained following the protocol described in section 4.2.1.4.

4.2.2.3 Infection of epithelial cell monolayer

4.2.2.3.1 Invasion of epithelial monolayer by *A. salmonicida*

To investigate the ability of *A. salmonicida* to penetrate the epithelial monolayer, RTgill-W1 cells were seeded onto transwells in a 12 well plate (Corning) with a growth area of 0.9 cm^2 and 3-micron pore size with a seeding density of 0.12×10^6 cells/insert. Blank inserts with only medium in the apical and basolateral side were maintained. Cells were maintained in L-15 medium supplemented with 10% FBS at 22 °C until confluency. The confluent cell monolayer was infected with *A. salmonicida* prepared in section 4.2.2.1 at a MOI of 10. At 5, 10, 15, 30 min, 1, 3 and 6 h post infection, 100 µL of growth medium from the basolateral side of each insert was collected into sterile 1.5 mL eppendorf tube and kept on ice. After each sampling, the basolateral compartments were replenished with 100 µL of fresh medium.

For the enumeration of live bacterial cells in the collected medium, the LIVE/DEAD BacLight Bacterial Viability and Counting Kit (Molecular probes, Invitrogen) containing SYTO and Propidium iodide (PI) was used. First a working solution of SYTO and PI was prepared in PBS (3 µL of SYTO + 3 µL of PI in 1.0 mL of PBS; 2x of recommended concentration of each component was used because of further 2-fold dilution). The solution was mixed properly and 100 µL of the solution was added into 100 µL of each sample, mixed gently and incubated for 15 min in dark. After incubation samples were analysed by flow cytometer (Beckman Coulter).

The percentage of bacterial cell invading through the monolayer with or without stimulation was calculated according to the equation mentioned below where the bacterial cell passing thorough the blank insert was considered as 100%.

$$Bacterial\ invasion\ through\ cell\ monolayer\ (\%) = \frac{Bacterial\ cells\ count\ in\ treated\ or\ untreated\ group\ \times 100}{Bacterial\ cell\ count\ in\ blank}$$

4.2.2.3.2 Modulation of epithelial monolayer by viral and bacterial PAMPs

To investigate the effectiveness of viral and bacterial PAMPs in modulating cellular integrity against bacterial infection, RTgill-W1 cells were pre-treated with, LPS and PGN 24 h before bacterial infection. A blank group without RTgill-W1 were also inoculated with bacteria while a control group with RTgill-W1 cells and bacteria were maintained. In the treatment groups, RTgill-W1 cells were stimulated with, 10 µg/mL LPS and 10 µg/mL PGN 24 h before infection. Another group for CyD treatment was also maintained where the RTgill-W1 cells were pre-treated with 2 µg/mL CyD 1 h before infection with *A. salmonicida* sub. *salmonicida*. The percentage of bacterial invasion through the epithelial monolayer was determined at 6 h post infection following the protocol of previous section.

In the control group, the percentage of bacteria invading through the monolayer was the percentage of bacterial cell passing through the blank insert while in the treatment groups the percentage of bacteria through the stimulated/treated monolayer was the percentage of bacteria passing through the stimulated/treated cell monolayer.

4.2.2.4 Antibacterial response of RTgill-W1 cells upon bacterial infection

To investigate the antibacterial response of RTgill-W1 cells to bacterial infection, RTgill-W1 cells were seeded onto the 12 well transwells (Corning) with a growth area of 0.9 cm^2 and 3-micron pore size with a seeding density of 0.12×10^6 cells/insert. Cells were maintained in L-15 medium supplemented with 10% FBS at 22 °C until confluency. The confluent cell monolayer was infected with *A. salmonicida* prepared according to the section 4.2.2.1 at a MOI of 10. The infection was continued for 3 and 6 h. Then cells were harvested using TRI-reagent for the extraction of total RNA following the protocol as explained in section 2.2.4.2.1 of chapter 2 and cDNA was synthesized using Maxima H Minus First Strand cDNA Synthesis Kit with dsDNase (Invitrogen) following the protocol

explained in section 4.2.4.1. Each cytokine and antimicrobial peptide primer pair (Table 4.2) was checked by conventional RT-PCR. The primers were designed, synthesized and validated by Primer Design Company. Each PCR product was then purified and ligated for DNA standard was generated following the protocols described in Chapter 2, section 2.2.5.

SYBR green based RT-qPCR was performed to quantify the mRNA transcripts of each gene using Roche LightCycler 480 instrument and Luminaries Color HiGreen qPCR Master Mix (Thermo Scientific) following the protocol described in section 4.2.4.3.

Table 4. 2: List of primers used for the study of expression of selected cytokines, innate immune gene and antimicrobial peptides in RTgill-W1 cells.

Target gene	Sequence (5'-3')	Ann. Temp. (°C)	Product size (bp)	Reference sequence Acc. No.
IL-8	F- GCTGCATTGAGACGGAAAGC R- ACATGATCTCAGTGTCTCTG	60	96	AY221022.1
CD209b	F- CACCTTAGCATCCTGCACAGCAA R- CGAGCTGTACGGTTGCCAGAAGTTAT	60	177	NM_001160495.1
rtCATH2	F- ACATGGAGGCAGAAGTTC R-GAGCCAAACCCAGGACGAGA	60	133	NM_001124463.1
omDB3	F- GCTTGTGGAATACAAGAGTCATCTGC R- GCATACATTCGGCCATGTACATCC	60	138	NM_001195183.2

4.2.2.5 Viral and bacterial PAMP induced immune response RTgill-W1 cells

Similar experiment as described in section 4.2.2.4 was conducted in triplicate where cells were stimulated with poly(I:C), LPS and PGN at a concentration of 10 μg/mL. Syber Green based RT-qPCR was conducted in Roche LightCycler 480 instrument following the protocols already explained.

4.2.3 Statistical analysis

TER data were analysed using 2-way repeated measure ANOVA followed by Bonferoni's multiple comparison using GraphPad prism version 6.0 (San Diego, CA, USA). RT-qPCR data were also analysed using 1-way ANOVA followed by Bonferoni's multiple comparison using GraphPad prism version 6.0. In all analyses, differences between groups were considered statistically significant at $p<0.01$ unless otherwise mentioned.

4.3 Results

4.3.1 Response of RTgill-W1 cells to Salmonid alphavirus subtype 2 (SAV-2) infection

SAV-2 was used as an infectious agent to investigate the cellular and molecular response of salmonid gill epithelial cell line RTgill-W1 upon viral infection. SAV-2 was grown in the laboratory and quantified the virus titer before used.

4.3.1.1 SAV- 2 culture in fish cell line

Three fish cell lines CHSE-214, CHH-1 and TO were initially tested for growing SAV-2 using two inoculation methods: (i) the adsorption inoculation method where virus was inoculated on preformed cell monolayers, and (ii) the simultaneous inoculation method where cell seeding, and virus inoculation were done simultaneously. Five different dilutions of the virus (10^{-1} to 10^{-5}) were used.

Cells were monitored everyday under the inverted microscope to check for CPE. CPE was found to form at day 5, 3 and 6 in CHSE-214, CHH-1 and TO cells respectively inoculated by adsorption method while in cells inoculated by the simultaneous method CPE started to form at day 4, 4 and 6 in CHSE-214, CHH-1 and TO cells respectively. Although, CPE started earlier in the CHH-1 cell line, CPE was much more progressive in CHSE-214 cells. Virus was harvested at day 18 from all the cells and was quantified by real time PCR. The highest viral RNA copy number was found in CHSE-214 cell inoculated with a dilution of 10^{-3}. For mass production of SAV in 25 cm^2 TC flasks, dilutions of 10^{-2} and 10^{-3} using both adsorption and simultaneous inoculation methods were inoculated. CPE started to form at day 4 and day 5 in adsorption inoculation with 10^{-2} and 10^{-3} respectively while in simultaneous inoculation method CPE started to form at day 5 in both dilutions. CPE was found to progress slowly up to day 10, later it progressed rapidly. The CPE was more progressive in the 10^{-3} dilution in simultaneous inoculation where at day 18 almost all the cells were detached from the surface of the flask. At day 20, virus was harvested from all four flasks of the simultaneous inoculation inoculated with a dilution of 10^{-3} (method section 4.2.1.1).

4.3.1.2 $TCID_{50}$ of SAV2, viral standard generation and viral copy number determination

Virus titter was done in CHSE-214 cells where a $TCID_{50}$ of $10^{6.35\pm0.2}$ per ml was detected. For the generation of a quantitative SAV-2 standard, viral RNA was extracted from the viral

supernatant. A target region was amplified by PCR, ligated into pCRII and RNA was transcribed from the plasmid (method section 4.2.3). A SAV-2 RNA standard from 10^7 - 10^1 copies per microliter was diluted using tRNA as the diluent. A standard curve was generated by three TaqMan probe based real time RT-qPCR runs of the entire RNA standard (Figure 4.4 show standard graph (r^2 = 0.9877, efficiency = 2.4 and sensitivity 10^1) (method section 4.2.3). The viral copy number in the stock was then also determined using TaqMan probe based real time RT-qPCR which gave copy number of around 10^7 per mL.

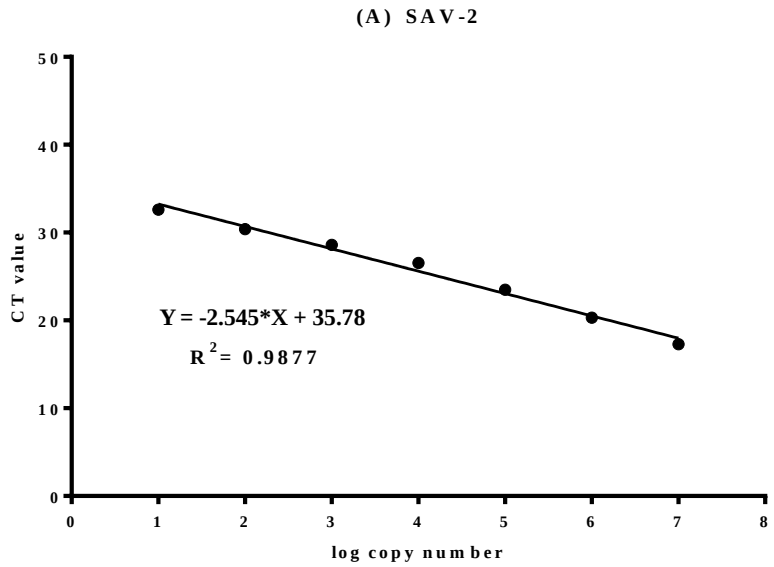

Figure 4.4: Standard curve of SAV-2. The graph was generated using the Log10 of copy number (X-axis) and the corresponding CT value (Y-axis). Each standard was run in duplicate and mean of three independent runs was used. Graph was generated and analysed using GraphPad Prism v. 6.0

4.3.1.3 Growth and replication of SAV-2 in RTgill-W1 cells

To investigate the load of SAV-2 in the cytoplasmic fraction of RNA of RTgill-W1 cells in a time dependent manner as a result of viral replication, cytosolic RNA was used where Taqman probe-based RT-qPCR was employed. Very low viral copy number was detected in the cytosolic RNA throughout the experimental period (Figure 4.5). However, significantly higher viral copy number was detected at 30 h post infection ($p<0.01$).

Further, to investigate the replication efficiency of SAV-2 in RTgill-W1 cells, cells were infected with SAV-2 at a concentration of MOI10, 1 and 0.1 using strand specific RT-qPCR. SAV-2 was found to replicate in the MOI 10 and 1 infected cells. In MOI0.1 infected cell replication was detected. Virus replication inside the RTgill-W1 cells was detected as early

as 6 h of post infection. However, viral replication was significantly higher at 12 and 24 h post infection ($p<0.01$).

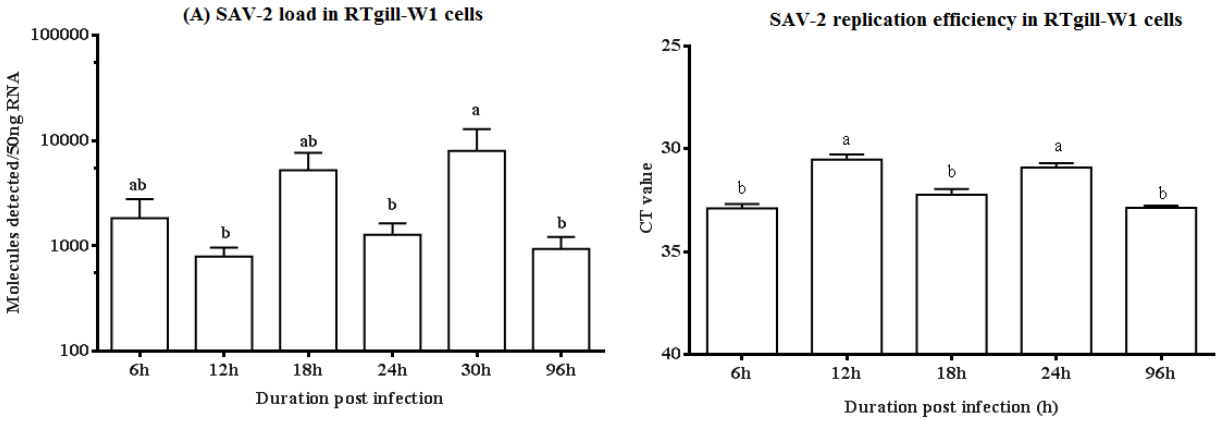

Figure 4.5: Viral load (A) and replication (B) in RTgill-W1 cells at different time points of post infection with SAV-2 at MOI 10. Viral copy number was determined using Taqman probe-based RT-qPCR and SAV-2 replicative strand was detected using strand specific RT-qPCR. Values are mean ± SEM. Data were analysed by One-Way ANOVA followed by Bonferoni's multiple comparison. Bar with different letters are significantly different with a level of significance $p<0.01$. Data were analysed using GraphPad prism version 6.0.

4.3.1.4 Effects of SAV-2 on cellular integrity

To investigate the effects of SAV-2 on TER, polarized RTgill-W1 cells in the transwell inserts were infected with SAV-2 at a concentration of MOI 10, 1 and 0.1. Before SAV2 infection, TER in each group was monitored overtime until it reached at peak and remained stable (16-20 $\Omega.cm^2$) in 72 to 96 h (Figure 4.6A). Post infection TER in the MOI 10 infected group started to decrease from as early as 30 min until 6 h post infection (hpi) and the decrease was significant at 1, 3 and 6 hpi ($p<0.005$) while in MOI 1 and MOI 0.1 infected group, TER was similar to the control group until 6 hpi (Figure 4.6B). However, TER in all the groups coincided at 24 hpi and then increased gradually until end of experiment in infected groups with some fluctuations where cells showed slightly significant higher resistance at 48 and 72 hpi in MOI 0.1 and 48 hpi in MOI 10 infected groups ($p<0.005$).

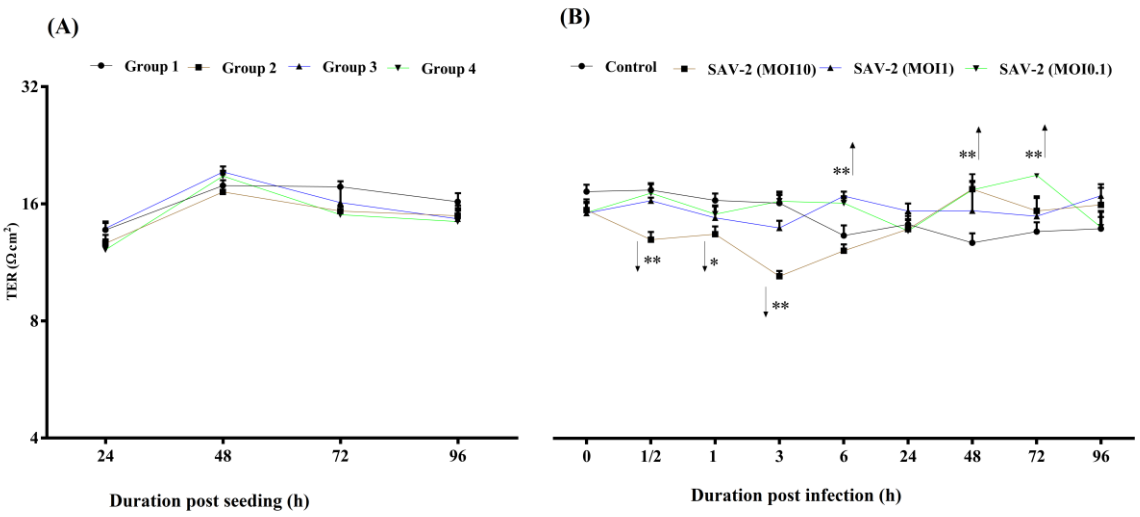

Figure 4.6: Modulation of transepithelial resistance (TER) of RTgill-W1 cells. (A) TER before infection where cells were seeded onto the transwells and left uninfected until TER reached at peak and remained stable. (B) TER in response to SAV-2 infection at MOI 10, 1 and 0.1 at different time points. In all cases 3 independent experiments in triplicate were conducted with 3 measurements at a single time point in each replicate. Values are mean ± SEM (n=3×3=9). TER of infected groups was compared to control group in each time point at the significance level of *=p<0.005, **=p<0.0005 using repeated measure two-way ANOVA, GraphPad Prism version 6.0.

4.3.1.5 Molecular response upon SAV-2 infection

To investigate the molecular response upon viral infection, tight junction related genes, genes related to TLR3 and RLR signaling pathways were tested. The expression patterns were monitored by SyberGreen based absolute qPCR where copy number was calculated from the standard curve (detailed in the method section). For each standard curve, co-efficient of determination (R^2), efficiency and sensitivity were calculated (Table 4.3).

Table 4. 3: Co-efficient of determination (r^2), efficiency and sensitivity for the target genes generated from the standard curve. Efficiency was calculated using the formula, $E = 10^{(-1/-slope)}$. E value of 2.0 is equivalent to 100% efficiency. N represent the number of qPCR run for each gene to make standard curve while sensitivity is the lowest copy number detected by qPCR.

Target	r^2	Efficiency	N	Sensitivity
TLR3	0.99	1.93	3	10^1
Mx2	0.99	1.95	3	10^1
ZO-1	0.99	1.93	3	10^1
RIG-I	0.99	1.88	3	10^2
MDA5	0.99	1.84	3	10^1
LGP2b	0.99	1.93	3	10^1
IPS1	0.99	1.87	3	10^1
TBK1	0.99	1.95	3	10^1
IRF3	0.99	1.82	3	10^1
PKR	0.99	1.80	3	10^1
ISG15	0.98	2.01	3	10^2
Viperin	0.99	1.95	3	10^2

Standard curve of each of the gene is presented in Appendix 2.2, Figure S2.2.

4.3.1.5.1 Expression of tight junction genes

SAV-2 was not found to induce the expression of tight junction regulatory gene ZO-1 (Figure 4.7) and tight junction gene claudin 3a and 8d (data not shown).

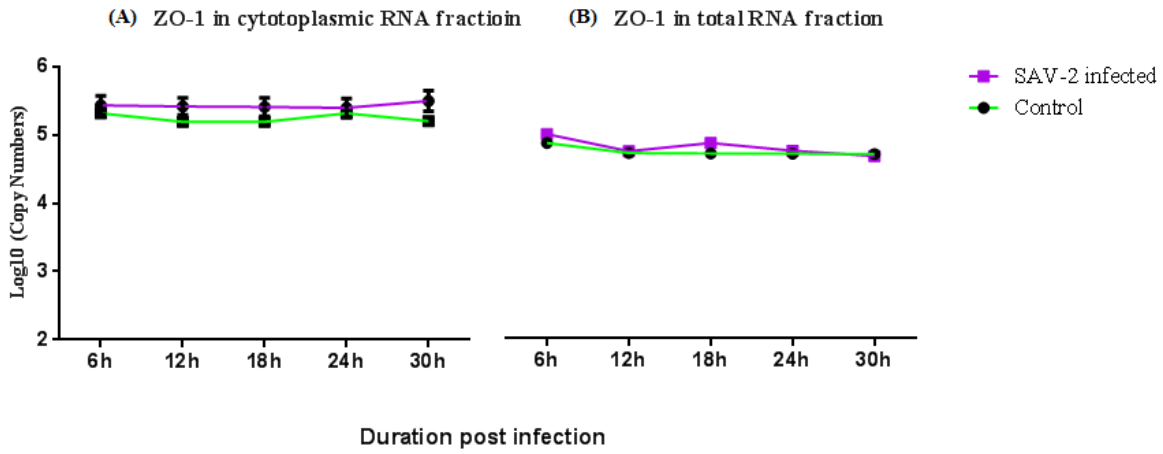

Figure 4.7: Expression of tight junction regulatory protein ZO-1 in cytoplasmic and total RNA fractions of RTgill-W1 cells. Cells were infected with SAV-2 for different time points and level of expression was compared between infected and control cells. One-way ANOVA, Bonferoni's multiple comparison was done to analyse the data where statistical significance was determined with the level of significance of $p<0.01$ using GraphPad Prism version 6.0. Green line denotes control group while purple line denotes SAV-2 infected group.

4.3.1.5.2 Antiviral response through TLR3 signaling pathway

Antiviral response of RTgill-W1 cells was detected in SAV-2 infected cells. Initially, three different MOI were used to infect the cells to optimize the virus concentration for the experiment. Expression of the response molecule, Mx2 was used as an indication of antiviral response where expression of Mx2 in RTgill-W1 cells infected with MOI 10 was higher than that of MOI 1 and MOI 0.1 in the cytoplasmic RNA at 96 h post infection. Expression of Mx2 in MOI 10 infected cells was around 2.5-fold higher than that of MOI 0.1 (Figure 4.8A). In control cells no expression of Mx2 was detected. Then for the final experiment virus concentration of MOI10 was used. As a low level of Mx2 expression had been detected in cytoplasmic RNA at 96 h post infection, the time course of Mx2 expression was monitored at 6h intervals in cytoplasmic and total RNA fractions from 6 h up to 30 h. In both cytoplasmic and total RNA fractions, the highest yield of Mx2 mRNA transcripts was observed at 30 h post infection with a significantly higher Mx2 copy number than at any of the other time points ($p<0.0001$; Figure 4.8B).

To investigate the endosomal sensor of dsRNA, TLR3 expression upon SAV-2 infection was investigated where a significantly higher copy number of TLR3 was detected in SAV-2 infected cells than that of non-infected cells at early stage of infection until 18h ($p<0.001$;

Figure 4.8C). Moreover, IFNβ expression upon infection was investigated where the expression remained stable but low throughout the experiment (data not shown).

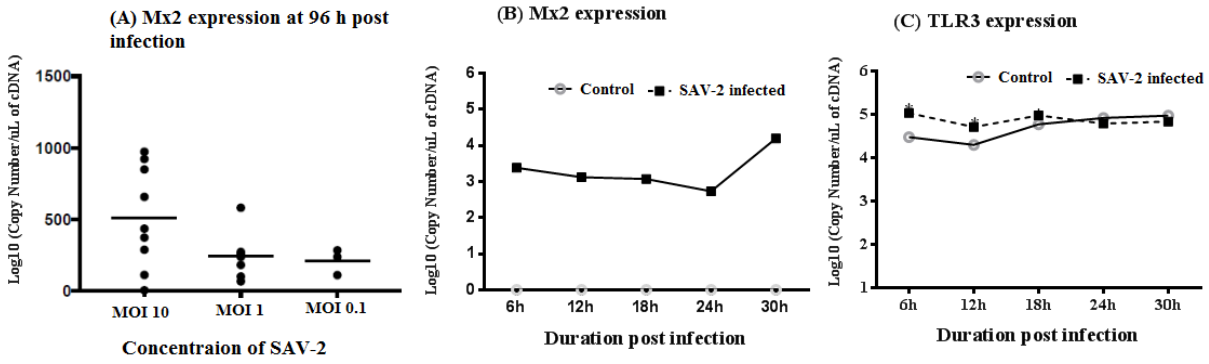

Figure 4.8: Expression profile of viral dsRNA receptor molecule TLR3 and antiviral response gene Mx2 in the cytoplasmic RNA of RTgill-W1 cells. (A) Expression of Mx2 after 96 h of post infection with SAV-2 at MOI of 10, 1 and 0.1 and (B) expression of Mx2 in control and SAV-2 infected cells. (C) TLR3 expression in control and SAV-2 infected RTgill-W1 cells at different post infection duration where in the control cells no expression of Mx2 was detected. One-way ANOVA, Bonferoni's multiple comparison was done to analyse the data where statistical significance was determined with $p<0.01$ using GraphPad Prism version 6.0.

4.3.1.5.3 Antiviral response through RLR signaling pathway

To investigate whether RTgill-W1 cells can sense SAV-2 by RLR signaling molecules and can activate the RLR signaling pathway, several genes associated with the pathway were selected. RIG-I, MDA5 and LGP2b were used as the perception molecules while IPS1 and TBK1 were used as integrating molecules. IRF3 was used as one of the transcription factors while PKR, ISG15 and viperin were used as antiviral response molecules.

4.3.1.5.3.1 Response upon poly(I:C)

Poly(I:C) is an analogue of dsRNA and is sensed by different host receptors. To investigate whether RTgill-W1 cells can sense poly(I:C) through cytoplasmic RLR molecules, cells were stimulated with poly(I:C) and expression pattern was monitored in cytoplasmic and total RNA fractions.

Poly(I:C) was found to enhance the upregulation of all of the tested receptor molecules RIG-I, MDA5 and LGP2b at all the time points in both cytoplasmic and total RNA ($p<0.0001$) except MDA5 at 6 and 30 h of post stimulation in cytoplasmic RNA and 30 h of post

stimulation in total RNA (Figure 4.9). Signaling molecules IPS1 and TBK1 remained stable upon stimulation while expression of IRF3 in both mRNA fractions was significantly and constitutively upregulated upon stimulation (Figure 4.10). All the interferon stimulated genes PKR, ISG15 and viperin constitutively and significantly upregulated in both cytoplasmic and total RNA upon stimulation ($p<0.0001$) (Figure 4.11).

4.3.1.5.3.2 Response upon SAV-2 infection

SAV-2 replicates in the cytoplasm where dsRNA is formed and is available to be sensed by host's sensors. To assess whether SAV-2 indeed triggers the expression of the molecules associated with RLR pathway, the parameters shown to respond to poly(I:C) stimulation were also measured upon SAV-2 infection.

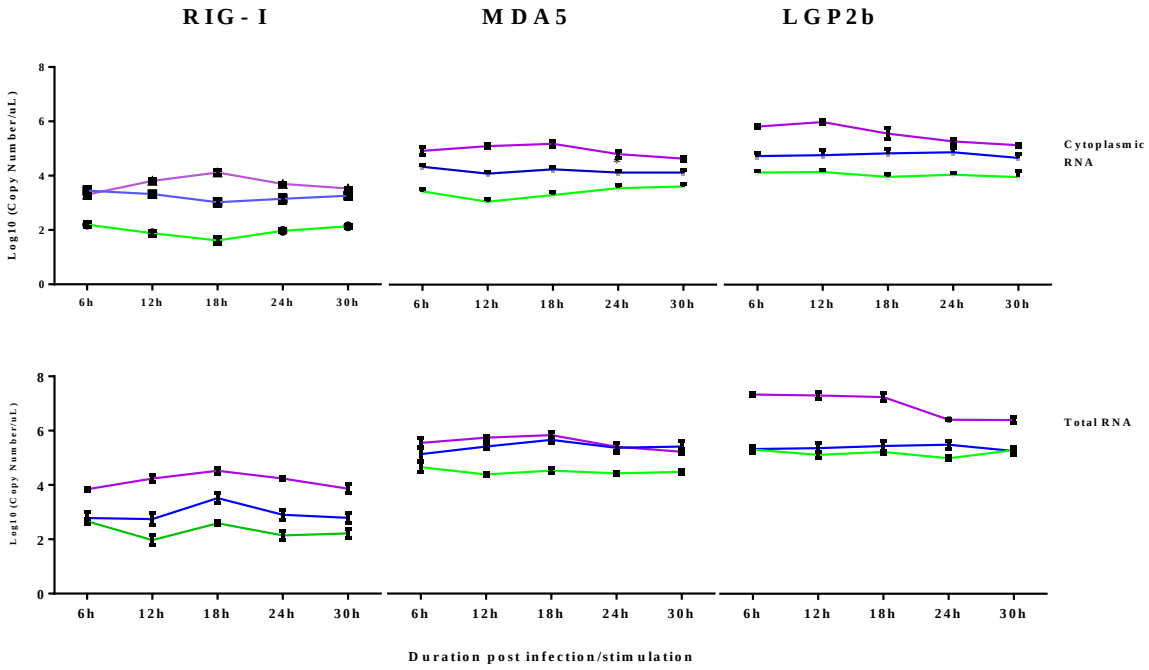

Figure 4.9: The absolute expression of dsRNA receptor molecules RIG-I, MDA5 and LGP2b in cytoplasmic and total RNA fractions of RTgill-W1 cells comparing between control and SAV-2 infected cells and Poly(I:C) stimulated cells at different time points. Data are mean ± SEM of three course independent experiment. One-way ANOVA, Bonferoni's multiple comparison was done to analyse the data where statistical significance was determined with $p<0.01$ using GraphPad Prism version 6.0. Green, blue and purple lines represent control, SAV-2 infected and poly(I:C) stimulated group respectively.

In the cytoplasmic RNA, the RIG-I mRNA transcript was significantly and constantly upregulated in response to SAV 2 infection which was significantly higher than the control

group at all time points ($p<0.0001$; Figure 4.9). Moreover, in total RNA, the mRNA transcript of RIG-I was upregulated at 12 and 24 h post infection in response to SAV2 (Figure 4.9). Expression of MDA5 in the cytoplasmic RNA was upregulated at the early stage of infection until18 h post infection and did remain unchanged at the late stage of SAV2 infection in both cytoplasmic and total RNA. Expression of LGP2b, a splice variant of LGP2 was also upregulated until 24 h post infection with a little decrease at 12 h in the cytoplasmic RNA ($p<0.0001$) while in the total RNA, the expression was found to be stable. In the cytoplasmic RNA, IPS1 remained stable in both control and infected cells throughout the experiment. However, in the total RNA fraction, IPS1 was downregulated at the early stage of infection at 6 ($p<0.01$) and 12 ($p<0.001$) h which was maintained to normal level at 18 and 24 h and again downregulated at 30 h ($p<0.001$) of infection. TBK1 in the cytoplasmic fraction was slightly upregulated at 12 ($p<0.01$), 18 ($p<0.01$) and 24 (0.001) h post infection. In the total RNA, TBK1 expression was unaffected by SAV-2 infection. In the cytoplasmic RNA, IRF3 was constitutively and significantly upregulated following SAV2 infection, while in total RNA expression was upregulated at 18 h post infection ($p<0.0001$) (Figure 4.10).

Interferon stimulated genes PKR upregulated upon SAV-2 induction at 12 h and onwards in cytoplasmic RNA fraction and remained unchanged except 18 h post induction in total RNA fraction. Other ISGs, ISG15 and Viperin were significantly upregulated throughout the experiment in the cytoplasmic RNA fraction ($p<0.0001$; Figure 4.11). In the total RNA fraction, ISG15 upregulated at all the time points except 24 h post SAV-2 infection.

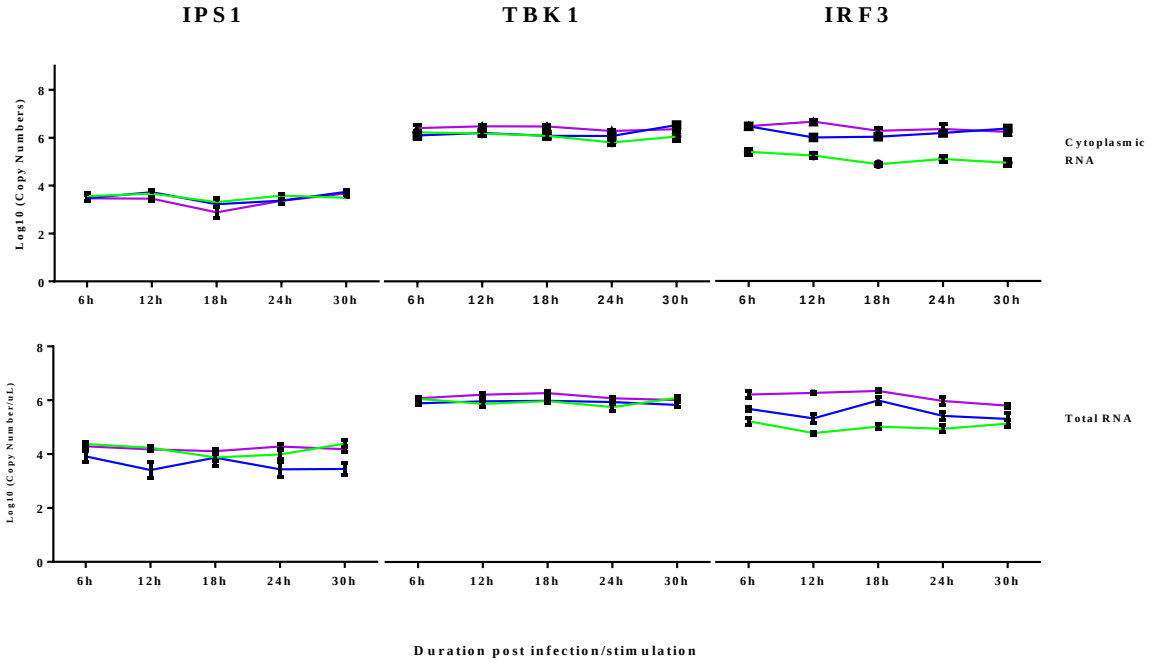

Figure 4.10: The absolute expression of the signaling molecules IPS1, TBK1 and IRF3 in the cytoplasmic and total RNA fractions of RTgill-W1 cells comparing between control and SAV-2 infected groups and control and poly(I:C) stimulated groups at different time points. Data are mean ± SEM of three course independent experiment. One-way ANOVA, Bonferoni's multiple comparison was done to analyse the data where statistical significance was determined with $p<0.01$ using GraphPad Prism version 6.0. Green, blue and purple lines represent control, SAV-2 infected and poly(I:C) stimulated group respectively.

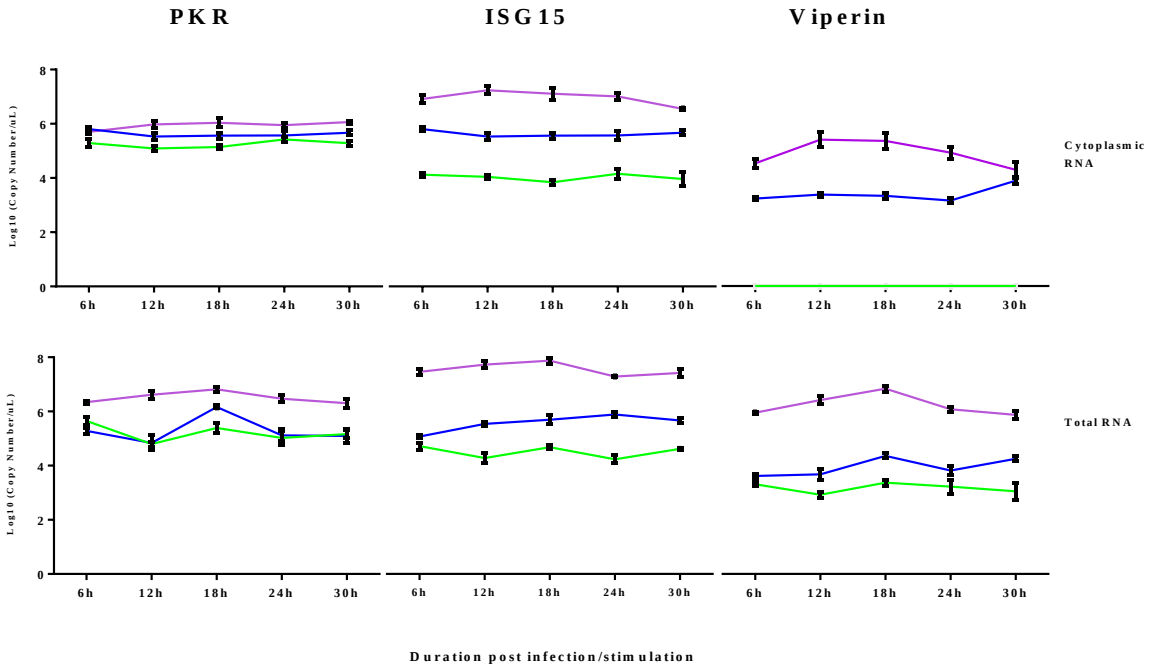

Figure 4.11: The absolute expression of the interferon stimulated genes PKR, ISG15 and viperin in the cytoplasmic and total RNA fractions of RTgill-W1 cells comparing between control and SAV-2 infected groups and control and poly(I:C) stimulated groups at different time points. Data are mean ± SEM of three course independent experiment. One-way ANOVA, Bonferoni's multiple comparison was done to analyse the data where statistical significance was determined with $p<0.01$ using GraphPad Prism version 6.0. Green, blue and purple lines represent control, SAV-2 infected and poly(I:C) stimulated group respectively.

The level of expression of each molecule at each time point has been demonstrated in Figure 4.12 (cytoplasmic RNA fraction) and 4.13 (total RNA fraction) where each rectangle represents replicate for respective gene, treatment group and duration.

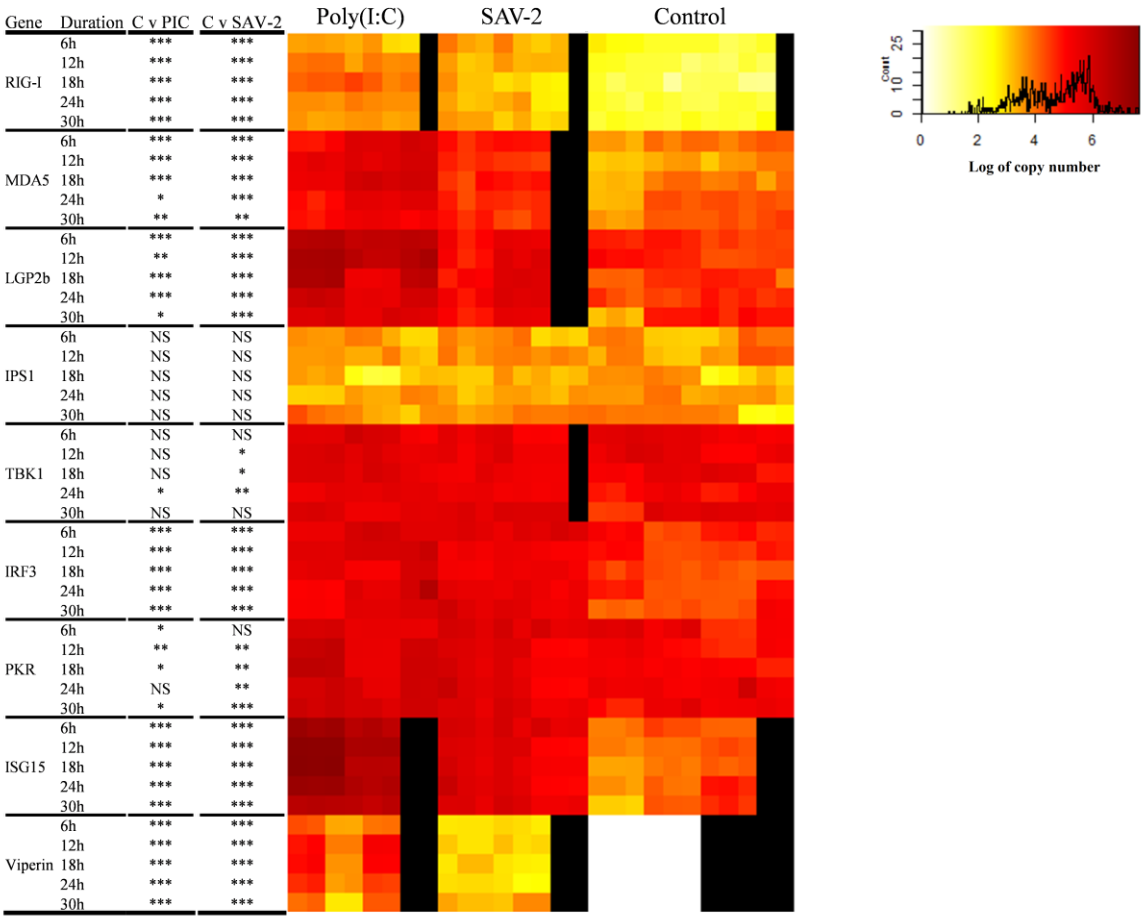

Figure 4.12: Heat map showing the absolute quantification of expression of mRNA transcripts of RLRs, integration and effector molecules in cytoplasmic RNA fraction RT-gill-W1 cells as depicted in the colour scale. Significant upregulation at $p<0.0001$, $p<0.001$ and $p<0.01$ were expressed by the asterisk ***, ** and * respectively. Black color in the heat map represents no sample.

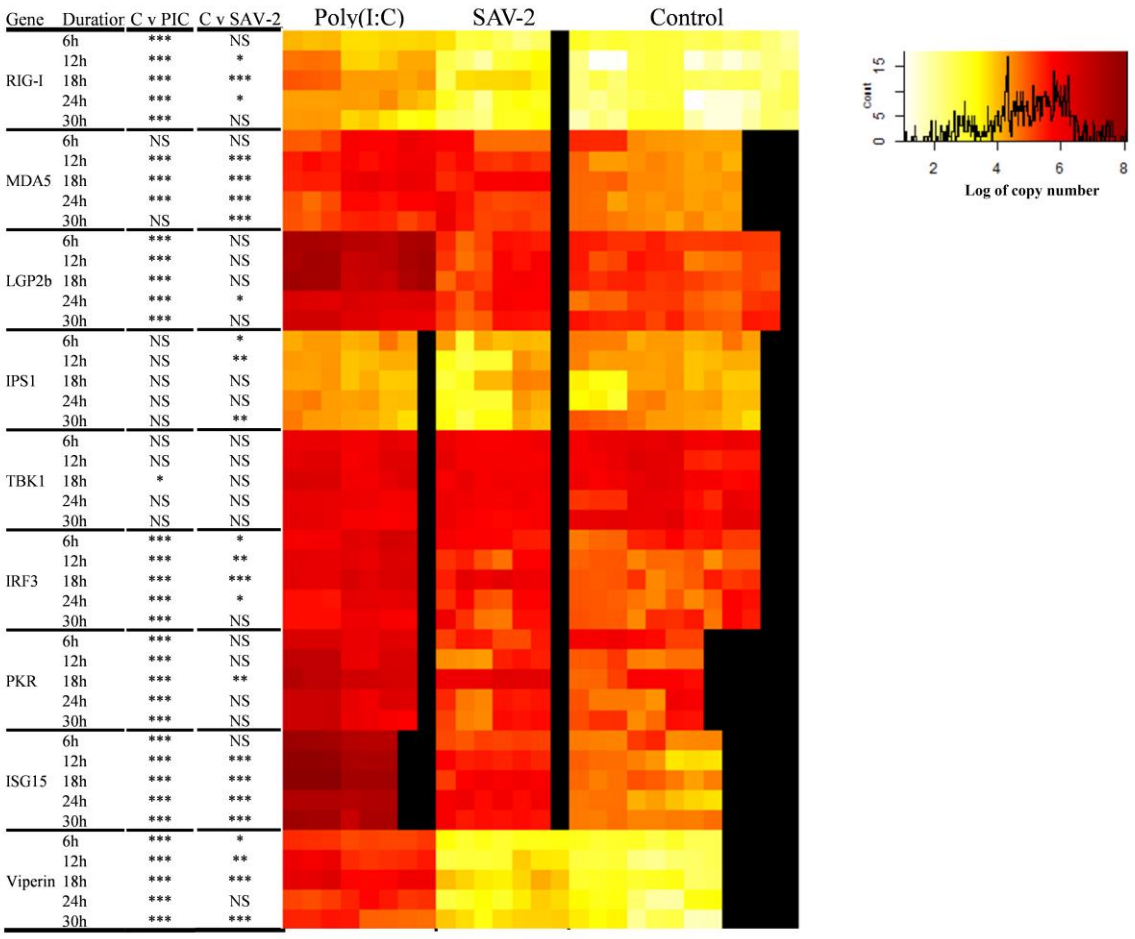

Figure 4.13: Heat map showing the absolute quantification of expression of mRNA transcripts of RLRs, integration and effector molecules in total RNA fraction of RT-gill-W1 cells as depicted in the colour scale. Significant upregulation or downregulation at $p<0.0001$, $p<0.001$ and $p<0.01$ were expressed by the asterisk ***, ** and * respectively. Black color in the heat map represents no sample.

4.3.2 *A. salmonicida* invasion model for RTgill-W1 cells

To investigate the barrier function of RTgill-W1 cells against bacterial infection, the cell monolayer was infected with *A. salmonicida*, a common pathogen of rainbow trout. Then the invasion of bacteria through the cell monolayer was studied by FACS analysis.

4.3.2.1 Rapid translocation of polarized RTgill-W1 cell monolayers

To investigate how fast pathogenic *A. salmonicida* sub. *salmonicida* can penetrate the epithelial monolayer, after apical infection of RTgill-W1 cells with bacteria, medium from the lower chamber of the transwell apparatus was sampled at different time points and bacterial load was determined flow cytometer using bacterial viability and counting kit.

The bacterial penetration was found to follow a time-dependent fashion where the recovery of *A. salmonicida* from the basolateral side at 5 min post-infection was less than 2% of the bacterial count from the basal side of blank insert with only medium and bacteria which remained stable until 1h of post-infection (Figure 4.14). The bacterial count increased to around 10% at 3 h and around 60% at 6 h of post-infection.

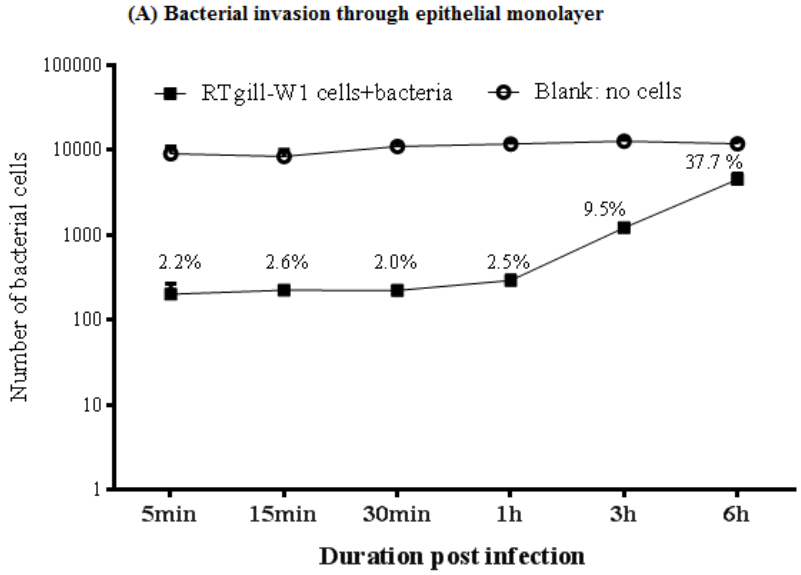

Figure 4.14: (A) Recovery of *A. salmonicida* subsp. *salmonicida* from the basolateral side of the transwells after penetration of polarized RTgill-W1 cell monolayers between 5 min and 6 h post-infection. RTgill-W1 cells were allowed to grow onto the transwells with 3µm pore size until they reached confluency. Each point is the mean cell count standard deviation by FACS analysis; each assay was done in triplicate for typical. Bacteria was recovered from 100 µL of L-15 medium from serosal side of the transwells. Sytox and propidium iodide were added into the sample and incubated for 15 min followed by FACS analysis by CytoFlex flow cytometer. The percentage represents the percentage of bacteria recovered from the transwells with RTgill-W1 cells compare to the blank (without cells).

4.3.2.2 Modulation of cellular integrity by viral and bacterial PAMPs against bacterial infection

To further investigate whether viral and bacterial PAMPs can modulate cellular integrity against bacterial infection, RTgill-W1 cells were pre-treated with poly(I:C), LPS and PGN 24 h before bacterial infection. Moreover, as bacterial invasion was very low until 3 h post-infection, the bacterial count was done only at 6 h of post infection. CyD which has been found to disrupt the cell monolayer (Chapter 3, section 3.2.1), was also used as a control treatment.

In the control group (RTgill-W1 cells + bacteria), around 45% bacterial cells were recovered from the basolateral side which was reduced to 7, 10 and 13% (Figure 4.15) when the RTgill-W1 cells were pre-treated with poly(I:C), LPS and PGN which were significantly lower than control group ($p<0.0001$, 0.0001 and 0.001 respectively). However, in the CyD treatment group, bacterial cell count in the basolateral side remained similar to the control group.

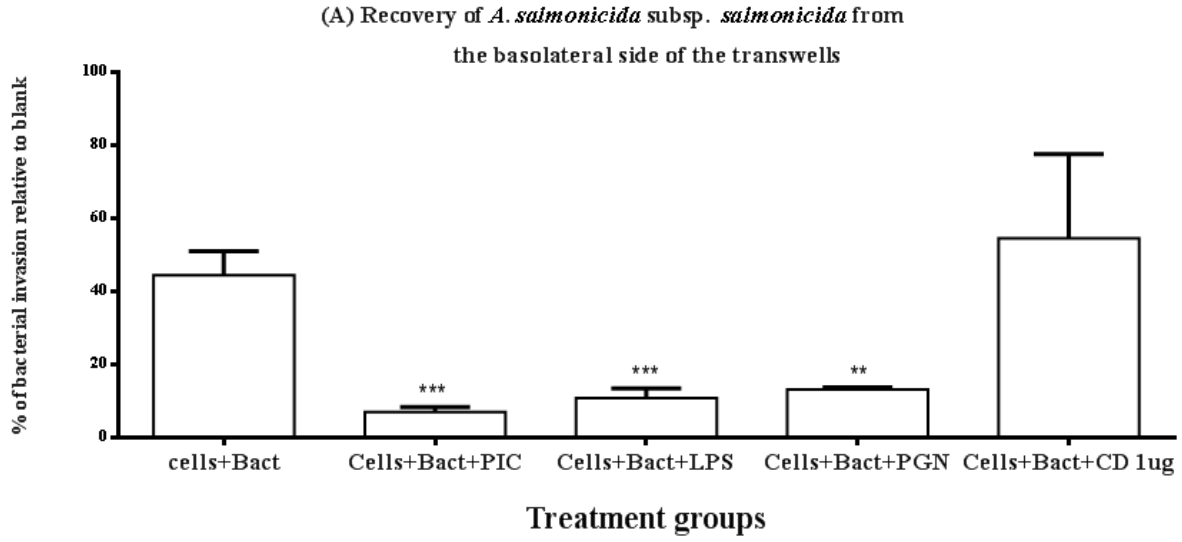

Figure 4.15: Percentage of recovery of *A. salmonicida* compared to blank after penetration of polarized RTgill-W1 cell monolayers at 6 h post-infection. RTgill-W1 cells were allowed to grow onto the transwells with 3µm pore size until reach confluency. For treatment groups with PAMPs, cells were pre-treated with respective PAMPs (poly(I:C), LPS and PGN) at 10 µg/ml 24 h before bacterial infection. For CyD treatment, cells were pre-treated with CyD at 1µg/ml 3 h (dose and duration optimized in Chapter 3, section 3.2.1) before bacterial infection. Data presented as mean ±SEM of cell count by FACS analysis where each assay was done in triplicate. Bacterial cells were recovered from 100 µL of L-15 medium from serosal side of the transwells after adding Sytox and propidium iodide and incubated for 15 min followed by FACS analysis by CytoFlex flow cytometer. One-way repeated measure ANOVA followed by Bonferoni's multiple comparison was conducted using GraphPad Prism 6.0 where the level of significance was $p<0.01$. Data were compared between control and treatment groups where ** and *** represent $p<0.001$ and $p<0,0001$ respectively

4.3.2.3 Molecular response upon bacterial infection

To further investigate the effects of *A. salmonicida* on RTgill-W1 cells at the molecular level, the expression of some selected gene markers was monitored. Pro-inflammatory cytokine, IL-8, innate immune gene C-type lectin CD209b and antimicrobial peptides rtCATH2 and omDB3 were tested. The expression pattern was monitored by SyberGreen based absolute qPCR. For absolute quantification of copy number of mRNA transcripts, DNA standard was generated for each gene (as described in the section 4.1.6). For each standard curve, co-efficient of determination (R^2), efficiency and sensitivity were calculated (Table 4.4).

Table 4. 4: Co-efficient of determination (r^2), efficiency and sensitivity for the target genes generated from the standard curve. Efficiency was calculated using the formula, $E = 10^{(-1/slope)}$. E value of 2.0 is equivalent to 100% efficiency. N represent the number of qPCR run for each gene to make standard curve while sensitivity is the lowest copy number detected by qPCR.

Target	r^2	Efficiency	N	Sensitivity
omDB3	0.99	1.91	3	10^1
IL-8	0.98	1.83	3	10^1
CD209b	0.96	1.86	3	10^1
rtCATH2	0.99	1.85	3	10^1

Standard curve of each of the gene is presented in Appendix 2.3, Figure S2.3.

4.3.2.3.1 Expression of cytokines (IL-8) and innate immune gene (CD209b) antimicrobial peptides (AMPs) in RTgill-W1 cells upon bacterial infection

The expression of the target genes was monitored upon infection for 3 and 6 h with typical *A. salmonicida*. IL-8 was significantly upregulated upon infection of *A. salmonicida* in both time points (Figure 4.16). Moreover, the innate immune gene C-type lectin CD209b was also significantly upregulated in similar fashion to IL-8. However, the antimicrobial peptide cathicidin (rtCATH2) was only upregulated significantly at late stage of infection with *A.*

salmonicida. Surprisingly, another antimicrobial peptide β-defensin (omDB3) was significantly downregulated at 6h of post infection with *A. salmonicida* ($p<0.001$).

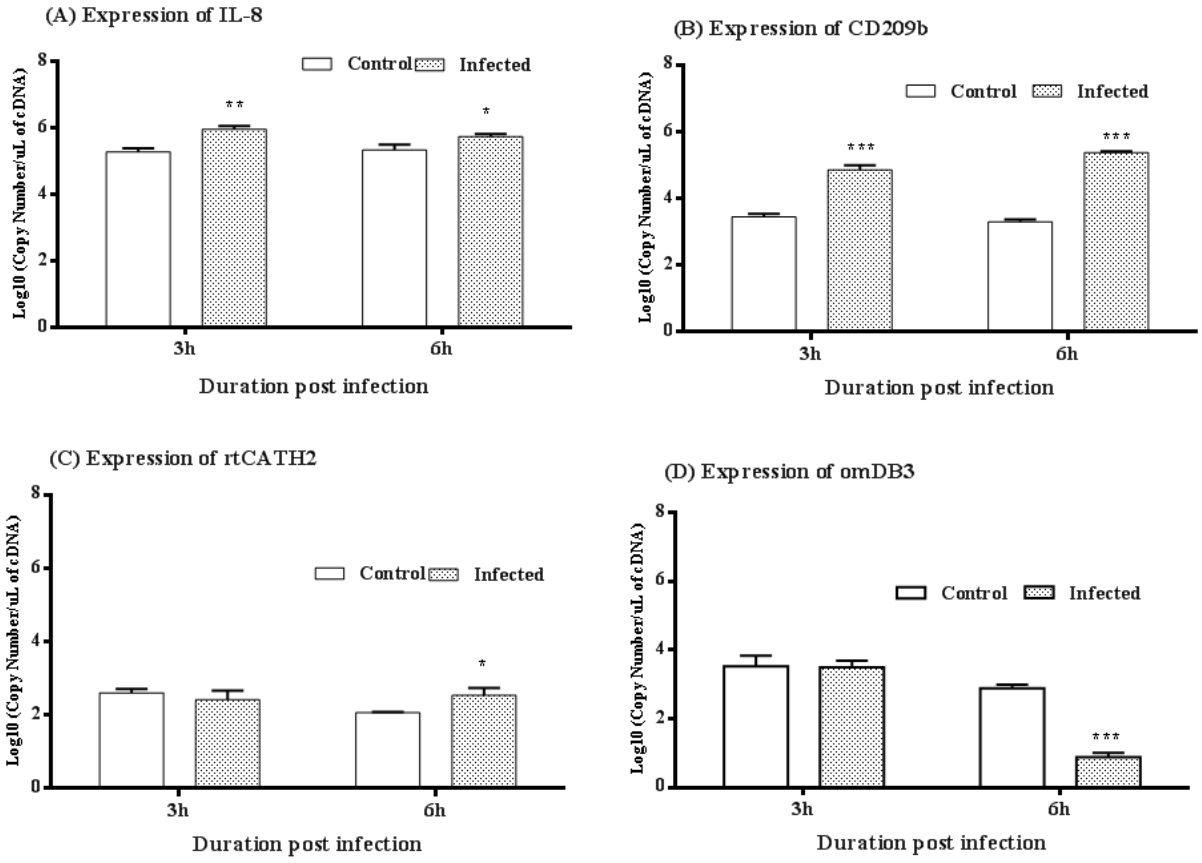

Figure 4.16: Expression of cytokine IL-8 (A), innate immune gene CD209b (B) and antimicrobial peptides rtCATH2 (C) and omDB3 (D) in RTgill-W1 cells after 3 and 6 h of infection with *A. salmonicida* subsp. salmonicida. Data have been presented as log10 copy number of mRNA transcripts (mean±SEM) of target gene per microlite of cDNA. Three course independent experiments were conducted each with biological duplicate where each replicate was a pooled sample of 2 inserts. One-way ANOVA followed by Bonferoni's multiple comparison was conducted to analyse the data where statistical significance was determined with $p<0.01$ using GraphPad Prism version 6.0. Data were compared between control and treatment groups at each time point where *, ** and *** represent $p<0.01$, $p<0.001$ and $p<0,0001$ respectively.

4.3.2.3.2 Expression of cytokine (IL-8) and innate immune gene (CD209b) antimicrobial peptides (AMPs) in RTgill-W1 cells upon viral and bacterial PAMP stimulation

Poly(I:C), LPS and PGN were used as stimulants in this study, to mimic viral and bacterial infection where poly(I:C) was found to significantly upregulate the expression of IL-8 and CD209b at both 3 and 6 h of stimulation and rtCATH2 at only 6 h of stimulation (Figure 4.17; $p<0.0001$). Another AMP, omDB3 remained stable upon stimulation.

LPS and PGN were found to upregulate the expression of IL-8 significantly at 3 h of stimulation ($p<0.001$) while at 6 h of stimulation, surprisingly, expression was found to be significantly downregulated ($p<0.001$). CD209b, rtCATH2 and omDB3 did not vary significantly upon stimulation ($p>0.01$).

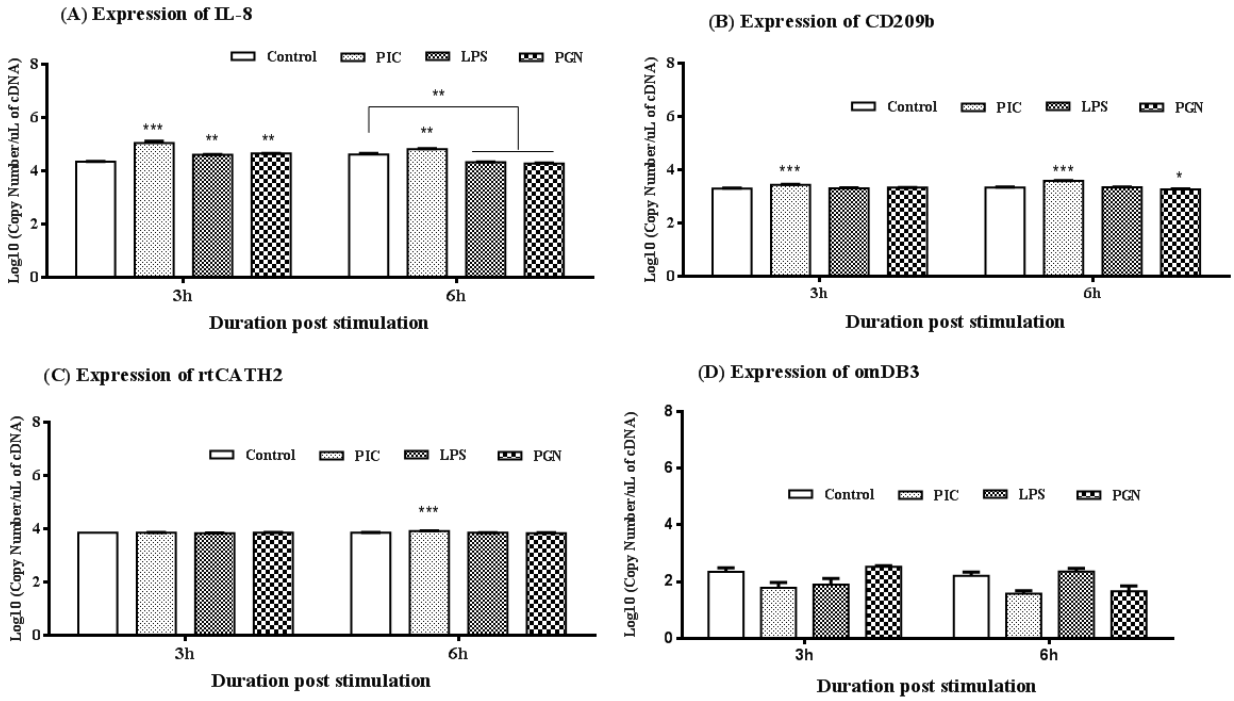

Figure 4.17: Expression of cytokine IL-8 (A), innate immune gene CD209b (B) and antimicrobial peptides rtCATH2 (C) and omDB3 (D) in RTgill-W1 cells after 3 and 6 h of stimulation with viral and bacterial PAMPs. Data have been presented as log10 copy number of mRNA transcripts (mean±SEM) of target gene per microlite of cDNA. Three course independent experiments were conducted each with biological duplicate where each replicate was a pooled sample of 2 inserts. One-way ANOVA followed by Bonferoni's multiple comparison was conducted to analyse the data where statistical significance was determined with $p<0.01$ using GraphPad Prism version 6.0. Data were compared between control and treatment groups at each time point where *, ** and *** represent $p<0.01$, $p<0.001$ and $p<0,0001$ respectively.

4.4 Discussion

4.4.1 SAV-2 infection and epithelial barrier function

To validate the response of RTgill-W1 cells to poly(I:C), a mimic of viral dsRNA, infections with SAV-2 virus were performed**.** Transepithelial electrical resistance (TER) measurement by milicell ERS volt-ohm meter and assessment of the expression of some selected tight junction genes by absolute RT-qPCR were performed. The experiments revealed a decrease of TER until 24 h post infection followed by a subsequent increase to a stable TER. Decreasing TER at an early stage of infection with a high viral concentration and recovery of TER at 24 h suggests a short-term loss of cellular integrity at early stages of virus entry. The transient loss of integrity may be due to the initial stress due to the microbial insult in the epithelial cell monolayer and later integrity recovers and even increases TER.

As no CPE was observed in the epithelial monolayer at any stage of infection, there might not be any damage to the cellular integrity. It is believed that microbial infection may cause leakage to the epithelial monolayer caused by the reduction of cellular integrity. Viruses especially can cause changes to the host cell morphology by damaging the cell cytoskeleton, which is connected to the tight junction regulatory protein ZO-1 and therefore can modulate or even break the cell to cell junctions (Kanlaya et al., 2009). This ultimately reduces cellular integrity which can be monitored by *in vitro* measurement of transepithelial electrical resistance. The observations made in RTgill-W1 cells post SAV infections have also been made in epithelial cell lines infected with other viruses. A drop of TER was reported in CaCo-2 and MDCK-1 cells post infection with rotavirus without any visible CPE (Svensson et al., 1991). Decrease of TER has also been found in CaCo-2 and KB cells (human squamous carcinoma cell line) within 30 min post infection by Coxsackie B viruses (Riabi et al., 2014).

In the present study, tight junction genes claudin 3a and 8d and tight junction regulatory gene ZO-1 were not modulated by SAV-2. Similar findings have been reported in mammalian cells. In primary human bronchial epithelial cells (HBECs), increased TER has been reported upon infection with respiratory syncytial virus (RSV). In this case, tight junction genes claudin and occludin were not upregulated by RSV infection just as observed in this study (Kast et al., 2017). Moreover, Porcine epidemic diarrhoea virus (PEDV) infection in Vero E6 (African green monkey kidney epithelial cells) and IPEC-J2 (porcine

intestinal epithelial cell clone J2) cells have not been found to have an effect on mRNA levels for claudin-1 while occludin mRNA expression was found to be significantly upregulated in virus infected cells at 24 and 48 h post infection in both cell lines (Luo et al., 2017).

In a study with alphavirus CHIKV, TER and ZO-1 expression were not modulated by apical or basolateral infection, for 24 h in non-polarized Vero and polarized Vero C1008 and HBMEC cells (Lim & Chu, 2014). However, effects of salmonid alphavirus on the cellular integrity and tight junctions of fish gill epithelia were not observed in this study. Thus, the current findings suggest that, salmonid gill epithelia have the ability to retain the barrier function when infected with salmonid alphavirus.

4.4.2 SAV-2 replication in RTgill-W1 cells

Alphavirus replication takes place inside the cytoplasm of host cells. To investigate the ability of SAV-2 to replicate in RTgill-W1 cells, strand specific RT-qPCR was employed to detect the replicative strand of SAV-2. The cytoplasmic RNA fraction was used to synthesize cDNA. SAV-2 was found to replicate in the cytosol of RTgill-W1 cells as early as 6 h post infection. A low level of replication (CT between 30 and 33) was detected in cells infected at MOI 10 and 1. Viral replication was significantly higher at 12 and 24 h post infection ($p<0.01$; Figure 4.1).

Low replication of SAV-2 was observed in several previous studies on salmonid alphavirus. SAV (1-6) was shown to replicate in heart and gill of Atlantic salmon parr at 2-8 weeks post challenge in gills yielding CT values for SAV-2 of around 35.5 at week 3 and 36.5 at week 8 (Graham et al., 2011). In another study, SAV-1 virus titers of 6.6, 7.1 and 6.4 (Log10 TCID50/g) from heart, kidney and gill respectively were determined at day 11 post challenge in Atlantic salmon parr (Herath et al., 2016). A low SAV titer (10^4 $TCID_{50}$/mL) has also been reported in RTG-2 cells (Graham et al., 2008), and in CHSE-214 cells (10^5 $TCID_{50}$/mL, SAV-1) (López-Dóriga et al., 2001). In contrast a higher titer of SAV-2 (around 10^7PFU/mL) has been reported in RTG-2 cells (Villoing et al., 2000).

Usually rhbadoviruses (-ssRNA) grow very fast and to high titers in cell culture. While a moderate titer of VHSV of around 10^6 $TCID_{50}$/mL was reported in RTG-2 cells (Campbell & Wolf, 1969), low replication and virus load of VHSV was reported in RTgill-W1 cells (Al-Hussinee et al., 2016). In the same study, a low titer of ISAV of 10^3 $TCID_{50}$/mL without any CPE was in contrast to *in vivo* studies in other cell types.

Various viruses have been shown to inhibit signaling pathways to prevent antiviral host responses. For example the nucleoprotein N of lyssavirus (a rhabdovirus) inhibits RIG-I recognition of viral RNA (Masatani et al., 2010). The V protein of paramyxoviruses is able to interact with MDA5 and block the interaction of MDA5 with MAVS and the subsequent downstream cascade whereas MAVS is selectively inhibited by influenza A and hepatitis viruses (Beachboard & Horner, 2016; Chan & Gack, 2016; Schulz & Mossman, 2016). NsP2 of the alphavirus CHIKV has been shown to induce cellular shutoff and promote viral replication by interacting with several host proteins (Bourai et al., 2012). However, overexpression of the innate immune response effector viperin has been found to strongly decreased CHIKV nsP2 expression levels in HEK293T cells (Teng et al., 2012). Many ISGs have been shown to directly block different phases of the viral replication cycle (Blondel et al., 2015).

Demonstrably RTgill-W1 cells have effective mechanism against -ssRNA virus such as VSHV (Al-Hussinee et al., 2016) and apparently also against +ssRNA viruses as demonstrated here. The overexpression of RLRs including RIG-I, MDA5 and LGP2b and ISGs including ISG15, PKR, Mx2 and viperin in RTgill-W1 cells upon SAV-2 infection indicate potentially strong interference with viral replication may be through conserved activation pathways in vertebrate history (as mentioned in Chapter 2).

4.4.3 TLR3 signaling and SAV-2 infection

TLR3 is one of the important TLRs sensing viral dsRNA (Edelmann et al., 2004). As demonstrated for poly(I:C) (chapter 2, section 2.1 and 2.2), In this study, SAV-2 was too found to upregulate TLR3 and subsequently IFNβ, and Mx2 in RTgill-W1 cells. TLR 3 upregulation had been shown in TO cells in response to SAV-3 infection (Xu et al., 2016). TLR3 and Mx mRNA transcripts have been shown to be upregulated by VHSV infection in rainbow trout liver (von Gersdorff Jørgensen et al., 2014). TLR3, interferon and Mx mRNA

transcripts have also been shown by VHSV induction in rainbow trout spleen (Abós et al., 2014). TLR3 upregulation in spleen of grass carp has also been reported upon infection with GCRV, a dsRNA virus (Su et al., 2009). Mx expression was also shown to be upregulated in the brain of European sea bass in response to Viral Nervous Necrosis Virus (VNNV, +ssRNA virus) infection (Valero et al., 2015). Responses to +ssRNA viruses appear TLR3 mediated not only in trout but also in other fish species. This suggest the activation of TLR3 signaling pathway by SAV-2 in RTgill-W1.

4.4.4 SAV-2 and poly(I:C) induced RLR expression

As a +ssRNA virus, SAV-2 forms dsRNA inside the cytoplasm of the host cells which is recognised by the host receptors. These receptors then transmit the downstream signals to other proteins to produce antiviral genes to inhibit viral replication. In this study, a low level of viral replication was detected as early as 6 h post infection using strand specific RT-qPCR. This was accompanied by early upregulation of mRNAs of RIG-I, MDA5.LGP2b and RLR family members.

The activation of the RIG-I signaling pathway depends on IPS1 which acts as an adaptor protein located in the outer mitochondrial membrane (Seth et al., 2006) where in association with TBK1 it initiates downstream signaling (Meylan et al., 2005). The upregulation of the receptor molecule RIG-I and the presence of IPS1 (constitutive expression) suggest the activation of RIG-I signaling pathway in RTgill-W1 cells. The further upregulation of transcription factor IRF3 and antiviral response molecules ISG15, Mx2, viperin and PKR confirm the activation of this pathway by SAV-2 infection.

One noteworthy finding in the present study is the significant upregulation of LGP2b which is in contrast to previous finding by Chang et al. (2011) which did not detect overexpression of LGP2b in trout fibroblast and macrophage cells in response to VHSV, even though RIG-I and MDA5 were overexpressed. Overexpression of LGP2b along with RIG-I and MDA5 in the present study, might play a role in inducing overexpression of downstream signalling genes IPS1, IRF3 and TBK1 and IFN stimulated genes ISG15, and viperin.

In this study, expression of ISGs including ISG15, viperin and PKR was found to be upregulated by SAV-2 and poly(I:C). Different molecules involved in the RIG-I signaling

pathway have been identified in different fishes and their induction by different viruses and viral PAMP have also been reported (Table 4.5). Upregulation of MDA5 and LGP2 by poly(I:C) stimulation or VHSV infection has been shown to result in significant increase of the Mx transcript in RTG-2 cells (M. Chang et al., 2011). PKR like gene, PKZ has also been found to be upregulated by poly(I:C) stimulation in Atlantic salmon head kidney (M. Chang et al., 2011). An orthologue of ISG15 in Atlantic salmon (AsISG15) has been found to be induced by poly(I:C) and ISAV infection (Røkenes et al., 2007). Moreover, viperin has been shown to be upregulated upon infection with infectious hematopoietic necrosis virus (IHNV) in rainbow trout fry (Purcell et al., 2011), and in rainbow trout leucocytes in response to infection with viral haemorrhagic septicaemia virus (VHSV) (Boudinot et al., 1999).

These reports and the results obtained here together suggest the activation of RIG-I and MDA5 and TLR3 (as shown in chapter 2) mediated antiviral response in RTgill-W1 cells upon SAV-2 and poly(I:C) induction.

4.4.5 Cytoplasmic vs total RNA

The majority of published gene-expression studies have used total cellular RNA where the inclusion of the nuclear transcriptome in the analyses might have a potential confounding impact (Solnestam et al., 2012). During RNA synthesis, mRNAs are transcribed, spliced, capped, and polyadenylated in the nucleus and the resulting steady-state RNA is transported from nucleus to cytoplasm via nuclear pore complexes for translation (Solnestam et al., 2012). The mRNA molecules that are not needed immediately to produce proteins, are retained in the nucleus (Prasanth et al., 2005).

For a more realistic view of cellular response using gene expression profiles, the nuclear and cytoplasmic RNA fractions should be analysed separately (Trask et al., 2009). In this study, mRNA fractions from the cytoplasm and total RNA from RTgill-W1cells were used for all gene expression experiments (methods in section 4.2.4.1). Expression patterns of different genes varied greatly in cytoplasmic and total RNA fractions. Most of the RLR molecules showed constitutive and stable expression in the cytosolic fraction while significant upregulation was noticed in total RNA. This is likely due to unprocessed mRNAs found in the nucleus.

Table 4. 5: Relevance of the findings of the current study to previous studies on fish RLRs

Targets	Fish species	Findings	Reference	Relevance to the present study
RIG-I, MAVS	Common carp	carp RIG-I and MAVS mRNAs were up-regulated in spleen, head kidney and intestine tissues in response to SVCV	(Feng et al., 2011)	In agreement to the present study for RIG-I.
IRF3		IRF-3 mRNAs transcripts were significantly up-regulated in different tissues of SVCV infected fish	(Feng et al., 2011)	Agreement with cytoplasmic RNA fraction but contrasting to the total RNA fraction
MDA5, LGP2, IRF3, MX and PKR	European sea bass	Upregulated in the brain in response to VNNV	(Valero et al., 2015)	Agreement except LGP2b and IRF3 expression in the total RNA. In total RNA fractions at 18 h PKR upregulated significantly
RIG-I, MDA5 and LGP2	Channel catfish	Significantly increased expression of the mRNA transcripts of RIG-I, MDA5 and LGP2 were detected in channel catfish virus and bacterial infected fish	(Rajendran et al., 2012)	In favour to the current study except LGP2b expression in the total RNA which is downregulated
MDA5	Sea perch	LjMDA5 was ubiquitously expressed and up-regulated significantly in all selected tissues in vivo post VNNV infection	(Jia et al., 2016)	Late stage expression of the present findings is in agreement with this finding
MDA5	Grass carp	Early stage up-regulation of MDA5 at 12- and 24-h following grass carp reovirus (GCRV) injection and thereafter decreased to normal level	(Su et al., 2010)	Relevance to the present study at 12- and 24-h expression
MDA5 and LGP2	Rainbow trout (RTG-2) cells	Up-regulated by poly(I:C) or VHSV infection resulting significant increase in Mx transcript	(Chang et al., 2011)	In agreement except LGP2b expression in the total RNA for SAV2 infection experiment.
LGP2	Black carp	LGP2 upregulated mRNA transcript in all the tested tissues except gill following infection by GCRV or SVCV	(Xiao et al., 2016)	Cytoplasmic mRNA transcript is in agreement but contrasting in the total RNA

	Mylopharyngodon piceus fin (MPF) cells (black carp cell line)	LGP2 up-regulated by poly(I:C) treatment, GCRV or SVCV infection, but not by LPS or PMA treatment.	(Xiao et al., 2016)	Cytoplasmic fraction in response to SAV 2 infection and both fractions in response to poly(I:C) stimulation support these findings.
TBK1	Black carp	Up-regulated by the stimulation of SVCV, GCRV	(Yan et al., 2017)	In response to SAV 2 induction, cytoplasmic mRNA transcript ubiquitously and total mRNA fraction at 18 h post infection in the present study are in agreement with the findings of these studies while TBK1 expression in both mRNA fractions except 18h in total mRNA fractions in response to poly(I:C) stimulation, does not agree to the findings related to poly(I:C) treatment.
	Grass carp	Up-regulated upon infection challenge with grass carp reovirus (GCRV) *in vivo* and *in vitro*	(Feng et al., 2014)	
	Common carp	Upregulated following SVCV infection.	(Feng et al., 2011)	
	Goldfish	Overexpression of TBK1 has been found to induce interferon production	(F. Sun et al., 2011)	
	Gilt-head sea bream	Upregulation upon infection with viral nervous necrosis virus (VNNV) in the brain of resistant to VNNV	(Valero et al., 2015)	
PKR	Zebra fish	Highly induced by poly(I:C) injection in vivo.	(Rothenburg et al., 2005)	both fractions in response to poly(I:C) stimulation, in agreement to all the findings related to poly(I:C) treatment
	Atlantic salmon	Upregulated by interferon in Atlantic salmon cell line, TO and by poly(I:C) stimulation in the head kidney.	(Bergan et al., 2008)	
	Rare minnow	Upregulated by virus (Grass carp reovirus) and bacteria *Aeromonas hydrophila*.	(Su et al., 2008)	
	Grass carp	Up-regulated after intraperitoneal (ip) injection with grass carp haemorrhagic virus.	(Hu et al., 2013)	
	Japanese flounder	Upregulated by viral infection and also found to inhibit the replication of rhabdovirus in flounder embryonic cells.	(Zhu et al., 2008)	
	Fugu	Significantly induced by poly(I:C) but not by LPS.	(del Castillo et al., 2012)	
	Rock bream	Upregulated at 12 h poly(I:C) injection.	(Zenke et al., 2010)	
ISG15	Atlantic salmon	Induced by poly(I:C) and ISAV infection.	(Røkenes et al., 2007)	ISG15 expression in response to SAV 2 and poly(I:C) in both cytoplasmic and total
	Grass carp and crucian carp	Upregulated by poly(I:C) and LPS.	(Zhang et al., 2007)	

	Atlantic cod	High expression of ISG15 by poly(I:C) stimulation but not with LPS.	(Seppola et al., 2007)	mRNA fractions in the present study is in agreement to all the previous findings.
		Upregulated after poly(I:C) stimulation.	(Furnes et al., 2009)	
	Japanese flounder	Highly induced by poly(I:C).	(Yasuike et al., 2011).	
Viperin (vig1)	Rainbow trout	High level of expression has been detected upon infection with viral haemorrhagic septicaemia virus (VHSV)	(Boudinot et al., 1999).	All the findings are in agreement with the findings of the current study.
	Rainbow trout (fry)	Upregulated upon infection with infectious hematopoietic necrosis virus (IHNV).	(Purcell et al., 2011)	
	Crucian carp	Overexpression of crucian carp viperin has been found to protect culture cells against grass carp reovirus (GCRV)	(Wang et al., 2014).	
	Mandarin fish	Viperin in gill has been shown to express only in virus infected and poly(I:C) induced fish.	(Sun & Nie, 2004).	
	Grass carp	Overexpression of viperin has been reported upon infection with GCRV	(B. Wang et al., 2014)	
	Tilapia	Upregulated upon induction with LPS and poly(I:C)	(Lee et al., 2013)	
	Rock bream	viperin has been shown to be upregulated upon infection with megalocytivirus	(cun Zhang et al., 2014).	
	Large yellow croaker	Significant upregulation of viperin has been reported upon in vivo poly(I:C) stimulation	Zhang et al. (2018)	
	TO cell line	Overexpressed upon interferon alpha stimulation	(Sun *et al.*, 2011).	
	Fathead minnow (FHM) cells (ATCC:	Viperin and a splice variant have been shown to be upregulated by Spring varimia of carp virus (SVCV) while poly(I:C) has been found to upregulate only viperin not the splice variant.	(Wang et al., 2019b)	

4.4.6 Bacterial invasion through epithelial monolayer

A. salmonicida is an infectious bacterium causing furunculosis in rainbow trout. To investigate the effects of this bacterium on trout gill epithelia, a bacterial invasion experiment was conducted in transwells. The ability of viral and bacterial PAMPs to prevent bacterial invasion through the RTgill-W1 cell monolayer was also investigated. *A. salmonicida* sub. *Salmonicida* was found to invade the epithelial monolayer as early as 5 min post infection even though a very low percentage of bacterial cells was recovered from the basolateral side of the transwell set which reached 60% at 6 h post infection. Rapid invasion by *Leptospira interrogans* (1.6%) as early as 15 min post infection (the earliest time point investigated) through polarized MDCK cell monolayers has been reported by Barocchi et al. (2002) which increased to 40% at 4 h post infection. Differential migration of different strains of *L. interrogans* through two human endothelial cell lines (HMEC-1 and EA.hy926) (Martinez-Lopez et al., 2010) which varied from 0% to 80% at 1 and 72 h post infection was reported. These findings suggest that RTgill-W1 cells have a similar efficiency as mammalian epithelial and endothelial cell lines to prevent bacterial invasion.

To further investigate the effectiveness of viral and bacterial PAMPs in reducing or preventing bacterial entry through the cell monolayer, RTgill-W1 cells were pre-stimulated with poly(I:C), LPS and PGN. The viral PAMP poly(I:C) and bacterial PAMPs LPS and PGN were found to reduce the percentage of bacterial invasion significantly. This may be linked to the ability of these PAMPs to increase the cellular integrity of epithelial cells (Chapter 2) and reduce the space for bacterial entry. No previous data on using PAMPs in a bacterial invasion model have been reported. Thus, the current report will facilitate further studies on the effectiveness of viral and bacterial PAMPs in preventing bacterial entry through epithelia for better understanding of the infective window.

Further to reveal the mechanism of bacterial entry, the actin cytoskeleton inhibitor CyD (Chapter 2), was used to pre-treat the cell monolayer. However, CyD was not found to promote bacterial invasion which is in accordance with the findings of Merien et al. (1997) who did not find any significant difference in invasion of pathogenic *Leptospira interrogans* through vero cells (African green monkey kidney fibroblast cells) after CyD treatment. This indicates actin independent invasion of *A. salmonicida* through the epithelial monolayer.

4.4.7 Bacterial infection and innate immunity

A major role in antiviral or antibacterial defense is played by the innate immune system in bony fish by acting as a barrier against the invasion of microbial pathogens (Aoki et al., 2013). To examine the response of RTgill-W1 cells to bacterial pathogen *A. salmonicida* and viral and bacterial PAMPs the expression of pro-inflammatory cytokines and antimicrobial peptides was investigated. An RT-qPCR quantification of IL-8 and CD209b as innate immune gene markers and of antimicrobial peptides defensin and catilicidin was employed.

IL8, a chemokine related to pro- inflammatory mechanism that directs immune cells to migrate to the infection sites (Reyes-Cerpa et al., 2012), was upregulated upon infection of RTgill-W1 cells with *A. salmonicida* as well as after stimulation with viral and bacterial PAMPs poly(I:C), LPS and PGN. These observations are supported by the literature as a recent study has also shown the upregulation of IL-8 in rainbow trout gills in response to typical *A. salmonicida* by a global transcriptome study (Rebl et al., 2014). Atlantic salmon macrophages have been shown to upregulate IL-8 expression upon infection with *A. salmonicida* (unpublished cited by Brown & Johnson 2008). Moreover, Brietzke et al. (2015) have shown IL-8 mRNA elevation in different tissues of rainbow trout upon infection with typical *A. salmonicida*. IL-8 has also been shown to upregulate in channel catfish after infection with *Edwardsiella ictaluri* (Chen et al., 2005).

LPS stimulation for 24 h has also been shown to induce IL-8 expression in primary cultures of rainbow trout leukocytes (Reyes-Cerpa et al., 2012). Moreover, PGN has also been reported to induce IL-8 expression in mammals (Cheon et al., 2008; Lee et al., 2015).

In the present study, CD209b, a C-type lectin receptor present on the surface of macrophages (and dendritic cells), was found to be upregulated by *A. salmonicida* infection and poly(I:C) stimulation while LPS and PGN did not induce its expression. CD209 has been speculated to be an important player in the immune response of rainbow trout against *A. salmonicida* as it is upregulated in the spleen of rainbow trout at mRNA and protein levels upon *A. salmonicida* infection (Long et al., 2015). The upregulation of CD209b has also been reported in rainbow trout cell lines RTgill-W1, RTL, RTS11 and RTG-2 upon infection with *Saprolegnia parasitica* for 16 and 24 h (De Bruijn et al., 2012). The results obtained in RTgill-W1 cells confirm these reports.

Cathilicidin (rtCATH2) and defensin are important AMPs that have been identified in various fishes. These two AMPS have been shown to have immunomodulatory functions in fish. The expression of cathilicidin and defensin in RTgill-W1 in response to pathogens or PAMPs was investigated. In the present study, rtCATH2 was upregulated in RTgill-W1 cells by *A. salmonicida* at 6h h post infection. However, among the tested PAMPs only poly(I:C) at 6 h post stimulation induced rtCATH2 expression. Upregulation of rtCATH2 in gill, head kidney and intestine, but not in liver of rainbow trout upon bacterial infection has been reported by Chang et al. (2006). Bacterial infection and bacterial DNA also induced the upregulation of rtCATH2 in CHSE-214 cells while purified LPS failed to upregulate the expression (Maier et al., 2008) as observed in the RTgill-W1 cells.

Further evidence comes from a study where rtCATH2 was shown to be induced in CHSE-212 and Atlantic cod larvae cells by bacterial infection and poly(I:C) stimulation showing a weak response in salmonid and a strong response in cod cells (Broekman et al., 2013).

The expression of another AMP, β-defensin was downregulated in RTgill-W1cells by the infection of *A. salmonicida* whereas no regulation was observed through the induction of viral and bacterial PAMPs. Cuesta et al. (2011) have also reported the failure of poly(I:C) and LPS stimulation to induce β-defensin mRNA transcript expression in gilthead seabream while β-defensin upregulation has been reported in Japanese medaka (*Oryzias latipes*) upon LPS injection (Zhao et al., 2009) which partially supports the findings of the present study. β-defensin including omDB-2 upregulation at early stage of stimulation (4h) with poly(I:C) has also been described in different tissues of rainbow trout while no induction has been detected at late stage of stimulation (24h) (Casadei et al., 2009). They also reported upregulation of omDB2 upon bacterial infection which was not observed in RTgill-W1 cells.

4.5 Conclusion

The findings of the current study suggest that trout gill epithelia have the ability to mount a defence against SAV-2 infection which can be induced to a greater extent by using poly(I:C) as an immuno-stimulant. SAV-2 replication was limited in RTgill-W1 cells which might be due to the activation of TLR3 and RLR signaling pathways by SAV-2 infection. Pre-treatment with poly(I:C), LPS and PGN were shown to reduce bacterial invasion through the trout gill epithelial cell monolayer. The mRNA expression of chemokine IL-8, innate immune marker CD209b and antimicrobial peptide cathilicidin were induced by viral and bacterial PAMPs suggesting the application of PAMPs in fish innate immunity.

Chapter 5
General discussion

5.1 Epithelium

Epithelium is a membranous tissue which is one of the basic cell types in animals covering internal and external surfaces of the body and its organs. Epithelium is composed of one or more layers of epithelial cells forming a polarized structure where the apical junctional complexes orchestrate the epithelial integrity and signaling across the epithelium (Tervonen et al., 2011).

5.2 Fish gill epithelial cells and cell lines

Fish gill epithelia cover the gill filament and lamellae and comprise of several cell types including pillar cells, pavement cells, mitochondria rich cells or chloride cells and mucous cells or goblet cells (Wilson & Laurent, 2002). Highly complex vasculature surrounded by a large surface area constitutes the fish gill (Evans et al., 2005). The surface area of fish gill has been recorded as 5412 cm^2 in freshwater carp (*Chirrhinus mrigalla*) (Palzenberger & Pohla, 1992). This large surface area separates the blood circulating through the gills from the external aquatic environment by a thin epithelial barrier (Evans et al., 2005). As a fish gill's main function is respiration which involves the uptake of oxygen from water across a huge surface area of tissue susceptibility to infection by different types of pathogens is a significant risk to the organism. Thus, the fish gill is a major portal of entry for pathogens. Structurally, fish gills are heterogeneous with different cell types and a complex branchial circulatory system, which makes it difficult to assess the contributions of each cell type to the various gill functions, particularly the defence mechanism. *In vitro* studies using primary and secondary fish gill cells minimize the cellular complexity and are widely used in immunological and toxicological studies. Accordingly, RTgill-W1 cells have been used for several but a limited number of *in vitro* studies. One of the important functions of epithelial cells is the barrier function through which epithelia control the movement of deleterious agents from the outside world to the interior of the fish body (Powell, 1981). This barrier between the external environment and the fish body protects the fish from being affected by microorganisms.

For basic research, use of fish gill cells is very limited. Ebner et al. (2007) have reported the pattern of activation of MAPK/ERK in RTgill-W1 cells. Moreover, Krumschnabel et al. (2007) has studied apoptotic mechanism in RTgill-W1 cells. These studies suggest that fish gill epithelial cells have similar functions as mammalian epithelial cells. The study of host-pathogen interaction using fish gill cells could allow researchers to elucidate the mechanisms of pathogen entry into and between the epithelial cells (Lee et al., 2009). The RTgill-W1 cell line has been shown to allow the growth of fish viruses like Atlantic salmon paramyxoviruses (ASPV) (Kvellestad et al., 2003) and infectious salmon anemia virus (ISAV) (Falk et al., 1997). These studies suggest the suitability of RTgill-W1 cell line for *in vitro* experiments.

5.3 Modulation of tight junction in fish gill epithelia

A major role in the innate immunity against microbial infection is played by the epithelial integrity of cells. The epithelial integrity of RTgill-W1 as measured by TER was found to increase if exposed to viral and bacterial PAMPs (Chapter 2. Section 2.1). The tight junction genes Claudin 8d and ZO-1 were found to be upregulated by viral and bacterial PAMPs which correlates to the observed increased epithelial resistance (Chapter 2. Section 2.3).

RTgill-W1 cell monolayer shows very low TER as has been shown in the current and previous studies even after stimulation (Claire, 2016; Trubitt et al., 2015) while in primary trout gill cells showed high TER in control and stimulated conditions in symmetrical and asymmetrical culture environments (Kelly & Wood, 2001a; Kelly and Wood, 2001b; Sandbichler et al., 2011) (Detail list in Appendix 3, Table S3.1). Trubitt et al. (2015) have shown cortisol induced an increase of TER in RTgill-W1 cells from around 40 Ω-cm^2 to 80 Ω-cm^2. In the same study, tetrabromocinnamic acid (an inhibitor of casein kinase 2) induced an increase of TER in RTgill-W1 cells which elevated from around 20 Ω-cm^2 to 27 Ω-cm^2. The low epithelial resistance observed in this study demonstrates the leakiness of RTgill-W1 cells.

Epithelial integrity is maintained mostly by tight junctions maintaining polarity and therefore the diverse molecular characteristics of apical and basolateral membranes (Jain et al., 2011). To investigate the barrier function of fish gill epithelia, cellular integrity was investigated upon viral infection and stimulation with viral and bacterial PAMPs. The

integrity measured in TER increased upon stimulation with viral and bacterial PAMPs as evidenced by the upregulation of the tight junction regulatory gene ZO-1 (Chapter 2). ZO-1 and other proteins related to cellular integrity were phosphorylated in RTgill-W1 cells (Chapter 3). ZO-1 was found to be phosphorylated on multiple serine residues in the protein sequence where S288 and S461 are common in control and stimulated groups and S1147 in MDP and poly(IC) stimulated cells. Several other studies have demonstrated the association between occludin phosphorylation by certain kinases and tight junction modulation. For example, ZO-1 phosphorylation and upregulation and subsequent increase of TER by Rho kinase in the human endothelial cell line ECV304; MAP kinases including ERK, p38/MAPK and JNK in MDCK cells; CK1 and PKC in MDCK cells; and PI3K in human adenocarcinoma have been reported (Dörfel & Huber, 2012). Taken together this suggests the modulation of tight junction gene expression and TER in PAMP stimulated RTGgill-W1 cells through activation of kinases. Moreover, poly(I:C) also activated the actin cytoskeleton signaling pathway which further suggests the modulation of cellular integrity by poly(I:C). Protein kinases also have roles in controlling cellular integrity. PKC, one of the kinases identified in the present study (Chapter 3, Section 3.3.5), has been shown to control the cell integrity pathway by controlling cell wall synthesis in fission yeast in response to external stimuli (Madrid et al., 2014).

5.4 The antiviral response is conserved in RTgill-W1 cells

For millions of years viruses and hosts are in continuous struggle that has driven the hosts to develop effective antiviral immune responses (Maxmen, 2017). The antiviral response initiates upon sensing viral gene materials or viral PAMPs by host's pattern recognition receptors (PRRs) including TLRs, RLRs and NLRs (Jun et al., 2016). Among TLRs, TLR3 is an important pattern recognition receptor that senses synthetic or viral dsRNA in the endosomal compartment of the cells. TLR3 signaling is important for interferon induction where interferon-α/β prevent viral replication by the induction of ISGs. The TLR3 mediated antiviral response has been reported in several fish species including rainbow trout (Abós et al., 2014; von Gersdorff Jørgensen et al., 2014) upon either poly(I:C) stimulation or viral infection (both dsRNA and ssRNA viruses). Zebrafish interferon has been shown to be induced by poly(I:C) in zebrafish liver cells (ZFL) (Altmann et al., 2003). *In vivo* infection with sole aquabirnavirus (solevirus) and poly(I:C) stimulation have been shown to induce Mx expression in Senegalese sole (Fernandez-Trujillo et al., 2008). In the present study,

mRNA expression of TLR3, IFN-β and Mx2 have been found to be upregulated by SAV-2 infection and poly(I:C) stimulation in RTgill-W1 cells.

Another important group of PRRs sensing viral RNA in the cytoplasmic compartment are the intracellular RLRs. The RLR family are ubiquitously expressed in the cytoplasm and regulate the production of interferon and interferon stimulated genes, thus playing a major role in the antiviral response (Zou et al., 2016). TLR independent and RIG-I mediated antiviral responses has been reported in mammals upon viral infection (Gack, 2014; Jiang et al., 2012; Reikine et al., 2014; Rothenfusser et al., 2005; Schlee, 2013). Poly(I:C) stimulation and viral infection have been shown to upregulate RLR molecules and RLR family members in a wide range of fish species (Chang et al., 2011; Xiao et al., 2016; Rothenburg et al., 2005; Furnes et al., 2009; Bergan et al., 2008; Røkenes et al., 2007; Zhang et al., 2007; Sun and Nie, 2004; Yasuike et al., 2011; Wang et al., 2019; Lee et al., 2013) as observed in mammals. In the present study three members of RLR molecules (RIG-I, MDA5, LGP2b) and RLR family members (TBK1, IRF3, PKR, ISG15 and viperin) were upregulated upon poly(I:C) stimulation and +ssRNA viral infection in salmonid gill epithelia.

RLRs and their family members have been shown to be present in the earliest animals from mammals to other vertebrates including fish which suggest that RLR mediated antiviral immunity is evolutionary conserved throughout vertebrate history as a result of co-evolutionary history with host cells and viruses (Levraud et al., 2013; Mukherjee et al., 2014; Zou et al., 2016). TLR mediated antiviral response is also thought to be conserved throughout the animal evolutionary history from drosophila to higher vertebrates (Zou et al., 2016). Thus, antiviral immunity in salmonid gill epithelia in response to viral infection and stimulation with viral particles is, of course, evolutionary conserved from earliest animals.

5.5 Bacterial pathogen and PAMPs mediated innate immune response in RTgill-W1 cells

Unlike the mechanisms of recognition of viral nucleic acids by TLR3 and RLRs and subsequent antiviral response pathways, recognition of bacterial molecules by host cells and subsequent innate immune responses are not well conserved among mammals and other vertebrates throughout evolutionary history. Bacterial molecules LPS, PGN and MDP recognition receptors are well conserved in mammals (Munford & Varley, 2006; Akira et

al., 2006; Dziarski, 2003) while among fish species these receptors are less conserved (Ribeiro et al., 2010) and some of the receptors are absent in some fish species. For example, TLR4 is absent in salmonid fishes (Reviewed by Palti, 2011). Some bony fishes including zebrafish and common carp possess orthologs of TLR4, however, TLR4 of this two fishes does not recognize LPS (Sepulcre et al., 2009). Iliev et al. (2005) have reported the absence of TLR4- mediated LPS recognition in fish. Recently, zebrafish caspy2 has been shown to recognise bacterial LPS (Zhang et al., 2018). Moreover, for use of the same ligands to induce innate immune signal transduction, fish cells require high concentrations which show lower or no induction in comparison to mammalian counterparts (Ribeiro et al., 2010). This might be because of the continuous exposure of fish to bacteria and bacterial molecules where the development of the gill microbiome has prompted a different set of recognition and response pathways.

In mammals, LPS is recognised by LPS binding protein (LBP), TLR4, and CD14 which also participate in this pathway (Reviewed by Rebl et al., 2010; Palti, 2011). Thus stimulation with LPS and subsequent production of interferon and interferon stimulated genes like Mx might follow the MyD88 pathway in mammals (Reviewed by Rebl et al. 2010). This involves the participation of both CD14 and MD2. The LBP like gene has been reported in some teleosts for example in Atlantic cod (Solstad et al., 2007). However, the other important molecules CD14 and myeloid differentiation protein 2 (MD2) have not yet been identified in teleost (Reviewed by Rebl et al., 2010). Thus, the pathway by which IFNβ and Mx2 are induced in trout gill epithelia in response to LPS stimulation is not clear and needs further investigation.

PGN, on the other hand, has been reported to induce interferon production in mammalian cells (Clua et al., 2017; Liu et al. 2004). In HEK293T cells, MDP has been shown to be sensed by NOD2 (Girardin et al., 2003; Inohara et al., 2003) and NOD2 expression has been reported in rainbow trout (Chang et al., 2011). Since there is a marked innate immune response (expression of IFNβ and Mx2) induced by PGN in RTgill-W1 cells (Chapter 2, Figure 2.5), it appears that MDP (a structural component of PGN) was indeed internalized (as shown in Chapter 2, Figure 2.9 A, B and 2.12). Thus, MDP might be sensed by NOD2 in RTgill-W1 cells which, of course, was further internalized and leading to the initiation of an antiviral response.

Interleukin-8 (IL-8) is an important chemokine that has been identified in several fishes including flounder (Choi et al., 2006), trout (Sangrador-Vegas et al., 2002), channel catfish (Chen et al., 2005) and lamprey (Najakshin et al., 1999). IL-8 has been shown to be induced by different bacteria and bacterial PAMPs such as LPS in different fish cells and tissues (Brietzke et al., 2015; Chen et al., 2005; Reyes-Cerpa et al., 2012). Li & Waldbieser (2006) reported the rapid induction (2 and 4 h) of IL-8 in the channel catfish spleen by LPS injection. In the present study, IL-8 has been found to be upregulated by *A. salmonicida* infection and stimulation with viral and bacterial PAMP. Another innate immune response effector, CD209b, was upregulated by *A. salmonicida* infection and viral and bacterial PAMP stimulation. CD209b has been shown to bind β-D-glucan and polysaccharides, thus functioning in the recognition and detection of bacteria (specifically Gram-negative), in phagocytosis and as positive regulator of endocytosis (Taylor et al., 2004). The upregulation of CD209b in trout gill epithelial cells suggests the potential use of PAMPs in augmenting immune response against bacterial infection.

As one of the first line of defences, along with innate immune responses, animals and animal cells produce a massive number of antimicrobial peptides (AMPs). A couple of AMPs, cathilicidin and defensin have been tested by quantitative RT-PCR in the present study to evaluate the ability of trout gill epithelial cell RTgill-W1 to express AMPs in response to bacterial pathogen and viral and bacterial PAMPs (Chapter 4). In the present study, rtCATH2 has been shown to be slightly upregulated by *A. salmonicida* infection and PAMP stimulation. Cathilicidin has been shown to be a potent antimicrobial agent expressed in different organs of rainbow trout (Chang et al., 2006). In some fishes cathilicidin has been shown to be highly active against Gram-negative bacteria, but not against Gram-positive bacteria, for example in cod (Broekman et al., 2011), while in hagfish cathilicidin has been shown to be active against both Gram-positive and -negative bacteria (Uzzell et al., 2003). In mammals, cathilicidins have been shown to possess immune and non-immune functions (reviewed by Choi et al., 2012). The immunomodulatory activities of cathilicidins in mammals are likely shared by their fish counterparts through a conserved evolutionary mechanism of the innate immune response (Masso-Silva & Diamond, 2014). Another AMP, β-defensin was downregulated by bacterial infection and was not induced by viral and bacterial PAMPs. Similar findings were reported by Cuesta et al. (2011) who have also

reported the failure of poly(I:C) and LPS stimulation to induce β-defensin mRNA transcript expression in gilthead seabream. This suggests that fish defensin expressed in gill epithelia might not be involved in innate immune response.

5.6 From perception to response: A cascade of events regulates immune response in RTgill-W1 cells

Antiviral response starts upon recognition of pathogens from the environment by the host PRRs. After perception, a cascade of events is required for signal transduction, a cellular process that converts primary extracellular signal into intracellular second messengers and even third or fourth messengers. The ultimate aim of the signal transduction process is the regulation of production of mRNA (transcription) and subsequent production of specific proteins (translation) (Figure 5.1). Both TLR3 and RLR recognize viral or synthetic dsRNA. While TLR3 recognizes dsRNA in the endosome, RLRs sense dsRNA in the cytoplasm and trigger innate immune responses (Figure 5.2). Upon sensing dsRNA, TLR3 or RLRs employ specific intracellular adaptor molecules to initiate respective signaling pathways. TBK1 and IKK-α/β are the kinases that can be activated by both TLR3 and RLRs where TBK1 phosphorylates IRF3/IRF7 and initiates interferon production, and IKK-α/β phosphorylates NF-κB and initiates pro- inflammatory cytokine production. These together play key roles in preventing viral infection (Kawai & Akira, 2008b). In RTgill-W1 cells the RLR signaling pathway was activated by SAV-2 infection and poly(I:C) stimulation as shown by the upregulation of signaling molecules upon recognition by the receptor molecules RIG-I, MDA5 and LGP2 (Chapter 4).

Integration of different molecules associated with specific signaling pathways is very important for the immediate and proper gene regulation through signal transduction against microbial pathogens. In these signal transduction mechanisms, protein expression, localization, activity and protein-protein interaction play critical roles which allow the cells to respond with high specificity and efficiency (Lee & Yaffe, 2016). A key player in this gene regulation is phosphorylation which activates the transcription factors associated with the expression of target genes (Hunter & Karin, 1992). Protein phosphorylation by specific kinases is a fundamental mechanism of increasing protein activity or expression of related genes for immune defence. TLR3 and RLR signaling pathways are further regulated by phosphorylation of various kinases and transcription factors. Sun et al. (2011) reported the phosphorylation in the RIG-I signaling pathway by casein kinase II (CKII) in the resting

stage of 293T cells while dephosphorylation occurred in RNA virus infected cells. Another study by Willemsen et al. (2017) reported death-associated protein kinase-1 (DAPK1, a Ca^{+2}/camodulin dependent serine/threonine kinase; CaMKII) to negatively regulate RIG-I/IRF3 signaling. Upon silencing DAPK1, increased transcriptional activity of IRF3 and a subsequent decrease in viral replication in human and mouse cell lines have been reported. Dixit & Kagan (2013) reported that IPS1, an important component of the RIG-I signaling pathway, promotes the activation of the transcription factors ATF-2/c-Jun through MAPK activation. ATF-2/c-Jun in turn induces transcription of IFN-β, IRF3/IRF7, and NF-κB. In this study, CKII and CaMKII were identified as actively phosporylating kinases in RTgill-W1 cells in all groups studied (Chapter 3) and most of the RIG-I signaling molecules were overexpressed in response to SAV-2 infection and poly(I:C) stimulation (Chapter 4).

Loegering & Lennartz (2011) reported the direct involvement of PKC in multiple steps of TLR signaling pathways. Johnson et al. (2007) have shown the role of PKC in the induction of interferon-β production in human dendritic cells by the activation of the TLR3 signaling pathway. They have also shown the inhibition of interferon-β expression by G6976 (a potent inhibitor of PKC). In another study, TLR3 has been shown to regulate the activation of p38-MAPK (Silva et al., 2004). In humans, TLR3 has five tyrosine residues two of which have been shown to be phosphorylated and to activate IRF3 and NF-κB mediated gene expression. The phosphorylation of tyrosine residues is involved in the activation TBK1 and subsequently induces the partial phosphorylation and activation of IRF3. Another two kinases PI3K and Akt kinase (PKB) have been shown to play role in the phosphorylation and activation of IRF3 in the nucleus (reviewed by Vercammen et al., 2008). The fully functioning IRF3 then initiates the production of interferon and interferon stimulated genes. In the present study, tyrosine phosphorylation covered 6% of total phosphosites detected in RTgill-W1 cells, even though no tyrosine kinase was identified. Moreover, PKB has been identified in this study (Chapter 3) which might be involved in TLR3 signaling pathway in trout gill epithelia. However, the role of RTK in immune response in fish requires further investigation.

In the present study, a number of signaling pathways have been found to be triggered by the stimulation with poly(I:C) and MDP (Chapter 3). One of the pathways is the MAPK signaling pathway which has been shown to play a central role in the induction of pro-

inflammatory cytokines and interferon production (Barton & Medzhitov, 2014). In eukaryotes, MAPK pathway has been reported to be involved in the cellular and molecular processes including cell cycle progression, cell proliferation, survival and differentiation, mRNA stabilization and translation and finally gene expression (reviewed in Plotnikov et al., 2011). Other MAPK associated pathways including JNK and p38 MAPK were found to be activated by viral and bacterial PAMPs.

Several effector molecules were found to be upregulated upon viral and bacterial pathogens and PAMPs (Figure 5.2). Upon SAV-2 infection and poly(I:C) stimulation interferon and ISGs including PKR, ISG15, Mx2 and viperin were found to be upregulated. IFNβ and Mx2 were also found to be induced by bacterial PAMPs LPS and PGN. A chemokine IL-8, an innate immune gene marker CD209b and an AMP cathilicidin were also found to be upregulated as explained in previous section.

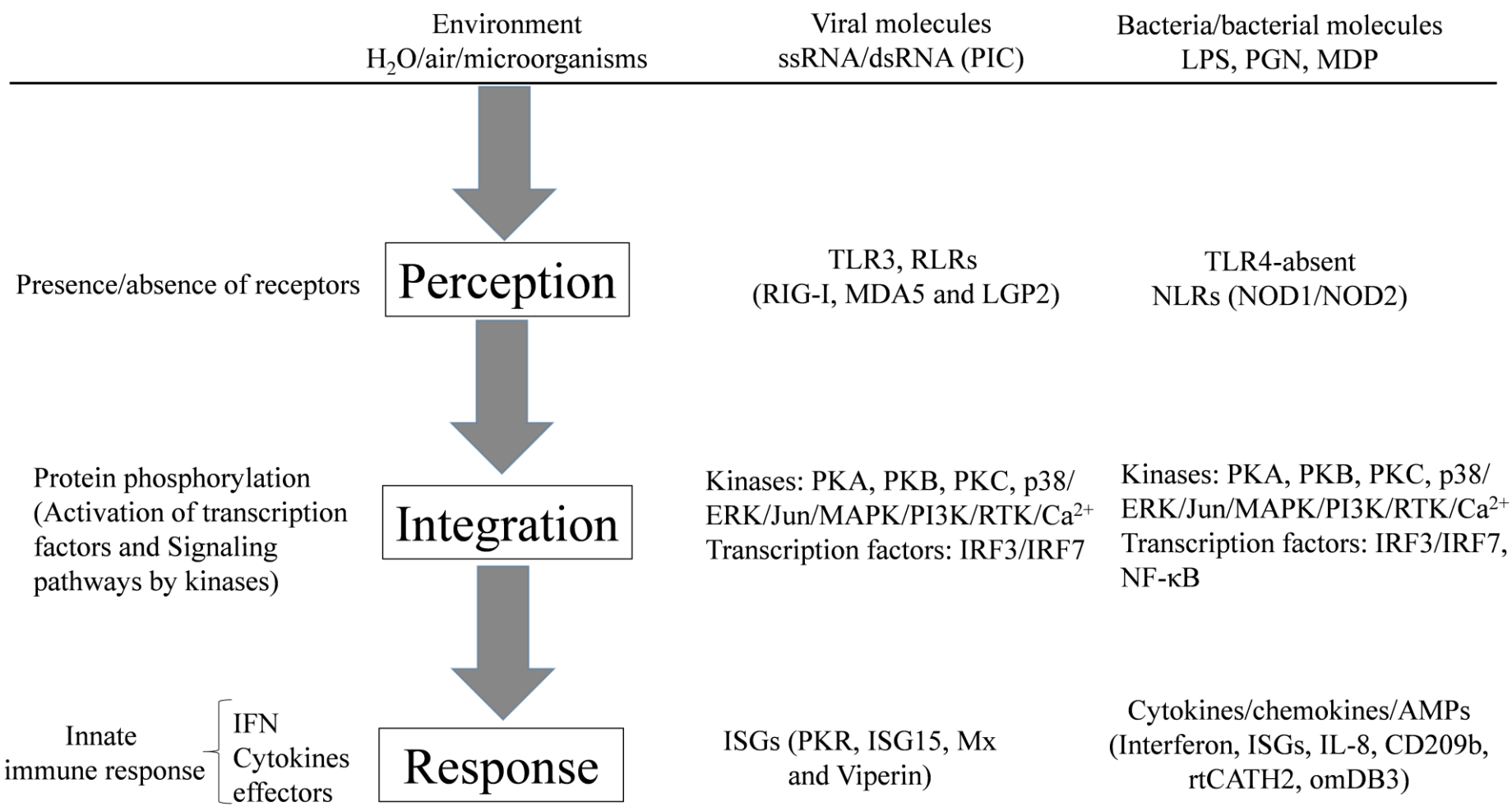

Figure 5.1: Innate immune response in salmonid gill epithelia. Upon perception of viral or bacterial molecules by host's sensors, a cascade of events is activated where protein phosphorylation plays central roles which lead to the production of interferon and pro-inflammatory cytokines

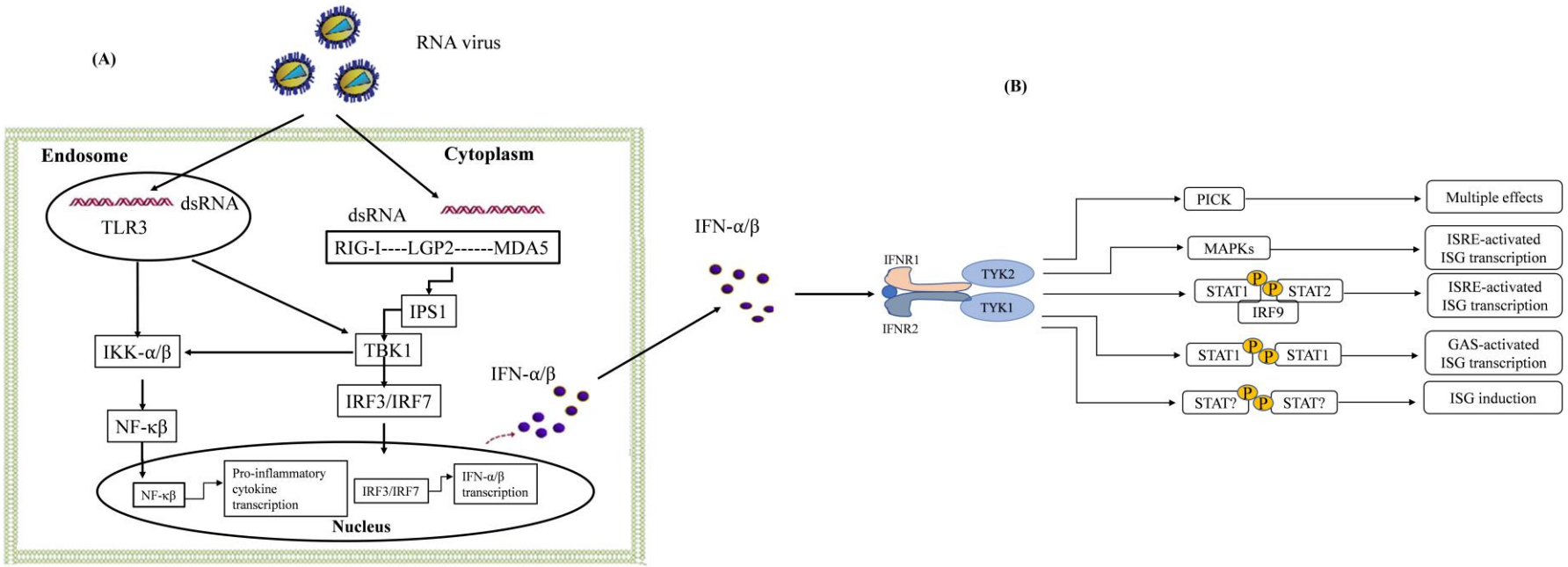

Figure 5.2: TLR3 and RLR cross talk. (A) TLR3 and RLR signalling pathways showing the common molecules, (B) pathway of activation of different kinases that leads to the transcription of ISGs from IFN-α/β (modified from Rodríguez Pulido & Sáiz 2017; Koshiba et al. 2011; McNab et al. 2015).

Chapter 6
General conclusions and future recommendations

6.1 Conclusions

Viral and bacterial PAMPs have been found to be able to induce the innate immune response in trout gill epithelia. The barrier function of trout gill epithelia was also found to be modulated to a greater extent by viral and bacterial PAMPs. The recognition and uptake pathways of LPS and PGN in RTgill-W1 cells were respectively shown to be by both actin dependent and independent endocytosis.

Salmonid alphavirus subtype 2 (SAV-2) which is responsible for sleeping disease in salmonids, has been found to multiply in trout gill epithelia at a low rate without affecting the barrier function of the epithelia. On the other hand, trout gill epithelium shows robust antiviral response upon SAV-2 infection triggered through the TLR3 and RIG-I signaling pathways. Viral and bacterial PAMPs were found to reduce bacterial invasion through salmonid gill epithelia.

Poly(I:C) triggered the phosphorylation in trout gill epithelia and activated different kinases and signaling pathways related to innate immunity. Taking together, RTgill-W1 cell line is an ideal *in vitro* biological model to study host-pathogen interaction.

6.2 Future perspectives

The present study suggests several future investigations. Other salmonid alphavirus subtypes should be tested in RTgill-W1 cells including viral replication, effects on barrier function and molecular responses in trout gill epithelia to better understand the barrier function of trout gill epithelia. The interactions between viral protein and host ISGs should be investigated by western blotting, confocal microscopy or flow cytometry to validate the antiviral activity of different ISGs in fish gills and for the potential therapeutic application in aquaculture. Some other aquatic viruses like IPNV, ISAV should be tested to complete knowledge on cellular and molecular responses of trout gill cells. A wide range of bacterial pathogens including Gram positive and negative bacteria should be used to study host-bacteria interactions and to identify potential therapeutic agents to prevent the bacterial infections. Some other cytokines and chemokines should be tested upon bacterial infection and PAMP stimulation. Viral and bacterial pathogens should be used to evaluate their effects

on protein phosphorylation in trout gill epithelia. A series of *in vivo* experiments including viral and bacterial challenge experiments to investigate the innate immune responses by transcriptomics and phosphoproteomics in salmonid gills, therapeutic use of poly(I:C) against the viral and bacterial infection are recommended to validate the *in vitro* findings found in this thesis. Finally, the expression of the innate immune effectors should be investigated by primary salmonid gill cell cultures to compare with the transwells.

References

Abós, B., Castro, R., Tafalla, C., González Granja, A., Barreda, D. R., & Havixbeck, J. J. (2014). Early Activation of Teleost B Cells in Response to Rhabdovirus Infection. *Journal of Virology*, *89*(3), 1768–1780.

Ahola, T., Laakkonen, P., Vihinen, H., & Kääriäinen, L. (1997). Critical residues of Semliki Forest virus RNA capping enzyme involved in methyltransferase and guanylyltransferase-like activities. *Journal of Virology*, *71*(1), 392–7.

Akerstrom, S., Mousavi-Jazi, M., Klingstrom, J., Leijon, M., Lundkvist, A., & Mirazimi, A. (2005). Nitric Oxide Inhibits the Replication Cycle of Severe Acute Respiratory Syndrome Coronavirus. *Journal of Virology*, *79*(3), 1966–1969.

Akira, S., Uematsu, S., & Takeuchi, O. (2006a). Pathogen recognition and innate immunity. *Cell*, *124*(4), 783–801.

Akira, S., Uematsu, S., & Takeuchi, O. (2006b). Pathogen Recognition and Innate Immunity. *Cell*, *124*(4), 783–801.

Alfano, C., Sanfelice, D., Babon, J., Kelly, G., Jacks, A., Curry, S., & Conte, M. R. (2004). Structural analysis of cooperative RNA binding by the La motif and central RRM domain of human La protein. *Nature Structural and Molecular Biology*, *11*(4), 323-329.

Al-Hussinee, L., Pham, P. H., Russell, S., Tubbs, L., Tafalla, C., Bols, N. C., Doxon, B. Lumsden, J. S. (2016). Temporary protection of rainbow trout gill epithelial cells from infection with viral haemorrhagic septicaemia virus IVb. *Journal of Fish Diseases*, *39*(9), 1099–1112.

Alexopoulou, L., Holt, A. C., Medzhitov, R., & Flavell, R. A. (2001). Recognition of double-stranded RNA and activation of NF-kappaB by Toll-like receptor 3. *Nature*, *413*(6857), 732–738.

Alonso, A., Sasin, J., Bottini, N., Friedberg, I., Friedberg, I., Osterman, A., Godzik, A., Hunter, T., Dixon, J.,& Mustelin, T.. (2004). Protein Tryrosin Phosphotase in the Human Genome. *Cell*, *117*, 699–711.

Altmann, S. M., Mellon, M. T., Distel, D. L., & Kim, C. H. (2003). Molecular and functional analysis of an interferon gene from the zebrafish, *Danio rerio*. *Journal of Virology*, *77*(3), 1992–2002.

Amaeze, N. H., Schnell, S., Sozeri, O., Otitoloju, A. A., Egonmwan, R. I., Arlt, V. M., & Bury, N. R. (2015). Cytotoxic and genotoxic responses of the RTgill-W1 fish cells in combination with the yeast oestrogen screen to determine the sediment quality of

Lagos lagoon, Nigeria. *Mutagenesis*, *30*(1), 117–127.

Andrés, V. & González, J. M. (2009). Role of A-type lamins in signaling, transcription, and chromatin organization. *Journal of Cell Biology*, *187*(7), 945-957.

Aoki, T., Hikima, J. ichi, Hwang, S. D., & Jung, T. S. (2013). Innate immunity of finfish: Primordial conservation and function of viral RNA sensors in teleosts. *Fish Shellfish Immunol*, *35*(6), 1689–1702.

Aoki, T., Hikima, J., Segovia, C., Jung, T., Kondo, H., & Hirono, I. (2011). Molecular immunity in the interaction between fish and pathogen for DNA vaccine. *Diseases in Asian Aquaculture VII*, 253–268.

Aquilino, C., Castro, R., Fischer, U., & Tafalla, C. (2014). Transcriptomic responses in rainbow trout gills upon infection with viral hemorrhagic septicemia virus (VHSV). *Developmental and Comparative Immunology*, *44*(1), 12-20.

Ardito, F., Giuliani, M., Perrone, D., Troiano, G., & Muzio, L. Lo. (2017). The crucial role of protein phosphorylation in cell signalingand its use as targeted therapy (Review). *International Journal of Molecular Medicine*, *40*(2), 271–280.

Arrington, J. V., Hsu, C. C., Elder, S. G., & Andy Tao, W. (2017). Recent advances in phosphoproteomics and application to neurological diseases. *Analyst*, *142*(23), 4373–4387.

Arthur, J. S. C., & Ley, S. C. (2013). Mitogen-activated protein kinases in innate immunity. *Nature Reviews Immunology*, *13*(9), 679–692.

Assefa, A., & Abunna, F. (2018). Maintenance of Fish Health in Aquaculture: Review of Epidemiological Approaches for Prevention and Control of Infectious Disease of Fish. *Veterinary Medicine International*, *2018*, 1-10.

Au, W., Moore, P. A., David, W., Tombal, B., Pitha, P. M., & Lafleur, D. W. (1998). Characterization of the Interferon Regulatory Factor-7 and Its Potential Role in the Transcription Activation of Interferon A Genes Characterization of the Interferon Regulatory Factor-7 and Its. *The Journal of Biological Chemistry*, *273*(44), 29210–29217.

Balachandran, S., Roberts, P. C., Brown, L. E., Truong, H., Pattnaik, A. K., Archer, D. R., & Barber, G. N. (2000). Essential role for the dsRNA-dependent protein kinase PKR in innate immunity to viral infection. *Immunity*, *13*(1), 129–141.

Balda, M. S., Whitney, J. A., Flores, C., González, S., Cereijido, M., & Matter, K. (1996). Functional dissociation of paracellular permeability and transepithelial electrical resistance and disruption of the apical-basolateral intramembrane diffusion barrier by

expression of a mutant tight junction membrane protein. *Journal of Cell Biology*, *134*(4), 1031–1049.

Baoprasertkul, P., Peatman, E., Somridhivej, B., & Liu, Z. (2006). Toll-like receptor 3 and TICAM genes in catfish: Species-specific expression profiles following infection with Edwardsiella ictaluri. *Immunogenetics*, *58*(10), 817–830.

Barford, D. (1996). Molecular mechanisms of the protein serine/threonine phosphatases. *Trends in Biochemical Sciences*, *21*(11), 407–412.

Barocchi, M. A., Ko, A. I., Galvão Reis, M., McDonald, K. L., & Riley, L. W. (2002). Rapid translocation of polarized MDCK cell monolayers by *Leptospira interrogans*, an invasive but nonintracellular pathogen. *Infection and Immunity*, *70*(12), 6926–6932.

Bartkova, S., Kokotovic, B., & Dalsgaard, I. (2017). Infection routes of Aeromonas salmonicida in rainbow trout monitored in vivo by real-time bioluminescence imaging. *Journal of Fish Diseases*, *40*(1), 73-82.

Barton, G. M., & Medzhitov, R. (2014). Toll-like receptor signaling pathways. *Science*, *5*, 1–8.

Bauer, H., Zweimueller-Mayer, J., Steinbacher, P., Lametschwandtner, A., & Bauer, H. C. (2010). The dual role of zonula occludens (ZO) proteins. *Journal of Biomedicine and Biotechnology*, *2010*, 1-11.

Beachboard, D. C., & Horner, S. M. (2016). Innate immune evasion strategies of DNA and RNA viruses. *Current Opinion in Microbiology*, *32*, 113–119.

Beck, B. H., Bakal, R. S., Brunner, C. J., & Grizzle, J. M. (2006). Virus distribution and signs of disease after immersion exposure to largemouth bass virus. *Journal of Aquatic Animal Health*, *18*(3), 176–183.

Beltran, L., & Cutillas, P. R. (2012). Advances in phosphopeptide enrichment techniques for phosphoproteomics. *Amino Acids*, *43*(3), 1009–1024.

Belvin, M. P., & Anderson, K. V. (1996). A conserved signaling pathway: The *Drosophila* Toll-Dorsal Pathway. *Annual Review of Cell and Developmental Biology*, *12*(1), 393–416.

Benson, K., Cramer, S., & Galla, H.-J. (2013). Impedance-based cell monitoring: barrier properties and beyond. *Fluids and Barriers of the CNS*, *10*(1), 5.

Bergan, V., Jagus, R., Lauksund, S., Kileng, Ø., & Robertsen, B. (2008). The Atlantic salmon Z-DNA binding protein kinase phosphorylates translation initiation factor 2 alpha and constitutes a unique orthologue to the mammalian dsRNA-activated protein

kinase R. *FEBS Journal*, *275*(1), 184–197.

Bergmann, S. M., Fichtner, D., Riebe, R., & Castric, J. (2008). First isolation and identification of sleeping disease virus (SDV) in Germany. *Bulletin of the European Association of Fish Pathologists*, *28*(4), 148–156.

Bernardet, J.F., Segers, P., Vancanneyt, M., Berthe, F., Kersters, K., & Vandamme, P. (1996). Cutting a Gordian Knot: Emended Classification and Description of the Genus Flavobacterium, Emended Description of the Family Flavobacteriaceae, and Proposal of Flavobacterium hydatis nom. nov. (Basonym, Cytophaga aquatilis Strohl and Tait 1978). *International Journal of Systematic Bacteriology*, *46*(1), 128–148.

Biacchesi, S., LeBerre, M., Lamoureux, A., Louise, Y., Lauret, E., Boudinot, P., & Bremont, M. (2009). Mitochondrial Antiviral Signaling Protein Plays a Major Role in Induction of the Fish Innate Immune Response against RNA and DNA Viruses. *Journal of Virology*, *83*(16), 7815–7827.

Biller-Takahashi, J. D., & Urbinati, E. C. (2014). Fish Immunology. The modification and manipulation of the innate immune system: Brazilian studies. *Annals of the Brazilian Academy of Sciences*, *86*(3), 1484–1506.

Blondel, D., Maarifi, G., Nisole, S., & Chelbi-Alix, M. K. (2015). Resistance to rhabdoviridae infection and subversion of antiviral responses. *Viruses*, *7*(7), 3675–3702.

Bols, N. C., Barlian, A., Chirino-Trejo, Caldwell, S. J., Goegan, P., & Lee, L. E. J. (1994). Development of a cell line from primary cultures of rainbow trout, *Oncorhynchus mykiss* (Walbaum), gills. *Journal of Fish Diseases*, *17*, 601–611.

Boltaña, S., Roher, N., Goetz, F. W., & MacKenzie, S. A. (2011). PAMPs, PRRs and the genomics of gram negative bacterial recognition in fish. *Developmental and Comparative Immunology*, *35*(12), 1195–1203.

Bonazzi, M., & Cossart, P. (2011). Impenetrable barriers or entry portals? The role of cell–cell adhesion during infection. *Journal of Cell Biology, 195*(3), 349-358.

Boneca, I. G. (2005). The role of peptidoglycan in pathogenesis. *Current Opinion in Microbiology*, *8*(1), 46–53.

Borkowski, A. W., Kuo, I. H., Bernard, J. J., Yoshida, T., Williams, M. R., Hung, N. J., Yu, B.D., Beck, L.A., & Gallo, R. L. (2015). Toll-like receptor 3 activation is required for normal skin barrier repair following UV damage. *Journal of Investigative Dermatology, 135*(2), 569–578.

Boucher, P., & Laurencin, F. B. (1996). Sleeping disease and pancreas disease:

comparative histopathology and acquired cross-protection. *Journal of Fish Diseases*, *19*(4), 303–310.

Boudinot, P., Massin, P., Blanco, M., Riffault, S., & Benmansour, A. (1999). vig-1, a new fish gene induced by the rhabdovirus glycoprotein, has a virus-induced homologue in humans and shares conserved motifs with the MoaA family. *Journal of Virology*, *73*(3), 1846–52.

Boudinot, P., Riffault, S., Salhi, S., Carrat, C., Sedlik, C., Mahmoudi, N., Charley, B., & Benmansour, A. (2000). Vesicular stomatitis virus and pseudorabies virus induce a vig1/cig5 homologue in mouse dendritic cells via different pathways. *Journal of General Virology*, *81*(11), 2675–2682.

Bourai, M., Lucas-Hourani, M., Gad, H. H., Drosten, C., Jacob, Y., Tafforeau, L., Cassonnet, P., Jones, L.M., Judith, D., Couderc, T., et al. (2012). Mapping of Chikungunya Virus Interactions with Host Proteins Identified nsP2 as a Highly Connected Viral Component. *Journal of Virology*, *86*(6), 3121–3134.

Bricknell, I., & Dalmo, R. A. (2005). The use of immunostimulants in fish larval aquaculture. *Fish and Shellfish Immunology*, *19*, 457–472.

Bridle, A. R., Morrison, R. N., & Nowak, B. F. (2006). The expression of immune-regulatory genes in rainbow trout, *Oncorhynchus mykiss*, during amoebic gill disease (AGD). *Fish and Shellfish Immunology*, *20*(3), 346–364.

Brietzke, A., Korytář, T., Jaros, J., Köllner, B., Goldammer, T., Seyfert, H. M., & Rebl, A. (2015). *Aeromonas salmonicida* infection only moderately regulates expression of factors contributing to toll-like receptor signaling but massively activates the cellular and humoral branches of innate immunity in rainbow trout (*Oncorhynchus mykiss*). *Journal of Immunology Research*, *2015*, 1-15.

Broekman, D. C., Gudmundsson, G. H., & Maier, V. H. (2013). Differential regulation of cathelicidin in salmon and cod. *Fish and Shellfish Immunology*, *35*(2), 532–538.

Broekman, D. C., Zenz, A., Gudmundsdottir, B. K., Lohner, K., Maier, V. H., & Gudmundsson, G. H. (2011). Functional characterization of codCath, the mature cathelicidin antimicrobial peptide from Atlantic cod (*Gadus morhua*). *Peptides*, *32*(10), 2044–2051.

Brown, L. L., & Johnson, S. C. (2008). Molecular interaction between fish pathogens and host aquatic animals. *Fisheries for Global Welfare and Environment. Memorial Book of the 5th World Fisheries Congress 2008.*, 12–288.

Bui, P., Bagherie-Lachidan, M., & Kelly, S. P. (2010). Cortisol differentially alters claudin

isoforms in cultured puffer fish gill epithelia. *Molecular and Cellular Endocrinology*, *317*, 120–126.

Bunai, K., & Yamane, K. (2005). Effectiveness and limitation of two-dimensional gel electrophoresis in bacterial membrane protein proteomics and perspectives. *Journal of Chromatography B: Analytical Technologies in the Biomedical and Life Sciences*, *815*(1–2), 227–236.

Burch, L. R., Scott, M., Pohler, E., Meek, D., & Hupp, T. (2004). Phage-peptide Display Identifies the Interferon-responsive, Death-activated Protein Kinase Family as a Novel Modifier of MDM2 and p21WAF1. *Journal of Molecular Biology*, *337*(1), 115–128.

Bustin, S. A., Benes, V., Garson, J. A., Hellemans, J., Huggett, J., Kubista, M., et al. (2009). The MIQE guidelines: Minimum information for publication of quantitative real-time PCR experiments. *Clinical Chemistry*, *55*(4), 611–622.

Campbell, J. B., & Wolf, K. (1969). Plaque assay and some characteristics of Egtved virus (virus of viral haemorrhagic septicaemia of Rainbow tout). *Canadian Journal Microbiology*, *15*, 635–637.

Camus, A. C. (2004). Channel Catfish Virus Disease. *SRAC publication*, *4702*, 1-4.

Cao, W., Baniecki, M. L., McGrath, W. J., Bao, C., Deming, C. B., Rade, J. J., et al. (2003). Nitric oxide inhibits the adenovirus proteinase in vitro and viral infectivity in vivo. *Faseb J*, *17*(15), 2345–2346.

Cargnello, M., & Roux, P. P. (2011). Activation and Function of the MAPKs and Their Substrates , the MAPK-Activated Protein Kinases. *Microbiology and Molecular Biology Reviews*, *75*(1), 50–83.

Casadei, E., Wang, T., Zou, J., González Vecino, J. L., Wadsworth, S., & Secombes, C. J. (2009). Characterization of three novel β-defensin antimicrobial peptides in rainbow trout (*Oncorhynchus mykiss*). *Molecular Immunology*, *46*(16), 3358–3366.

Casani, D., Randelli, E., Costantini, S., Facchiano, A. M., Zou, J., Martin, S., et al. (2009). Molecular characterisation and structural analysis of an interferon homologue in sea bass (*Dicentrarchus labrax* L.). *Molecular Immunology*, *46*(5), 943–952.

Castric, J., Laurencin, F. B., Bremont, M., Jeffroy, J., Ven, A. L., & Bearzotti, M. (1997). Isolation of the virus responsible for sleeping disease in experimentally infected rainbow trout (*Onchorhynchus mykiss*). *Bulletin of the European Association of Fish Pathologists*, *17 (1)*(27), 27–30.

Chan, Y. K., & Gack, M. U. (2016). Viral evasion of intracellular DNA and RNA sensing.

Nature Reviews Microbiology, *14*(6), 360–373.

Chang, C., Zhang, Y., Zou, J., Nie, P., & Secombes, C. J. (2006). Two Cathelicidin Genes Are Present in both Rainbow Trout (*Oncorhynchus mykiss*) and Atlantic Salmon (*Salmo salar*). *Society*, *50*(1), 185–195.

Chang, M., Collet, B., Nie, P., Lester, K., Campbell, S., Secombes, C. J., & Zou, J. (2011). Expression and Functional Characterization of the RIG-I-Like Receptors MDA5 and LGP2 in Rainbow Trout (*Oncorhynchus mykiss*). *Journal of Virology*, *85*(16), 8403–8412.

Chang, M., Nie, P., Collet, B., Secombes, C. J., & Zou, J. (2009). Identification of an additional two-cysteine containing type i interferon in rainbow trout *Oncorhynchus mykiss* provides evidence of a major gene duplication event within this gene family in teleosts. *Immunogenetics*, *61*(4), 315–325.

Chang, M., Wang, T., Nie, P., Zou, J., & Secombes, C. J. (2011). Cloning of two rainbow trout nucleotide-binding oligomerization domain containing 2 (NOD2) splice variants and functional characterization of the NOD2 effector domains. *Fish and Shellfish Immunology*, *30*(1), 118–127.

Chang, M. X., Nie, P. & Wei, L. L. (2007). Short and long peptidoglycan recognition proteins (PGRPs) in zebrafish, with findings of multiple PGRP homologs in teleost fish. *Molecular Immunology*, *44*(11), 3005–3023.

Chasiotis, H., Kolosov, D., Bui, P., & Kelly, S. P. (2012a). Tight junctions, tight junction proteins and paracellular permeability across the gill epithelium of fishes: A review. *Respiratory Physiology and Neurobiology*, *184*(3), 269–281.

Chasiotis, H., Kolosov, D., & Kelly, S. P. (2012b). Permeability properties of the teleost gill epithelium under ion-poor conditions. *AJP: Regulatory, Integrative and Comparative Physiology*, *302*, R727–R739.

Chasiotis, H., Wood, C. M., & Kelly, S. P. (2010). Cortisol reduces paracellular permeability and increases occludin abundance in cultured trout gill epithelia. *Molecular and Cellular Endocrinology*, *323*(2), 232–8.

Chen, E. Y., Tan, C. M., Kou, Y., Duan, Q., Wang, Z., Meirelles, G. V., Clark, N. R., & Ma'yan, A. (2013). Enrichr: Interactive and collaborative HTML5 gene list enrichment analysis tool. *BMC Bioinformatics*, *14*(128), 1-14.

Chen, L., He, C., Baoprasertkul, P., Xu, P., Li, P., Serapion, J., et al. (2005). Analysis of a catfish gene resembling interleukin-8: cDNA cloning, gene structure, and expression after infection with Edwardsiella ictaluri. *Developmental and Comparative*

Immunology, *29*(2), 135–142.

Cheon, I. S., Woo, S. S., Kang, S. S., Im, J., Yun, C. H., Chung, D. K., et al. (2008). Peptidoglycan-mediated IL-8 expression in human alveolar type II epithelial cells requires lipid raft formation and MAPK activation. *Molecular Immunology*, *45*(6), 1665–1673.

Chi, H., Zhang, Z., Bøgwald, J., Zhan, W., & Dalmo, R. A. (2011). Cloning, expression analysis and promoter structure of TBK1 (TANK-binding kinase 1) in Atlantic cod (*Gadus morhua* L.). *Fish & Shellfish Immunology*, *30*(4–5), 1055–1063.

Chin, K.-C., & Cresswell, P. (2001). Viperin (cig5), an IFN-inducible antiviral protein directly induced by human cytomegalovirus. *Proceedings of the National Academy of Sciences*, *98*(26), 15125–15130.

Choi, J., Snovida, S. I., Bomgarden, R., Rogers, J. C., & Scientific, T. F. (2017). Sequential enrichment from Metal Oxide Affinity Chromatography (SMOAC), a phosphoproteomics strategy for the separation of multiply phosphorylated from monophosphorylated peptides .

Choi, K. Y., Chow, L. N. Y., & Mookherjee, N. (2012). Cationic host defence peptides: Multifaceted role in immune modulation and inflammation. *Journal of Innate Immunity*, *4*(4), 361–370.

Choi, W., Lee, E. Y., & Choi, T. J. (2006). Cloning and sequence analysis of the β2-microglobulin transcript from flounder, *Paralichthys olivaceous*. *Molecular Immunology*, *43*(10), 1565–1572.

Ciani, B., Layfield, R., Cavey, J. R., Sheppard, P. W., & Searle, M. S. (2003). Structure of the Ubiquitin-associated Domain of p62 (SQSTM1) and Implications for Mutations That Cause Paget's Disease of Bone. *Journal of Biological Chemistry*, *278*(39), 37409-37412.

Claire, L. (2016). *Development and Uses of a Primary Fish Gill Cell Culture System to investigate the Uptake, Efflux and Metabolism of Pharmaceuticals in Ecotoxicology*. A thesis submitted to King's College London.

Claude, P., & Goodenough, D. A. (1973). Fracture faces of zonulae occludentes from "tight" and "leaky" epithelia. *Journal of Cell Biology*, *58*(2), 390–400.

Clua, P., Kanmani, P., Zelaya, H., Tada, A., Humayun Kober, A. K. M., Salva, S., et al. (2017). Peptidoglycan from immunobiotic lactobacillus rhamnosus improves resistance of infant Mice to respiratory syncytial viral infection and secondary *Pneumococcal pneumonia*. *Frontiers in Immunology*, *8*(944), 1-15.

Clem, L.W., Sizemore, R.C., Ellsaesser, C.F. and Muller, N.W. (1985). Monocytes as accessory cells in fish immune responses. *Developmental and comparative immunology*, *9*, 803–809.

Comstock, A. T., Ganesan, S., Chattoraj, A., Faris, A. N., Margolis, B. L., Hershenson, M. B., & Sajjan, U. S. (2011). Rhinovirus-Induced Barrier Dysfunction in Polarized Airway Epithelial Cells Is Mediated by NADPH Oxidase 1. *Journal of Virology*, *85*(13), 6795–6808.

Cuesta, A., Meseguer, J., & Esteban, M. Á. (2011). Molecular and functional characterization of the gilthead seabream β-defensin demonstrate its chemotactic and antimicrobial activity. *Molecular Immunology*, *48*(12–13), 1432–1438.

Cummins, P. M. (2012). Occludin: One Protein, Many Forms. *Molecular and Cellular Biology*, *32*(2), 242–250.

Cutillas, P. R. (2015). Role of phosphoproteomics in the development of personalized cancer therapies. *Proteomics - Clinical Applications*, *9*(3–4), 383–395.

Dalsgaard, I., & Madsen, L. (2000). Bacterial pathogens in rainbow trout, *Oncorhynchus mykiss* (Walbaum), reared at Danish freshwater farms. *Journal of Fish Diseases*, *23*(3), 199-209.

Dauber, B., & Wolff, T. (2009). Activation of the antiviral kinase PKR and viral countermeasures. *Viruses*, *1*(3), 523–544.

De Bruijn, I., Belmonte, R., Anderson, V. L., Saraiva, M., Wang, T., Van West, P., & Secombes, C. J. (2012). Immune gene expression in trout cell lines infected with the fish pathogenic oomycete Saprolegnia parasitica. *Developmental and Comparative Immunology*, *38*(1), 44–54.

Declercq, A. M., H. F., Van Den Broeck, W., Bossier, P., & Decostere, A. (2013). Veterinary Research Full text Columnaris disease in fish a review with emphasis on bacterium-host interactions. *Veterinary Research*, *44*(27), 1-17.

De Castro, D. G., Clarke, P. A., Al-Lazikani, B., & Workman, P. (2013). Personalized Cancer Medicine: Molecular Diagnostics, Predictive biomarkers, and Drug Resistance. *Clinical Pharmacology and Therapeutics*, *93*(3), 252–259.

de Groot, R. J., Rumenapf, T., Kuhn, R. J., Strauss, E. G., & Strauss, J. H. (1991). Sindbis virus RNA polymerase is degraded by the N-end rule pathway. *Proc Natl Acad Sci U S A*, *88*(20), 8967–8971.

del Castillo, C. S., Hikima, J. ichi, Ohtani, M., Jung, T. S., & Aoki, T. (2012). Characterization and functional analysis of two PKR genes in fugu (Takifugu

rubripes). *Fish and Shellfish Immunology*, *32*(1), 79–88.

Delom, F., & Chevet, E. (2006). Phosphoprotein analysis: from proteins to proteomes. *Proteome Science*, *4*, 15.

Department of Agriculture. (2009). Disease strategy: Furunculosis (Version 2.0). In: Australian Aquatic Veterinary Emergency Plan (AQUAVETPLAN), Australian Government Department of Agriculture, Canberra, ACT.

Deribe, Y. L., Pawson, T., & Dikic, I. (2010). Post-translational modifications in signal integration. *Nature Structural and Molecular Biology*, *17*(6), 666–672.

DeWitte-Orr, S. J., & Mossman, K. L. (2010). dsRNA and the innate antiviral immune response. *Future Virology*, *5*(3), 325–341.

Dinarello, C., Arend, W., Sims, J., Immunology, M., Smith, D., Blumberg, H., et al. (2010). IL-1 family nomenclature. *Nature Immunology*, *11*(11), 973.

Dixit, E., & Kagan, J. C. (2013). Intracellular Pathogen Detection by RIG-I-Like Receptors. *Advances in Immunology*, Elsevier Inc., *117*, 99-125.

Dorantes-Aranda, J. J., Waite, T. D., Godrant, A., Rose, A. L., Tovar, C. D., Woods, G. M., & Hallegraeff, G. M. (2011). Novel application of a fish gill cell line assay to assess ichthyotoxicity of harmful marine microalgae. *Harmful Algae*, *10*(4), 366–373.

Dörfel, M. J., & Huber, O. (2012). Modulation of tight junction structure and function by kinases and phosphatases targeting occludin. *Journal of Biomedicine and Biotechnology*, *2012*.

Dunlevy, F., McElvaney, N. G., & Greene, C. M. (2010). TLR3 Sensing of Viral Infection. *Open Infectious Diseases Journal*, *4*(1), 1–10.

Dutta, D., & Donaldson, J. G. (2012). Intended specificity and unintended consequences. *Cellular Logistics*, *2*(4), 203–208.

Dziarski, R. (2003). Recognition of bacterial peptidoglycan by the innate immune system. *Cellular and Molecular Life Sciences*, *60*(9), 1793–1804.

Dziarski, R. (2004). Peptidoglycan recognition proteins (PGRPs). *Molecular Immunology*, *40*(12), 877–886.

Ebbesson, L. O. E., Tipsmark, C. K., Holmqvist, B., Nilsen, T., Andersson, E., Stefansson, S. O., & Madsen, S. S. (2005). Nitric oxide synthase in the gill of Atlantic salmon : colocalization with and inhibition of Na + , K + -ATPase, 1011–1017.

Ebner, H. L., Blatzer, M., Nawaz, M., & Krumschnabel, G. (2007). Activation and nuclear translocation of ERK in response to ligand-dependent and -independent stimuli in liver and gill cells from rainbow trout. *The Journal of Experimental Biology*, *210*(Pt

6), 1036–45.

Edelmann, K. H., Richardson-Burns, S., Alexopoulou, L., Tyler, K. L., Flavell, R. A., & Oldstone, M. B. A. (2004). Does Toll-like receptor 3 play a biological role in virus infections? *Virology*, *322*(2), 231–238.

Emmenegger, E. J., Glenn, J. A., Winton, J. R., Batts, W. N., Gregg, J. L., & Hershberger, P. K. (2014). Molecular identification of erythrocytic necrosis virus (ENV) from the blood of Pacific herring (*Clupea pallasii*). *Veterinary Microbiology*, *174*(1–2), 16–26.

Emmerich, R., & Weibel, E. (1894). Ueber eine durch Bacterien erzeugte Seuche unter den Forellen. *Archiv für Hygiene*, *21*, 1-21.

Essbauer, S., & Ahne, W. (2001). Viruses of lower vertebrates. *Journal of Veterinary Medicine, Series B*, *48*(6), 403–475.

Evans, D. H., Piermarini, P. M., & Choe, K. P. (2005). The Multifunctional Fish Gill: Dominant Site of Gas Exchange, Osmoregulation, Acid-Base Regulation, and Excretion of Nitrogenous Waste. *Physiological Reviews*, *85*, 97–177.

Eyngor, M. Z., Rachel, T., Japhette, E. K., Berkowitz, A. B., Hillel, T. S., Lev, M., Hurvitz, A., Galeotti, M., Bacharach, E., & Eldar, A. (2014). Identification of a novel RNA virus lethal to tilapia. *Journal of Clinical Microbiology*, *52*(12), 4137–4146.

Falk, K., Namork, E., Rimstad, E., Mjaaland, S., & Dannevig, B. H. (1997). Characterization of infectious salmon anemia virus, an orthomyxo-like virus isolated from Atlantic salmon (*Salmo salar* L.). *Journal of Virology*, *71*(12), 9016–23.

FAO. (2012). The State of World Fisheries and Aquaculture, *Food and Agriculture Oraganization of the United Nations*, Rome, 209.

FAO. (2014). *The state of world fisheries and aquaculture*. *Food and Agriculture Oraganization of the United Nations*, Rome, 223.

FAO. (2016). *The State of World Fisheries and Aquaculture 2016. Contributing to food security and nutrition for all.* Rome. 200.

FAO. (2018). *The State of Agricultural Commodity Markets 2018. Agricultural trade, climate change and food security*. *Agricultural trade, climate change and food security*, Rome, 92.

Feng, H., Liu, H., Kong, R., Wang, L., Wang, Y., Hu, W., & Guo, Q. (2011). Expression profiles of carp IRF-3/-7 correlate with the up-regulation of RIG-I/MAVS/TRAF3/TBK1, four pivotal molecules in RIG-I signaling pathway. *Fish and Shellfish Immunology*, *30*(4–5), 1159–1169.

Feng, H., Zhang, Q.-M., Zhang, Y.-B., Li, Z., Zhang, J., Xiong, Y.-W., Wu, M. & Gui, J.-F. (2016). Zebrafish IRF1, IRF3, and IRF7 Differentially Regulate IFNΦ1 and IFNΦ3 Expression through Assembly of Homo- or Heteroprotein Complexes. *The Journal of Immunology*, *197*(5), 1893–1904.

Feng, X., Su, J., Yang, C., Yan, N., Rao, Y., & Chen, X. (2014). Molecular characterizations of grass carp (*Ctenopharyngodon idella*) TBK1 gene and its roles in regulating IFN-I pathway. *Developmental and Comparative Immunology*, *45*(2), 278–290.

Fernandez-Trujillo, A., Ferro, P., Garcia-Rosado, E., Infante, C., Alonso, M. C., Bejar, J., et al. (2008). Poly I:C induces Mx transcription and promotes an antiviral state against sole aquabirnavirus in the flatfish Senegalese sole (*Solea senegalensis* Kaup). *Fish and Shellfish Immunology*, *24*(3), 279–285.

Fijan, N., Sulimanović, D., Bearzotti, M., Muzinić, D., Zwillenberg, L. O., Chilmonczyk, S., Vautherot, J.F., & de Kinkelin, P. (1983). Some properties of the Epithelioma papulosum cyprini (EPC) cell line from carp *Cyprinus carpio*. *Annales de l'Institut Pasteur / Virologie*, *134*(2), 207–220.

Foster, S. J., Smith, T. J., & Blackman, S. A. (2000). Autolysins of Bacillus subtilis: multiple enzymes with multiple functions. *Microbiology*, *146*(2), 249–262.

Francis-Floyd, R. (2013). An introduction to fish health management. The fish site. University of Florida IFAS extension. 1-5.

Fred, P., & Meyer. (1997). Aquaculture disease and health management. Aquaculture in Animal Science symposium, MAS, 82nd Annual Meeting, Ames, IA, United States.

Fringuelli, E., Rowley, H. M., Wilson, J. C., Hunter, R., Rodger, H., & Graham, D. A. (2008). Phylogenetic analyses and molecular epidemiology of European salmonid alphaviruses (SAV) based on partial E2 and nsP3 gene nucleotide sequences. *Journal of Fish Diseases*, *31*(11), 811–823.

Furnes, C., Kileng, Ø., Rinaldo, C. H., Seppola, M., Jensen, I., & Robertsen, B. (2009). Atlantic cod (*Gadus morhua* L.) possesses three homologues of ISG15 with different expression kinetics and conjugation properties. *Developmental and Comparative Immunology*, *33*(12), 1239–1246.

Furuse, M., & Tessuaki Hirase, Masahiko Itoh, Akira Nagafuchi, Shigenobu Yonemura, S. T. and S. T. (1993). Occludin: A Novel Integral Membrane Protein Localizing at Tight Junctions, *123*(6), 1777–1788.

Gack, M. U. (2014). Mechanisms of RIG-I-Like Receptor Activation and Manipulation by

Viral Pathogens. *Journal of Virology*, *88*(10), 5213–5216.

Gao, J. J., Filla, M. B., Fultz, M. J., Vogel, S. N., Russell, S. W., & Murphy, W. J. (1998). Autocrine/Paracrine IFN-αβ Mediates the Lipopolysaccharide-Induced Activation of Transcription Factor Stat1α in Mouse Macrophages: Pivotal Role of Stat1 α in Induction of the Inducible Nitric Oxide Synthase Gene. *The Journal of Immunology*, *161*, 4803–4810.

Garmashova, N., Atasheva, S., Kang, W., Weaver, S. C., Frolova, E., & Frolov, I. (2007). Analysis of Venezuelan Equine Encephalitis Virus Capsid Protein Function in the Inhibition of Cellular Transcription. *Journal of Virology*, *81*(24), 13552–13565.

Girardin, S. E., Boneca, I. G., Viala, J., Chamaillard, M., Labigne, A., Thomas, G., et al. (2003). Nod2 is a general sensor of peptidoglycan through muramyl dipeptide (MDP) detection. *Journal of Biological Chemistry*, *278*(11), 8869–8872.

Giuliani, A., Pirri, G., & Nicoletto, S. F. (2007). *Antimicrobial peptides: An overview of a promising class of therapeutics*. *Central European Journal of Biology* (Vol. 2).

Gonzalez-Mariscal, L., Betanzos, A., Nava, P., & Jaramilo, B. E. (2003). Tight junction proteins. *Progress in Biophysics and Molecular Biology*, *81*(1), 1–44.

Gottlieb, T. a, Ivanov, I. E., Adesnik, M., & Sabatini, D. D. (1993). Actin filaments play a critical role in endocytosis at the apical but not the basolateral surface of polarized epithelial cells. *J. Cell Biol.*, *120*(3), 695–710.

Graham, D. A., Frost, P., Mclaughlin, K., Rowley, H. M., Gabestad, I., Gordon, A., & Mcloughlin, M. F. (2011). A comparative study of marine salmonid alphavirus subtypes 1-6 using an experimental cohabitation challenge model. *Journal of Fish Diseases*, *34*(4), 273–286.

Graham, D. A., Rowley, H. M., Fringuelli, E., Bovo, G., Manfrin, A., McLoughlin, M. F., et al. (2007). First laboratory confirmation of salmonid alphavirus infection in Italy and Spain. *Journal of Fish Diseases*, *30*(9), 569–572.

Graham, D. A., Rowley, H. M., Walker, I. W., Weston, J. H., Branson, E. J., & Todd, D. (2003). First isolation of sleeping disease virus from rainbow trout, *Oncorhynchus mykiss* (Walbaum), in the United Kingdom. *J Fish Dis*, *26*(11–12), 691–694.

Graham, D. A., Wilson, C., Jewhurst, H., & Rowley, H. (2008). Cultural characteristics of salmonid alphaviruses - Influence of cell line and temperature. *Journal of Fish Diseases*, *31*(11), 859–868.

Grand View Research, I. (2015). Aquaculture Market Analysis By Culture Environment (Fresh Water, Marine Water, Brackish Water), By Product (Carps, Crustaceans,

Mackerel, Milkfish, Mollusks, Salmon, Sea bass, Sea bream, Trout) And Segment Forecasts To 2020. Grand View Research Inc., USA.

Gu, J., Dai, S., Liu, H., Cao, Q., Yin, S., Lai, K.P., Tse, W. K. F., Wong, C. K. C., & Shi, H. (2018). Identification of immune-related genes in gill cells of Japanese eels (Anguilla japonica) in adaptation to water salinity changes. *Fish and Shellfish Immunology, 73*, 288-296.

Guo, S., Al-Sadi, R., Said, H. M., & Ma, T. Y. (2013). Lipopolysaccharide causes an increase in intestinal tight junction permeability in vitro and in vivo by inducing enterocyte membrane expression and localization of TLR-4 and CD14. *American Journal of Pathology*, *182*(2), 375–387.

Guo, T. (2015). *Salmonid alphavirus infection in Atlantic salmon - viral properties and host responses to infection*. Norwegian University of Life Sciences.

Haller, O., & Kochs, G. (2002). Interferon-Induced Mx Proteins: Dynamin-Like GTPases with Antiviral Activity. *Traffic*, 3(10), 710-717.

Hancock, R. E. (2000). Cationic antimicrobial peptides: towards clinical applications. *Expert Opinion on Investigational Drugs*, *9*(8), 1723–1729.

Hancock, R. E. W., & Diamond, G. (2000). The role of cationic antimicrobial peptides in innate host defences. *Trends in Microbiology*, *8*(9), 402–410.

Hayashi, F., Means, T. K., & Luster, A. D. (2003). Toll-like receptors stimulate human neutrophil function. *Blood*, *102*(7), 2660–2669. https://doi.org/10.1182/blood-2003-04-1078

Healy, L. L., Cronin, J. G., & Sheldon, I. M. (2015). Polarized Epithelial Cells Secrete Interleukin 6 Apically in the Bovine Endometrium1. *Biology of Reproduction*, *92*(6), 1–12.

Helbig, K. J., & Beard, M. R. (2014). The role of viperin in the innate antiviral response. *Journal of Molecular Biology*, *426*, 1210–1219.

Helbig, K. J., Carr, J. M., Calvert, J. K., Wati, S., Clarke, J. N., Eyre, N. S., et al. (2013). Viperin Is Induced following Dengue Virus Type-2 (DENV-2) Infection and Has Anti-viral Actions Requiring the C-terminal End of Viperin. *PLoS Neglected Tropical Diseases*, *7*(4), e2178, 1-14.

Herath, T. K., Ferguson, H. W., Weidmann, M. W., Bron, J. E., Thompson, K. D., Adams, A., et al. (2016). Pathogenesis of experimental salmonid alphavirus infection in vivo: An ultrastructural insight. *Veterinary Research*, *47*(1), 1–11.

Hinson, E. R., Joshi, N. S., Chen, J. H., Rahner, C., Jung, Y. W., Wang, X., Kaech, S.M.,

& Cresswell, P. (2010). Viperin Is Highly Induced in Neutrophils and Macrophages during Acute and Chronic Lymphocytic Choriomeningitis Virus Infection. *The Journal of Immunology*, *184*(10), 5723–5731.

Hiscott, J., Grandvaux, N., Sharma, S., Tenoever, B. R., Servant, M. J., & Linn, R. (2003). Convergence of the NF-κB and Interferon Signaling Pathways in the Regulation of Antiviral Defance and Apoptosis. *Annals New York Academy of Sciences*, *10*(237–248).

Hiscott, J., Lacoste, J., & Lin, R. (2006). Recruitment of an interferon molecular signaling complex to the mitochondrial membrane: Disruption by hepatitis C virus NS3-4A protease. *Biochemical Pharmacology*, *72*(11), 1477–1484.

Hjeltnes, B., Bornø, G., Jansen, M. D., Haukaas, A., & Walde, C. (Eds.). (2017). The Health Situation in Norwegian Aquaculture 2016, Norwegian Veterinary Institute.

Hjortaas, M. J., Skjelstad, H. R., Taksdal, T., Olsen, A. B., Johansen, R., Bang-Jensen, B., et al. (2013). The first detections of subtype 2-related salmonid alphavirus (SAV2) in Atlantic salmon, *Salmo salar* L., in Norway. *Journal of Fish Diseases*, *36*(1), 71–74.

Holland, J. W., Bird, S., Williamson, B., Woudstra, C., Mustafa, A., Wang, T., Zou, J., Blaney, S.C., Collet, B., & Secombes, C. J. (2008). Molecular characterization of IRF3 and IRF7 in rainbow trout, *Oncorhynchus mykiss*: Functional analysis and transcriptional modulation. *Molecular Immunology*, *46*(2), 269–285.

Hornberg, J. J., Bruggeman, F. J., Binder, B., Geest, C. R., Bij De Vaate, A. J. M., Lankelma, J. Ørpetveit, I., & Westerhoff, H. V. (2005). Principles behind the multifarious control of signal transduction: ERK phosphorylation and kinase/phosphatase control. *FEBS Journal*, *272*(1), 244–258.

Hounmanou, Y. M.G., Mdegela, R. H., Dougnon, T. V., Achoh, M. E., Mhongole, O. J., Agadjihouèdé, H., Gangbè, L., & Dalsgaard, A. (2018). Tilapia lake virus threatens tilapiines farming and food security: Socio-economic challenges and preventive measures in Sub-Saharan Africa. *Aquaculture*, *493*, 123-129.

Hu, D., Mayeda, A., Trembley, J. H., Lahti, J. M., & Kidd, V. J. (2003). CDK11 complexes promote pre-mRNA splicing. *Journal of Biological Chemistry*, *278*(10), 8623–8629.

Huising, M. O., Stet, R. J. M., Savelkoul, H. F. J., & Verburg-Van Kemenade, B. M. L. (2004). The molecular evolution of the interleukin-1 family of cytokines; IL-18 in teleost fish. *Developmental and Comparative Immunology*, *28*(5), 395–413.

Hu, Y.-S., Li, W., Li, D.-M., Liu, Y., Fan, L.-H., Rao, Z.-C., et al. (2013). Cloning,

expression and functional analysis of PKR from grass carp (*Ctenopharyngodon idellus*). *Fish & Shellfish Immunology*, *35*(6), 1874–1881.

Huang, L. Y., Stuart, C., Takeda, K., D'Agnillo, F., & Golding, B. (2016). Poly(I:C) induces human lung endothelial barrier dysfunction by disrupting tight junction expression of claudin-5. *PLoS ONE*, *11*(8), 1–16.

Huerta-Cepas, J., Szklarczyk, D., Forslund, K., Cook, H., Heller, D., Walter, M. C., et al. (2016). EGGNOG 4.5: A hierarchical orthology framework with improved functional annotations for eukaryotic, prokaryotic and viral sequences. *Nucleic Acids Research*, *44*(D1), D286–D293.

Hultmark, D., Engström, Å., Bennich, H., Kapur, R., & Boman, H. G. (1982). Insect Immunity: Isolation and Structure of Cecropin D and Four Minor Antibacterial Components from Cecropia Pupae. *European Journal of Biochemistry*, *127*(1), 207–217.

Hunter, T. (1995). Protein kinases and phosphatases: The Yin and Yang of protein phosphorylation and signaling. *Cell*, *80*(2), 225–236.

Hunter, T., & Karin, M. (1992). The regulation of transcription by phosphorylation. *Cell*, *70*(3), 375–387.

Hyndman, K. A., Choe, K. P., Havird, J. C., Rose, R. E., Piermarini, P. M., & Evans, D. H. (2006). Neuronal nitric oxide synthase in the gill of the killifish, *Fundulus heteroclitus*, *144*, 510–519.

Hyoung, J. K., Oseko, N., Nishizawa, T., & Yoshimizu, M. (2009). Protection of rainbow trout from infectious hematopoietic necrosis (IHN) by injection of infectious pancreatic necrosis virus (IPNV) or Poly(I:C). *Diseases of Aquatic Organisms*, *83*(2), 105–113.

Idowu, T. A., Adedji, H. A., & Sogbesan, O. A. (2017). Fish Diseases and Health Management in Aquaculture Production. *International Journal of Environmental & Argricultural science*, *1*(1), 1-6.

Iliev, D. B., Roach, J. C., Mackenzie, S., Planas, J. V., & Goetz, F. W. (2005). Endotoxin recognition: In fish or not in fish? *FEBS Letters*, *579*(29), 6519–6528.

Inohara, N., Ogura, Y., Fontalba, A., Gutierrez, O., Pons, F., Crespo, J., Fukase, K., Inamura, S., Kusumoto, S., Hashimoto, M., Foster, S.J., Moran, A.P., Fernandez-Luna, J.L., & Nuñez, G. (2003). Host recognition of bacterial muramyl dipeptide mediated through NOD2: Implications for Crohn's disease. *Journal of Biological Chemistry*, *278*(8), 5509–5512.

Inouye, K. (1996). An overview of health management of cold-water fish and shrimp in Japanese aquaculture. *In* Health Management in Asian Aquaculture. Proceedings of the Regional Expert Consultation on Aquaculture Health Management in Asia and the Pacific. R. P. Subasinghe, J. R. Arthur & M. Shariff (eds.), p. 104–114. FAO Fisheries Technical Paper No. 360, Rome, FAO. 142 p.

Ito, Y., Kawamura, I., Kohda, C., Tsuchiya, K., Nomura, T., & Mitsuyama, M. (2005). Seeligeriolysin O, a protein toxin of Listeria seeligeri, stimulates macrophage cytokine production via Toll-like receptors in a profile different from that induced by other bacterial ligands. *International Immunology*, *17*(12), 1597–1606.

Jacobs, B. L., & Langland, J. O. (1996). When two strands are better than one: the mediators and modulators of the cellular responses to double-stranded RNA. *Virology*, *219*(2), 339–49.

Jain, S., Suzuki, T., Seth, A., Samak, G., & Rao, R. (2011). Protein kinase Cζ phosphorylates occludin and promotes assembly of epithelial tight junctions. *Biochemical Journal*, *437*(2), 289–299.

Jang, J. H., Kim, H. & Cho, J. H. (2013). Rainbow trout peptidoglycan recognition protein has an anti-in fl ammatory function in liver cells. *Fish and Shellfish Immunology*, *35*, 1838–1847.

Jensen, I., Albuquerque, A., Sommer, A.-I., & Robertsen, B. (2002). Effect of poly I:C on the expression of Mx proteins and resistance against infection by infectious salmon anaemia virus in Atlantic salmon. *Fish & Shellfish Immunology*, *13*(4), 311–326.

Jensen, I., & Robertsen, B. (2002). Effect of double-stranded RNA and interferon on the antiviral activity of Atlantic salmon cells against infectious salmon anemia virus and infectious pancreatic necrosis virus. *Fish & Shellfish Immunology*, *13*(3), 221–241.

Jansen, M. D., Dong, H. T., & Mohan, C. V. (2018). Tilapia lake virus: a threat to the global tilapia industry? *Reviews in Aquaculture*, 1-5.

Jensen, V., & Robertsen, B. (2000). Cloning of an Mx cDNA from Atlantic halibut (*Hippoglossus hippoglossus*) and characterization of Mx mRNA expression in response to double-stranded RNA or infectious pancreatic necrosis virus. *Journal of Interferon & Cytokine Research : The Official Journal of the International Society for Interferon and Cytokine Research*, *20*(8), 701–10.

Jeon, Y. J., Yoo, H. M., & Chung, C. H. (2010). ISG15 and immune diseases. *Biochimica et Biophysica Acta - Molecular Basis of Disease*, *1802*(5), 485–496.

Jia, P., Jia, K., Chen, L., Le, Y., Jin, Y., Zhang, J., Zhu, L., Zhang, L., & Yi, M. (2016).

Identification and characterization of the melanoma differentiation - associated gene 5 in sea perch, *Lateolabrax japonicus*. *Developmental and Comparative Immunology*, *61*, 161–168.

Jiang, X., Kinch, L. N., Brautigam, C. A., Chen, X., Du, F., Grishin, N. V., & Chen, Z. J. (2012). Ubiquitin-Induced Oligomerization of the RNA Sensors RIG-I and MDA5 Activates Antiviral Innate Immune Response. *Immunity*, *36*(6), 973–959.

Johnson, J., Albarani, V., Nguyen, M., Goldman, M., Willems, F., & Aksoy, E. (2007). Protein kinase Cα is involved in interferon regulatory factor 3 activation and type I interferon-β synthesis. *Journal of Biological Chemistry*, *282*(20), 15022–15032.

Jones, S. R. M., Bruno, D. W., Madsen, L., & Peeler, E. J. (2015). Disease management mitigates risk of pathogen transmission from maricultured salmonids. *Aquaculture Environment Interactions*, *6*, 119–134.

Jose, J., Snyder, J., & Kuhn, R. (2009). A structural and functional perspective of alphavirus replication and assembly. *Future Microbiol*, *4*, 30.

Jou, T. S., Schneeberger, E. E., & Nelson, W. J. (1998). Structural and functional regulation of tight junctions by RhoA and Rac1 small GTPases. *Journal of Cell Biology*, *142*(1), 101–115.

Kanlaya, R., Pattanakitsakul, S. N., Sinchaikul, S., Chen, S. T., & Thongboonkerd, V. (2009). Alterations in actin cytoskeletal assembly and junctional protein complexes in human endothelial cells induced by dengue virus infection and mimicry of leukocyte transendothelial migration. *Journal of Proteome Research*, *8*(5), 2551–2562.

Kasamatsu, J., Oshiumi, H., Matsumoto, M., Kasahara, M., & Seya, T. (2010). Phylogenetic and expression analysis of lamprey toll-like receptors. *Developmental and Comparative Immunology*, *34*(8), 855–865.

Kast, J. I., McFarlane, A. J., Głobińska, A., Sokolowska, M., Wawrzyniak, P., Sanak, M., et al. (2017). Respiratory syncytial virus infection influences tight junction integrity. *Clinical and Experimental Immunology*, *190*(3), 351–359.

Kato, G., Miyazawa, H., Nakayama, Y., Ikari, Y., Kondo, H., Yamaguchi, T., Sano, M., & Fischer, U. (2018). A Novel Antigen-Sampling Cell in the Teleost Gill Epithelium With the Potential for Direct Antigen Presentation in Mucosal Tissue. *Frontiers in Immunology*, *9*(2166), 1-12.

Kato, H., Takeuchi, O., Sato, S., Yoneyama, M., Yamamoto, M., Matsui, K., et al. (2006). Differential roles of MDA5 and RIG-I helicases in the recognition of RNA viruses. *Nature*, *441*(7089), 101–105.

Kawai, T., & Akira, S. (2008a). Toll-like receptor and RIG-1-like receptor signaling. *Annals of the New York Academy of Sciences*, *1143*, 1–20.

Kawai, T., & Akira, S. (2008b). Toll-like Receptor and RIG-1-like Receptor Signaling. *Annals of the New York Academy of Sciences*, *1143*(1), 1–20.

Kawai, T., Takahashi, K., Sato, S., Coban, C., Kumar, H., Kato, H., et al. (2005). IPS-1, an adaptor triggering RIG-I- and Mda5-mediated type I interferon induction. *Nature Immunology*, *6*(10), 981–988.

Kelly, S. P., & Wood, C. M. (2001a). Effect of cortisol on the physiology of cultured pavement cell epithelia from freshwater trout gills. *Am J Physiol Regulatory Integrative Comp Physiol*, *281*(3), 811–820.

Kelly, S. P., & Wood, C. M. (2001b). The Physiological Effects of 3,5′,3′-Triiodo-l-thyronine Alone or Combined with Cortisol on Cultured Pavement Cell Epithelia from Freshwater Rainbow Trout Gills. *General and Comparative Endocrinology*, *123*(3), 280–294.

Kennedy, D. A., Kurath, G., Brito, I. L., Purcell, M. K., Read, A. F., Winton, J. R., & wargo, A. R. (2016). Potential drivers of virulence evolution in aquaculture. *Evolutionary Applications*, 9(2), 344-354.

Kielian, M., Chanel-Vos, C. & Liao, M. (2010). Alphavirus entry and membrane fusion. *Viruses*, *2*(4), 796–825.

Kim, M. Y., Jang, J. H., Lee, J. W., & Cho, J. H. (2010). Molecular cloning and characterization of peptidoglycan recognition proteins from the rockfish, *Sebastes schlegeli*. *Fish and Shellfish Immunology*, *28*(4), 632–639.

Kim, Y.-S., Yoon, J.-W., Han, H.-J., Suebsing, R., & Kim, J.-H. (2011). Prevalence and Characterization of Typical *Aeromonas salmonicida* Chum Salmon Isolates in Korea. *Fisheries and Aquatic Sciences*, *14*(4), 347–354.

Kitao, Y., Kono, T., Korenaga, H., Iizasa, T., Nakamura, K., Savan, R., & Sakai, M. (2009). Characterization and expression analysis of type I interferon in common carp Cyprinus carpio L. *Molecular Immunology*, *46*(13), 2548–2556.

Koch, H., Wilhelm, M., Ruprecht, B., Beck, S., Frejno, M., Klaeger, S., & Kuster, B. (2016). Phosphoproteome Profiling Reveals Molecular Mechanisms of Growth-Factor-Mediated Kinase Inhibitor Resistance in EGFR-Overexpressing Cancer Cells. *Journal of Proteome Research*, *15*(12), 4490–4504.

Kohli, G., Hu, S., Clelland, E., Di Muccio, T., Rothenstein, J., & Peng, C. (2003). Cloning of transforming growth factor-β1 (TGF-β1) and its type II receptor from zebrafish

ovary and role of TGF-β1 in oocyte maturation. *Endocrinology*, *144*(5), 1931–1941.

Kolosov, D., Bui, P., Chasiotis, H., & Kelly, S. P. (2013). Claudins in teleost fishes. *Tissue Barriers*, *1*(3), e25391.

Koshiba, T., Bashiruddin, N., & Kawabata, S. (2011). Mitochondria and antiviral innate immunity. *International Journal of Biochemistry and Molecular Biology*, *2*(3), 257–262.

Kozera, B., & Rapacz, M. (2013). Reference genes in real-time PCR. *Journal of Applied Genetics*, *54*(4), 391-406.

Krumschnabel, G., Maehr, T., Nawaz, M., Schwarzbaum, P. J., & Manzl, C. (2007). Staurosporine-induced cell death in salmonid cells: The role of apoptotic volume decrease, ion fluxes and MAP kinase signaling. *Apoptosis*, *12*(10), 1755–1768.

Kuleshov, M. V., Jones, M. R., Rouillard, A. D., Fernandez, N. F., Duan, Q., Wang, Z., et al. (2016). Enrichr: a comprehensive gene set enrichment analysis web server 2016 update. *Nucleic Acids Research*, *44*, W90–W97.

Kumar, G., Menanteau-Ledouble, S., Saleh, M., & El-Matbouli, M. (2015). *Yersinia ruckeri*, the causative agent of enteric redmouth disease in fish. *Veterinary Research*, *46*(1), 1–10.

Kumar, M., & Carmichael, G. G. (1998). Antisense RNA: function and fate of duplex RNA in cells of higher eukaryotes. *Microbiology and Molecular Biology Reviews : MMBR*, *62*(4), 1415–34.

Kvellestad, A., Dannevig, B. H., & Falk, K. (2003). Isolation and partial characterization of a novel paramyxovirus from the gills of diseased seawater-reared Atlantic salmon (*Salmon salar* L.). *Journal of General Virology*, *84*(8), 2179–2189.

Kwon, O. K., Kim, S. J., Lee, Y. M., Lee, Y. H., Bae, Y. S., Kim, J. Y., et al. (2016). Global analysis of phosphoproteome dynamics in embryonic development of zebrafish (*Danio rerio*). *Proteomics*, *16*(1), 136–149.

Langevin, C., van der Aa, L. M., Houel, A., Torhy, C., Briolat, V., Lunazzi, A., Harmache, A., Bremont, M., Levraud, J. - P., & Boudinot, P. (2013). Zebrafish ISG15 Exerts a Strong Antiviral Activity against RNA and DNA Viruses and Regulates the Interferon Response. *Journal of Virology*, *87*(18), 10025–10036.

LaStarza, M. W., Lemm, J. A., & Rice, C. M. (1994). Genetic analysis of the nsP3 region of Sindbis virus: evidence for roles in minus-strand and subgenomic RNA synthesis. *Journal of Virology*, *68*(9), 5781–91.

Latorre, I. J., Roh, M. H., Frese, K. K., Weiss, R. S., Margolis, B., & Javier, R. T. (2005).

Viral oncoprotein-induced mislocalization of select PDZ proteins disrupts tight junctions and causes polarity defects in epithelial cells. *Journal of Cell Science*, *118*(Pt 18), 4283–4293.

Lazarovici, P., & Primor, Naftali ; Loew, L. M. (1986). Purification and Pore Forming Activity of Two Hydrophobic Polypeptides from the Secretion of the Red Sea Moses Sole (*Pardachirus marmoratus*). *J Biol Chem*, *261*, 16704–13.

Lee, C. W., Chung, S. W., Bae, M. J., Song, S., Kim, S. P., & Kim, K. (2015). Peptidoglycan up-regulates CXCL8 expression via multiple pathways in monocytes/macrophages. *Biomolecules and Therapeutics*, *23*(6), 564–570.

Lee, L. E. J., Dayeh, V. R., Schirmer, K., & Bols, N. C. (2009). Applications and potential uses of fish gill cell lines: examples with RTgill-W1. *In Vitro Cellular and Developmental Biology - Animal*, 45, 127-134.

Lee, M. J., & Yaffe, M. B. (2016). Protein regulation in signal transduction. *Cold Spring Harbor Perspectives in Biology*, *8*(6), 1–20.

Lee, P. Y., Knight, R., Smit, J. M., Wilschut, J., & Griffin, D. E. (2002). A single mutation in the E2 glycoprotein important for neurovirulence influences binding of Sindbis virus to neuroblastoma cells. *Journal of Virology*, *76*(12), 6302–6310.

Lee, S. H., Peng, K. C., Lee, L. H., Pan, C. Y., H, A. L., Her, G. M., et al. (2013). Characterization of tilapia (*Oreochromis niloticus*) viperin expression, and inhibition of bacterial growth and modulation of immune-related gene expression by electrotransfer of viperin DNA into zebrafish muscle. *Veterinary Immunology and Immunopathology*, *151*(3–4), 217–228.

Leighton, I. A., Dalby, K. N., Barry Caudwell, F., Cohen, P. T. W., & Cohen, P. (1995). Comparison of the specificities of p70 S6 kinase and MAPKAP kinase-1 identifies a relatively specific substrate for p70 S6 kinase: the N-terminal kinase domain of MAPKAP kinase-1 is essential for peptide phosphorylation. *FEBS Letters*, *375*(3), 289–293.

Lemeer, S., Jopling, C., Gouw, J., Mohammed, S., Heck, A. J. R., Slijper, M., & den Hertog, J. (2008). Comparative Phosphoproteomics of Zebrafish Fyn/Yes Morpholino Knockdown Embryos. *Molecular & Cellular Proteomics*, *7*(11), 2176–2187.

Lemeer, S., Pinkse, M. W. H., Mohammed, S., Van Breukelen, B., Hertog, J. Den, Slijper, M., & Heck, A. I. R. (2008). Online automated *in vivo* zebrafish phosphoproteomics: From large-scale analysis down to a single embryo. *Journal of Proteome Research*, *7*(4), 1555–1564.

Lenschow, D. J. (2010). Antiviral properties of ISG15. *Viruses*, *2*(10), 2154–2168.

Levraud, J.-P., Langevin, C., Palha, N., Passoni, G., Boudinot, P., & Aleksejeva, E. (2013). The Antiviral Innate Immune Response in Fish: Evolution and Conservation of the IFN System. *Journal of Molecular Biology*, *425*(24), 4904–4920.

Li, R. W., & Waldbieser, G. C. (2006). Production and utilization of a high-density oligonucleotide microarray in channel catfish, *Ictalurus punctatus*. *BMC Genomics*, *7*, 1–7.

Li, H., Yang, G., Li, T., Yang, H., & An, L. (2017). Molecular characterization of a fish-specific toll-like receptor 22 (TLR22) gene from common carp (*Cyprinus carpio* L.): Evolutionary relationship and induced expression upon immune stimulants. *Fish and Shellfish Immunology*, *63*, 74–86.

Li, J. H., Chang, M. X., Xue, N. N., & Nie, P. (2013). Functional characterization of a short peptidoglycan recognition protein, PGRP5 in grass carp *Ctenopharyngodon idella*. *Fish and Shellfish Immunology*, *35*(2), 221–230.

Li, J. H., Yu, Z. L., Xue, N. N., Zou, P. F., Hu, J. Y., Nie, P. & Chang, M. X. (2014). Molecular cloning and functional characterization of peptidoglycan recognition protein 6 in grass carp *Ctenopharyngodon idella*. *Developmental and Comparative Immunology*, *42*(2), 244–255.

Li, M. O., Wan, Y. Y., Sanjabi, S., Robertson, A. -K. L., & Flavell, R. A. (2006). Transforming Growth Factor-B Regulation of Immune Responses, *Annual Review of Immunology*, *24*(1), 99–146.

Lu, L. F., Li, S., Lu, X. B., & Zhang, Y. A. (2015). Functions of the two zebrafish MAVS variants are opposite in the induction of IFN1 by targeting IRF7. *Fish and Shellfish Immunology*, 4I5(2), 574–582.

Lu, L. F., Li, S., Lu, X. B., & Zhang, Y. A. (2010). Cloning, mRNA expression, and recombinant expression of peptidoglycan recognition protein II gene from large yellow croaker (*Pseudosciaena crocea*). *Molecular Biology Reports*, *37*(8), 3897–3908.

Lieschke, G. J., & Trede, N. S. (2009). Fish immunology. *Current Biology*, *19*(16), 678–682.

Lim, P. J., & Chu, J. J. H. (2014). A Polarized Cell Model for Chikungunya Virus Infection: Entry and Egress of Virus Occurs at the Apical Domain of Polarized Cells. *PLoS Neglected Tropical Diseases*, *8*(2), e2661, 1-15.

Lindenmann, J., Lane, C.A., & Hobson, D. (1963). The resistance of A2G mice to

orthomyxoviruses. *J Immunol*, *90*, 942–951.

Liongue, C., & Ward, A. C. (2007). Evolution of Class I cytokine receptors. *BMC Evolutionary Biology*, *7*(120), 1-15.

Litchfield, D. W. (2003). Protein kinase : structure, regulation and role in cellular decisions of life and death. *Biochemical Journal*, *369*(1), 1–15.

Litwack, G. (2018). Blood and Lymphatic System, Chapter 21 of Human Biochemistry, 681-708. Elsevier Inc., Los Angeles, CA, United States.

Liu, G., Zhai, Q., Schaffner, D., Popova, T., Hayford, A., Bailey, C., & Alibek, K. (2004). Bacillus alcalophilus peptidoglycan induces IFN-α-mediated inhibition of vaccinia virus replication. *FEMS Immunology and Medical Microbiology*, *42*(2), 197–204.

Liu, Y., & Chance, M. R. (2014). Integrating phosphoproteomics in systems biology. *Computational and Structural Biotechnology Journal*, *10*(17), 90–97.

Lobigs, M., Zhao, H. X., & Garoff, H. (1990). Function of Semliki Forest virus E3 peptide in virus assembly: replacement of E3 with an artificial signal peptide abolishes spike heterodimerization and surface expression of E1. *J Virol*, *64*(9), 4346–4355.

Lockhart, K., Gahlawat, S. K., Soto-Mosquera, D., Bowden, T. J., & Ellis, A. E. (2004). IPNV carrier Atlantic salmon growers do not express Mx mRNA and poly I:C-induced Mx response does not cure the carrier state. *Fish and Shellfish Immunology*, *17*(4), 347–352.

Loegering, D. J., & Lennartz, M. R. (2011). Protein kinase C and toll-like receptor signaling. *Enzyme Research*, *2011*, 1-7.

Long, M., Zhao, J., Li, T., Tafalla, C., Zhang, Q., Wang, X., et al. (2015). Transcriptomic and proteomic analyses of splenic immune mechanisms of rainbow trout (*Oncorhynchus mykiss*) infected by *Aeromonas salmonicida* subsp. *salmonicida*. *Journal of Proteomics*, *122*, 41–54.

Long, S., Milev-Milovanovic, I., Wilson, M., Bengten, E., Clem, L. W., Miller, N. W., & V.G.Chinchar. (2006). Identification and expression analysis of interferon gamma genes in channel catfish. *Fish & Shellfish Immunology*, *21*, 42–59.

Loo, Y.-M., & Gale, M. (2012). Immune Signaling by RIG-I-like Receptors.pdf, *34*(5), 680–692.

López-Dóriga, M. V., Smail, D. A., Smith, R. J., Castric, J., Doménech, A., Smith, P. D., & Ellis, A. E. (2001). Isolation of salmon pancreas disease virus (SPDV) in cell culture and its ability to protect against infection by the "wild-type" agent. *Fish and Shellfish Immunology*, *11*(6), 505–522.

Loyer, P., Trembley, J. H., Katona, R., Kidd, V. J., & Lahti, J. M. (2005). Role of CDK / cyclin complexes in transcription and RNA splicing, *17*, 1033–1051.

Lu, X.-J., Ning, Y.-J., Liu, H., Nie, L., & Chen, J. (2018). A Novel Lipopolysaccharide Recognition Mechanism Mediated by Internalization in Teleost Macrophages. *Frontiers in Immunology*, *9*(November), 1–18.

Lucitt, M. B., Price, T. S., Pizarro, A., Wu, W., Yocum, A. K., Seiler, C., et al. (2008). Analysis of the Zebrafish Proteome during Embryonic Development. *Molecular & Cellular Proteomics*, *7*(5), 981–994.

Luo, X., Guo, L., Zhang, J., Xu, Y., Gu, W., Feng, L., & Wang, Y. (2017). Tight Junction Protein Occludin Is a Porcine Epidemic Diarrhea Virus Entry Factor. *Journal of Virology*, *91*(10), e00202-17.

Lutfalla, G., Roest Crollius, H., Stange-Thomann, N., Jaillon, O., Mogensen, K., & Monneron, D. (2003). Comparative genomic analysis reveals independent expansion of a lineage-specific gene family in vertebrates: the class II cytokine receptors and their ligands in mammals and fish. *BMC Genomics*, *4*(1), 29.

M, P. (1984). *Bergey's manual of of systematic bacteriology*. (N. R. Krieg, Ed.). Baltimore: The Williams & Wilkins Co.

Ma, X., Helgason, E., Phung, Q. T., Quan, C. L., Iyer, R. S., Lee, M. W., et al. (2012). Molecular basis of Tank-binding kinase 1 activation by transautophosphorylation. *Proceedings of the National Academy of Sciences*, *109*(24), 9378–9383.

Madrid, M., Jimenez, R., Sanchez-Mir, L., Soto, T., Franco, A., Vicente-Soler, J., et al. (2014). Multiple layers of regulation influence cell integrity control by the PKC ortholog P in fission yeast. *Journal of Cell Science*, *128*(2), 266–280.

Magi, B., Bini, L., Marzocchi, B., Liberatori, S., Raggiaschi, R., & Pallini, V. (1999). Immunoaffinity Identification of 2-DE Separated Proteins. *Methods in Molecular Biology*, *112*, 431-443.

Magnadottir, B. (2010). Immunological control of fish diseases. *Marine Biotechnology*, *12*(4), 361–379.

Mahlapuu, M., Håkansson, J., Ringstad, L., & Björn, C. (2016). Antimicrobial Peptides: An Emerging Category of Therapeutic Agents. *Frontiers in Cellular and Infection Microbiology*, *6*(194), 1–12.

Maier, V. H., Schmitt, C. N. Z., Gudmundsdottir, S., & Gudmundsson, G. H. (2008). Bacterial DNA indicated as an important inducer of fish cathelicidins. *Molecular Immunology*, *45*(8), 2352–2358.

Manning, G., Whyte, D. B., Martinez, R., Hunter, T., & Sudarsanam, S. (2002). The protein kinase complement of the human genome. *Science (New York, N.Y.), 298*, 1912-1219.

Marilyn G. Farquhar, and G. E. P. (1963). Junctional complexes in various epithelia. *The Journal of Cell Biology*, *17*, 375–412.

Martinez-Lopez, D. G., Fahey, M., & Coburn, J. (2010). Responses of human endothelial cells to pathogenic and non-pathogenic Leptospira species. *PLoS Neglected Tropical Diseases*, *4*(12), 1–11.

Masatani, T., Ito, N., Shimizu, K., Ito, Y., Nakagawa, K., Sawaki, Y., et al. (2010). Rabies Virus Nucleoprotein Functions To Evade Activation of the RIG-I-Mediated Antiviral Response. *Journal of Virology*, *84*(8), 4002–4012.

Masso-Silva, J. A., & Diamond, G. (2014). Antimicrobial peptides from fish. *Pharmaceuticals*, *7*(3), 265–310.

Matsuo, A., Oshiumi, H., Tsujita, T., Mitani, H., Kasai, H., Yoshimizu, M., Matsumoto, M., & Seya, T. (2008). Teleost TLR22 recognizes RNA duplex to induce IFN and protect cells from birnaviruses. *Journal of immunology (Baltimore, Md. : 1950)*, *181*(5), 3474–85.

Matsumoto, M., Kikkawa, S., Kohase, M., Miyake, K., & Seya, T. (2002). Establishment of a monoclonal antibody against human Toll-like receptor 3 that blocks double-stranded RNA-mediated signaling. *Biochemical and Biophysical Research Communications*, *293*(5), 1364–1369.

Maxmen, A. (2017). A billion-year arms race against viruses shaped our evolution. *Nature*, 1–3.

May, J. A., Ratan, H., Glenn, J. R., Lösche, W., Spangenberg, P., & Heptinstall, S. (1998). GPIIb-IIIa antagonists cause rapid disaggregation of platelets pre-treated with cytochalasin D. Evidence that the stability of platelet aggregates depends on normal cytoskeletal assembly. *Platelets*, *9*(3–4), 227–232.

Mayuri, Geders, T. W., Smith, J. L., & Kuhn, R. J. (2008). Role for Conserved Residues of Sindbis Virus Nonstructural Protein 2 Methyltransferase-Like Domain in Regulation of Minus-Strand Synthesis and Development of Cytopathic Infection. *Journal of Virology*, *82*(15), 7284–7297.

McCarthy, K. M., Skare, I. B., Stankewich, M. C., Furuse, M., Tsukita, S., Rogers, R. A., Lynch, R. D., & Schneeberger, E. E. (1996). Occludin is a functional component of the tight junction. *Journal of cell science*, *109*, 2287-2298.

McGinnis, S., & Madden, T. L. (2004). BLAST: At the core of a powerful and diverse set of sequence analysis tools. *Nucleic Acids Research*, *32*(W20-W25).

McKee, R., Gerlach, G. F., Jou, J., Cheng, C. N., & Wingert, R. A. (2014). Temporal and spatial expression of tight junction genes during zebrafish pronephros development. *Gene Expression Patterns*, *16*(2), 104–113.

McLoughlin, M. F., & Graham, D. A. (2007). Alphavirus infections in salmonids - A review. *Journal of Fish Diseases*, *30*(9), 511–531.

McNab, F., Mayer-Barber, K., Sher, A., Wack, A., & O'Garra, A. (2015). Type I interferons in infectious disease. *Nat Rev Immunol*, *15*(2), 87–103.

Mehta, D. R., Ashkar, A. A., & Mossman, K. L. (2012). The nitric oxide pathway provides innate antiviral protection in conjunction with the type I interferon pathway in fibroblasts. *PLoS ONE*, *7*(2). e31688, 1-12.

Merien, F., Baranton, g., & perolat, p. (1997). Invasion of Vero Cells and Induction of Apoptosis in Macrophages by Pathogenic Leptospira interrogans Are Correlated with Virulence. *Infection and Immunity*, *65*(2), 729–738.

Meyer, F. (2016). Viral interactions with components of the splicing machinery. In *Progress in Molecular Biology and Translational Science*, *142*(241–268).

Meyer, F. P. (1991). Aquaculture disease and health management. *Journal of Animal Science*, *69*, 4201-4208.

Meylan, E., Curran, J., Hofmann, K., Moradpour, D., Binder, M., Bartenschlager, R., & Tschopp, J. (2005). Cardif is an adaptor protein in the RIG-I antiviral pathway and is targeted by hepatitis C virus. *Nature Letters*, *437*(7062), 1167–1172.

Meylan, E., Tschopp, J., & Karin, M. (2006). Intracellular pattern recognition receptors in the host response. *Nature*, *442*(7098), 39–44.

Mikkelsen, S. S., Jensen, S. B., Chiliveru, S., Melchjorsen, J., Julkunen, I., Gaestel, M., et al. (2009). RIG-I-mediated activation of p38 MAPK is essential for viral induction of interferon and activation of dendritic cells. Dependence on TRAF2 and TAK1. *Journal of Biological Chemistry*, *284*(16), 10774–10782.

Mistri, A., Kumari, U., Mittal, S., & Mittal, A. K. (2018). Immunohistochemical localization of nitric oxide synthase (NOS) isoforms in epidermis and gill epithelium of an angler catfish, Chaca chaca (Siluriformes, Chacidae). *Tissue and Cell*, *55*(September), 25–30.

Monte, M. M., Wang, T., Holland, J. W., Zou, J., & Secombes, C. J. (2013). Cloning and characterization of rainbow trout interleukin-17A/F2 (IL-17A/F2) and IL-17 receptor

a: Expression during infection and bioactivity of recombinant IL-17A/F2. *Infection and Immunity*, *81*(1), 340–353.

Montoya, A., Beltran, L., Casado, P., Rodríguez-Prados, J. C., & Cutillas, P. R. (2011). Characterization of a TiO_2 enrichment method for label-free quantitative phosphoproteomics. *Methods*, *54*(4), 370–378.

Mookherjee, N., Brown, K. L., Bowdish, D. M. E., Doria, S., Falsafi, R., Hokamp, K., et al. (2006). Modulation of the TLR-Mediated Inflammatory Response by the Endogenous Human Host Defense Peptide LL-37. *The Journal of Immunology*, *176*(4), 2455–2464.

Moore, J. D., Ototake, M., & Nakanishi, T. (1998). Particulate antigen uptake during immersion immunisation of fish: The effectiveness of prolonged exposure and the roles of skin and gill. *Fish & Shellfish Immunology*, *8*(6), 393–407.

Mukherjee, K., Korithoski, B., & Kolaczkowski, B. (2014). Ancient origins of vertebrate-specific innate antiviral immunity. *Molecular Biology and Evolution*, *31*(1), 140–153.

Munford, R. S., & Varley, A. W. (2006). Shield as Signal: Lipopolysaccharides and the Evolution of Immunity to Gram-Negative Bacteria. *PLoS Pathogens*, *2*(6), e67.

Munro, A. L. S., & Hastings, T. S. (1993). Furunculosis. In: Inglis V, Roberts, RJ, Bromage, NR (eds.) Bacterial diseases of fish, pp 122-142. Blackwell Scientific Publishers, London.

Najakshin, A. M., Mechetina, L. V., Alabyev, B. Y., & Taranin, A. V. (1999). Identification of an IL-8 homolog in lamprey (*Lampetra fluviatilis*): Early evolutionary divergence of chemokines. *European Journal of Immunology*, *29*(2), 375–382.

Neumann, N. F., Fagan, D., & Belosevic, M. (1995). Macrophage activating factor(s) secreted by mitogen stimulated goldfish kidney leukocytes synergize with bacterial lipopolysaccharide to induce nitric oxide production in teleost macrophages. *Developmental and Comparative Immunology*, *19*(6), 473–482.

Newman, R. H., Zhang, J., & Zhu, H. (2014). Toward a systems-level view of dynamic phosphorylation networks. *Frontiers in Genetics*, *5*(AUG), 1–22.

Nie, L., Zhang, Y. sheng, Dong, W. ren, Xiang, L. xin, & Shao, J. zhong. (2015). Involvement of zebrafish RIG-I in NF-κB and IFN signaling pathways: Insights into functional conservation of RIG-I in antiviral innate immunity. *Developmental and Comparative Immunology*, *48*(1), 95–101.

Nitta, Y., Ding, P., & Zhang, Y. (2014). Identification of additional MAP kinases activated

upon PAMP treatment. *Plant Signaling and Behavior*, *9*(11), e976155-1-e976155-3.

Nygaard, R., Husgard, S., Sommer, A. I., Leong, J.-A. A., & Robertsen, B. (2000). Induction of Mx protein by interferon and double-stranded RNA in salmonid cells. *Fish & Shellfish Immunology*, *10*(5), 435–450.

O'Shea, J. P., Chou, M. F., Quader, S. A., Ryan, J. K., Church, G. M., & Schwartz, D. (2013). PLogo: A probabilistic approach to visualizing sequence motifs. *Nature Methods*, *10*(12), 1211–1212.

Ohtani, M., Hikima, J. ichi, Kondo, H., Hirono, I., Jung, T. S., & Aoki, T. (2011). Characterization and antiviral function of a cytosolic sensor gene, MDA5, in Japanese flounder, *Paralichthys olivaceus*. *Developmental and Comparative Immunology*, *35*(5), 554–562.

OIE. (2018). Infection with salmonid alphavirus. *OIE Aquatic Animal Disease Cards*, 1–14.

Olsen, J. V., Blagoev, B., Gnad, F., Macek, B., Kumar, C., Mortensen, P., & Mann, M. (2006). Global, In Vivo, and Site-Specific Phosphorylation Dynamics in Signaling Networks. *Cell*, *127*(3), 635–648.

Onyiah, J. C., & Colgan, S. P. (2016). Cytokine responses and epithelial function in the intestinal mucosa. *Cellular and Molecular Life Sciences*, 73(22), 4203-4212.

Ortega-Villaizan, M., Chico, V., Falco, A., Perez, L., Coll, J. M., & Estepa, A. (2009). The rainbow trout TLR9 gene and its role in the immune responses elicited by a plasmid encoding the glycoprotein G of the viral haemorrhagic septicaemia rhabdovirus (VHSV). *Molecular Immunology*, *46*(8-9), 1710-1717.

Oshiumi, H., Tsujita, T., Shida, K., Matsumoto, M., Ikeo, K., & Seya, T. (2003). Prediction of the prototype of the human Toll-like receptor gene family from the pufferfish, *Fugu rubripes*, genome. *Immunogenetics*, *54*(11), 791–800.

Palti, Y. (2011). Toll-like receptors in bony fish: From genomics to function. *Developmental and Comparative Immunology*, *35*(12), 1263–1272.

Palti, Y., Rodriguez, M. F., Gahr, S. A., Purcell, M. K., Rexroad, C. E., & Wiens, G. D. (2010). Identification, characterization and genetic mapping of TLR1 loci in rainbow trout (*Oncorhynchus mykiss*). *Fish and Shellfish Immunology*, *28*(5-6), 918-926.

Palzenberger, M., & Pohla, H. (1992). Gill surface area of water-breathing freshwater fish. *Reviews in Fish Biology and Fisheries*, *2*(3), 187–216.

Pankiv, S., Clausen, T. H., Lamark, T., Brech, A., Bruun, J. A., Outzen, H., Øvervatn, A., Bjørkøy, G., & Johansen, T. (2007). p62/SQSTM1 Binds Directly to Atg8/LC3 to

Facilitate Degradation of Ubiquitinated Protein Aggregates by Autophagy. Journal of Biological Chemistry, 282(33), 24131-24145.

Part, P., Norrgren, L., Bergstrom, E., & Sjoberg, P. (1993). Primary Cultures of Epithelial Cells From Rainbow Trout Gills, *232*, 219–232.

Pearce, L. R., Komander, D., & Alessi, D. R. (2010). The nuts and bolts of AGC protein kinases. *Nature Reviews Molecular Cell Biology*, *11*(1), 9–22.

Pearson, R. B., & Kemp, B. E. (1991). Protein Kinase Phosphorylation Site Sequences and Consensus Specificity Motifs: Tabulations. *Methods in Enzymology*, *200*, 62–81.

Pearson, W. R. (2014). An Introduction to Sequence Similarity ("Homology ") Searching. *Current Protocols in Bioinformatics*, 1–9.

Phelan, P. E., Mellon, M. T., & Kim, C. H. (2005). Functional characterization of full-length TLR3, IRAK-4, and TRAF6 in zebrafish (Danio rerio). *Molecular Immunology*, *42*(9), 1057–1071.

Pinna, L. A., & Ruzzene, M. (1996). How do protein kinases recognize their substrates? *Biochimica et Biophysica Acta - Molecular Cell Research*, *1314*(3), 191–255.

Plant, K. P., Harbottle, H., & Thune, R. L. (2005). Poly I:C induces an antiviral state against Ictalurid Herpesvirus 1 and Mx1 transcription in the channel catfish (*Ictalurus punctatus*). *Developmental and Comparative Immunology*, *29*(7), 627–635.

Plant, K. P., & Thune, R. L. (2004). Cloning and characterisation of a channel catfish (*Ictalurus punctatus*) Mx gene. *Fish & Shellfish Immunology*, *16*(3), 391–405.

Platanias, L. C. (2005). Mechanisms of type-I- and type-II-interferon-mediated signalling. *Nature Reviews Immunology*, *5*(5), 375–386.

Plotnikov, A., Zehorai, E., Procaccia, S., & Seger, R. (2011). The MAPK cascades: Signaling components, nuclear roles and mechanisms of nuclear translocation. *Biochimica et Biophysica Acta - Molecular Cell Research*, *1813*(9), 1619–1633.

Poltorak A, He X, Smirnova I, Liu MY, Van Huffel C, Du X, et al. (1998). Defective LPS signaling in C3H/HeJ and C57BL/10ScCr mice: mutations in Tlr4 gene. *Science*, *282*(5396), 2085–2088.

Powell, D. W. (1981). Barrier function of epithelia. *The American Journal of Physiology*, *241*(4), G275–G288. Retrieved from

Poynter, S. J., Weleff, J., Soares, A. B., & DeWitte-Orr, S. J. (2015b). Class-A scavenger receptor function and expression in the rainbow trout (*Oncorhynchus mykiss*) epithelial cell lines RTgutGC and RTgill-W1. *Fish and Shellfish Immunology*, *44*(1), 138–146.

Prasanth, K. V., Prasanth, S. G., Xuan, Z., Hearn, S., Freier, S. M., Bennett, C. F., et al. (2005). Regulating gene expression through RNA nuclear retention. *Cell*, *123*(2), 249–263.

Pratte, Z. A., Besson, M., Hollman, R. D., & Stewarta, F. J. (2018). The Gills of Reef Fish Support a Distinct Microbiome Influenced by Host-Specific Factors. *Applied and Environmental Microbiology*, *84*(9), 1-15.

Purcell, M. K., Kurath, G., Garver, K. A., Herwig, R. P., & Winton, J. R. (2004). Quantitative expression profiling of immune response genes in rainbow trout following infectious haematopoietic necrosis virus (IHNV) infection or DNA vaccination. *Fish and Shellfish Immunology*, *17*(5), 447–462.

Purcell, M. K., Marjara, I. S., Batts, W., Kurath, G., & Hansen, J. D. (2011). Transcriptome analysis of rainbow trout infected with high and low virulence strains of Infectious hematopoietic necrosis virus. *Fish and Shellfish Immunology*, *30*(1), 84–93.

Puttinaowarat, S., Thompson, K.D., & Adams, A. (2000). Mycobacteriosis: detection and identification of aquatic *Mycobacterium* species. Fish Veterinary Journal, *5*, 6- 21.

Qian, T., Wang, K., Mu, Y., Ao, J., & Chen, X. (2013). Molecular characterization and expression analysis of TLR 7 and TLR 8 homologs in large yellow croaker (*Pseudosciaena crocea*). *Fish and Shellfish Immunology*, 35(3), 671-679.

Racioppi, L., & Means, A. R. (2012). Calcium/calmodulin-dependent protein kinase kinase 2: Roles in signaling and pathophysiology. *Journal of Biological Chemistry*, *287*(38), 31658–31665.

Rajendran, K. V., Zhang, J., Liu, S., Peatman, E., Kucuktas, H., Wang, X., et al. (2012). Pathogen recognition receptors in channel catfish: II. Identification, phylogeny and expression of retinoic acid-inducible gene I (RIG-I)-like receptors (RLRs). *Developmental and Comparative Immunology*, *37*(3–4), 381–389.

Rakers, S., Niklasson, L., Steinhagen, D., Kruse, C., Schauber, J., Sundell, K., & Paus, R. (2013). Antimicrobial peptides (AMPs) from fish epidermis: Perspectives for investigative dermatology. *Journal of Investigative Dermatology*, *133*(5), 1140–1149.

Rebl, A., Goldammer, T., & Seyfert, H.-M. (2010). Toll-like receptor signaling in bony fish. *Veterinary Immunology and Immunopathology*, *134*(3–4), 139–50.

Rebl, A., Korytář, T., Köbis, J. M., Verleih, M., Krasnov, A., Jaros, J., et al. (2014). Transcriptome Profiling Reveals Insight into Distinct Immune Responses to *Aeromonas salmonicida* in Gill of Two Rainbow Trout Strains. *Marine*

Biotechnology, *16*(3), 333–348.

Rebouças, E. de. L., Costa, J. J. do. N., Passos, M. J., Passos, J. R. de S., Hurk, R. van den S., & José, R. V. (2013). Real Time PCR and Importance of Housekeeping Genes for Normalization and Quantification of mRNA Expression in Different Tissues. *Brazilian Archives of Biology and Technology*, *56*(1), 143-154.

Reikine, S., Nguyen, J. B., & Modis, Y. (2014). Pattern recognition and signaling mechanisms of RIG-I and MDA5. *Frontiers in Immunology*, *5*(JUL).

Reiland, S., Messerli, G., Baerenfaller, K., Gerrits, B., Endler, A., Grossmann, J., et al. (2009). Large-Scale Arabidopsis Phosphoproteome Profiling Reveals Novel Chloroplast Kinase Substrates and Phosphorylation Networks. *Plant Physiology*, *150*(2), 889–903.

Rendell, J. L., Fowler, S., Cockshutt, A., & Currie, S. (2006). Development-dependent differences in intracellular localization of stress proteins (hsps) in rainbow trout, Oncorhynchus mykiss, following heat shock. *Comparative Biochemistry and Physiology - Part D: Genomics and Proteomics*, *1*(2), 238-252.

Reyes-Cerpa, S., Maisey, K., Reyes-Lpez, F., Toro-Ascuy, D., Mara, A., & Imarai, M. (2012). Fish Cytokines and Immune Response. *New Advances and Contributions to Fish Biology*, 3–58.

Riabi, S., Harrath, R., Gaaloul, I., Bouslama, L., Nasri, D., Aouni, M., et al. (2014). Study of Coxsackie B viruses interactions with Coxsackie Adenovirus receptor and Decay-Accelerating Factor using Human CaCo-2 cell line. *Journal of Biomedical Science*, *21*(1), 1–9.

Ribeiro, C. M. S., Hermsen, T., Taverne-Thiele, A. J., Savelkoul, H. F. J., & Wiegertjes, G. F. (2010). Evolution of recognition of ligands from Gram-positive bacteria: similarities and differences in the TLR2-mediated response between mammalian vertebrates and teleost fish. *Journal of Immunology (Baltimore, Md. : 1950)*, *184*(5), 2355–68.

Ritter, M., Mennerich, D., Weith, A., & Seither, P. (2005). Characterization of Toll-like receptors in primary lung epithelial cells: strong impact of the TLR3 ligand poly(I:C) on the regulation of Toll-like receptors, adaptor proteins and inflammatory response. *Journal of inflammation*, *2*(16), 1-25.

Robertsen, B. (2006). The interferon system of teleost fish. *Fish and Shellfish Immunology*, *20*(2), 172–191.

Robertsen, B. (2008). Expression of interferon and interferon-induced genes in salmonids

in response to virus infection, interferon-inducing compounds and vaccination. *Fish and Shellfish Immunology*, *25*(4), 351–357.

Robertsen, B., Bergan, V., Røkenes, T., Larsen, R., & Albuquerque, A. (2003). Atlantic salmon interferon genes: cloning, sequence analysis, expression, and biological activity. *Journal of Interferon & Cytokine Research : The Official Journal of the International Society for Interferon and Cytokine Research*, *23*(10), 601–612.

Robertsen, B., Trobridge, G., & Leong, J.-A. (1997). Molecular cloning of double stranded RNA inducible mx genes from atlantic salmon (*saimo salar* L.). *Developmental & Comparative Immunology*, *21*(5), 397–412.

Rodriguez, M. F., Wiens, G. D., Purcell, M. K., & Palti, Y. (2005). Characterization of Toll-like receptor 3 gene in rainbow trout (*Oncorhynchus mykiss*). *Immunogenetics*, *57*(7), 510–519.

Rodríguez Pulido, M., & Sáiz, M. (2017). Molecular Mechanisms of Foot-and-Mouth Disease Virus Targeting the Host Antiviral Response. *Frontiers in Cellular and Infection Microbiology*, *7*(252), 1–9.

Roher, N., Callol, A., Planas, J. V, Goetz, F. W., & MacKenzie, S. a. (2011). Endotoxin recognition in fish results in inflammatory cytokine secretion not gene expression. *Innate Immunity*, *17*(1), 16–28.

Røkenes, T. P., Larsen, R., & Robertsen, B. (2007). Atlantic salmon ISG15: Expression and conjugation to cellular proteins in response to interferon, double-stranded RNA and virus infections. *Molecular Immunology*, *44*(5), 950–959.

Rossi, A. G., Sawatzky, D. A., Walker, A., Ward, C., Sheldrake, T. A., Riley, N. A., et al. (2006). Cyclin-dependent kinase inhibitors enhance the resolution of inflammation by promoting inflammatory cell apoptosis. *Nature Medicine*, *12*(9), 1056–1064.

Rothenburg, S., Deigendesch, N., Dittmar, K., Koch-Nolte, F., Haag, F., Lowenhaupt, K., & Rich, A. (2005). A PKR-like eukaryotic initiation factor 2alpha kinase from zebrafish contains Z-DNA binding domains instead of dsRNA binding domains. *Proceedings of the National Academy of Sciences of the United States of America*, *102*(5), 1602–7.

Rothenfusser, S., Goutagny, N., DiPerna, G., Gong, M., Monks, B. G., Schoenemeyer, A., et al. (2005). The RNA Helicase Lgp2 Inhibits TLR-Independent Sensing of Viral Replication by Retinoic Acid-Inducible Gene-I. *The Journal of Immunology*, *175*(8), 5260–5268.

Roussel, A., Lescar, J., Vaney, M. C., Wengler, G., Wengler, G., & Rey, F. A. (2006).

Structure and interactions at the viral surface of the envelope protein E1 of semliki forest virus. *Structure*, *14*(1), 75–86.

Saint-Jean, S. R., & Pérez-Prieto, S. I. (2006). Interferon mediated antiviral activity against salmonid fish viruses in BF-2 and other cell lines. *Veterinary Immunology and Immunopathology*, *110*(1–2), 1–10.

Sandbichler, A. M., Egg, M., Schwerte, T., & Pelster, B. (2011). Claudin 28b and F-actin are involved in rainbow trout gill pavement cell tight junction remodeling under osmotic stress. *The Journal of Experimental Biology*, *214*, 1473–1487.

Sangrador-Vegas, A., Lennington, J. B., & Smith, T. J. (2002). Molecular cloning of an IL-8-like CXC chemokine and tissue factor in rainbow trout (Oncorhynchus mykiss) by use of suppression subtractive hybridization. *Cytokine*, *17*(2), 66–70.

Sanz, M. A., Pbrezs, L., & Carrasco, L. (1994). Semliki Forest Virus 6K Protein Modifies Membrane Permeability. *Biochemistry*, *269*(16), 12106–12110.

Satoh, T., Kato, H., Kumagai, Y., Yoneyama, M., Sato, S., Matsushita, K., et al. (2010). LGP2 is a positive regulator of RIG-I- and MDA5-mediated antiviral responses. *Proceedings of the National Academy of Sciences*, *107*(4), 1512–1517.

Sausville, E. A. (2002). Complexities in the development of cyclin-dependent kinase inhibitor drugs. *Trends in Molecular Medicine*, *8*(4 Suppl.), 32–37.

Sayed, M., Pelech, S., Wong, C., Marotta, A., & Salh, B. (2001). Protein kinase is involved in G2 arrest and apoptosis following spindle damage in epithelial cells. *Oncogene*, *20*(48), 6994–7005.

Schlee, M. (2013). Master sensors of pathogenic RNA - RIG-I like receptors. *Immunobiology*, *218*(11), 1322–1335.

Schachte, J. H. (1983). Bacterial gill disease. In: Meyer, F. P., Warren, J. W., Carey, T. G., eds. A guide to integrated fish health management in the Great Lakes Basin. Ann Arbor, Michigan, USA: *Great Lakes Fishery Commission*, Special Publication 83-2, 181-184.

Schliwa, M. (1982). Action of Cytochalasin D on Cytoskeletal Networks H. *The Journal of Cell Biology*, *92*, 79–91.

Schmidt-Posthaus, H., Diserens, N., Hjortaas, M. J., Knüsel, R., Hirschi, R., & Taksdal, T. (2014). First outbreak of sleeping disease in Switzerland: Disease signs and virus characterization. *Diseases of Aquatic Organisms*, *111*(2), 165–171.

Schulz, K. S., & Mossman, K. L. (2016). Viral evasion strategies in type I IFN signaling - A summary of recent developments. *Frontiers in Immunology*, *7*(NOV), 1–10.

Schwartz, D., & Gygi, S. P. (2005). An iterative statistical approach to the identification of protein phosphorylation motifs from large-scale data sets. *Nature Biotechnology*, *23*(11), 1391–1398.

Secombes, C. J., Hardie, L. J., & Daniels, G. (1996). Cytokines in fish: an update. *Fish & Shellfish Immunology*, *6*(4), 291–304.

Sen, G. C. (2001). Viruses and Interferons. *Annu. Rev. Microbiol.*, *55*, 255–281.

Seo, J. Y., Yaneva, R., Hinson, E. R., & Cresswell, P. (2011). Human cytomegalovirus directly induces the antiviral protein viperin to enhance infectivity. *Science*, *332*(6033), 1093–1097.

Seppola, M., Stenvik, J., Steiro, K., Solstad, T., Robertsen, B., & Jensen, I. (2007). Sequence and expression analysis of an interferon stimulated gene (ISG15) from Atlantic cod (*Gadus morhua* L.). *Developmental and Comparative Immunology*, *31*(2), 156–171.

Sepulcre, M. P., Alcaraz-Perez, F., Lopez-Munoz, A., Roca, F. J., Meseguer, J., Cayuela, M. L., & Mulero, V. (2009). Evolution of Lipopolysaccharide (LPS) Recognition and Signaling: Fish TLR4 Does Not Recognize LPS and Negatively Regulates NF- B Activation. *The Journal of Immunology*, *182*(4), 1836–1845.

Seth, R. B., Sun, L., & Chen, Z. J. (2006). Antiviral innate immunity pathways. *Cell Research*, *16*(2), 141–147.

Seth, R. B., Sun, L., Ea, C. K., & Chen, Z. J. (2005). Identification and characterization of MAVS, a mitochondrial antiviral signaling protein that activates NF-κB and IRF3. *Cell*, *122*(5), 669–682.

Severa, M., Coccia, E. M., & Fitzgerald, K. A. (2006). Toll-like receptor-dependent and -independent Viperin gene expression and counter-regulation by PRDI-binding factor-1/BLIMP1. *Journal of Biological Chemistry*, *281*(36), 26188–26195.

Shahsavarani, A, McNeill, B., Galvez, F., Wood, C. M., Goss, G. G., Hwang, P.-P., & Perry, S. F. (2006). Characterization of a branchial epithelial calcium channel (ECaC) in freshwater rainbow trout (*Oncorhynchus mykiss*). *The Journal of Experimental Biology*, *209*, 1928–1943.

Sheth, P., Delos Santos, N., Seth, A., LaRusso, N. F., & Rao, R. K. (2007). Lipopolysaccharide disrupts tight junctions in cholangiocyte monolayers by a c-Src-, TLR4-, and LBP-dependent mechanism. *AJP: Gastrointestinal and Liver Physiology*, *293*(1), G308–G318.

Shimazu, R., Akashi, S., Ogata, H., Nagai, Y., Fukudome, K., Miyake, K., & Kimoto, M.

(1999). MD-2, a molecule that confers lipopolysaccharide responsiveness on Toll-like receptor 4. *The Journal of Experimental Medicine*, *189*(11), 1777–82.

Shrivastav, M., & Niewold, T. B. (2013). Nucleic acid sensors and type I interferon production in systemic lupus erythematosus. *Frontiers in Immunology*, *4*(319), 1–10.

Silva, A.M., Whitmore, M., Xu, Z., Jiang, Z., Li, X., & Williams, B. R. G. (2004). Protein Kinase R (PKR) Interacts with and Activates Mitogen-activated Protein Kinase Kinase 6 (MKK6) in Response to Double-stranded RNA Stimulation. *Journal of Biological Chemistry*, *279*(36), 37670–37676.

Smrzlic, I. V., Kapetanovic, D., Valic, D., Teskeredzic, E., Mcloughlin, M. F., & Fringuelli, E. (2013). First laboratory confirmation of sleeping disease virus (SDV) in Croatia, *33*(3), 78–83.

Solem, S. T., Jorgensen, J. B., & Robertsen, B. (1995). Stimulation of respiratory burst and phagocytic activity in Atlantic salmon (*Salmo salar* L.) macrophages by lipopolysaccharide. *Fish & Shellfish Immunology*, *5*, 475–491.

Solnestam, B. W., Stranneheim, H., Hällman, J., Käller, M., Lundberg, E., Lundeberg, J., & Akan, P. (2012). Comparison of total and cytoplasmic mRNA reveals global regulation by nuclear retention and miRNAs. *BMC Genomics*, *13*(1), 1-9.

Solstad, T., Stenvik, J., & Jørgensen, T. (2007). mRNA expression patterns of the BPI/LBP molecule in the Atlantic cod (*Gadus morhua* L.). *Fish and Shellfish Immunology*, *23*(2), 260–271.

Song, F., Hu, Y., Wang, Y., Smith, D. E., & Jiang, H. (2018). Functional characterization of human peptide/histidine transporter 1 in stably transfected MDCK cells. *Molecular Pharmaceutics*, *15*(2), 385-393.

Srinivasan, B., Kolli, A. R., Esch, M. B., Abaci, H. E., Michael Shuler, L., & Hickman, J. J. (2016). TEER measurement techniques for in vitro barrier model systems (Vol. 20).

Stachura, D. L., Svoboda, O., Campbell, C. A., Espín-Palazón, R., Lau, R. P., Zon, L. I., et al. (2013). The zebrafish granulocyte colony-stimulating factors (Gcsfs): 2 Paralogous cytokines and their roles in hematopoietic development and maintenance. *Blood*, *122*(24), 3918–3928.

Staeheli, P., Yu, Y. X., Grob, R., & Haller, O. (1989). A double-stranded RNA-inducible fish gene homologous to the murine influenza virus resistance gene Mx. *Molecular and Cellular Biology*, *9*(7), 3117–3121.

Stanley, A. C., & Lacy, P. (2010). Pathways for Cytokine Secretion. *Physiology*, *25*(4), 218–229.

Stentiford, G. D., Sritunyalucksana, K., Flegel, T. W., Williams, B. A. P., Withyachumnarnkul, B., Itsathitphaisarn, O., & Bass, D. (2018). Tilapia lake virus threatens tilapiines farming and food security: Socio-economic challenges and preventive measures in Sub-Saharan Africa. *Aquaculture, 493*, 123-129

Stevenson, B. R., Siliciano, J. D., Mooseker, M. S., & Goodenough, D. A. (1986). Identification of ZO-1: A high molecular weight polypeptide associated with the tight junction (Zonula Occludens) in a variety of epithelia. *Journal of Cell Biology*, *103*(3), 755–766.

Su, J., Huang, T., Dong, J., Heng, J., Zhang, R., & Peng, L. (2010). Molecular cloning and immune responsive expression of MDA5 gene, a pivotal member of the RLR gene family from grass carp *Ctenopharyngodon idella*. *Fish and Shellfish Immunology*, *28*(4), 712–718.

Su, J., Jang, S., Yang, C., Wang, Y., & Zhu, Z. (2009). Genomic organization and expression analysis of Toll-like receptor 3 in grass carp (*Ctenopharyngodon idella*). *Fish and Shellfish Immunology*, *27*(3), 433–439.

Su, J., Zhu, Z., & Wang, Y. (2008). Molecular cloning, characterization and expression analysis of the PKZ gene in rare minnow *Gobiocypris rarus*. *Fish and Shellfish Immunology*, *25*(1–2), 106–113.

Sugiyama, N., Nakagami, H., Mochida, K., Daudi, A., Tomita, M., Shirasu, K., & Ishihama, Y. (2008). Large-scale phosphorylation mapping reveals the extent of tyrosine phosphorylation in Arabidopsis. *Molecular Systems Biology*, *4*(193).

Sun, B. J., & Nie, P. (2004). Molecular cloning of the viperin gene and its promoter region from the mandarin fish Siniperca chuatsi. *Veterinary Immunology and Immunopathology*, *101*(3–4), 161–170.

Sun, B., Skjaeveland, I., Svingerud, T., Zou, J., Jorgensen, J., & Robertsen, B. (2011). Antiviral Activity of Salmonid Gamma Interferon against Infectious Pancreatic Necrosis Virus and Salmonid Alphavirus and Its Dependency on Type I Interferon. *Journal of Virology*, *85*(17), 9188–9198.

Sun, F., Zhang, Y.-B., Liu, T.-K., Shi, J., Wang, B., & Gui, J.-F. (2011). Fish MITA Serves as a Mediator for Distinct Fish IFN Gene Activation Dependent on IRF3 or IRF7. *The Journal of Immunology*, *187*(5), 2531–2539.

Sun, Z., Ren, H., Liu, Y., Teeling, J. L., & Gu, J. (2011). Phosphorylation of RIG-I by Casein Kinase II Inhibits Its Antiviral Response. *Journal of Virology*, *85*(2), 1036–1047.

Sundaram, M. (2006). RTK/Ras/MAPK signaling. *WormBook*, ed. The *C. elegans* Research Community, WormBook.

Suzuki, M., Hisamatsu, T., & Podolsky, D. (2003). Gamma interferon augments the intracellular pathway for lipopolysaccharide (LPS) recognition in human intestinal epithelial cells through coordinated up-regulation. *Infection and Immunity*, *71*(6), 3503–3511.

Svensson, L., Finlay, B. B., Bass, D., von Bonsdorff, C. H., & Greenberg, H. B. (1991). Symmetric infection of rotavirus on polarized human intestinal epithelial (Caco-2) cells. *Journal of Virology*, *65*(8), 4190–7.

Svendsen, Y. S., Dalmo, R. A., & Bögwaldt, J. (1999). Tissue localization of Aeromonas salmonicida in Atlantic salmon, *Salmo salar* L., following experimental challenge. *Journal of Fish Disease*, *22*, 125-131.

Svingerud, T., Solstad, T., Sun, B., Nyrud, M. L. J., Kileng, O., Greiner-Tollersrud, L., & Robertsen, B. (2012). Atlantic Salmon Type I IFN Subtypes Show Differences in Antiviral Activity and Cell-Dependent Expression: Evidence for High IFNb/IFNc-Producing Cells in Fish Lymphoid Tissues. *The Journal of Immunology*, *189*(12), 5912–5923.

Tafalla, C., Figueras, A., & Novoa, B. (1999). Role of nitric oxide on the replication of viral haemorrhagic septicemia virus (VHSV), a fish rhabdovirus. *Veterinary Immunology and Immunopathology*, *72*(3–4), 249–256.

Tafalla, C., Figueras, A., & Novoa, B. (2001). Viral hemorrhagic septicemia virus alters turbot Scophthalmus maximus macrophage nitric oxide production. *Diseases of Aquatic Organisms*, *47*(2), 101–107.

Takami, I., Kwon, S. R., Nishizawa, T., & Yoshimizu, M. (2010). Protection of Japanese flounder Paralichthys olivaceus from viral hemorrhagic septicemia (VHS) by Poly(I:C) immunization. *Diseases of Aquatic Organisms*, *89*(2), 109–115.

Taylor, P. R., Brown, G. D., Herre, J., Williams, D. L., Willment, J. A., & Gordon, S. (2004). The Role of SIGNR1 and the -Glucan Receptor (Dectin-1) in the Nonopsonic Recognition of Yeast by Specific Macrophages. *The Journal of Immunology*, *172*(2), 1157–1162.

Teng, T. S., Foo, S. S., Simamarta, D., Lum, F. M., Teo, T. H., Lulla, A., et al. (2012). Viperin restricts chikungunya virus replication and pathology. *Journal of Clinical Investigation*, *122*(12), 4447–4460.

Tervonen, T. A., Partanen, J. I., Saarikoski, S. T., Myllynen, M., Marques, E., Paasonen,

K., et al. (2011). Faulty epithelial polarity genes and cancer. *Advances in Cancer Research*, *111*, 97-161.

Tipsmark, C. K., & Madsen, S. S. (2003). Regulation of Na + / K + -ATPase activity by nitric oxide in the kidney and gill of the brown trout (*Salmo trutta*), 1503–1510.

The World Bank, 2013. Fish to 2030: Prospects for fisheries and aquaculture (No. 83177). The World Bank.

Thwaite, R., Ji, J., Torrealba, D., Coll, J., Sabés, M., Villaverde, A., Roher, N. (2018). Protein nanoparticles made of recombinant viral antigens: A promising biomaterial for oral delivery of Fish Prophylactics. *Frontiers in Immunology*, *9*(1652), 1-12.

Torati, L. S., Migaud, H., Doherty, M. K., Siwy, J., Mullen, W., Mesquita, P. E. C., & Albalat, A. (2017). Comparative proteome and peptidome analysis of the cephalic fluid secreted by Arapaima gigas (Teleostei: Osteoglossidae) during and outside parental care. *PLoS ONE*, *12*(10), 1–20.

Torres-Flores, J. M., & Arias, C. F. (2015). Tight Junctions Go Viral! *Viruses*, *7*(9), 5145-5154

Tort, L., Balasch, J. C., & Mackenzie, S. (2003). Fish immune system. A crossroads between innate and adaptive responses. *Immunologia*, *22*, 277–286.

Trask, H. W., Cowper-Sal-lari, R., Sartor, M. A., Gui, J., Heath, C. V., Renuka, J., et al. (2009). Microarray analysis of cytoplasmic versus whole cell RNA reveals a considerable number of missed and false positive mRNAs. *Rna*, *15*(10), 1917–1928.

Trobridge, G. D., Chiou, P. P., & Leong, J. a. (1997). Cloning of the rainbow trout (*Oncorhynchus mykiss*) Mx2 and Mx3 cDNAs and characterization of trout Mx protein expression in salmon cells. *Journal of Virology*, *71*(7), 5304–5311.

Trubitt, R. T., Rabeneck, D. B., Bujak, J. K., Bossus, M. C., Madsen, S. S., & Tipsmark, C. K. (2015). Transepithelial resistance and claudin expression in trout RTgill-W1 cell line: Effects of osmoregulatory hormones. *Comparative Biochemistry and Physiology Part A: Molecular & Integrative Physiology*, *182*, 45–52.

Tsan, M.-F., & Gao, B. (2009). Heat shock proteins and immune system. *Journal of Leukocyte Biology*, 85(6), 905-910.

Uzzell, T., Stolzenberg, E. D., Shinnar, A. E., & Zasloff, M. (2003). Hagfish intestinal antimicrobial peptides are ancient cathelicidins. *Peptides*, *24*(11), 1655–1667.

Valero, Y., Morcillo, P., Meseguer, J., Buonocore, F., Esteban, M. A., Chaves-Pozo, E., & Cuesta, A. (2015). Characterization of the IFN pathway in the teleost fish gonad against vertically transmitted viral nervous necrosis virus. *Journal of General*

Virology, *96*(8), 2176–2187.

Van Der Does, A. M., Bogaards, S. J. P., Ravensbergen, B., Beekhuizen, H., Van Dissel, J. T., & Nibbering, P. H. (2010). Antimicrobial peptide hLF1-11 directs granulocyte-macrophage colony-stimulating factor-driven monocyte differentiation toward macrophages with enhanced recognition and clearance of pathogens. *Antimicrobial Agents and Chemotherapy*, *54*(2), 811–816.

Valenzuela-Miranda, D., Boltaña, S., Cabrejos, M. E., Yáñez, J. M., & Gallardo-Escárate, C. (2015). High-throughput transcriptome analysis of ISAV-infected Atlantic salmon Salmo salar unravels divergent immune responses associated to head-kidney, liver and gills tissues. *Fish and Shellfish Immunology*, *45*(2), 367-377.

Vercammen, E., Staal, J., & Beyaert, R. (2008). Sensing of viral infection and activation of innate immunity by toll-like receptor 3. *Clinical Microbiology Reviews*, *21*(1), 13–25.

Verhelst, J., Hulpiau, P., & Saelens, X. (2013). Mx Proteins: Antiviral Gatekeepers That Restrain the Uninvited. Microbiology and Molecular Biology Reviews, 77(4). 551-566.

Villen, J., Beausoleil, S. A., Gerber, S. A., & Gygi, S. P. (2007). Large-scale phosphorylation analysis of mouse liver. *Proceedings of the National Academy of Sciences*, *104*(5), 1488–1493.

Villoing, S., Béarzotti, M., Chilmonczyk, S., Castric, J., & Brémont, M. (2000). Rainbow trout sleeping disease virus is an atypical alphavirus. *Journal of Virology*, *74*(1), 173–83.

von Gersdorff Jørgensen, L., Tafalla, C., Castro, R., Buchmann, K., Pignatelli, J., Abós, B., & González Granja, A. (2014). Early Immune Responses in Rainbow Trout Liver upon Viral Hemorrhagic Septicemia Virus (VHSV) Infection. *PLoS ONE*, *9*(10), e111084.

Wallace, I. S., McKay, P., & Murray, A. G. (2017). A historical review of the key bacterial and viral pathogens of Scottish wild fish. *Journal of Fish Diseases*, *40*(12), 1741-1756.

Walker, P. J., & Winton, J. R. (2010). Emerging viral diseases of fish and shrimp. *Veterinary Research*, *41*(6), 1-24.

Wang, B., Zhang, Y. B., Liu, T. K., Shi, J., Sun, F., & Gui, J. F. (2014). Fish viperin exerts a conserved antiviral function through RLR-triggered IFN signaling pathway. *Developmental and Comparative Immunology*, *47*(1), 140–149.

Wang, F., Jiao, H., Liu, W., Chen, B., Wang, Y., Chen, B., Lu, Y., Su, J., Zhang, Y., &

Liu, X. (2019). The antiviral mechanism of viperin and its splice variant in spring viremia of carp virus infected fathead minnow cells. *Fish and Shellfish Immunology*, *86*, 805–813.

Wang, T., Hanington, P. C., Belosevic, M., & Secombes, C. J. (2008). Two Macrophage Colony-Stimulating Factor Genes Exist in Fish That Differ in Gene Organization and Are Differentially Expressed. *The Journal of Immunology*, *181*(5), 3310–3322.

Wang, X., Bian, Y., Cheng, K., Gu, L. F., Ye, M., Zou, H., Sun, S.S., & He, J. X. (2013). A large-scale protein phosphorylation analysis reveals novel phosphorylation motifs and phosphoregulatory networks in Arabidopsis. *Journal of Proteomics*, *78*, 486–498.

Ward, M., Secombes, C. J., Grabowski, P. S., Campos-perez, J. J., & Ellis, A. E. (2003). The gills are an important site of iNOS expression in rainbow trout *Oncorhynchus mykiss* after challenge with the Gram-positive pathogen Renibacterium salmoninarum. *Immunology*, *99*(1), 153–161.

Wayman, G. A., Tokumitsu, H., Davare, M. A., & Soderling, T. R. (2011). Analysis of CaM-kinase signaling in cells. *Cell Calcium*, *50*(1), 1–8.

Weaver, B. K., Kumar, K. P., & Reich, N. C. (1998). Interferon regulatory factor 3 and CREB-binding protein/p300 are subunits of double-stranded RNA-activated transcription factor DRAF1. *Molecular and Cellular Biology*, *18*(3), 1359–1368.

Wettenhall, R. E. H., Aebersold, R. H., & Hood, L. E. (1991). Solid-Phase Sequencing of 32P-Labeled Phosphopeptides at Picomole and Subpicomole Levels, *201*(1988), 186–199.

Whitehead, A., Roach, J. L., Zhang, S., & Galvez, F. (2011). Genomic mechanisms of evolved physiological plasticity in killifish distributed along an environmental salinity gradient. *Proceedings of the National Academy of Sciences*, *108*(15), 6193–6198.

Wiklund, T., & Dalsgaard, I. (1998). Occurrence and significance of atypical *Aeromonas salmonicida* in non-salmonid and salmonid fish species: A review. *Diseases of Aquatic Organisms*, *32*(1), 49–69.

Willemsen, J., Wicht, O., Wolanski, J. C., Baur, N., Bastian, S., Haas, D. A., et al. (2017). Phosphorylation-Dependent Feedback Inhibition of RIG-I by DAPK1 Identified by Kinome-wide siRNA Screening. *Molecular Cell*, *65*(3), 403–415.e8.

Wilson, J. M., & Laurent, P. (2002). Fish gill morphology: Inside out. *Journal of Experimental Zoology*, *293*(3), 192–213.

Xiao, J., Yan, J., Chen, H., Li, J., Tian, Y., & Feng, H. (2016). LGP2 of black carp plays

an important role in the innate immune response against SVCV and GCRV. *Fish and Shellfish Immunology*, *57*, 127–135.

Xu, C., Evensen, Ø., & Munang'andu, H. M. (2016). De novo transcriptome analysis shows that SAV-3 infection upregulates pattern recognition receptors of the endosomal toll-like and RIG-I-like receptor signaling pathways in macrophage/dendritic like TO-cells. *Viruses*, *8*(4), 1–16.

Xu, L. G., Wang, Y. Y., Han, K. J., Li, L. Y., Zhai, Z., & Shu, H. B. (2005). VISA is an adapter protein required for virus-triggered IFN-β signaling. *Molecular Cell*, *19*(6), 727–740.

Yamaguchi, T., Takizawa, F., Fischer, U., & Dijkstra, J. (2015). Along the Axis between Type 1 and Type 2 Immunity; Principles Conserved in Evolution from Fish to Mammals. *Biology*, *4*(4), 814–859.

Yamamoto, M., Sato, S., & Hemmi, H. (2003). Role of Adaptor TRIF in the MyD88-Independent Toll-Like Receptor Signaling Pathway. *Science*, *301*(August), 640–643.

Yamanaka, R., & Xanthopoulos, K. G. (2004). Development of improved Sindbis virus-based DNA expression vector. *DNA Cell Biol*, *23*(2), 75–80.

Yan, C., Xiao, J., Li, J., Chen, H., Liu, J., Wang, C., & Feng, C. (2017). TBK1 of black carp plays an important role in the innate immune response against SVCV and GCRV. *Fish and Shellfish Immunology*, *69*, 108–118.

Yang, C., Su, J., Huang, T., Zhang, R., & Peng, L. (2011). Identification of a retinoic acid-inducible gene I from grass carp (*Ctenopharyngodon idella*) and expression analysis in vivo and in vitro. *Fish & Shellfish Immunology*, *30*(3), 936–943.

Yap, W. H., Tay, A., Brenner, S., & Venkatesh, B. (2003). Molecular cloning of the pufferfish (Takifugu rubripes) Mx gene and functional characterization of its promoter. *Immunogenetics*, *54*, 705–713.

Yasuike, M., Kondo, H., Hirono, I., & Aoki, T. (2011). Identification and characterization of Japanese flounder, Paralichthys olivaceus interferon-stimulated gene 15 (Jf-ISG15). *Comparative Immunology, Microbiology and Infectious Diseases*, *34*(1), 83–91.

Yeung, A. T. Y., Gellatly, S. L., & Hancock, R. E. W. (2011). Multifunctional cationic host defence peptides and their clinical applications. *Cellular and Molecular Life Sciences*, *68*(13), 2161–2176.

Yibing, Z., Qiya, Z., Dequan, X. U., Chengyu, H. U., & Jianfang, G. U. I. (2003). Identification of antiviral- relevant genes in the cultured fish cells induced by UV-

inactivated virus. *Chinese Science Bulletin*, *48*(6), 581–588.

Yoneyama, M., Suhara, W., & Fujita, T. (2002). Control of IRF-3 activation by phosphorylation. *Journal of Interferon & Cytokine Research : The Official Journal of the International Society for Interferon and Cytokine Research*, *22*(1), 73–76.

Yoon, S., & Seger, R. (2006). The extracellular signal-regulated kinase: Multiple substrates regulate diverse cellular functions. *Growth Factors*, *24*(1), 21–44.

Yu, F. F., Zhang, Y. B., Liu, T. K., Liu, Y., Sun, F., Jiang, J., & Gui, J. F. (2010). Fish virus-induced interferon exerts antiviral function through Stat1 pathway. *Molecular Immunology*, *47*(14), 2330–2341.

Yuki, T., Yoshida, H., Akazawa, Y., Komiya, A., Sugiyama, Y., & Inoue, S. (2011). Activation of TLR2 Enhances Tight Junction Barrier in Epidermal Keratinocytes. *The Journal of Immunology*, *187*(6), 3230–3237.

Zenke, K., Nam, Y. K., & Kim, K. H. (2010). Molecular cloning and expression analysis of double-stranded RNA-dependent protein kinase (PKR) in rock bream (Oplegnathus fasciatus). *Veterinary Immunology and Immunopathology*, *133*(2–4), 290–295.

Zhang, B. cun, Zhang, J., Xiao, Z. zhong, & Sun, L. (2014). Rock bream (*Oplegnathus fasciatus*) viperin is a virus-responsive protein that modulates innate immunity and promotes resistance against megalocytivirus infection. *Developmental and Comparative Immunology*, *45*(1), 35–42.

Zhang, J., Liu, C., Zhao, S., Guo, S., & Shen, B. (2018). Molecular characterization and expression analyses of the Viperin gene in Larimichthys crocea (Family: Sciaenidae). *Developmental and Comparative Immunology*, *79*, 59–66.

Zhang, L., Chen, W. Q., Hu, Y. W., Wu, X. M., Nie, P., & Chang, M. X. (2016). TBK1-like transcript negatively regulates the production of IFN and IFN-stimulated genes through RLRs-MAVS-TBK1 pathway. *Fish and Shellfish Immunology*, *54*, 135–143.

Zhang, Y. B., Wang, Y. L., & Gui, J. F. (2007). Identification and characterization of two homologues of interferon-stimulated gene ISG15 in crucian carp. *Fish and Shellfish Immunology*, *23*(1), 52–61.

Zhang, Y., Zheng, X., Wang, Z., Gu, Z., Wang, W., Hu, T., Hou, M., Wang, W., Gu, Z., Wang, Q., Zhang, R., Zhang, Y., & Wang, Q. (2018). Sensing of cytosolic LPS through caspy2 pyrin domain mediates noncanonical inflammasome activation in zebrafish. *Nature Communications*, *9*(3052), 1-12.

Zhai, J. V. B., Beausoleil, S. A., Mintseris, J., & Gygi, S. P. (2008). Phosphoproteome analysis of drosophila melanogaster embryos. *Journal of Proteome Research*, *7*(4),

1675–1682.

Zhao, J. G., Zhou, L., Jin, J. Y., Zhao, Z., Lan, J., Zhang, Y. Bin, Zhang, Q.Y., & Gui, J. F. (2009). Antimicrobial activity-specific to Gram-negative bacteria and immune modulation-mediated NF-κB and Sp1 of a medaka β-defensin. *Developmental and Comparative Immunology*, *33*(4), 624–637.

Zhong, J., & Kyriakis, J. M. (2007). Dissection of a Signaling Pathway by Which Pathogen-associated Molecular Patterns Recruit the JNK and p38 MAPKs and Trigger Cytokine Release, *282*(33), 24246–24254.

Zhou, Z. X., Zhang, B. C., & Sun, L. (2014). Poly(I:C) induces antiviral immune responses in Japanese flounder (*Paralichthys olivaceus*) that require TLR3 and MDA5 and is negatively regulated by Myd88. *PLoS ONE*, *9*(11), 1–14.

Zhu, B., He, Q., Xiang, J., Qi, F., Cai, H., Mao, J., Zhang, C., Zhang, Q., Li, H., Wang, T., & Yu, W. (2017). Quantitative Phosphoproteomic Analysis Reveals Key Mechanisms of Cellular Proliferation in Liver Cancer Cells. *Scientific Reports*, *7*(1), 1–12.

Zhu, H., Cong, J. P., & Shenk, T. (1997). Use of differential display analysis to assess the effect of human cytomegalovirus infection on the accumulation of cellular RNAs: induction of interferon-responsive RNAs. *Proceedings of the National Academy of Sciences of the United States of America*, *94*(25), 13985–90.

Zhu, R., Zhang, Y.B., Zhang, Q.Y., & Gui, J.F. (2008). Functional domains and the antiviral effect of the double-stranded RNA-dependent protein kinase PKR from *Paralichthys olivaceus*. *Journal of Virology*, *82*(14), 6889–6901.

Zolnierowicz, S., & Bollen, M. (2000). Protein phosphorylation and protein phosphatases, De Panne, Belgium, September 19-24, 1999. *EMBO Journal*, *19*(4), 483–488.

Zou, J, Grabowski, P, Cunningham, C and Secombes, C. (1999). Molecular cloning of interleukin 1beta from rainbow trout *Oncorhynchus mykiss* reveals no evidence of an ice cut site. *Cytokine*, *11*(8), 552–560.

Zou, J., Bird, S., Truckle, J., Bols, N., Horne, M., & Secombes, C. (2004). Identification and expression analysis of an IL-18 homologue and its alternatively spliced form in rainbow trout (*Oncorhynchus mykiss*). *European Journal of Biochemistry*, *271*(10), 1913–1923.

Zou, J., Castro, R., & Tafalla, C. (2016). Antiviral Immunity: Origin and Evolution in Vertebrates. In *The Evolution of the Immune System: Conservation and Diversification* (173–204). Elsevier Inc.

Zou, J., Gorgoglione, B., Taylor, N. G. H., Summathed, T., Lee, P. T., Panigrahi, A.,

Genet, C., Chen, Y-M., Chen, T-Y., Hassan, M.U., Mughal, S.M., Boudinot, P., & Secombes, C. J. (2014). Salmonids have an extraordinary complex type I IFN system: characterization of the IFN locus in rainbow trout *Oncorhynchus mykiss* reveals two novel IFN subgroups. *Journal of Immunology (Baltimore, Md. : 1950)*, *193*, 2273–86.

Zou, J., & Secombes, C. (2016). The Function of Fish Cytokines. *Biology*, *5*(23), 1-35.

Zou, P. F., Chang, M. X., Li, Y., Zhang, S. H., Fu, J. P., Chen, S. N., & Nie, P. (2015). Higher antiviral response of RIG-I through enhancing RIG-I/MAVS-mediated signaling by its long insertion variant in zebrafish. *Fish and Shellfish Immunology*, *43*(1), 13–24.

Zou, P. F., Chang, M. X., Xue, N. N., Liu, X. Q., Li, J. H., Fu, J. P., Chen, S.N., & Nie, P. (2014). Melanoma differentiation-associated gene 5 in zebrafish provoking higher interferon-promoter activity through signalling enhancing of its shorter splicing variant. *Immunology*, *141*(2), 192–202.

Appendices

Appendix 1: Protocols

Appendix 1.1: RNA extraction protocol using TRI-reagent (Sigma)

This RNA extraction protocol was adapted for cells growing onto 12 well plate/12 well transwells

Step 1: Cell lysis

1. Cells were washed twice with1 ml of PBS.
2. 500 µL of TRI-Reagent was added in each well.
3. Cell lysate was collected in 2 mL screw capped tube.
4. Kept in -20 °C or directly used for RNA extraction.

Step 2: Phase Separation

1. If from frozen, was allowed to thaw at room temperature (RT), then 100 µL BCP (per mL TRI Reagent used) was added and the tube was shaken vigorously by hand for 15 seconds.
2. Samples were incubated at room temperature for 15 min.
3. Samples were centrifuged at 16900 × g for 15 min, at 4ºC.
4. After centrifugation, the upper aqueous phase was transferred to a new tube without disturbing the interface.

Step 3: RNA precipitation

1. ½ volume (half of total volume of upper phase) of RNA precipitation solution (prepared in house with 1.2M NaCl and 0.8M Sodium Citrate Sesquihydrate in nuclease free water, 0.2 nm filter sterilized) and the same ½ volume of isopropanol were added and mixed properly by inverting gently for 4-6 times followed by incubation for 10 min at room temperature.
2. Sample was then centrifuged at 16900 × g for 15 min, at 4ºC. The RNA precipitate forms a gel like pellet on the side/bottom of the tube.

Step 4: RNA Wash

1. The supernatant was removed carefully without disturbing the pellet by pipetting and the pellet was washed with 1 mL of 75% ethanol for 15 mins at RT.
2. The pellet was flicked to lift the pellet from the bottom and invert a few times so that the entire surface of the pellet and tube are washed, then centrifugation at 16900 × g for 15 min, at room temperature was done.

3. Most of the supernatant was removed carefully by pipetting.
4. The sample was re-spined for just 2 pulses and all the remaining ethanol was removed with a small volume pipette (preferable 10-20 µL).
5. Finally, the RNA was air dried at room temp for 5 min.

Step 5: Dissolving the RNA

1. RNA pellet was re-suspended in an appropriate amount of RNase free water
2. RNA was incubated at RT for 30-60 min with gentle flicking of the tubes every 10 min to aid resuspension.
3. RNA was kept at -70^{o}C overnight.

Step 6: RNA quantification

1. RNA was thawed and quantified by Nanodrop

2. An aliquot of RNA (250 ng) was used for gel run to check the integrity of the RNA. For this, 250 ng of RNA was incubated at 65 °C for 2 min (preferable in thermocycler), and chilled on ice.

1. Required volume of loading dye was added into the RNA and run on 1.5% agarose gel to check the quality of RNA (a good quality RNA gives 2 band as Figure
2. RNA was stored at -70^{o}C until further use.

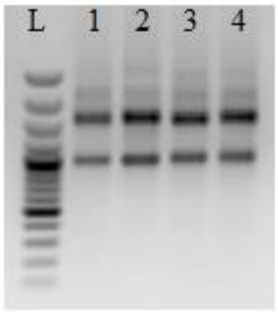

Figure 1.1: Agarose gel electrophoresis of RNA. L, 100 bp marker, 1-4 RNA sample.

Appendix 1.2: Protocol for cDNA extraction using Superscript III (Invitrogen)

1. Each component was thawed, mixed and centrifuged before use.
2. Combine the following component in PCR tube

Component	Amount
RNA up to 5 µg of total RNA	X µL
Primer: 50 µM oligo(dT)	1 µL
10 mM dNTP mix	1 µL
DEPC-treated water	Y µL (to make up 10 µL

3. Tube was incubated at 65°C for 5 min, then placed on ice for at least 1 min.
4. The following cDNA Synthesis Mix was prepared, adding each component in the indicated order.

Component	1 reaction
10X RT buffer	2 µL
25 mM MgCl2	4 µL
0.1 M DTT	2 µL
RNaseOUT™ (40 U/µL)	1 µL
SuperScript® III RT (200 U/µL)	1 µL

5. 10 µL of cDNA Synthesis Mix to each RNA/primer mixture was added, mixed gently, and collected by brief centrifugation and then incubated for 50 min at 50°C
6. The reaction was terminated by incubating at 85°C for 5 min. Then chilled on ice.
7. The reaction was collected by brief centrifugation. And then 1 µL of RNase H was added to each tube and incubated the tubes for 20 min at 37°C.
8. cDNA synthesis reaction was stored at −20°C or used for PCR immediately.

Appendix 1.3: PCR clean-up protocol
Using Nucleospin PCR clean-up and Gel extraction kit (Macherey-Nagel)

Step 1: Adjusting DNA binding condition

1. Volume of PCR product was adjusted to 50 µL with miliQ water
2. 2 volume of NTI buffer (100 µL of buffer) was added into PCR product

Step 2: Binding DNA

1. A PCR clean-up column was placed into a 2 mL collection tube
2. PCR product and NTI mixture was transferred into the column
3. Centrifuged for 30s at 11,000 *g*
4. Flow-through was discarded
5. Column was placed back into the tube

Step 3: Washing silica membrane

1. 700 µl NT3 buffer was added into the column
2. Centrifuged for 30s at 11,000 *g*
3. Flow-through was discarded
4. Column was placed back into the tube

Step 4: Drying silica membrane

1. The column with collection tube was entrifuged for 1 min at 11,000 *g* to remove the NT3 buffer completely

Step 5: DNA elution

1. PCR clean-up column was placed into a new 1.5 mL microcentrifuge tube.
2. 20 µL NE buffer (previously incubated at 72°C) was added into the column, incubated for 2 min at 72°C.
3. Centrifuged for 1 min at 11,000 *g*
4. Column was discarded and the tube with supernatant as ultrapure PCR product was kept at -20°C until further use.

(For the higher efficiency, at the beginning sufficient volume of NE buffer was taken into a tube and incubated at 72°C)

Appendix 1.4: Plasmid extraction protocol

Using NucleoSpin plasmid DNA purification kit (Macherey-Nagel)

The overnight grown bacterial culture used for plasmid extraction.

1. Tube with bacterial culture was centrifuged at 11000*g* for 30 seconds
2. The supernatant was discarded
3. Then 150 µL of buffer A1 was added and vortexed to re-suspend the pellet completely
4. Then 250 µL of buffer A2 was added and inverted for 5 times – (avoiding vortex)
5. The tube was incubated for 2 min at RT to lyse the cells
6. Then 350 µL of buffer A3 was added and inverted until lysate has turned colourless
7. Centrifuged for 3 min at full speed (16000*g*)
8. A nucleaspin plasmid EasyPure column was placed into a collection tube
9. Clear supernatant was added onto the spin column
10. Centrifuged for 30s at 2000*g*
11. Flow-through was discarded
12. Then 450 µL of buffer AQ was added into the spin column
13. Centrifuged for 1 min at full speed (16000*g*)
14. Tube was discarded
15. The spin column was placed into a new 1.5 ml Eppendorf tube
16. Then 50 µL pre-heated (at 72°C) buffer AE was added onto the membrane and incubate at 72 °C for 2 min
17. Centrifuged for 1 min at full speed (16000*g*)
18. The column was discarded and the tube with supernatant was kept
19. Nano drop was performed to quantify the plasmid DNA
20. Plasmid DNA was kept at -20 °C

(For the higher efficiency, at the beginning sufficient volume of AE buffer was taken into a tube and incubated at 72°C).

Appendix 1.5: Titration of virus for infectivity study

After a virus is propagated in cell culture, we need to know the infectivity titre of the virus. This can be determined by inoculating increasing dilutions of the virus to a cell line based on CPE seen in different dilutions. Viral titter is the lowest concentration of a virus that still infects cells. To determine the titter, several dilutions are prepared, such as 10^{-1}, 10^{-2}, 10^{-3}, 10^{-4} and so forth. This is virus specific as well as cell line.

There are mainly two methods for the determination of virus titter. One is the adsorption inoculation method where virus is inoculated on a preformed cell monolayer and another is the simultaneous inoculation method where cells and virus are inoculated at the same time.

1. Adsorption inoculation method

For the adsorption inoculation method CHSE-214 cells were seeded on to two 96 well plates at a seeding density of 0.03×10^{6} cells/well. Two 96 well plates were seeded one for 10-fold dilution and another for 5-fold dilution and incubated overnight at 22 °C with 4% CO_2.

2. Simultaneous inoculation method

For simultaneous inoculation method virus and cells are inoculated at the same time. First the plate for simultaneous inoculation is inoculated with virus supernatant and the kept in the incubator and then cells are harvested and seeded onto the plate.

SAV-2 keeping at 4°C was used for adsorption and simultaneous inoculation for 10-fold and 5-fold dilutions across the plate.

Titration Method

Perform virus titration using an appropriate dilution series for the virus concerned. Here is the example of 10-fold dilution series.

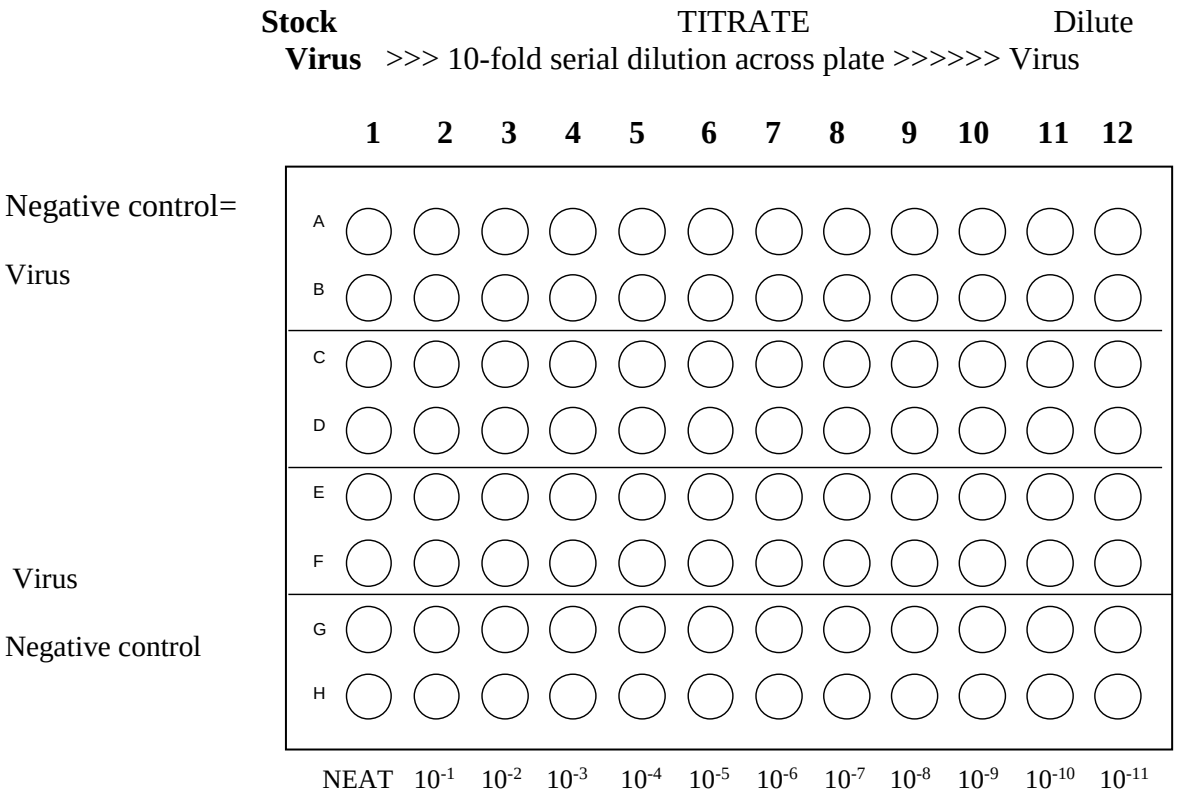

Virus titration method

1. Add 90 µl of diluent (HBSS+2%serum) to all wells of the 96 well plate except the first wells of column 1.
2. Add 100µl of diluent (HBSS+2%serum) to the first well of row A and row H (controls).
3. Add 100 µl of the virus preparation to the first well of rows B to G.
4. FOR EACH ROW, make ten–fold dilutions across the plate by transferring 10µl into the next well across the plate, and mix well at each stage. Use a different tip for each well (to minimise the potential carry over of virus across the titration plate).
5. Remember to discard 10µl from the last wells to the discard container.
6. Nescofilm the plate and incubate at appropriate temperature/CO_2 incubator.

7. Trypsinise a recently prepared 25cm^2 flask of cells and re-suspend cells in approximately 13 ml medium. Follow the method for 'Preparing subcultures of a fish

cell line' (page 5-6) up to point 8. At this point add 13mls medium and re-suspend the cells by gently pipetting up and down.

8. Dispense 1.5ml of cell suspension into each channel of a high walled reservoir.
9. Starting from the last well in the row add 100µl of cell suspension to each well using the multi-channel pipette and the high walled reservoirs. (RHS, low concentration of virus to LHS, high concentration of virus)
10. Label plate with name and date of preparation. Please do not obscure any wells of the plate with marker pen. Keep all writing to the edges.
11. Seal titration/neutralisation plate using Nescofilm around the perimeter, taking care not to disrupt or mix the contents of the wells.
12. Incubate the inoculated cell culture plate at appropriate temperature for virus culture but also within the normal temperature range for those particular cells.
13. Check the plate every day for 1 week and record results.

Appendix 1.7: Protocol for PCR product clean up using DNA Clean & Concentrator-5 (Zymo Research)

1. In a 1.5 mL microcentrifuge tube, 5 volumes of DNA Binding Buffer were added to each volume of PCR product
2. Mixed briefly by vortexing
3. The mixture was transferred to a provided Zymo-Spin Column in a collection tube
4. Centrifuged at *10,000 - 16,000 x g* for 30 seconds
5. Flow-through was discarded
6. Then 200 µL DNA Wash Buffer was added to the column
7. Centrifuged at *10,000 - 16,000 x g* for 30 seconds
8. The flow-through was discarded and back into collection tube
9. Steps 6 – 8 were repeated
10. The column was transferred to a 1.5 mL microcentrifuge tube
11. Then 15-20 µL DNA Elution Buffer or water was directly added to the column matrix and incubated at room temperature for one min.
12. Centrifuged for 30 seconds to elute the PCR product
13. Nano drop was performed to quantify the PCR product
14. Ultrapure PCR product was used immediately or stored at −20°C for future use.

Appendix 1.7: Protocol for cDNA synthesis using Maxima H Minus Synthesis Master Mix

1. The following components were combined in a PCR tube

Component	Amount
10XdsDNase	1 µL
10XdsDNase buffer	1 µL
RNA up to 500 ng of cytoplasmic or total RNA	X µL
DEPC-treated water	Y µL (to make up 10 µL

2. The reaction was mixed gently and briefly centrifuged
3. Tube was incubated at 37 °C for 2 min, then placed on ice for at least 1 min.
4. The following cDNA Synthesis Mix was prepared, adding each component in the indicated order.

Component	1 reaction
5X Maxima cDNA H Minus Synthesis Master Mix	4 µL
DEPC-treated water	6 µL

5. The reaction was mixed gently and briefly centrifuged
6. Tube was incubated at 25 °C for 10 min, 50 °C for 15 min and termination at 85°C for 5 min.
7. The cDNA synthesis reaction was stored at −20°C or used for PCR immediately.

Appendix 1.8: Plasmid DNA extraction protocol

Using High Pure Plasmid Isolation Kit (Roche) with some modifications

The overnight grown bacterial culture used for plasmid extraction.

1. The bacterial culture was centrifuged at 11000*g* for 30 seconds
2. The supernatant was discarded
3. Then cell pellet was resuspended in 250 µL of suspension buffer supplemented with RNase followed by addition of 250 µL lysis buffer
4. The mixture was incubated for 5 min at room temperature followed by addition of 300 µL of chilled binding buffer and then centrifuged for 10 min at maximum speed.
5. Clear supernatant was transferred to high pure filter tube followed by centrifugation at maximum speed for 1 min.
6. Flow-through was discarded
7. Then 500 µL wash buffer I was added
8. Centrifuged for 1 min at 13000*g*
9. Flow through was discarded
10. Then 700 µL wash buffer II was added
11. Centrifuged for 1 min at 13000*g* followed by an additional 1min centrifugation after discarding flow through
12. The filter tube was placed into a new 1.5 ml Eppendorf tube
13. Then 30 µL of elution buffer was added and centrifuged for 1 min at 13000*g*
14. The column was discarded and the tube with supernatant was kept
15. Nano drop was performed to quantify the plasmid DNA
16. Plasmid DNA was kept at -20 °C

Appendix 2: DNA standard curves

Appendix 2.1: Plasmid DNA standard of antiviral and tight junction genes used in the study

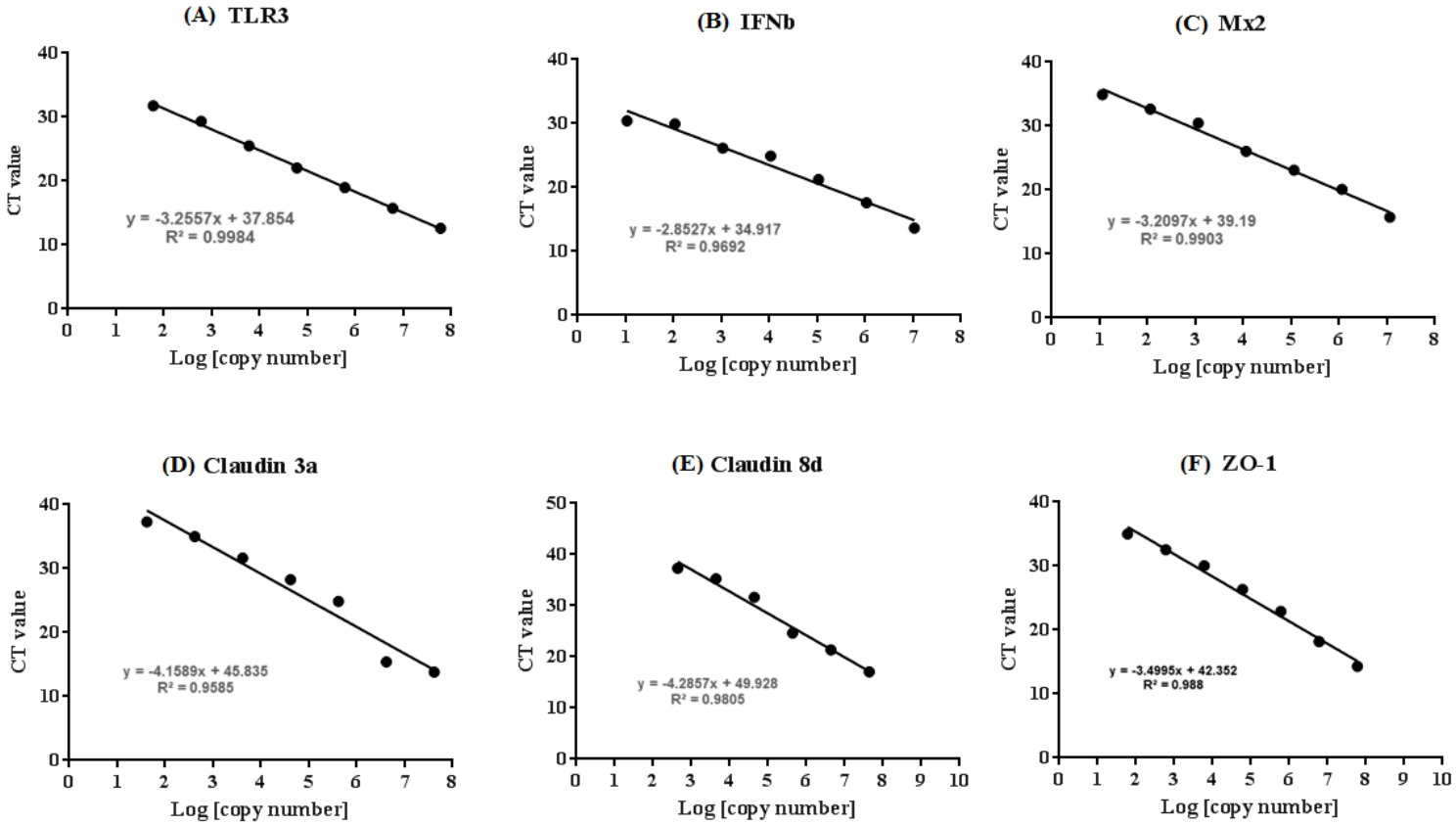

Figure S 2.1: Plasmid DNA standard of antiviral gene TLR3 (A), IFNb (B), MX2 (C) and tight junction genes claudin 3a (D), claudin 8d and ZO-1 (F). Each standard curve was generated with the average CT values of each concentration of standard of three independent runs.

Appendix 2.2a: Plasmid DNA standard of RLRs and related genes used in the study

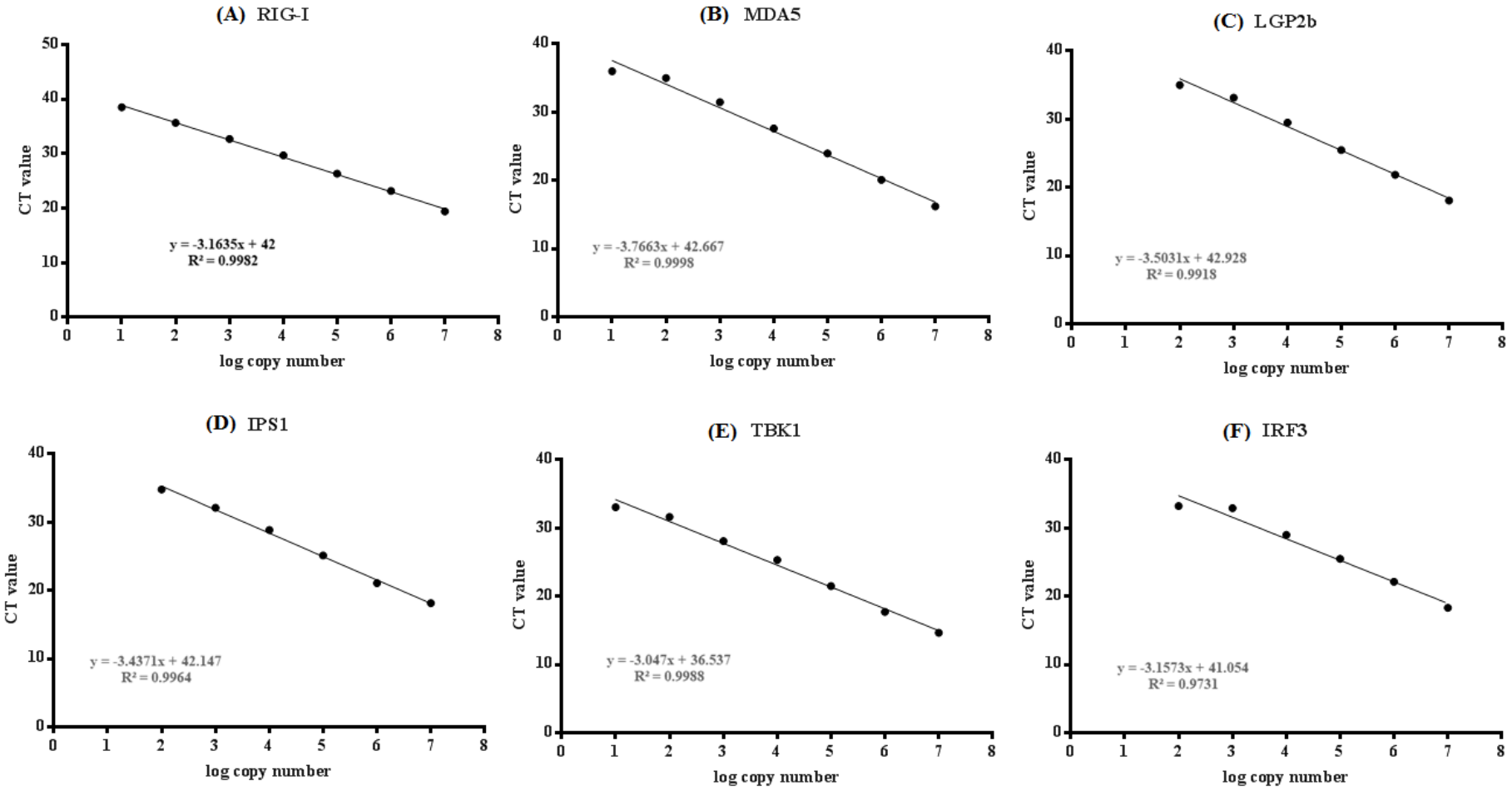

Figure S 2.2a: Plasmid DNA standard of RLRs and associated molecules. Each standard curve was generated with the average CT values of each concentration of standard of three independent runs.

Appendix 2.2b: Plasmid DNA standard of RLRs and related genes used in the study

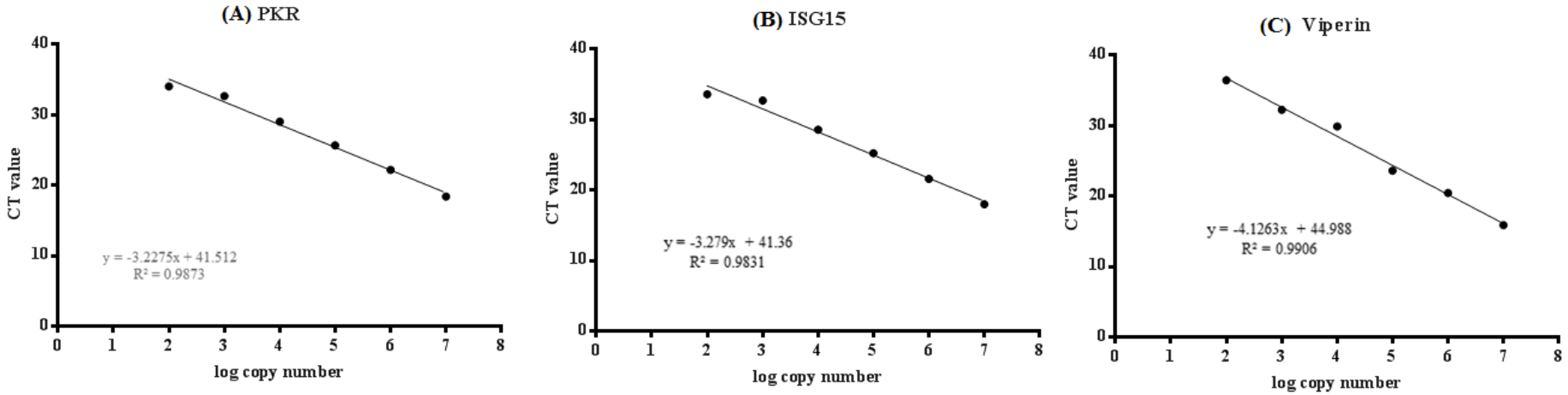

Figure S 2.2b: Plasmid DNA standard of ISGs namely PKR (A), ISG15 (B) and viperin (C). Each standard curve was generated with the average CT values of each concentration of standard of three independent runs.

Appendix 2.3: Plasmid DNA standard of cytokines and antimicrobial peptide genes used in the study

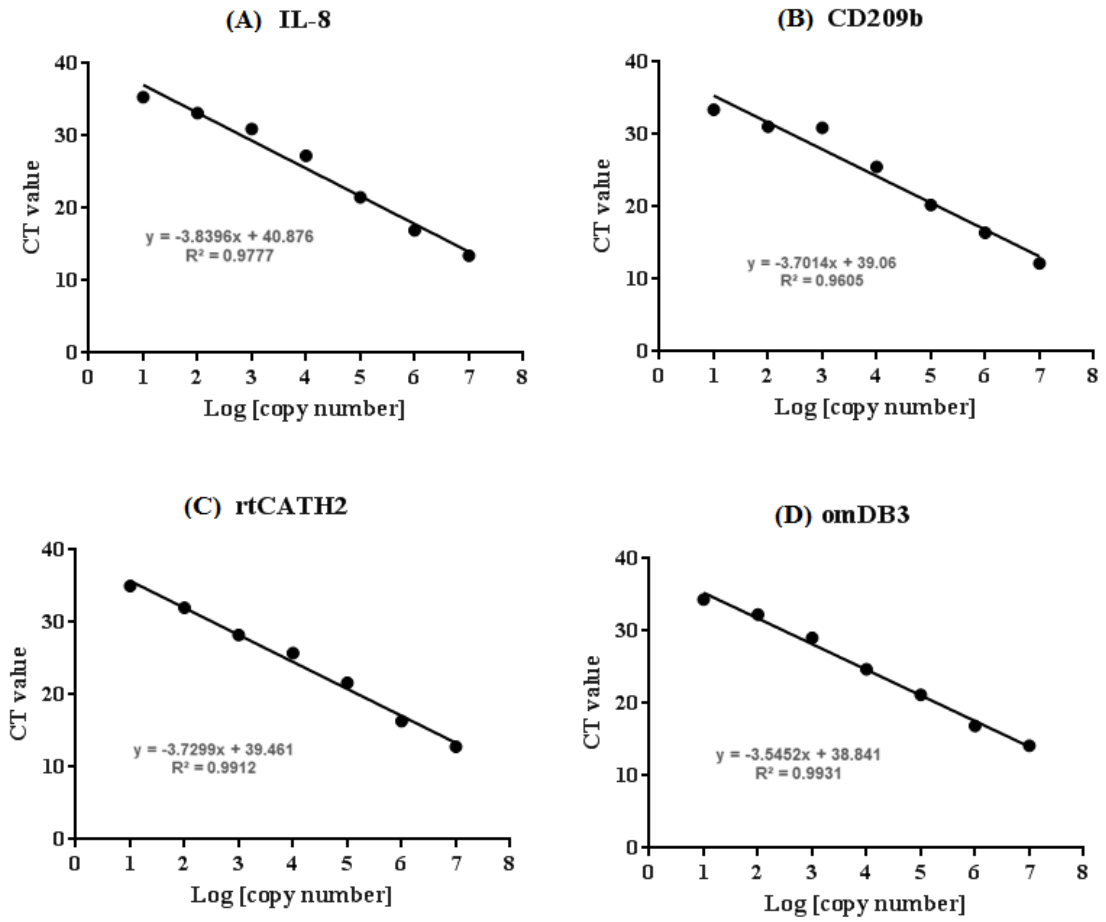

Figure S2.3: Plasmid DNA standard of cytokine IL-8(A), innate immune gene CD209b (B) antimicrobial peptide rtCATH2 (C) and omDB3 (D). Each standard curve was generated with the average CT values of each concentration of standard of three independent runs.

Appendix 3: Transwell literature and supplementary phosphoproteome information

Supplementary Table S3.1: Literature on use of transwell system

SL	Instrument used to measure TER	Findings	Experimental animal and tissue	References
1	Custom modified EVOM Voltohmmeter (World Precision Instruments, Sarasota, FL, USA).	In symmetrical and SSI, TER observed in control group as 5026 ± 127 Ωcm^2 in 6-9 days	Sea bass (*Dicentrarchus labrax*) gill	(Avella et al., 1999)
2	,,	TER value nearly 30 KΩ cm^2 in pre-exposure period while decreased to ~7.7 kΩ cm^2 after exposure to sea water (SW).	puffer fish (*Tetraodon nigroviridis*) gill	(Bui & Kelly, 2015)
3	,,	Highest TER of 3.5 kΩcm^2 by day 6 of seeding	rainbow trout gill primary cells	(Wood & Part 1997)
4	,,	Initial TER was measured as 3 kΩcm^2 in symmetrical culture condition in SSI	rainbow trout gill	(Carlsson & Pärt, 2001)
5	,,	Highest TER of 1150 ± 46 Ωcm^2 after 36-42 h of seeding in SSI	Gold fish *Carrasius auratus*	(Chasiotis & Kelly, 2011)
6	,,	In gold fish, TER of 1.75 and 1.25 K Ωcm^2 at 48 and 96 h of seeding in one experiment and 1 K Ωcm^2 in another experiment where TER was observed as 2.5 K Ωcm^2 in rainbow trout gill epithelia after 96 h of seeding	Gold fish *Carrasius auratus* and Rainbow trout	(Chasiotis & Kelly, 2011a)
7	,,	TER of nearly 2900 Ωcm^2 in symmetrical and nearly 10000 Ωcm^2 asymmetrical culture condition was observed.	rainbow trout gill	(Chasiotis et al., 2010)
8	,,	TER was found as 1.2, 1.5 and 1.8 K Ωcm^2 respectively after 24 h of seeding.	Gold fish	(Chasiotis et al., 2012)
9	,,	TER values as high as 2,000 Ω cm^2	MDCK cells	(Damek-Poprawa et al., 2013)

10	,,	TER observed between 1.3 and 34 kΩcm^2 in DSI whereas, between 1.2 and 21 kΩcm^2 in SSI preparations.	rainbow trout gill	(Fletcher et al., 2000)
11	,,	The plateau TER of control and cortisol- treated (1000 ng/ml cortisol) inserts was 3.79 ± 0.35 and 24.38 ± 0.70 KΩ cm^2, respectively.	rainbow trout gill	(Kelly & Wood, 2001a)
12	,,	TER found as 18.2±2.7 kΩcm^2 at day 7 in control group which increased up to 31 kΩcm^2 and gradually dropped to 10 kΩcm^2 and remained nearly constant.	rainbow trout gill	(Kelly & Wood, 2001b)
13	,,	TER values as 18.00± 3.41 kΩ cm^2 and 27.05±2.60 kΩ cm^2 in freshwater rainbow trout gill epithelia in symmetrical and asymmetrical culture condition.	rainbow trout gill	(Kelly & Wood, 2003)
14	,,	TER values ranged between 27.33 ± 2.49 kΩ cm^2 and 24.82±2.79 kΩ cm^2 in control and cortisol-treated rainbow trout gill epithelia respectively.	rainbow trout gill	(Kelly & Wood, 2008)
15	,,	Symmetrical culture condition in SSI had TER values nearly 4 kΩ cm^2 in control condition.	rainbow trout gill	(Kolosov & Kelly, 2013)
16	,,	TER in primary culture of rainbow trout gill cells was measured as 22.8±6 kΩ cm^2 in control group	rainbow trout gill	(Leguen et al., 2011)
17	,,	TER in control Nile tilapia gill epithelia in SSI was 1.83 ± 0.19 kΩ cm^2 in symmetrical culture condition while TER in asymmetrical culture conditions was 18.58±0.83 kΩ cm^2.	Nile tilapia gill	(Kelly & Wood, 2002)
18	,,	TER in SSI and symmetrical control cultures has been recorded as 10 kΩ cm^2 after 24 hrs of seeding in pre-stress and control conditions.	rainbow trout gill	(Sandbichler et al., 2011)

19	,,	TER of 6.84 ± 1.99 kΩcm^2 in control and 13.54 ± 2.30 kΩcm^2 in continuous cortisol treatment cells	rainbow trout gill	(Sandbichler et al., 2011)
20	,,	TER values have been reported as 2.5 ± 0.9 kΩ cm^2 in symmetrical control cultures and 4.3 ± 1.3 kΩcm^2 in symmetrical cortisol-treated cultures.	rainbow trout gill	(Sandbichler et al., 2011)
21	,,	Found TER as 0.98± 0.09 KΩ cm^2 in control and 1.09± 0.23 KΩ cm^2 oPRL treated after 6 days culture of freshwater In asymmetrical culture condition, found TER values higher than 10 KΩ cm^2 in control group and nearly 22 KΩ cm^2 in oPRL treated group after 3 h of exposure to apical freshwater.	rainbow trout gill	(Kelly & Wood, 2002)
22	,,	TER as 7.6±1.4 kΩcm^2 in control culture	rainbow trout gill	(Shahsavarani et al., 2006)
23	,,	TER value nearly 13 KΩ cm^2 in control group of primary rainbow trout gill cells.	rainbow trout gill	(Smith et al., 2001)
24	,,	TER values as 18.1 ± 1.3 kΩ cm^2 after 8 days in DSI	Rainbow trout primary gill epithelia	(Stott et al., 2014)
25	,,	TER between 20 and 80 Ωcm^2 which remained stable for at least the following 6–12 days	RTgill-W1	(Trubitt et al., 2015)
26	,,	TER reached a plateau of approximately 30 kΩ cm^2 by Day 9, while the first 3 days the value was nearly zero kΩ cm^2. At day 6 and 7, TER value was nearly 8, 13 and 17, 22 kΩ cm^2 respectably in two treatments.	rainbow trout gill	(Wood et al., 2002)
27	,,	Symmetrical culture condition in DSI had TER values nearly 34 kΩ cm^2 in control condition at day 7.	rainbow trout gill	(Zhou et al., 2003)
28	,,	TER of 25–30 kΩ cm^2 (plateau phase) in 7–9 days in DSI in symmetrical condition	rainbow trout gill	(Zhou et al., 2005)

29	,,	TER reached at 5000–8000 Ωcm^2 in DSI in symmetrical condition while 12,000–15,000 Ωcm^2 at 3h in asymmetrical condition.	Nile tilapia gill	(Zhou et al., 2006)
30	Millicel-ERS	TER values were observed between 141±81 and 711±79 Ωcm^2 in different models.	Caco-2/TC7 cells	(Da Violante et al., 2004)
31	,,	TER measures nearly 500 Ωcm^2 in Caco-2 and 100-300 Ωcm^2 in Caco-2 co-culture with HT29-MTX.	Caco-2 and HT29-MTX	(Béduneau et al., 2014)
32	,,	TER values were detected as 283±70 Ωcm^2 in Caco-2 cells and 60±17 to 122±31 Ωcm^2 in co-culture.	Caco-2, HT29-MTX and Raji	(Bazes et al., 2011)
33	,,	TER was observed in control and treated cells as nearly 275 to 500 Ωcm^2 and 50-500 Ωcm^2 respectively	RBE4 cells	(Balbuena et al., 2010)
34	,,	Maximum TER value was 152 Ωcm^2 which was detected at 4-5 days.	A549 cells	(Tavana et al., 2011)
35	,,	Mean TER values ranged between 100 and 1200 Ωcm^2 in different cells.	Caco-2, IEC-18 and HCEC cells	(Steensma et al., 2004)
36	,,	TER was measured between 140 and 180 Ωcm^2.	A549 cells	(Rothen-Rutishauser et al., 2005)
37	,,	TER was measured between 170 and 1470 Ωcm^2 in mono and co-culture.	16HBE140-, A549 and hAEpC cells	(Lehmann et al., 2011)
38	,,	TER values detected in different cells in different duration ranged between 147±27 and 463 ±54 Ωcm^2.	Caco-2 and Raji	(des Rieux et al., 2007)
39	,,	TER values were 120 and 140 Ωcm^2 in submerged and air-exposed cultures respectably.	A549	(Blank et al., 2006)
40	,,	Observed TER as 500 to 1300 Ωcm^2 in different groups.	Caco-2	(Ferruzza et al., 2012)
41	,,	Maximum TER value was detected as nearly 3000 Ωcm^2.	NHBE cell line	(Oshima et al., 2011)

Table S3.2. List of proteins identified in different treatment groups from rainbow trout gill epithelial cells RTgill-W1 with their functional groups, associated genes in zebra fish and human

Uniprot or NCBI ID for rainbow trout	Zebrafish gene symbol	Human gene symbol	Protein name	Functional group[1]	Localization	Treatment group
P26351	tmsb4x	TMSB4Y	Thymosin beta-11	N	Cytoplasmic	All
XP_021479457.1			rho GTPase-activating protein 32-like isoform X1	T	Nuclear	PIC
XP_020339660.1			SLIT-ROBO Rho GTPase-activating protein 2-like	T	Extracellular	PIC
XP_021476300.1			rho GTPase-activating protein 12-like	T	Nuclear	PIC
XP_024236905.1			rho GTPase-activating protein 39-like isoform X2	T	Nuclear	PIC
A0A060W1R7	-	-	Phosphate transporter	P	Plasmamembrane	Control+PIC
XP_021476300.1	arhgap12b	ARHGAP12	rho GTPase-activating protein 12-like	T	nuclear	PIC
XP_020317074.1	ssb	SSB	lupus La protein homolog B-like	A	nuclear	All
XP_021439759.1	sqstm1	SQSTM1	sequestosome-1-like	J	nuclear	All
Q5KT34	hsp70l	HSPA1L	Heat shock 70kDa protein	O		All
XP_021415075.1	lmna	LMNA	lamin-A-like	DY	nuclear	All
A0A060VVL3	eif3c	EIF3CL	Eukaryotic translation initiation factor 3 subunit C	J	Cytoplasmic	All
XP_021417537.1	ahnak	AHNAK	neuroblast differentiation-associated protein AHNAK-like	O	Cytoplasmic_ nuclear	All
XP_020342305.1	srsf3a	SRSF3	serine/arginine-rich splicing factor 3-like	A	nuclear	All
XP_021427140.1	gsk3b	GSK3B	glycogen synthase kinase-3 beta-like isoform X4	G	Cytoplasmic_ nuclear	All
XP_021459134.1	sgta	SGTA	small glutamine-rich tetratricopeptide repeat-containing protein alpha-like	S	Cytoplasmic _nuclear	Control+PIC
A0A060WCN2	rps6	RPS6	40S ribosomal protein S6	J	Cytoplasmic	Control+PIC
XP_020340664.1	srsf9	SRSF9	serine/arginine-rich splicing factor 9-like	A	nuclear	All
XP_021478340.1	dbh	DBH	dopamine beta-hydroxylase	E	extracellular	PIC

XP_021438926.1	ahnak	AHNAK	neuroblast differentiation-associated protein AHNAK-like	S	nuclear	All
XP_021417537.1	ahnak	AHNAK	neuroblast differentiation-associated protein AHNAK-like	s	nuclear	All
XP_021480987.1	myh9a	MYH9	myosin-9-like isoform X2	Z	Endoplasmic reticulum	All
A0A060X654	aco2	ACO2	Aconitate hydratase, mitochondrial	C	mitochondrial	Control+PIC
XP_021415820.1	abcf1	ABCF1	ATP-binding cassette sub-family F member 1-like	J	nuclear	All
XP_021435177.1	pdcl3	PDCL3	phosducin-like protein 3	T	Cytoplasmic	Control+PIC
A0A060XB41	gapdhs	GAPDHS	Glyceraldehyde-3-phosphate dehydrogenase	G	Cytoplasmic	All
A0A060YAX6	mcm2	MCM2	DNA helicase	K	nuclear	All
XP_021417046.1	sqstm1	SQSTM1	sequestosome-1-like	J	Cytoplasmic	All
XP_021458415.1	srsf9	SRSF9	serine/arginine-rich splicing factor 9-like	A	nuclear	All
XP_021430220.1	srrm1	SRRM1	serine/arginine repetitive matrix protein 1-like isoform X1	A	nuclear	All
A0A1S3SB33	snw1	SNW1	SNW domain-containing protein 1-like	AB	Cytoplasmic	All
A0A060XAK4	map2	MAP2	Microtubule-associated protein	Z	nuclear	PIC
XP_021430686.1	dync1h1	DYNC1H1	Cytoplasmicplasmic dynein 1 heavy chain 1	Z	Cytoplasmic	All
A0A1S3N9Q2	zgc:55733	CH17-409J4.1	heterogeneous nuclear ribonucleoprotein C-like isoform X3	A	nuclear	All
A7UH96	map4k4	MAP4K4	Mitogen-activated protein kinase kinase kinase kinase 4-like protein	T	nuclear	MDP+PIC
XP_021471377.1	adamts9	ADAMTS9	A disintegrin and metalloproteinase with thrombospondin motifs 20-like	O	plasma membrane	All
XP_021467095.1	srsf5b	SRSF5	serine/arginine-rich splicing factor 5-like isoform X2	A	nuclear	All
XP_021461826.1	srsf9	SRSF9	serine/arginine-rich splicing factor 9-like isoform X1	A	extracellular	All
XP_021456437.1	akap12b	AKAP12	A-kinase anchor protein 12 isoform X1	T	nuclear	All
XP_021440312.1	srrm1	SRRM1	serine/arginine repetitive matrix protein 1-like	A	nuclear	All
XP_020309176.1	nifk	NIFK	syntaxin-4-like	U	nuclear	All
XP_021458386.1	parvaa	PARVA	alpha-parvin-like isoform X1	Z	nuclear	All

XP_021468057.1	ccdc6a	CCDC6	coiled-coil domain-containing protein 6-like	S	nuclear	All
A0A060WML4	coro1b	CORO1B	Coronin		nuclear	All
XP_020322254.1	map2k2b	MAP2K2	dual specificity mitogen-activated protein kinase kinase 2-like	T	Cytoplasmic_ nuclear	All
XP_021447377.1	srsf1b	SRSF1	serine/arginine-rich splicing factor 1B-like isoform X1	A	nuclear	All
XP_021428409.1	hivep1	HIVEP1	zinc finger protein 40-like isoform X1	K	nuclear	PIC
XP_020315797.1	prkar1ab	PRKAR1A	cAMP-dependent protein kinase type I-alpha regulatory subunit-like	T	nuclear	All
XP_021413834.1	myh9a	MYH9	myosin-9-like isoform X2	S	nuclear	Control+PIC
A0A1S3RBB5	limd2	LIMD2	LIM domain-containing protein 2-like isoform X1	T	nuclear	All
XP_021454842.1	fnbp1l	FNBP1L	formin-binding protein 1-like isoform X2	Z	nuclear	All
XP_021436746.1	rnf213b	RNF213	E3 ubiquitin-protein ligase rnf213-beta-like isoform X8	O	Plasmamembrane	PIC
XP_021465920.1	ccdc114	CCDC114	coiled-coil domain-containing protein 63	S	Cytoplasmic	PIC
XP_021478308.1	add1	ADD1	alpha-adducin-like	TZ	nuclear	PIC
XP_021412395.1	add3a	ADD3	gamma-adducin-like	TZ	nuclear	Control+PIC
Q53HX4	map2k2a	MAP2K2	MAPK /ERK kinase	T	Cytoplasmic	All
XP_021420114.1	larp1	LARP1	la-related protein 1	JO	nuclear	All
XP_021458770.1	tcp11l1	TCP11L1	T-complex protein 11-like protein 1	T	Cytoplasmic	All
A0A1S3QC57	pdha1a	PDHA2	Pyruvate dehydrogenase E1 component subunit alpha	C	Cytoplasmic	Control+PIC
NP_001117896.1	map2k2a	MAP2K2	MAPK /ERK kinase	T	Cytoplasmic	All
XP_021460427.1	lmnb2	LMNB2	lamin-B2	DY	nuclear	All
XP_020346920.1	pea15	PEA15	astrocytic phosphoprotein PEA-15-like	D	plasma membrane	PIC
B5XE27	ensab	ENSA	alpha-endosulfine	TU	Cytoplasmic	All
XP_021464580.1	itsn1	ITSN1	intersectin-1-like isoform X3	T	nuclear	All
XP_021476221.1	neurod6a	NEUROD6	neurogenic differentiation factor 6	K	nuclear	PIC
XP_021460036.1	tpra	TPR	nucleoprotein TPR-like	U	nuclear	PIC
A0A060VQQ6	fkbp8	FKBP8	Peptidylprolyl isomerase	O	endoplasmic reticulum	PIC

XP_021429469.1	ahi1	AHI1	jouberin isoform X1	T	nuclear	PIC
XP_024263477.1	eef1da	EEF1D	elongation factor 1-delta-like	K	Cytoplasmic	PIC
XP_021458987.1	uhrf1	UHRF1	E3 ubiquitin-protein ligase UHRF1 isoform X1	K	nuclear	PIC
XP_021439199.1	trappc11	TRAPPC11	trafficking protein particle complex subunit 11	U	Cytoplasmic	PIC
Q6L767	raf1a	RAF1	Serine/threonine protein kinase RAF1	T		PIC
XP_024261818.1	tcea1	TCEA1	transcription elongation factor A protein 1-like isoform X1	K	mitochondrial	PIC
XP_021442370.1	tp53bp1	TP53BP1	TP53-binding protein 1	L	Cytoplasmic_ nuclear	PIC
XP_021418521.1	prpf4bb	PRPF4B	serine/threonine-protein kinase PRP4 homolog	nuclear		All
XP_021469369.1	jun	JUN	transcription factor AP-1-like	K	Cytoplasmic	MDP+PIC
XP_021431726.1	cbx1b	CBX1	chromobox protein homolog 1-like isoform X1	B	nuclear	Control+PIC
XP_021453040.1	ptpn4a	PTPN4	tyrosine-protein phosphatase non-receptor type 4 isoform X4	T	nuclear	PIC
XP_021431200.1	wdr24	WDR24	WD repeat-containing protein 24-like isoform X2	U	mitochondrial	PIC
A0A060XAI2	itgb1a	ITGB1	Integrin beta	W	Plasmamembrane	PIC
XP_020330313.1	cdk2	CDK2	cyclin-dependent kinase 2		Cytoplasmic _nuclear	All
XP_021478144.1	sh2d3ca	SH2D3C	SH2 domain-containing protein 3C-like	T	Cytoplasmic	PIC
XP_021439502.1	map7d3	MAP7D3	ensconsin-like isoform X8	S	nuclear	PIC
XP_021420688.1	calcoco2	CALCOCO2	calcium-binding and coiled-coil domain-containing protein 2-like	Z	Cytoplasmic	PIC
XP_021432999.1	cdc123	CDC123	cell division cycle protein 123 homolog	D	Cytoplasmic _nuclear	All
XP_021438069.1	tbx4	TBX4	T-box transcription factor TBX4-like	K	nuclear	PIC
XP_021454979.1	prrc2c	PRRC2C	protein PRRC2C-like	S	nuclear	PIC
XP_021452805.1	ssb	SSB	lupus La protein homolog B-like	A	nuclear	All
XP_021431031.1	ccdc186	CCDC186	coiled-coil domain-containing protein 186	W	nuclear	PIC
XP_021439469.1	dgkaa	DGKA	diacylglycerol kinase theta-like	I	Cytoplasmic	PIC
A0A060W1Z3	xrn2	XRN2	5'-3' exoribonuclease	A	nuclear	Control+PIC
XP_021456912.1	usp24	USP24	biquitin carboxyl-terminal hydrolase 24-like	O	nuclear	All

XP_021423224.1	mcm2	MCM2	DNA replication licensing factor mcm2-like	K	nuclear	All
XP_021476751.1	ostf1	OSTF1	osteoclast-stimulating factor 1	T	Cytoplasmic	All
XP_021420675.1	cbx1b	CBX1	chromobox protein homolog 1 isoform X1	B	nuclear	All
XP_021417045.1	canx	CANX	calnexin-like	O	Cytoplasmic	Control+PIC
XP_021479552	rps3	RPS3	40S ribosomal protein S3-like	J	mitochondrial	All
XP_021474353.1	pold3	POLD3	DNA polymerase delta subunit 3 isoform X1	L	nuclear	All
XP_021434739.1	ppig	PPIG	peptidyl-prolyl cis-trans isomerase G	O	nuclear	All
XP_021446638.1	prrc2b	PRRC2B	protein PRRC2B-like isoform X5	S	Endoplasmic reticulum	PIC
XP_021458154.1	prrc2b	PRRC2B	protein PRRC2B-like isoform X2	S	nuclear	PIC
XP_021447025.1	ccdc82	CCDC82	coiled-coil domain-containing protein 82-like	S	nuclear	PIC
XP_021429897.1	klc1a	KLC1	kinesin light chain 1-like isoform X2	Z	Cytoplasmic	All
XP_021478624.1	rictorb	RICTOR	rapamycin-insensitive companion of mTOR-like isoform X1	D	nuclear	PIC
XP_021441892.1	sltm	SLTM	SAFB-like transcription modulator	K	nuclear	All
XP_021456220.1	lbr	LBR	lamin-B receptor-like	I	plasma membrane	All
XP_021423882.1	irf2bp2b	IRF2BP2	interferon regulatory factor 2-binding protein 2-B-like	K	nuclear	PIC
XP_021479352.1	bckdk	BCKDK	-methyl-2-oxobutanoate dehydrogenase [lipoamide]	T	mitochondrial	All
XP_021452802.1	ppig	PPIG	peptidyl-prolyl cis-trans isomerase G-like	O	nuclear	PIC
XP_021466982.1	fntb	FNTB	protein farnesyltransferase subunit beta-like	O	extracellular	PIC
XP_021446580.1	ddx54	DDX54	ATP-dependent RNA helicase DDX54	A	nuclear	PIC
XP_021427993.1	top2b	TOP2B	DNA topoisomerase 2-beta-like	B	nuclear	All
XP_021467718.1	cad	CAD	CAD protein isoform X2	F	Cytoplasmic	All
XP_021415194.1	chd4a	CHD4	chromodomain-helicase-DNA-binding protein 4-like	K	nuclear	Control+PIC
A0A1S3SFE2	tmpoa	TMPO	lamina-associated polypeptide 2, isoform beta-like isoform X7	D	nuclear	All
C0PUT2	flna	FLNA	Filamin-A	Z	nuclear	All
XP_021415751.1	map7d1b	MAP7D1	MAP7 domain-containing protein 1-like isoform X7	Z	nuclear	PIC

XP_021435215.1	cwc22	CWC22	pre-mRNA-splicing factor CWC22 homolog isoform X1	A	nuclear	PIC
XP_024249913.1	rb1	RB1	retinoblastoma-associated protein	D	nuclear	All
XP_021468770.1	chd7	CHD7	chromodomain-helicase-DNA-binding protein 7	K	nuclear	All
XP_021472273.1	hspg2	HSPG2	basement membrane-specific heparan sulfate proteoglycan core protein-like	T	plasma membrane	PIC
XP_021430202.1	marcksl1a	MARCKSL1	MARCKS-related protein-like	S	nuclear	All
XP_021427379.1	zfpm2a	ZFPM2	zinc finger protein ZFPM2-lik	K	Cytoplasmic _nuclear	Control+PIC
XP_021464990.1	cep68	CEP68	entrosomal protein of 68 kDa-like		nuclear	PIC
XP_021473878.1	mink1	MINK1	misshapen-like kinase 1 isoform X6	T	Endoplasmic reticulum	Control+PIC
XP_021474808.1	patl1	PATL1	protein PAT1 homolog 1-like	J	extracellular	PIC
A0A060XTD4	jak2b	JAK2	Tyrosine-protein kinase	T	Cytoplasmic	Control+PIC
XP_021419524.1	ppp1r12a	PPP1R12A	protein phosphatase 1 regulatory subunit 12A-like isoform X1	OT	nuclear	Control+PIC
XP_021420296.1	nolc1	NOLC1	nucleolar and coiled-body phosphoprotein 1 isoform X5	S	nuclear	All
P_021421553.1	ikzf4	IKZF4	zinc finger protein Eos-like	K	nuclear	PIC
XP_021454181.1	dnah5	DNAH5	dynein heavy chain 8, axonemal	Z	mitochondrial	All
XP_021427372.1	prrc2a	PRRC2A	protein PRRC2A-like isoform X1	S	nuclear	PIC
A0A060XUS8	dhh	DHH	Hedgehog protein	T	mitochondrial	PIC
XP_021438852.1	rnf20	RNF20	E3 ubiquitin-protein ligase BRE1A-like	O	nuclear	Control+PIC
XP_021457356.1	lmnb1	LMNB1	lamin-B1	DY	nuclear	PIC
XP_021466280.1	itga5	ITGA5	integrin alpha-5-like	W	extracellular	PIC
XP_020362322.1	tuba8l	TUBA8	tubulin alpha-8 chain-like	Z	mitochondrial	All
XP_021440620.1	tacc3	TACC3	transforming acidic coiled-coil-containing protein 3-like isoform X2	S	nuclear	All
XP_021418498.1	cdk13	CDK13	cyclin-dependent kinase 13-like	T	nuclear	Control+PIC
XP_021459894.1	prrc2c	PRRC2C	protein PRRC2C-like	S	nuclear	Control+PIC
XP_021471773.1	exosc10	EXOSC10	exosome component 10	J	nuclear	PIC
XP_020357923.1	rbmx	RBMY1J	RNA-binding motif protein, X chromosome-like isoform X1	K	nuclear	All

XP_021415580.1	tra2a	TRA2A	transformer-2 protein homolog alpha-like	A	nuclear	All
XP_021479399.1	bcl7ba	BCL7B	B-cell CLL/lymphoma 7 protein family member B-A-like	S	mitochondrial	Control+PIC
XP_021443245.1	tekt1	TEKT1	tektin-1	Z	Cytoplasmic	PIC
XP_021412770.1	wipf2b	WIPF2	WAS/WASL-interacting protein family member 2-like	Z	nuclear	PIC
A0A1S3Q1N9, XP_021415540.1	cbx3a	CBX3	chromobox protein homolog 3-like isoform X1	B	nuclear	All
XP_021415540.1	cbx3a	CBX3	chromobox protein homolog 3-like isoform X1	B	nuclear	All
XP_021438214.1	proca1	PROCA1	mucin-5AC-like	I	nuclear	PIC
XP_021441805.1	btbd10b	BTBD10	BTB/POZ domain-containing protein 10-like	S	plasma membrane	PIC
W5S0M1	ptges3a	PTGES3	Peroxiredoxin 4	O		Control+PIC
XP_021481712.1	srrm2	SRRM3	serine/arginine repetitive matrix protein 2-like isoform X2	A	nuclear	All
C1BF32	ptges3a	PTGES3	Prostaglandin E synthase 3	O	Cytoplasmic	All
A0A060VN95	dis3l2	DIS3L2	DIS3-like exonuclease 2	J	Cytoplasmic _nuclear	PIC
XP_021449714.1	lmna	LMNA	lamin-A-like	DY	nuclear	PIC
XP_021427551.1	sfpq	SFPQ	splicing factor, proline- and glutamine-rich-like	A	Cytoplasmic	All
XP_021479384.1	dyrk1ab	DYRK1A	dual specificity tyrosine-phosphorylation-regulated kinase 1A-like isoform X3	T	Cytoplasmic _nuclear	Control+PIC
XP_020307840.1	eif4h	EIF4H	eukaryotic translation initiation factor 4H-like isoform X1	J	nuclear	PIC
XP_021470616.1	acin1b	ACIN1	apoptotic chromatin condensation inducer in the nucleus-like	B	nuclear	All
A0A060W734	ciapin1	CIAPIN1	Anamorsin	J	nuclear	Control+PIC
XP_021445248.1	eif4g3b	EIF4G3	extended synaptotagmin-2-B-like isoform X1		nuclear	PIC
XP_021445248.1	eif4g3b	EIF4G3	eukaryotic translation initiation factor 4 gamma 3-like isoform X13	J		PIC
XP_021465211.1	ncl	NCL	nucleolin	AJ	nuclear	All
XP_021447382.1	rpl23a	RPL23A	60S ribosomal protein L23a-like	J	Cytoplasmic	PIC
A0A060XX58	ncapd2	NCAPD2	Condensin complex subunit 1	BD	Cytoplasmic _nuclear	All

XP_021428051.1	abcf1	ABCF1	ATP-binding cassette sub-family F member 1-like isoform X2	J	Cytoplasmic	PIC
A0A060VNP2	esyt2a	ESYT2	C12orf43	S	endoplasmic reticulum	All
XP_021480998.1	pdcl3	PDCL3	ubinuclein-2-like isoform X2	KT	Cytoplasmic	PIC
XP_021432914.1	rpap3	RPAP3	RNA polymerase II-associated protein 3-like isoform X1	J	Cytoplasmic _nuclear	PIC
XP_021454383.1	api5	API5	apoptosis inhibitor 5-like	T	Cytoplasmic _nuclear	All
P_020321066.1	ssh2b	SSH2	protein phosphatase Slingshot homolog 2-like isoform X2	V	nuclear	PIC
XP_021460839.1	rbm15b	RBM15B	putative RNA-binding protein 15B	S	nuclear	PIC
XP_020349866.1	rpl22l1	RPL22L1	60S ribosomal protein L22-like 1	J	nuclear	All
A0A060VRL5	katna1	KATNA1	Katanin p60 ATPase-containing subunit A1	O	Cytoplasmic	PIC
XP_021436210.1	ptprea	PTPRE	receptor-type tyrosine-protein phosphatase epsilon-like isoform X2	S	Cytoplasmic	PIC
XP_021480762.1	poldip3	POLDIP3	polymerase delta-interacting protein 3-like isoform X1	A	Cytoplasmic	PIC
XP_021427160.1	pdxkb	PDXK	pyridoxal kinase-like	H	Cytoplasmic	PIC
XP_021449661.1	phf3	PHF3	PHD finger protein 3-like	K	nuclear	PIC
XP_021423059.1	lsp1	LSP1	non-muscle caldesmon-like	T	nuclear	Control+PIC
XP_021471795.1	ube4b	UBE4B	ubiquitin conjugation factor E4 B isoform X4	O	nuclear	All
A0A060XMQ3	u2af2b	U2AF2	U2 snRNP auxiliary factor large subunit	A	nuclear	All
XP_021425993.1	fblim1	FBLIM1	filamin-binding LIM protein 1-like	S	nuclear	MDP+PIC
XP_021419904.1	snd1	SND1	staphylococcal nuclease domain-containing protein 1-like	K	Cytoplasmic	Control+PIC
XP_021430107.1	srsf11	SRSF11	serine/arginine-rich splicing factor 11-like isoform X1	A	extracellular	Control+PIC
XP_020308207.1	map7d3	MAP7D3	ensconsin-like isoform X1	Z	nuclear	PIC
XP_021426653.1	pspc1	PSPC1	paraspeckle component 1-like	K	Cytoplasmic	Control+PIC
XP_021453368.1	mphosph8	MPHOSPH8	M-phase phosphoprotein 8-like isoform X3	B	nuclear	PIC
XP_021469759.1	ranbp3b	RANBP3	ran-binding protein 3-like isoform X1	U	nuclear	PIC
XP_021451121.1	map7d1a	MAP7D1	MAP7 domain-containing protein 1-like	Z	nuclear	PIC

O93245	ar	AR	Androgen receptor beta	T	nuclear	PIC
XP_024253232.1	fubp3	FUBP3	far upstream element-binding protein 3-like isoform X8	A	Cytoplasmic _cytoskeleton	PIC
XP_021419484.1	parpbp	PARPBP	PCNA-interacting partner-like	L	nuclear	PIC
XP_021454601.1	cdkn1ba	CDKN1B	cyclin-dependent kinase inhibitor 1B-like	T	nuclear	PIC
XP_021467118.1	papola	PAPOLB	poly(A) polymerase type 3	A	nuclear	PIC
XP_020317820.1	itga4	ITGA4	integrin alpha-4-like	W	extracellular	MDP+PIC
XP_021480553.1	smg9	SMG9	protein SMG9 isoform X2	A	plasma membrane	PIC
XP_021430418.1	mtfr1l	MTFR1L	mitochondrial fission regulator 1-like isoform X1	K	mitochondrial	All
NP_001265967.1	sap30l	SAP30L	Histone deacetylase complex subunit SAP30L	K	nuclear	PIC
NP_001167391.1	aldoaa	ALDOA	fructose-bisphosphate aldolase A	G	Cytoplasmic	All
XP_021456165.1	itpkb	ITPKB	inositol-trisphosphate 3-kinase B-like	I	extracellular	PIC
XP_024295229.1	scaf11	SCAF11	protein SCAF11-like	O	nuclear	All
XP_021419608.1	scaf11	SCAF11	protein SCAF11-like	A	nuclear	All
XP_021458454.1	nup155	NUP155	uclear pore complex protein Nup155	UY	Cytoplasmic	PIC
XP_021461664.1	pdlim2	PDLIM2	PDZ and LIM domain protein 2-like isoform X2	TZ	mitochondrial	PIC
P_021443651.1	synrg	SYNRG	synergin gamma-like isoform X3	TU	nuclear	PIC
XP_020338646.1	ift52	IFT52	intraflagellar transport protein 52 homolog	W	Cytoplasmic	PIC
A0A060XY23	mep1b	MEP1B	Metalloendopeptidase	O	plasma membrane	PIC
XP_021454850.1	bend5	BEND5	BEN domain-containing protein 5-like isoform X2	S	nuclear	PIC
XP_021427847.1	akap9	AKAP9	A-kinase anchor protein 9-like isoform X8	T	nuclear	PIC
A0A1S3Q8Y9	scrib	SCRIB	protein scribble homolog isoform X13	S	nuclear	All
XP_020351123.1	srsf2a	SRSF8	serine/arginine-rich splicing factor 2-like	A	nuclear	PIC
XP_021448119.1	rnf146	RNF146	E3 ubiquitin-protein ligase rnf146-like	O	nuclear	PIC
XP_024276922.1	dock7	DOCK7	dedicator of Cytoplasmickinesis protein 7 isoform X9	T	endoplasmic reticulum	Control+PIC
XP_021465597.1	smarcc2	SMARCC2	SWI/SNF complex subunit SMARCC2-like	B	nuclear	PIC

XP_021430590.1	ndufaf1	NDUFAF1	complex I intermediate-associated protein 30, mitochondrial	S	mitochondrial	PIC
XP_021440829.1	pnn	PNN	pinin-like	Z	nuclear	PIC
A0A1S3PUV7	rras2	RRAS2	ras-related protein R-Ras2 isoform X1	S	extracellular	PIC
XP_021423409.1	cdkn1bb	CDKN1B	cyclin-dependent kinase inhibitor 1B	T	nuclear	PIC
XP_021476489.1	cdk13	CDK13	cyclin-dependent kinase 13-like isoform X2	T	nuclear	All
XP_021459082.1	rabgap1l	RABGAP1L	rab GTPase-activating protein 1-like	T	nuclear	PIC
XP_021476126.1	cct5	CCT5	T-complex protein 1 subunit epsilon	O	Cytoplasmic	PIC
XP_021465141.1	frmd4ba	FRMD4B	FERM domain-containing protein 4B-like isoform X5	Z	plasma membrane	PIC
XP_021412677.1	sept9b	40057	neuronal-specific septin-3-like isoform X1	DTZ	Cytoplasmic _nuclear	PIC
XP_021469967.1	lig1	LIG1	DNA ligase 1-like	L	nuclear	PIC
XP_021441910.1	tcf12	TCF12	transcription factor 12 isoform X5	K	nuclear	PIC
XP_021431928.1	snx20	SNX20	sorting nexin-20	U	Cytoplasmic	PIC
XP_021430325.1	iars2	IARS2	isoleucine--tRNA ligase, mitochondrial	J	mitochondrial	PIC
XP_021424998.1	strip1	STRIP1	striatin-interacting protein 1 homolog	S	Cytoplasmic	PIC
XP_021470667.1	fxr2	FXR2	fragile X mental retardation syndrome-related protein 1-like	A	nuclear	Control+PIC
XP_021444732.1	nfatc4	NFATC4	nuclear factor of activated T-cells, Cytoplasmicplasmic 4-like	K	nuclear	PIC
XP_021449500.1	smarcc1a	SMARCC1	SWI/SNF complex subunit SMARCC1	B	nuclear	All
A0A060W7T9	aclya	ACLY	ATP-citrate synthase	C	Cytoplasmic	Control+PIC
A0A060Z0A8	pds5b	PDS5B	bad matching	D	mitochondrial	PIC
XP_021418579.1	asap1b	ASAP1	arf-GAP with SH3 domain, ANK repeat and PH domain-containing protein 1-like isoform X1	T	nuclear	PIC
XP_021460938.1	mapkapk5	MAPKAPK5	MAP kinase-activated protein kinase 5-like isoform X2	T	Cytoplasmic	PIC
XP_021464499.1	prkx	PRKX	cAMP-dependent protein kinase catalytic subunit PRKX-like		mitochondrial	PIC
XP_021432988.1	pfkfb3	PFKFB3	6-phosphofructo-2-kinase/fructose-2,6-bisphosphatase 3-like isoform X1	G	nuclear	PIC
XP_021456230.1	cd2ap	CD2AP	CD2-associated protein-like isoform X3	D/Z/T	mitochondrial	Control+PIC

A0A060ZEH8	papss1	PAPSS1	Adenylyl-sulfate kinase	F	nuclear	Control+PIC
XP_021427476.1	nelfe	NELFE	negative elongation factor E-like isoform X1	K	nuclear	PIC
XP_021465957.1	eif4enif1	EIF4ENIF1	eukaryotic translation initiation factor 4E transporter-like isoform X1	J	extracellular	PIC
XP_021428272.1	slc30a8	SLC30A8	regulation of nuclear pre-mRNA domain-containing protein 1A-like isoform X2	A	nuclear	PIC
XP_021473547.1	prr11	PRR11	proline-rich protein 11-like isoform X2	S	mitochondrial	PIC
XP_024241945.1	pnisr	PNISR	arginine/serine-rich protein PNISR-like isoform X1	S	nuclear	PIC
XP_021474937.1	pcm1	PCM1	pericentriolar material 1 protein-like isoform X1	Z	nuclear	PIC
XP_021419722.1	zc3hc1	ZC3HC1	nuclear-interacting partner of ALK-like isoform X1	S	extracellular	PIC
XP_020344432.1	iqgap1	IQGAP1	ras GTPase-activating-like protein	T	extracellular	PIC
A0A060Y486	kif23	KIF23	Kinesin-like protein	Z	nuclear	Control+PIC
XP_021470370.1	papolg	PAPOLG	poly(A) polymerase gamma-like	A	plasma membrane	PIC
XP_021446539.1	cicb	CIC	protein ca3ua homolog	K	nuclear	PIC
XP_021462871.1	ctdspl2a	CTDSPL2	CTD small phosphatase-like protein 2 isoform X1		nuclear	PIC
XP_021437744.1	arhgef1b	ARHGEF1	rho guanine nucleotide exchange factor 1-like	T	Cytoplasmic	PIC
A0A1S3MJG6	tbc1d15	TBC1D15	TBC1 domain family member 15-like	T	plasma membrane	PIC
XP_021430154.1	zfyve19	ZFYVE19	abscission/NoCut checkpoint regulator	S	mitochondrial	PIC
XP_021448714.1	nacad	NACAD	mucin-17-like isoform X1	K	nuclear	PIC
A0A060WAA1	gpatch8	GPATCH8			nuclear	PIC
XP_021476532.1	atxn2	ATXN2	ataxin-2-like	A	mitochondrial	PIC
XP_021457298.1	map3k1	MAP3K1	mitogen-activated protein kinase kinase kinase 1 isoform X1	T	nuclear	PIC
XP_021453584.1	phf11	PHF11	PHD finger protein 11-like isoform X2	K	nuclear	PIC
XP_021416851.1	foxo4	FOXO4	forkhead box protein O4	K	nuclear	PIC
XP_020341969.1, XP_021413269.1	igf2bp1	IGF2BP1	insulin-like growth factor 2 mRNA-binding protein 1 isoform X1	A	Cytoplasmic	PIC
XP_021432795.1	ppp1r12a	PPP1R12A	protein phosphatase 1 regulatory subunit 12A-like isoform X9	OT	nuclear	Control+PIC

XP_021441573.1	dync1li2	DYNC1LI2	Cytoplasmicplasmic dynein 1 light intermediate chain 2-like isoform X1	N	mitochondrial	PIC
XP_021443363.1	ccdc9	CCDC9	coiled-coil domain-containing protein 9-like isoform X2	S	nuclear	PIC
XP_021460778.1	tmcc3	TMCC3	transmembrane and coiled-coil domains protein 3-like isoform X1	S	plasma membrane	PIC
C1BFZ7	ndufs7	NDUFS7	NADH dehydrogenase iron-sulfur protein 7, mitochondrial	C	mitochondrial	PIC
XP_024242025.1	sec24c	SEC24C	protein transport protein Sec24C-like	U	nuclear	PIC
XP_021413419.1	trim33l	TRIM28	transcription intermediary factor 1-alpha-like	O	nuclear	PIC
XP_021447324.1	alg5	ALG5	dolichyl-phosphate beta-glucosyltransferase	M	extracellular	PIC
XP_020310264.1	znf292b	ZNF292	zinc finger protein 292-like	nuclear		PIC
NP_001167240.1	akt1s1	AKT1S1	Proline-rich AKT1 substrate 1	T	nuclear	PIC
XP_021428626.1	evx1	EVX1	homeobox protein XHOX-3-like	K	nuclear	PIC
XP_021467890.1	ubr7	RP11-371E8.4	putative E3 ubiquitin-protein ligase UBR7	T	Cytoplasmic	Control+PIC
XP_021438926.1	ahnak	AHNAK	neuroblast differentiation-associated protein AHNAK-like	O	Cytoplasmic	PIC
XP_021455136.1	serbp1a	SERBP1	plasminogen activator inhibitor 1 RNA-binding protein-like isoform X4	J	nuclear	PIC
XP_021467627.1	igf2r	IGF2R	cation-independent mannose-6-phosphate receptor-like	T	plasma membrane	PIC
XP_021473170.1	sh3pxd2b	SH3PXD2B	SH3 and PX domain-containing protein 2B-like isoform X3	C	nuclear	PIC
XP_021454947.1	rabggta	RABGGTA	geranylgeranyl transferase type-2 subunit alpha	O	Cytoplasmic	PIC
XP_021455047.1	fryl	FRYL	protein furry homolog-like isoform X10	S	plasma membrane	PIC
A0A060YNW5	dusp1	DUSP1	Dual specificity protein phosphatase	V	plasma membrane	PIC
XP_021469626.1	sugp1	SUGP1	SURP and G-patch domain-containing protein 1-like	S	nuclear	PIC
XP_024279969.1	celf2	CELF2	CUGBP Elav-like family member 2 isoform X11	A	Cytoplasmic _nuclear	PIC
ACN58663.1	psmd11b	PSMD11	26S proteasome non-ATPase regulatory subunit 11, partial	O	Cytoplasmic	PIC

XP_020327183.1	xirp2a	XIRP2	xin actin-binding repeat-containing protein 2-like	TZ	Cytoplasmic	PIC
XP_021457465.1	odf2a	ODF2	outer dense fiber protein 2-like isoform X2	Z	nuclear	PIC
A0A060XPG0	mvda	MVD	Diphosphomevalonate decarboxylase	I	Cytoplasmic _nuclear	PIC
XP_021422086.1	csde1	CSDE1	cold shock domain-containing protein E1-like isoform X12	J	nuclear	PIC
XP_021417540.1	synpo	SYNPO	synaptopodin-like isoform X1	S	nuclear	PIC
XP_021478237.1	wdr91	WDR91	WD repeat-containing protein 91	S	extracellular	PIC
XP_021460781.1	zfr	ZFR	zinc finger RNA-binding protein-like	C	nuclear	PIC
XP_021421461.1	atf7a	RP11-793H13.10	cyclic AMP-dependent transcription factor ATF-7-like isoform X5	K	nuclear	PIC
XP_020308224.1	arhgef6	ARHGEF6	rho guanine nucleotide exchange factor 6-like isoform X1	T	nuclear	All
XP_021424546.1	tacc1	TACC1	transforming acidic coiled-coil-containing protein 1-like	S	nuclear	PIC
XP_021448247.1	slc4a7	SLC4A7	sodium bicarbonate cotransporter 3-like, partial	P	extracellular	PIC
XP_021474011.1	atrx	ATRX	transcriptional regulator ATRX-like	K	plasma membrane	All
XP_021456107.1	igf2r	IGF2R	cation-independent mannose-6-phosphate receptor-like	T	plasma membrane	PIC
XP_021473208.1	pwwp2a	PWWP2A	PWWP domain-containing protein 2A-like	S	nuclear	PIC
XP_021419104.1	tmpoa	TMPO	lamina-associated polypeptide 2, isoforms beta/gamma-like isoform X2	S	periplasmic	PIC
XP_021431770.1	kctd2	KCTD2	BTB/POZ domain-containing protein KCTD5-like	S	nuclear	PIC
XP_021425240.1	slc2a1b	SLC2A1	solute carrier family 2, facilitated glucose transporter member 1-like		plasma membrane	All
P_021420027.1	kmt2ca	KMT2C	histone-lysine N-methyltransferase 2C-like		nuclear	PIC
XP_021429951.1	tacc3	TACC3	transforming acidic coiled-coil-containing protein 3-like	S	nuclear	PIC
A0A060WTG1	ybx1	YBX1	nuclease-sensitive element-binding protein 1-like isoform X2	J	nuclear	PIC
XP_021466471.1	nol8	NOL8	nucleolar protein 8	S	nuclear	PIC

XP_021442129.1	cpsf6	CPSF6	cleavage and polyadenylation specificity factor subunit 7-like isoform X2	A	nuclear	PIC
XP_021471729.1	ndrg3b	NDRG3	protein NDRG3-like isoform X5	S	Cytoplasmic	PIC
XP_021443382.1	baz1b	BAZ1B	tyrosine-protein kinase BAZ1B-like	T	nuclear	PIC
XP_021479768.1	pdlim4	PDLIM4	PDZ and LIM domain protein 4-like	TZ	nuclear	PIC
XP_024230633.1	yes1	YES1	tyrosine-protein kinase Ye	mitochondrial		PIC
P_021423546.1	sh3pxd2aa	SH3PXD2A	SH3 and PX domain-containing protein 2A-like isoform X2	C	nuclear	PIC
XP_021419890.1	slc41a2b	SLC41A2	solute carrier family 41 member 2-like	P	plasma membrane	PIC
XP_021430362.1	kif13ba	KIF13B	kinesin-like protein KIF13B	Z	nuclear	PIC
XP_020358161.1	rapgef2	RAPGEF2	rap guanine nucleotide exchange factor 2 isoform X2	S	nuclear	PIC
P_020341796.1	taok2a	TAOK2	serine/threonine-protein kinase TAO2 isoform X2	T	nuclear	PIC
XP_021422254.1	vapb	VAPB	vesicle-associated membrane protein-associated protein B-like isoform X1	U	plasma membrane	PIC
XP_021479505.1	vps11	VPS11	vacuolar protein sorting-associated protein 11 homolog	U	Cytoplasmic	PIC
XP_021428177.1	chkb	CHKB-CPT1B	choline/ethanolamine kinase	I	Cytoplasmic	PIC
A0A060WUI1	aldoaa	ALDOA	Fructose-bisphosphate aldolase	G	Cytoplasmic	PIC
XP_021468445.1	sec62	SEC62	translocation protein SEC62-like	U	nuclear	PIC
XP_021457356.1	lmnb1	LMNB1	lamin-B1	DY	Cytoplasmic	PIC
XP_021417149.1	zbtb33	ZBTB33	transcriptional regulator Kaiso	K	nuclear	PIC
XP_021463255.1	cpsf6	CPSF6	cleavage and polyadenylation specificity factor subunit 7-like isoform X1	A	nuclear	PIC
XP_021454164.1	utrn	UTRN	utrophin-like	Z	nuclear	PIC
XP_021471861.1	csde1	CSDE1	cold shock domain-containing protein E1-like isoform X8	k	nuclear	PIC
XP_020317393.1	rbm45	RBM45	RNA-binding protein 45-like	S	Cytoplasmic _nuclear	PIC
A0A060X9N5	sf3b3	SF3B3		A	Cytoplasmic _nuclear	PIC
XP_021451939.1	baiap2l1b	BAIAP2L1	brain-specific angiogenesis inhibitor 1-associated protein 2-like protein 1	T	extracellular	PIC

XP_021473697.1	flot2a	FLOT2	flotillin-2a	UZ	Cytoplasmic	PIC
XP_020313968.1	atp2a2b	ATP2A2	sarcoplasmic/endoplasmic reticulum calcium ATPase 2-like isoform X2	P	plasma membrane	PIC
XP_020336675.1	ccnd2a	CCND2	1/S-specific cyclin-D2 isoform X1	D	extracellular	PIC
XP_021416130.1	anp32e	ANP32E	acidic leucine-rich nuclear phosphoprotein 32 family member E-like	T	nuclear	PIC
XP_021413021.1	tomm20b	TOMM20	mitochondrial import receptor subunit TOM20 homolog	U	extracellular	PIC
XP_021420218.1	taf6	TAF6	transcription initiation factor TFIID subunit 6-like isoform X1	K	nuclear	PIC
XP_021438876.1	arhgef6	ARHGEF6	rho guanine nucleotide exchange factor 6-like	T	nuclear	PIC
XP_021440826.1	ctage5	CTAGE6	cTAGE family member 5-like isoform X8	J	Cytoplasmic	PIC
XP_020328076.1	srsf5b	SRSF5	serine/arginine-rich splicing factor 5-like isoform X2	A	nuclear	Control+PIC
XP_021458140.1	gpsm1b	GPSM1	G-protein-signaling modulator 1-like	T	extracellular	PIC
A0A060YZ54	arhgef7b	ARHGEF7	bad matching	T	extracellular	PIC
XP_021460947.1	hsp90b1	HSP90B1	endoplasmin-like	O	Cytoplasmic	PIC
A0A060WE27	atp6v0a2a	ATP6V0A2	V-type proton ATPase subunit a	C	plasma membrane	PIC
XP_021461659.1	rab11fip1a	RAB11FIP1	titin-like isoform X1	S	nuclear	PIC
A0A060VPK5	cnn3b	CNN3	Calponin	Z	Cytoplasmic	PIC
XP_021413811.1	ilf3b	ILF3	interleukin enhancer-binding factor 3 isoform X2	J	endoplasmic reticulum	All
A0A060VWT9	rnf217	RNF217	RBR-type E3 ubiquitin transferase	O	Cytoplasmic _nuclear	PIC
XP_021434978.1	safb	SAFB	scaffold attachment factor B2-like isoform X1	K	nuclear	All
A0A060W0C6	top2a	TOP2A	DNA topoisomerase 2	B	nuclear	All
XP_021429354.1	wdhd1	WDHD1	WD repeat and HMG-box DNA-binding protein 1 isoform X1	S	nuclear	All
XP_021455314.1	nasp	NASP	histone-binding protein N1/N2-like isoform X1	BD	nuclear	PIC
XP_021421617.1	cbx5	CBX5	chromobox protein homolog 5-like	B	nuclear	Control+PIC
XP_021463802.1	polr2m	POLR2M	early endosome antigen 1-like	K	nuclear	PIC
XP_021458500.1	rai14	RAI14	ankycorbin-like isoform X1	nuclear		All

XP_021468954.1	toe1	TOE1	target of EGR1 protein 1-like	L	nuclear	All
XP_021439667.1	ctnnd1	CTNND1	catenin delta-1	TW	nuclear	All
XP_021429616.1	irf2bpl	IRF2BPL	interferon regulatory factor 2-binding protein-like	K	nuclear	Control+PIC
XP_021442908.1	iws1	IWS1	protein IWS1 homolog	K	nuclear	All
A0A060W6N3	lect2l	LECT2	uncharacterized	S	extracellular	PIC
XP_021419110.1	calua	CALU	calumenin-A-like isoform X1	TU	extracellular	MDP+PIC
XP_021473945.1	ercc6l	ERCC6L	DNA excision repair protein ERCC-6-like isoform X2	KL	nuclear	MDP+PIC
XP_021459326.1	safb	SAFB	scaffold attachment factor B2-like isoform X2	K	nuclear	MDP+PIC
XP_021418844.1	iws1	IWS1	protein IWS1 homolog isoform X1	K	nuclear	MDP+PIC
A0A060WE49	kpna2	KPNA2	Importin subunit alpha	U	Cytoplasmic _nuclear	All
XP_021465682.1	atf7a	RP11-793H13.10	cyclic AMP-dependent transcription factor ATF-7-like isoform X6	K	nuclear	PIC
XP_021420911.1	usp31	USP31	ubiquitin carboxyl-terminal hydrolase 31-like	O	mitochondrial	PIC
XP_021477387.1	morc2	MORC2	MORC family CW-type zinc finger protein 2A-like isoform X2	D	nuclear	MDP+PIC
XP_021462858.1	tjp1a	TJP1	tight junction protein ZO-1 isoform X11	T	nuclear	All
A0A060WGZ9	psma3	PSMA3	Proteasome subunit alpha type	O	Cytoplasmic _nuclear	All
A0A060WHD0	wnt11r	WNT11	Protein Wnt	T	extracellular	Control+PIC
NP_001153993.1	fth1a	FTMT	Ferritin, heavy subunit	P	Cytoplasmic	All
XP_021427474.1	skiv2l	SKIV2L	helicase SKI2W	A	Cytoplasmic	Control+PIC
XP_021459691.1	eif4g2a	EIF4G2	eukaryotic translation initiation factor 4 gamma 2-like	J	Cytoplasmic	PIC
XP_021456229.1	trim44	TRIM44	tripartite motif-containing protein 44-like isoform X1	S	extracellular	PIC
XP_021424996.1			putative RNA-binding protein 15	K	nuclear	Control
A0A060WJD0	lta4h	LTA4H	Leukotriene A(4) hydrolase	EIOV	Cytoplasmic	MDP+PIC
XP_021454809.1	pak2b	PAK2	serine/threonine-protein kinase PAK 2-like isoform X2	S	mitochondrial	PIC
XP_021479558.1	capn5b	CAPN5	calpain-5-like	OT	mitochondrial	PIC

XP_021441376.1	wdr43	WDR43	WD repeat-containing protein 43-like	S	nuclear	All
XP_021471344.1	srsf6a	SRSF6	serine/arginine-rich splicing factor 6-like	A	nuclear	Control+PIC
XP_021413250.1	cbx1a	CBX1	chromobox protein homolog 1-like	B	nuclear	All
XP_020359488.1	eif4h	EIF4H	eukaryotic translation initiation factor 4H-like isoform X2	J	nuclear	All
XP_021413914.1	ddx5	DDX5	probable ATP-dependent RNA helicase DDX5 isoform X1	A	nuclear	All
XP_021479220.1	rps6kb1b	RPS6KB1	ribosomal protein S6 kinase beta-1-like isoform X2	T	Cytoplasmicplasmic_nuclear	PIC
XP_021455731.1	pum2	PUM2	pumilio homolog 2-like isoform X5	J	nuclear	All
XP_021468674.1	pcyt1aa	PCYT1A	choline-phosphate cytidylyltransferase A-like	I	nuclear	PIC
XP_021423892.1	psen2	PSEN2	presenilin-2	T	Cytoplasmic	Control+PIC
XP_021429038.1	cfap44	CFAP44	cilia- and flagella-associated protein 44	S	nuclear	Control+PIC
XP_021460965.1	smn1	SMN2	survival motor neuron protein 1-like	A	nuclear	All
XP_021437541.1	tmem120a	TMEM120A	transmembrane protein 120A-like	S	Cytoplasmic	PIC
XP_021414111.1	dek	DEK	protein DEK-like isoform X1	B	nuclear	All
XP_021466363.1	ncoa5	NCOA5	nuclear receptor coactivator 5 isoform X2	UY	nuclear	Control+PIC
XP_020313564.1	pi4kaa	PI4KA	phosphatidylinositol 4-kinase alpha-like isoform X1	T	plasmamembrane	PIC
A0A060X7V7	mapk14b	MAPK14	Mitogen-activated protein kinase	K	Cytoplasmic	PIC
XP_021412908.1	trim25	TRIM25	E3 ubiquitin/ISG15 ligase TRIM25-like isoform X1	O	nuclear	All
XP_024235446.1	phrf1	PHRF1	PHD and RING finger domain-containing protein 1-like isoform X1	O	nuclear	Control+PIC
XP_021479535.1	mark4a	MARK4	MAP/microtubule affinity-regulating kinase 4-like isoform X2	T	nuclear	MDP+PIC
XP_021465514.1	nucks1a	NUCKS1	nuclear ubiquitous casein and cyclin-dependent kinase substrate 1-like	T	nuclear	All
XP_021422062.1	spen	SPEN	msx2-interacting protein isoform X3	K	nuclear	MDP+PIC
XP_021433892.1	rbm4.2	RBM14-RBM4	RNA-binding protein 4.1-like isoform X3	A	nuclear	All
XP_021433911.1	eml3	EML3	echinoderm microtubule-associated protein-like 3 isoform X1	S	nuclear	PIC

XP_021428007.1	anln	ANLN	anillin-like isoform X1	DZ	nuclear	PIC
A0A060XDM3	stmn1b	STMN1	Stathmin	Z	nuclear	PIC
XP_021478448.1	fam169ab	FAM169A	soluble lamin-associated protein of 75 kDa-like	S	Cytoplasmic _nuclear	PIC
A0A060XNQ2	smc4	SMC4	Structural maintenance of chromosomes protein	BD	mitochondrial	All
XP_024236216.1	ciz1a	CIZ1	cip1-interacting zinc finger protein-like isoform X3	S	nuclear	MDP+PIC
XP_024299836.1	abi2b	ABI2	abl interactor 2-like isoform X2	T	mitochondrial	PIC
XP_021472426.1	cbx5	CBX5	chromobox protein homolog 5-like	B	nuclear	Control+PIC
XP_021441913.1	znf280d	ZNF280B	zinc finger protein 280D	K	nuclear	Control+PIC
XP_021425058.1	nucks1a	NUCKS1	nuclear ubiquitous casein and cyclin-dependent kinase substrate 1-like isoform X1	T	nuclear	All
XP_021428072.1	nsun2	NSUN2	tRNA (Cytoplasmicsine(34)-C(5))-methyltransferase-like isoform X1	A	nuclear	All
XP_021471434.1	tpx2	TPX2	targeting protein for Xklp2-like isoform X1	Z	nuclear	Control+PIC
XP_021469599.1	cactin	CACTIN	cactin-like	T	nuclear	PIC
ACO07861.1	ptges3a	PTGES3	Prostaglandin E synthase 3	O	extracellular	All
XP_021457136.1	hdlbpa	HDLBP	vigilin	I	Cytoplasmic	Control+PIC
XP_021457627.1	purba	PURB	transcriptional activator protein Pur-beta-like	K	Cytoplasmic	All
XP_021475652.1	taok3a	TAOK3	serine/threonine-protein kinase TAO3-like	T	nuclear	MDP+PIC
A0A060Y668	cav1	CAV1	Caveolin	T	plasma membrane	MDP+PIC
XP_021432401.1	lrit2	LRIT2	leucine-rich repeat, immunoglobulin-like domain and transmembrane domain-containing protein 2	T	plasma membrane	Control+PIC
XP_021417518.1	g3bp1	G3BP1	ras GTPase-activating protein-binding protein 1-like	T	Cytoplasmic	All
XP_021461836.1	morc2	MORC2	MORC family CW-type zinc finger protein 2A-like isoform X1	D	nuclear	MDP+PIC
XP_021440591.1	rbm12b	RBM12B	RNA-binding protein 12B-like	S	nuclear	Control+PIC
XP_021436768.1	exoc7	EXOC7	exocyst complex component 7 isoform X11	U	Cytoplasmic	PIC
XP_021439069.1	hnrnph1	HNRNPH1	heterogeneous nuclear ribonucleoprotein H-like	A	nuclear	Control+PIC

XP_021419839.1	nap1l4a	NAP1L4	nucleosome assembly protein 1-like 4 isoform X1	BD	nuclear	Control+PIC
XP_021475129.1	g3bp2	G3BP2	ras GTPase-activating protein-binding protein 2-like isoform X2	T	Cytoplasmic	All
XP_021480823.1	rangap1a	RANGAP1	ran GTPase-activating protein 1-like isoform X1	T	Cytoplasmic	MDP+PIC
XP_021463402.1	nipa2	NIPA2	magnesium transporter NIPA2 isoform X1	G	plasma membrane	All
XP_021449693.1	gpatch4	GPATCH4	G patch domain-containing protein 4	AD	nuclear	MDP+PIC
XP_021415506.1	cdca7b	CDCA7L	cell division cycle-associated 7-like protein	D	nuclear	Control+PIC
XP_021449193.1			protein DEK-like isoform X2	|B	nuclear	Control
XP_024264953.1	tacc2	TACC2	transforming acidic coiled-coil-containing protein 2-like isoform X2	S	nuclear	PIC
A0A060Z608	tp53	TP53	Cellular tumor antigen p53	K	nuclear	All
XP_021414894.1	rbbp6	RBBP6	E3 ubiquitin-protein ligase RBBP6-like	O	nuclear	PIC
A9Z0N2			Ribosomal protein S3	J	mitochondrial	Control
C0KIP5	tk1	TK1	Thymidine kinase	F	Cytoplasmic	All
C1BEG9	stmn1b	STMN1	Stathmin	Z	nuclear	PIC
C1BER5	syap1	SYAP1	Synapse-associated protein 1	U	Cytoplasmic	All
C1BF68	psma3	PSMA3	Proteasome subunit alpha type	O	Cytoplasmic	All
C1BH87	ppa1b	PPA1	Inorganic pyrophosphatase	C	Cytoplasmic	All
C1BHT0	rbm8a	RBM8A	RNA-binding protein 8A	A	nuclear	PIC
Q1XG85	pum2	PUM2	Pumilio-2B	J	nuclear	MDP+PIC

[1]Functional groups: A= RNA processing and modification, B= Chromatin structure and dynamics, C =Energy production and conversion, D =Cell cycle control, cell division, chromosome partitioning, E =Amino acid transport and metabolism, F= Nucleotide transport and metabolism, G = Carbohydrate transport and metabolism, H = Coenzyme transport and metabolism, I =Lipid transport and metabolism, J= Translation, ribosomal structure and biogenesis, K =Transcription, L = Replication, recombination and repair, N =Cell motility, O =Post-translational modification, protein turnover, and chaperones, P =Inorganic ion transport and metabolism, S =Function unknown, T =Signal transduction mechanisms, U =Intracellular trafficking, secretion, and vesicular transport, V =Defence mechanisms, W =Extracellular structure and Z =Cytoskeleton. PIC denotes poly(I:C).

Table S3.3: Predicted pathways identified from the phospho-proteins using *Enrichr* tool. Pathways that are significantly enriched was selected.

Pathways	Adjusted p-value			Control_ Associated genes	MDP_ Associated genes	Poly(I:C)_ Associated genes
	Control	MDP	PIC			
Spliceosome	0.00	0.00	0.00	SNW1;HSPA1L;U2AF2;SRSF1;TRA2A;SRSF3;ACIN1;SRSF5;SRSF9	DDX5;SNW1;HSPA1L;U2AF2;SRSF1;TRA2A;SRSF3;ACIN1;SRSF5;SRSF9	DDX5;SF3B3;HSPA1L;RBM8A;SRSF1;SNW1;U2AF2;TRA2A;SRSF3;ACIN1;SRSF5;SRSF6;SRSF8;SRSF9
Salmonella infection	0.02	0.00	0.01	TJP1;DYNC1H1;MYH9;FLNA;KLC1	TJP1;DYNC1H1;JUN;MYH9;FLNA;KLC1	TJP1;DYNC1H1;JUN;DYNC1LI2;MYH9;FLNA;MAPK14;KLC1
HIF-1 signaling pathway	0.02		0.02	PDHA2;MAP2K2;RPS6;SLC2A1;ALDOA		PDHA2;MAP2K2;PFKFB3;CDKN1B;RPS6KB1;RPS6;SLC2A1;ALDOA
Citrate cycle (TCA cycle)	0.03			ACLY;PDHA2;ACO2		
Herpes simplex infection	0.03	0.01	0.01	SRSF1;CDK2;SRSF3;SRSF5;JAK2;SRSF9	JUN;SRSF1;CDK2;SRSF3;SRSF5;TP53;SRSF9	JUN;EEF1D;SRSF1;CDK2;SRSF3;TAF6;SRSF5;SRSF6;JAK2;TP53;SRSF8;SRSF9
Epstein-Barr virus infection	0.04	0.01	0.03	RB1;GSK3B;SNW1;HSPA1L;CDK2;SND1	RB1;GSK3B;JUN;SNW1;HSPA1L;CDK2;TP53	RB1;GSK3B;JUN;SNW1;CDKN1B;PSMD11;HSPA1L;CDK2;MAPK14;TP53;SND1
Viral carcinogenesis	0.04	0.02		RB1;SNW1;CDK2;SCRIB;CHD4;SND1	RB1;JUN;SNW1;CDK2;SCRIB;TP53	
Prostate cancer	0.04	0.01	0.00	RB1;GSK3B;MAP2K2;CDK2	RB1;GSK3B;MAP2K2;CDK2;TP53	RB1;GSK3B;AR;MAP2K2;CDKN1B;CDK2;RAF1;TP53;HSP90B1
Apoptosis		0.01	0.05		JUN;MAP2K2;LMNA;TP53;LMNB2;TUBA8	JUN;MAP2K2;LMNA;RAF1;TP53;LMNB2;TUBA8;LMNB1
Influenza A		0.02			GSK3B;JUN;MAP2K2;HSPA1L;TRIM25;KPNA2	
RNA transport		0.02	0.00		SMN2;TACC3;EIF3CL;ACIN1;RANGAP1;SRRM1	NUP155;RBM8A;RANGAP1;SRRM1;PNN;FXR2;TPR;SMN2;TACC3;EIF3CL;ACIN1;EIF4G3;EIF4G2
Thyroid cancer		0.02	0.03		MAP2K2;CCDC6;TP53	MAP2K2;TPR;CCDC6;TP53
MAPK signaling pathway		0.02	0.00		JUN;MAP2K2;HSPA1L;TAOK3;FLNA;TP53;MAP4K4	JUN;MAP3K1;MAP2K2;HSPA1L;DUSP1;RRAS2;MAPK14;TAOK3;STMN1;TAOK2;RAPGEF2;FLNA;MAPKAPK5;RAF1;TP53;PAK2;MAP4K4
Cell cycle		0.02	0.03		RB1;GSK3B;CDK2;TP53;MCM2	RB1;GSK3B;CDK7;CCND2;CDKN1B;CDK2;TP53;MCM2
Focal adhesion		0.02	0.01		GSK3B;JUN;ITGA4;CAV1;FLNA;PARVA	ITGB1;GSK3B;JUN;CCND2;PPP1R12A;ITGA4;CAV1;FLNA;PARVA;ITGA5;RAF1;PAK2
Bladder cancer		0.02			RB1;MAP2K2;TP53	
Hepatitis B		0.03	0.01		RB1;JUN;MAP2K2;CDK2;TP53	RB1;JUN;MAP3K1;MAP2K2;CDKN1B;CDK2;RAF1;TP53;HSPG2;NFATC4
Pathways in cancer		0.04	0.04		RB1;GSK3B;JUN;MAP2K2;CDK2;CCDC6;SLC2A1;TP53	RB1;ITGB1;GSK3B;JUN;CDKN1B;MAP2K2;SLC2A1;HSP90B1;AR;WNT11;TPR;CDK2;CCDC6;ARHGEF1;RAF1;TP53
Endometrial cancer		0.04			GSK3B;MAP2K2;TP53	

Non-small cell lung cancer	0.05		RB1;MAP2K2;TP53	
Proteoglycans in cancer		0.00		ITGB1;DDX5;MAP2K2;PPP1R12A;CAV1;RPS6;RRAS2;IQGAP1;MAPK14;HSPG2;WNT11;RPS6KB1;FLNA;ARHGEF1;ITGA5;RAF1;TP53
Regulation of actin cytoskeleton		0.00		ITGB1;MAP2K2;PPP1R12A;ITGA4;RRAS2;IQGAP1;SSH2;ABI2;TMSB4Y;MYH9;ARHGEF1;ITGA5;ARHGEF7;RAF1;PAK2;ARHGEF6
ErbB signaling pathway		0.02		GSK3B;JUN;MAP2K2;CDKN1B;RPS6KB1;RAF1;PAK2
HTLV-I infection		0.02		RB1;GSK3B;JUN;RANBP3;MAP3K1;SLC2A1;RRAS2;NFATC4;POLD3;CCND2;WNT11;CANX;TP53
mRNA surveillance pathway		0.03		PNN;CPSF6;RBM8A;PAPOLG;ACIN1;PAPOLB;SRRM1
Neurotrophin signaling pathway		0.03		GSK3B;JUN;MAP3K1;MAP2K2;PSEN2;MAPK14;RAF1;TP53
Prolactin signaling pathway		0.03		GSK3B;CCND2;MAP2K2;MAPK14;RAF1;JAK2
Leishmaniasis		0.03		ITGB1;JUN;MARCKSL1;ITGA4;MAPK14;JAK2
Insulin signaling pathway		0.05		GSK3B;MAP2K2;RPS6KB1;PRKAR1A;EXOC7;RPS6;FLOT2;RAF1

Table S3.4: Predicted kinases identified from the phospho-proteins using *Enrichr* tool. Kinases that are significantly enriched was selected.

Kinases	Adjusted p value			Control _Associated genes	MDP_ Associated genes	Poly(I:C)_ Associated genes
	Control	MDP	PIC			
CDK2	7.81E-20	6.32E-23	8.32E-32	RB1;AHNAK;CHD7;NOLC1;CHD4;ADD3;LMNB2;LARP1;LMNA;RPS3;LBR;SRSF11;USP24;SMARCC1;API5;ATRX;UBE4B;PRPF4B;SRRM1;ACLY;ILF3;SNW1;PRKAR1A;NCL;CDK2;XRN2;CCDC6;TACC3;PPIG;SQSTM1;SRSF9;MCM2	RB1;AHNAK;SYAP1;CHD7;NOLC1;NUCKS1;SMC4;LMNB2;LARP1;LMNA;RPS3;TK1;LBR;USP24;JUN;SMARCC1;API5;ATRX;UBE4B;PRPF4B;RANGAP1;SRRM1;PUM2;ILF3;SNW1;PRKAR1A;NCL;CDK2;CCDC6;TACC3;PPIG;SQSTM1;TP53;SRSF9;MCM2	RB1;CDKN1B;SYAP1;CHD7;NUCKS1;CHD4;SMC4;LMNB2;LMNB1;EIF4ENIF1;STMN1;TK1;CIC;SYNPO;LBR;CAST;SMARCC1;PCYT1A;LIG1;ATRX;UBE4B;PRPF4B;RANGAP1;EML3;SRRM1;ACLY;DYNC1LI2;ILF3;PRKAR1A;HNRNPH1;NCL;XRN2;AKT1S1;PPIG;SQSTM1;TP53;SRSF9;MCM2;AHNAK;UHRF1;NOLC1;PDS5B;ADD3;ADD1;ARHGAP12;LARP1;MAP2;TPR;LMNA;RPS3;RBBP6;TP53BP1;SRSF11;USP24;JUN;API5;PRRC2A;PUM2;ZC3HC1;TPX2;CDK7;SNW1;RPS6KB1;CDK2;CCDC6;TACC3;EIF4G2
GSK3B	1.17E-19	2.08E-19	4.85E-27	RB1;TOP2A;GSK3B;AHNAK;ITSN1;CTNND1;DOCK7;CHD4;ADD3;LMNA;RPS3;FLNA;LBR;USP24;SMARCC1;API5;SGTA;PRPF4B;SRRM1;TJP1;ACLY;SFPQ;SNW1;NCL;CANX;CCDC6;TACC3;PPIG;SQSTM1;MCM2;ARHGEF6	RB1;TOP2A;GSK3B;AHNAK;ITSN1;CTNND1;SYAP1;SMC4;LMNA;RPS3;FLNA;LBR;MAP4K4;USP24;SPEN;JUN;SMARCC1;API5;PRPF4B;SRRM1;TJP1;SFPQ;SNW1;NCL;CCDC6;TACC3;PPIG;SQSTM1;TP53;MCM2;ARHGEF6	RB1;TOP2A;GSK3B;CDKN1B;ITSN1;CTNND1;SYAP1;DOCK7;HDLBP;CHD4;SMC4;LMNB1;EIF4ENIF1;CCND2;PAPOLG;STMN1;CIC;SYNPO;LBR;SMARCC1;SMARCC2;PCYT1A;PRPF4B;SRRM1;ACLY;SFPQ;NCL;CANX;PPIG;SQSTM1;TP53;MCM2;ARHGEF6;AHNAK;PDS5B;ADD3;ADD1;ARHGAP12;MAP2;LMNA;RPS3;FLNA;RBBP6;TP53BP1;PDLIM4;MAP4K4;USP24;SPEN;JUN;ODF2;API5;SGTA;TJP1;TPX2;ANLN;SNW1;RPS6KB1;CCDC6;TACC3;TAF6
MAPK14	3.28E-12	3.47E-13	1.33E-23	RB1;SMARCC1;AHNAK;ATRX;DOCK7;NOLC1;PRPF4B;CHD4;IWS1;SRRM1;TJP1;ACLY;ILF3;SNW1;NCL;CANX;TACC3;FLNA;SKIV2L;SQSTM1;LBR	RB1;SPEN;JUN;SMARCC1;DDX5;AHNAK;ATRX;NOLC1;PRPF4B;RANGAP1;IWS1;SRRM1;TJP1;ILF3;SNW1;NCL;G3BP2;TACC3;FLNA;SQSTM1;LBR;TP53	RB1;PHF3;CDKN1B;DOCK7;HDLBP;CHD4;EIF4ENIF1;CCND2;PAPOLG;STMN1;LBR;SMARCC1;ATRX;PRPF4B;BAZ1B;RANGAP1;SRRM1;AR;ACLY;ILF3;NCL;CANX;AKT1S1;MAPKAPK5;SQSTM1;TP53;DDX5;AHNAK;NOLC1;IWS1;ARHGAP12;MAP2;G3BP2;HIVEP1;FLNA;PDLIM4;SPEN;JUN;MAPK14;NFATC4;TJP1;TPX2;ANLN;SNW1;RPS6KB1;TACC3;TCEA1;SKIV2L;TAF6
CDK1	2.01E-11	5.03E-14	9.40E-23	RB1;TOP2A;TOP2B;SMARCC1;AHNAK;SGTA;NOLC1;PRPF4B;LMNB2;SRRM1;ACLY;SNW1;U2AF2;NCL;CANX;LMNA;RPS3;FLNA;SKIV2L;SQSTM1;LBR;TMPO	RB1;TOP2A;TOP2B;ERCC6L;AHNAK;NOLC1;NUCKS1;LMNB2;U2AF2;LMNA;RPS3;FLNA;TK1;LBR;TMPO;MAP4K4;SPEN;SMARCC1;PRPF4B;RANGAP1;SRRM1;SNW1;NCL;SQSTM1;TP53	RB1;TOP2A;TOP2B;ERCC6L;NUCKS1;LMNB2;LMNB1;STMN1;TK1;CIC;LBR;TMPO;SMARCC1;SMARCC2;PCYT1A;LIG1;DUSP1;PRPF4B;RANGAP1;SRRM1;AR;ACLY;EEF1D;NCL;CANX;AKT1S1;SQSTM1;TP53;AHNAK;NOLC1;PDS5B;ADD1;U2AF2;MAP2;TPR;LMNA;RPS3;FLNA;RBBP6;TP53BP1;PDLIM4;MAP4K4;SPEN;ODF2;SGTA;ZC3HC1;TPX2;ANLN;CDK7;SNW1;NASP;RPS6KB1;SKIV2L
RPS6KA3	9.46E-10	8.74E-09	1.35E-21	TOP2B;GSK3B;SMARCC1;AHNAK;ITSN1;RPS6;NOLC1;PRPF4B;KIF23;ADD3;SRRM1;ACLY;LMNA;FLNA;SKIV2L;PPIG;LBR	TOP2B;USP8;GSK3B;SMARCC1;AHNAK;ITGA4;ITSN1;NOLC1;PRPF4B;SRRM1;PUM2;LMNA;FLNA;PPIG;TP53;LBR	TOP2B;GSK3B;CDKN1B;AHNAK;ITSN1;NOLC1;ATP2A2;FOXO4;PDS5B;YBX1;ADD3;ADD1;ARHGAP12;PNN;TRIM28;MAP2;STMN1;PEA15;LMNA;FLNA;CIC;PAK2;LBR;USP8;SMARCC1;RANBP3;RBM15;SMARCC2;ITGA4;SYNRG;RPS6;PRPF4B;KIF23;SRRM1;PUM2;NFATC4;AR;TPX2;ACLY;SKIV2L;PPIG;RAF1;TP53
PRKCB	1.25E-09	1.43E-11	3.56E-10	TOP2A;GSK3B;AHNAK;CTNND1;NOLC1;UBE4B;SAFB;ADD3;SRRM1;PSMA3;ILF3;LMNA;FLNA;LBR;TMPO	TOP2A;GSK3B;AHNAK;CTNND1;NOLC1;UBE4B;SAFB;RANGAP1;SRRM1;PSMA3;ILF3;LMNA;FLNA;LTA4H;TP53;LBR;TMPO	TOP2A;GSK3B;AHNAK;CTNND1;NOLC1;ADD3;ADD1;LMNB1;STMN1;PEA15;LMNA;FLNA;LTA4H;PAPOLB;PAK2;LBR;TMPO;PCYT1A;UBE4B;SAFB;RANGAP1;SRRM1;PSMA3;ILF3;TP53
MAPK1	4.28E-09	7.81E-09	5.26E-15	TOP2A;GSK3B;AHNAK;CAD;CHD4;SAFB;KLC1;SRRM1;AKAP12;LARP1;XRN2;LMNA;CDK2;RPS3;JAK2;RAI14	TOP2A;GSK3B;JUN;AHNAK;CAD;SAFB;KLC1;SMC4;SRRM1;AKAP12;LARP1;LMNA;CDK2;RPS3;TP53;RAI14	TOP2A;GSK3B;CDKN1B;AHNAK;CHD4;KLC1;SMC4;AKAP12;EIF4ENIF1;LARP1;STMN1;LMNA;TPR;RPS3;CIC;JAK2;JUN;DUSP1;EXOC7;CAD;SAFB;SRRM1;NFATC4;ZC3HC1;AR;TPX2;RPS6KB1;HNRNPH1;XRN2;CDK2;MAPKAPK5;TAF6;RAF1;TP53;RAI14

CHEK1	1.25E-09	2.01E-08	4.77E-16	RB1;MAP2K2;SLTM;SCAF11;LMNA;MINK1;CHD7;CCDC6;PRRC2C;CDK13;KPNA2;ADD3	RB1;SPEN;MAP2K2;SLTM;SCAF11;LMNA;CHD7;CCDC6;CDK13;KPNA2;TP53	RB1;POLDIP3;CHD7;HDLBP;YBX1;ADD3;ADD1;TRIM28;LMNA;HIVEP1;TP53BP1;KPNA2;SPEN;MAP2K2;LIG1;SCAF11;MINK1;PRRC2C;PRRC2B;EML3;ZC3HC1;SLTM;CCDC6;CDK13;TP53
AKT1	1.17E-08	1.39E-07	1.16E-12	GSK3B;SMARCC1;SSB;ITSN1;RPS6;ACLY;ILF3;LMNA;CDK2;RPS3;FLNA;ACIN1;LBR	USP8;GSK3B;ILF3;SMARCC1;SSB;ITSN1;LMNA;CDK2;RPS3;FLNA;ACIN1;LBR	GSK3B;CDKN1B;PFKFB3;ITSN1;FOXO4;YBX1;MAP2;PEA15;LMNA;RPS3;FLNA;RICTOR;LBR;USP8;SMARCC1;SSB;RANBP3;SMARCC2;RPS6;AR;ACLY;ILF3;AKT1S1;CDK2;ACIN1;RAF1
MAPK3	8.19E-07	6.92E-07	3.26E-12	TOP2A;GSK3B;SNW1;CANX;LMNA;CDK2;CAD;CCDC6;RPS3;JAK2;KLC1	TOP2A;GSK3B;JUN;SNW1;LMNA;CDK2;CAD;CCDC6;RPS3;KLC1;TP53	TOP2A;GSK3B;CDKN1B;KLC1;STMN1;LMNA;RPS3;CIC;JAK2;JUN;RANBP3;DUSP1;EXOC7;CAD;BAZ1B;NFATC4;ZC3HC1;AR;SNW1;RPS6KB1;CANX;CDK2;CCDC6;RAF1;TP53
PRKACA	2.34E-06	1.31E-05	1.67E-07	RB1;GSK3B;PPP1R12A;SSB;AHNAK;CBX3;SRSF1;CAD;NOLC1;ADD3;AKAP12;POLD3;ACLY;FLNA	RB1;GSK3B;SSB;AHNAK;ITGA4;CBX3;SRSF1;CAD;NOLC1;AKAP12;POLD3;FLNA;TP53	RB1;GSK3B;PFKFB3;AHNAK;UHRF1;SRSF1;NOLC1;ADD3;ADD1;AKAP12;POLD3;MAP2;STMN1;TPR;FLNA;PDLIM4;PPP1R12A;SSB;ITGA4;CBX3;CAD;NFATC4;ACLY;AKAP9;MAPKAPK5;RAF1;TP53
PRKACB	5.31E-06	4.01E-07	1.40E-05	BCKDK;AHNAK;CBX3;FLNA;PRPF4B;PPIG;SRRM1;ABCF1	BCKDK;AHNAK;CBX3;FLNA;PRPF4B;PPIG;TP53;SRRM1;ABCF1	BCKDK;AHNAK;CBX3;STMN1;FLNA;PRPF4B;PPIG;RAF1;TP53;SRRM1;ABCF1;LMNB1
MAPK9	1.72E-05	1.40E-08	1.96E-13	USP24;MAP2K2;XRN2;ITSN1;RPS3;TMPO;MCM2;ARHGEF6	PURB;USP24;JUN;MAP2K2;ITSN1;RPS3;TP53;TMPO;MCM2;ARHGEF6;MAP4K4	USP24;JUN;MAP2K2;ITSN1;FOXO4;BAZ1B;ADD1;ARHGAP12;NFATC4;LMNB1;PURB;RPS6KB1;XRN2;STMN1;RPS3;MAPKAPK5;SYNPO;TP53;TMPO;MCM2;ARHGEF6;MAP4K4
ATM	6.10E-05	0.0004	3.13E-08	RNF20;WDHD1;RPS6;LMNA;CANX;CCDC6;PRPF4B;CHD4	WDHD1;JUN;TAOK3;LMNA;CCDC6;PRPF4B;TP53	RNF20;WDHD1;JUN;SMARCC2;RPS6;PSEN2;PRPF4B;CHD4;NASP;TAOK3;TRIM28;LMNA;TPR;CANX;CCDC6;PAPOLB;TP53BP1;TP53
SGK1	3.83E-05	0.000	4.45E-05	GSK3B;AHNAK;PRPF4B;KIF23;LBR;SRRM1	GSK3B;AHNAK;PRPF4B;LBR;SRRM1	GSK3B;CDKN1B;AHNAK;PRPF4B;KIF23;RICTOR;FOXO4;LBR;SRRM1
CSNK2A1	9.18E-05	4.01E-07	1.17E-07	TOP2A;PSMA3;SSB;CBX5;PTGES3;CANX;CBX1;MYH9;ABCF1;MCM2	TOP2A;JUN;SSB;PTGES3;CAV1;CBX1;DEK;RANGAP1;PSMA3;MYH9;TP53;ABCF1;MCM2	TOP2A;JUN;SSB;CDKN1B;CBX5;LIG1;PTGES3;CAV1;CBX1;PSEN2;DEK;RANGAP1;IGF2R;PSMA3;RPS6KB1;EEF1D;STMN1;PEA15;CANX;MYH9;TP53;ABCF1;MCM2
CSNK2A2	9.39E-05	3.34E-07	1.05E-08	TOP2A;AKAP12;PSMA3;SSB;CBX3;NCL;CANX;PPIG;MCM2	TOP2A;AKAP12;JUN;PSMA3;SSB;CBX3;NCL;CAV1;PPIG;TP53;MAP4K4;MCM2	TOP2A;JUN;SSB;LIG1;CBX3;CAV1;HDLBP;PSEN2;BAZ1B;ADD1;AKAP12;PSMA3;NCL;CANX;AKT1S1;PPIG;SYNPO;ARHGEF7;UTRN;TP53;MAP4K4;MCM2
PRKCA	0.000	0.000	1.05E-08	TOP2A;GSK3B;PPP1R12A;NCL;RPS6;CTNND1;LMNA;MYH9;PRPF4B;ADD3;CORO1B;TMPO	TOP2A;GSK3B;DDX5;NCL;CTNND1;LMNA;MYH9;PRPF4B;TP53;CORO1B;TMPO	PHF3;ITGB1;TOP2A;GSK3B;DDX5;CDKN1B;PFKFB3;CTNND1;IQGAP1;FOXO4;ADD3;CORO1B;ADD1;PDLIM2;MAP2;PEA15;LMNA;TP53BP1;TMPO;PPP1R12A;RBM15;RPS6;PRPF4B;AR;TPX2;ANLN;HNRNPH1;NCL;MYH9;RAF1;TP53
CSNK1E	9.80E-05	1.35E-07	1.93E-06	TOP2B;AHNAK;CTNND1;PRPF4B;PPIG;SRRM1;ABCF1	PURB;TOP2B;AHNAK;CTNND1;G3BP1;PRPF4B;PPIG;TP53;SRRM1;ABCF1	TOP2B;AHNAK;SYNRG;CTNND1;PSEN2;PRPF4B;BAZ1B;SRRM1;PURB;G3BP1;PPIG;TP53;PAK2;ABCF1
RPS6KC1	6.10E-05			GSK3B;RPS6;FLNA;LBR		
RPS6KL1	6.10E-05			GSK3B;RPS6;FLNA;LBR		
PRKDC	0.004		4.41E-06	PPP1R12A;RPS6;LMNA;CANX;PRPF4B;LSP1		JUN;PPP1R12A;RPS6;ATP2A2;PRPF4B;LSP1;ANLN;NASP;RPS6KB1;LMNA;TPR;CANX;PAPOLB;TP53BP1;RAF1;TP53
RPS6KA6	7.95E-05			GSK3B;RPS6;FLNA;LBR		
RPS6KA1	0.003			GSK3B;RPS6;FLNA;LSP1		

AURKB	0.006	0.000	0.000	RB1;CBX5;AHNAK;KIF23	RB1;AHNAK;NSUN2;DEK;TP53	RB1;CBX5;AHNAK;NSUN2;ATP2A2;KIF23;DEK;TP53;NELFE
CDK15		0.000			RB1;LMNA;TP53;LBR	
AURKA		0.000			GSK3B;TACC3;TP53;MCM2	
CDK18		0.000			RB1;LMNA;TP53;LBR	
CDK11A		0.000			RB1;LMNA;TP53;LBR	
PLK3		3.43E-05			TOP2A;JUN;CALU;TP53	
MTOR		0.000	0.000		JUN;LARP1;AHNAK;FLNA;SRRM1	JUN;LARP1;AHNAK;RPS6KB1;AKT1S1;FLNA;PATL1;NFATC4;SRRM1
CDK14		0.000			RB1;LMNA;TP53;LBR	
MAPK8			9.41E-07			CAST;JUN;RBM15;SMARCC2;AHNAK;FOXO4;NFATC4;AR;EIF4ENIF1;DYNC1LI2;NASP;RPS6KB1;STMN1;LMNA;MAPKAPK5;TP53BP1;CIC;TP53;MAP4K4
MAPK10			8.08E-06			JUN;PCYT1A;RPS6KB1;SYAP1;ITSN1;STMN1;CCDC6;PDS5B;IQGAP1;ADD1;ARHGAP12;LMNB1
SRC			9.03E-05			CDKN1B;DGKA;CAV1;CTNND1;ASAP1;ARHGAP12;CNN3;AR;SFPQ;SH3PXD2A;RPS6KB1;SH3PXD2B;G3BP1;MYH9;JAK2;RAF1;PAK2

Figure S3.1: List of motifs identified in RTgill-W1 cells at different substrates in the phospho-peptide data

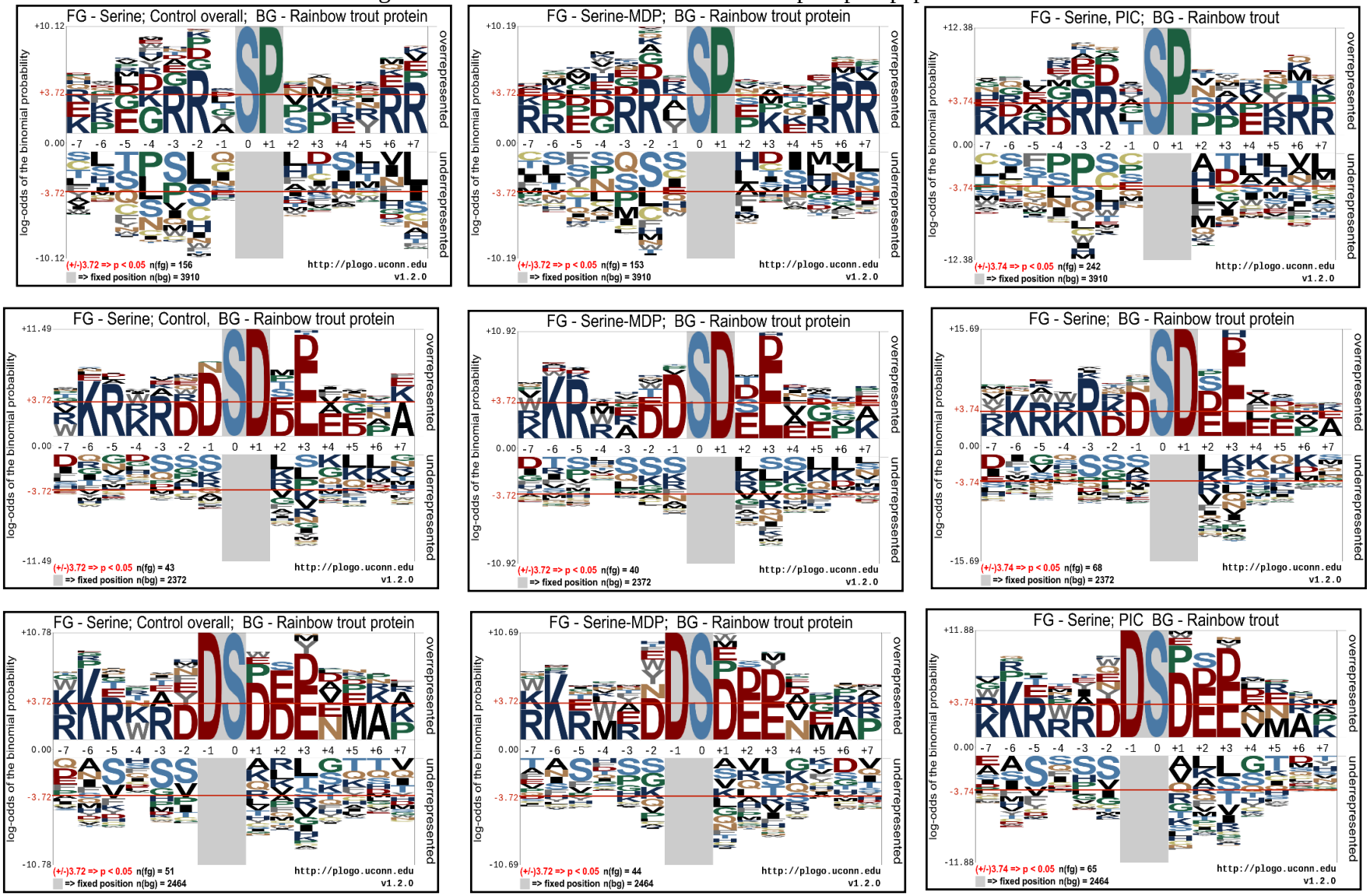

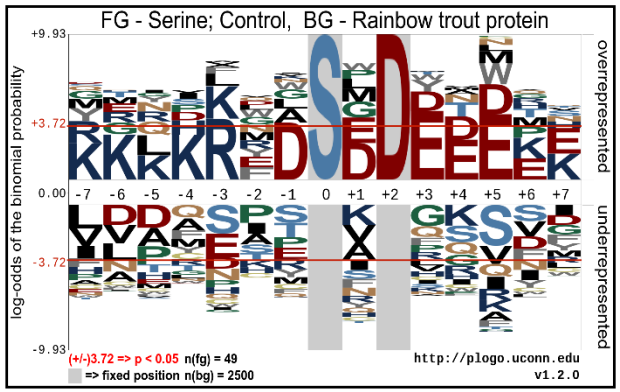
FG - Serine; Control, BG - Rainbow trout protein
log-odds of the binomial probability
overrepresented
underrepresented
+9.93
+3.72
0.00
-3.72
-9.93
-7 -6 -5 -4 -3 -2 -1 0 +1 +2 +3 +4 +5 +6 +7
(+/-)3.72 => p < 0.05 n(fg) = 49
=> fixed position n(bg) = 2500
http://plogo.uconn.edu
v1.2.0

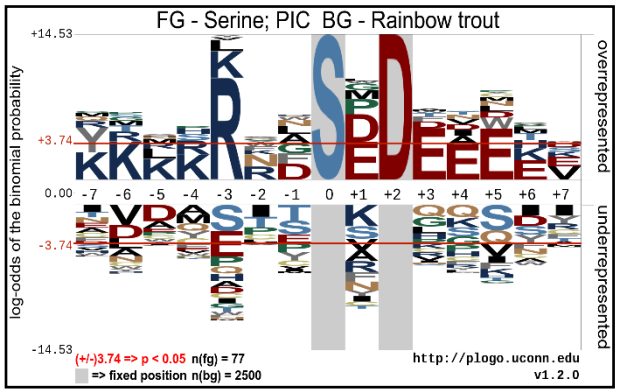
FG - Serine; PIC BG - Rainbow trout
log-odds of the binomial probability
overrepresented
underrepresented
+14.53
+3.74
0.00
-3.74
-14.53
-7 -6 -5 -4 -3 -2 -1 0 +1 +2 +3 +4 +5 +6 +7
(+/-)3.74 => p < 0.05 n(fg) = 77
=> fixed position n(bg) = 2500
http://plogo.uconn.edu
v1.2.0

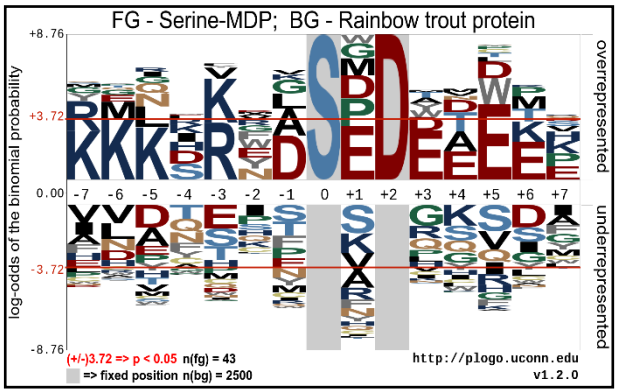
FG - Serine-MDP; BG - Rainbow trout protein
log-odds of the binomial probability
overrepresented
underrepresented
+8.76
+3.72
0.00
-3.72
-8.76
-7 -6 -5 -4 -3 -2 -1 0 +1 +2 +3 +4 +5 +6 +7
(+/-)3.72 => p < 0.05 n(fg) = 43
=> fixed position n(bg) = 2500
http://plogo.uconn.edu
v1.2.0

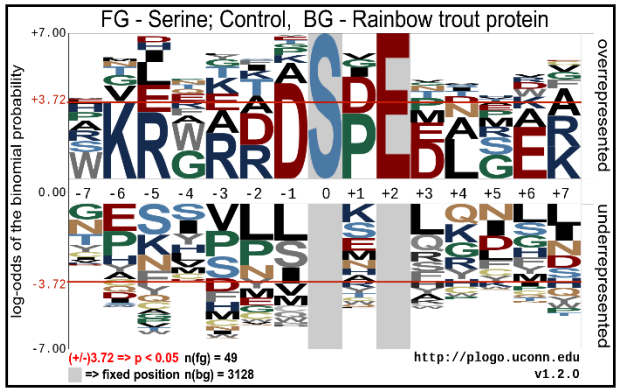
FG - Serine; Control, BG - Rainbow trout protein
log-odds of the binomial probability
overrepresented
underrepresented
+7.00
+3.72
0.00
-3.72
-7.00
-7 -6 -5 -4 -3 -2 -1 0 +1 +2 +3 +4 +5 +6 +7
(+/-)3.72 => p < 0.05 n(fg) = 49
=> fixed position n(bg) = 3128
http://plogo.uconn.edu
v1.2.0

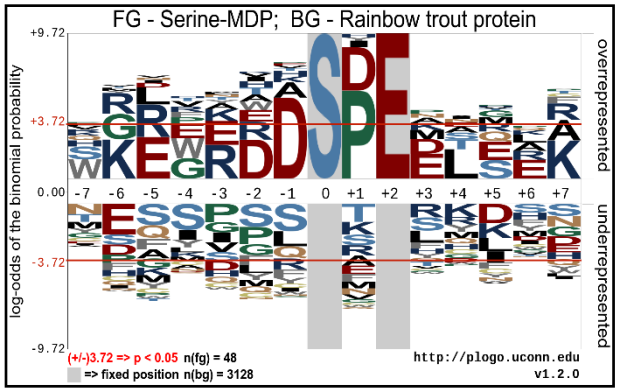
FG - Serine-MDP; BG - Rainbow trout protein
log-odds of the binomial probability
overrepresented
underrepresented
+9.72
+3.72
0.00
-3.72
-9.72
-7 -6 -5 -4 -3 -2 -1 0 +1 +2 +3 +4 +5 +6 +7
(+/-)3.72 => p < 0.05 n(fg) = 48
=> fixed position n(bg) = 3128
http://plogo.uconn.edu
v1.2.0

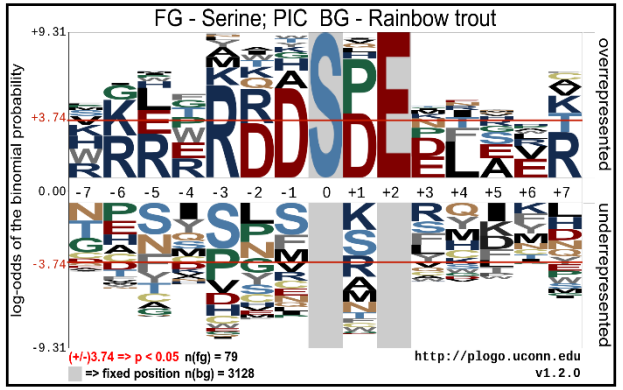
FG - Serine; PIC BG - Rainbow trout
log-odds of the binomial probability
overrepresented
underrepresented
+9.31
+3.74
0.00
-3.74
-9.31
-7 -6 -5 -4 -3 -2 -1 0 +1 +2 +3 +4 +5 +6 +7
(+/-)3.74 => p < 0.05 n(fg) = 79
=> fixed position n(bg) = 3128
http://plogo.uconn.edu
v1.2.0

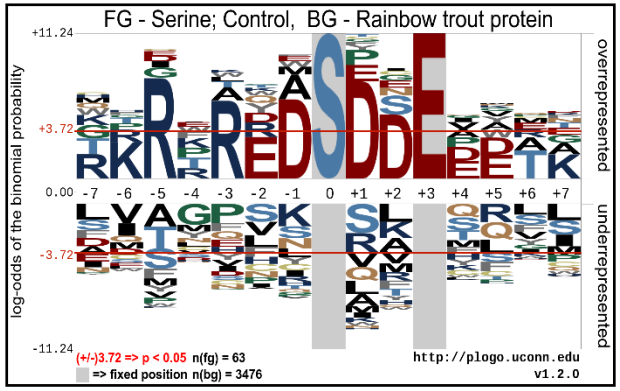
FG - Serine; Control, BG - Rainbow trout protein
log-odds of the binomial probability
overrepresented
underrepresented
+11.24
+3.72
0.00
-3.72
-11.24
-7 -6 -5 -4 -3 -2 -1 0 +1 +2 +3 +4 +5 +6 +7
(+/-)3.72 => p < 0.05 n(fg) = 63
=> fixed position n(bg) = 3476
http://plogo.uconn.edu
v1.2.0

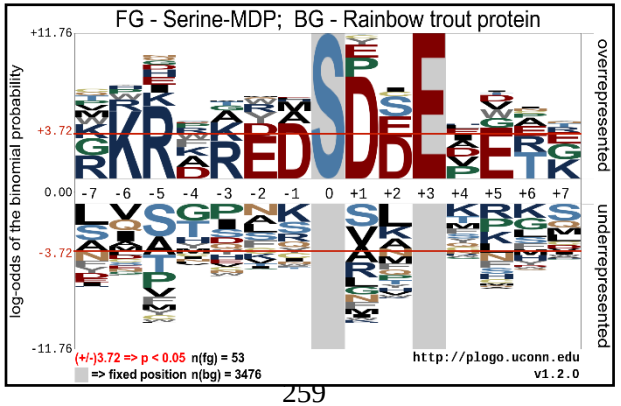
FG - Serine-MDP; BG - Rainbow trout protein
log-odds of the binomial probability
overrepresented
underrepresented
+11.76
+3.72
0.00
-3.72
-11.76
-7 -6 -5 -4 -3 -2 -1 0 +1 +2 +3 +4 +5 +6 +7
(+/-)3.72 => p < 0.05 n(fg) = 53
=> fixed position n(bg) = 3476
http://plogo.uconn.edu
v1.2.0

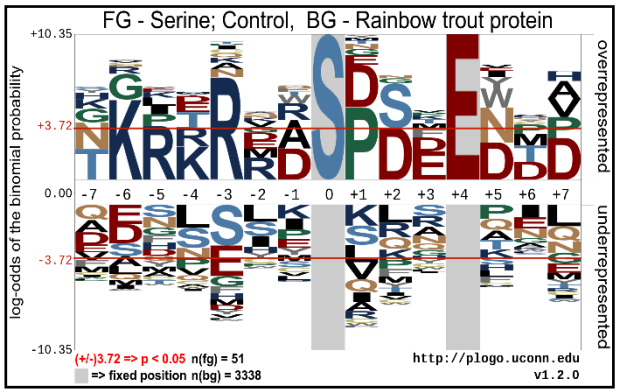
FG - Serine; Control, BG - Rainbow trout protein
log-odds of the binomial probability
overrepresented
underrepresented
(+/-)3.72 => p < 0.05 n(fg) = 51
=> fixed position n(bg) = 3338
http://plogo.uconn.edu
v1.2.0

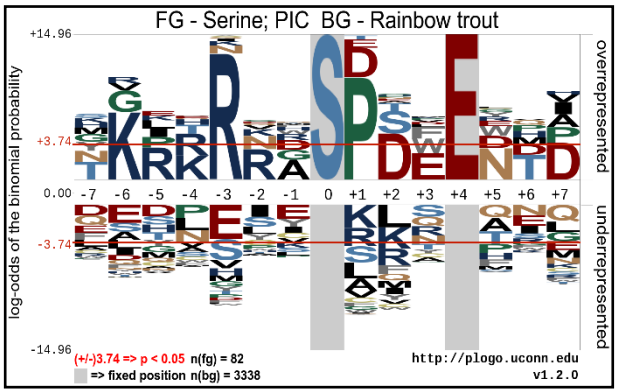
FG - Serine; PIC BG - Rainbow trout
log-odds of the binomial probability
overrepresented
underrepresented
(+/-)3.74 => p < 0.05 n(fg) = 82
=> fixed position n(bg) = 3338
http://plogo.uconn.edu
v1.2.0

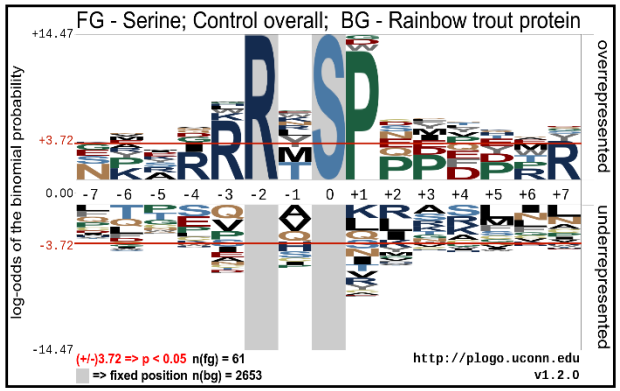
FG - Serine; Control overall; BG - Rainbow trout protein
log-odds of the binomial probability
overrepresented
underrepresented
(+/-)3.72 => p < 0.05 n(fg) = 61
=> fixed position n(bg) = 2653
http://plogo.uconn.edu
v1.2.0

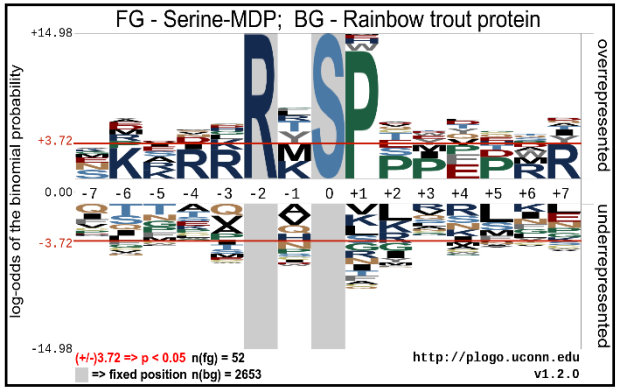
FG - Serine-MDP; BG - Rainbow trout protein
log-odds of the binomial probability
overrepresented
underrepresented
(+/-)3.72 => p < 0.05 n(fg) = 52
=> fixed position n(bg) = 2653
http://plogo.uconn.edu
v1.2.0

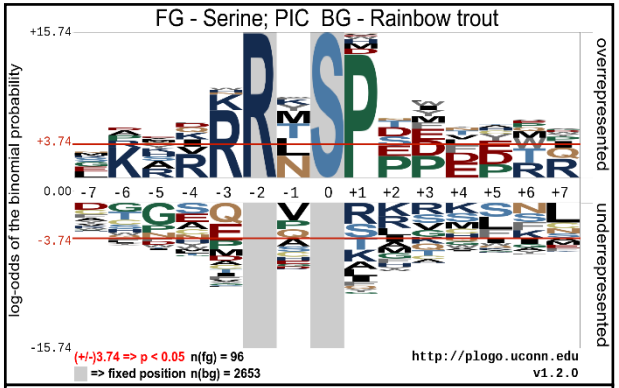
FG - Serine; PIC BG - Rainbow trout
log-odds of the binomial probability
overrepresented
underrepresented
(+/-)3.74 => p < 0.05 n(fg) = 96
=> fixed position n(bg) = 2653
http://plogo.uconn.edu
v1.2.0

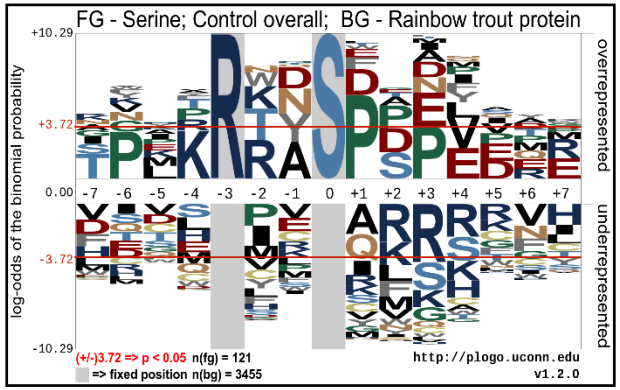
FG - Serine; Control overall; BG - Rainbow trout protein
log-odds of the binomial probability
overrepresented
underrepresented
(+/-)3.72 => p < 0.05 n(fg) = 121
=> fixed position n(bg) = 3455
http://plogo.uconn.edu
v1.2.0

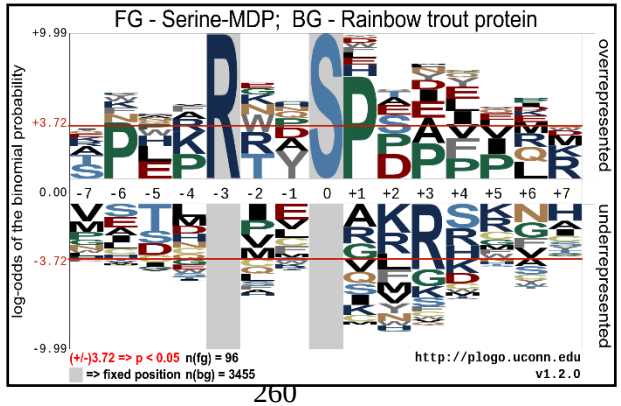
FG - Serine-MDP; BG - Rainbow trout protein
log-odds of the binomial probability
overrepresented
underrepresented
(+/-)3.72 => p < 0.05 n(fg) = 96
=> fixed position n(bg) = 3455
http://plogo.uconn.edu
v1.2.0

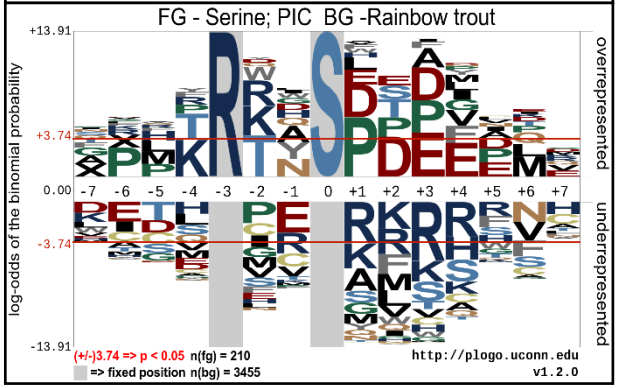
FG - Serine; PIC BG -Rainbow trout
log-odds of the binomial probability
overrepresented
underrepresented
(+/-)3.74 => p < 0.05 n(fg) = 210
=> fixed position n(bg) = 3455
http://plogo.uconn.edu
v1.2.0

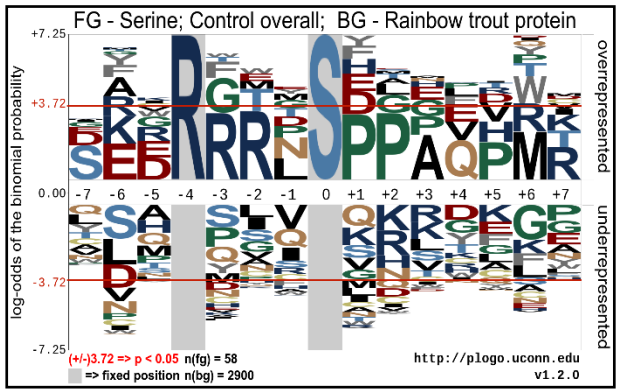
FG - Serine; Control overall; BG - Rainbow trout protein
log-odds of the binomial probability
overrepresented
underrepresented
+7.25
+3.72
0.00
-3.72
-7.25
-7 -6 -5 -4 -3 -2 -1 0 +1 +2 +3 +4 +5 +6 +7
(+/-)3.72 => p < 0.05 n(fg) = 58
=> fixed position n(bg) = 2900
http://plogo.uconn.edu
v1.2.0

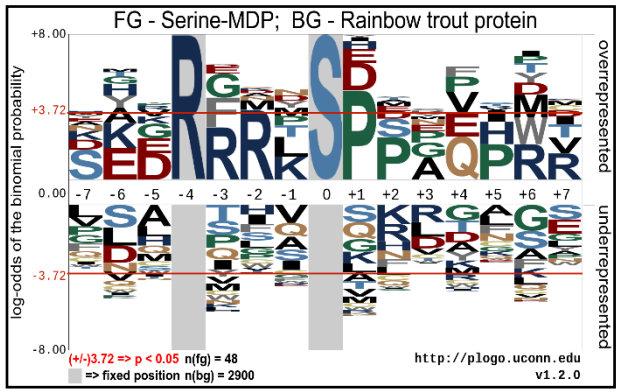
FG - Serine-MDP; BG - Rainbow trout protein
log-odds of the binomial probability
overrepresented
underrepresented
+8.00
+3.72
0.00
-3.72
-8.00
-7 -6 -5 -4 -3 -2 -1 0 +1 +2 +3 +4 +5 +6 +7
(+/-)3.72 => p < 0.05 n(fg) = 48
=> fixed position n(bg) = 2900
http://plogo.uconn.edu
v1.2.0

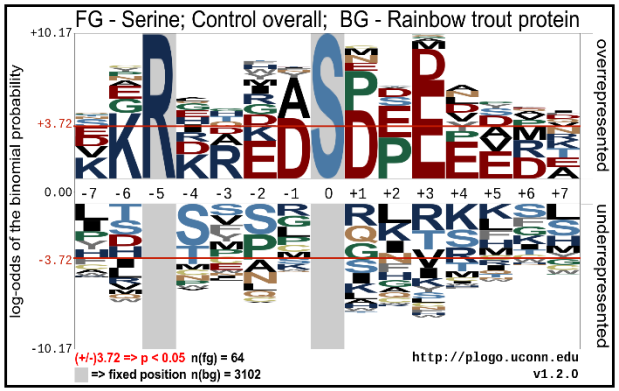
FG - Serine; Control overall; BG - Rainbow trout protein
log-odds of the binomial probability
overrepresented
underrepresented
+10.17
+3.72
0.00
-3.72
-10.17
-7 -6 -5 -4 -3 -2 -1 0 +1 +2 +3 +4 +5 +6 +7
(+/-)3.72 => p < 0.05 n(fg) = 64
=> fixed position n(bg) = 3102
http://plogo.uconn.edu
v1.2.0

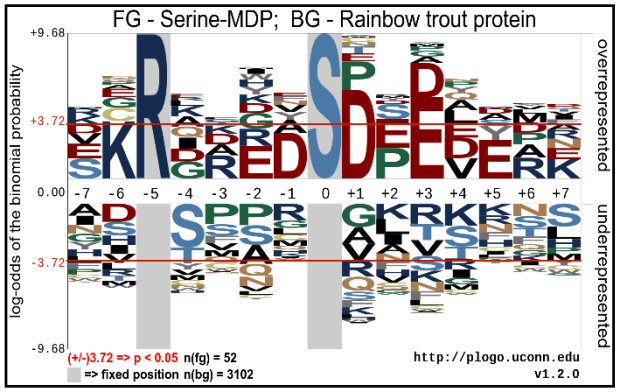
FG - Serine-MDP; BG - Rainbow trout protein
log-odds of the binomial probability
overrepresented
underrepresented
+9.68
+3.72
0.00
-3.72
-9.68
-7 -6 -5 -4 -3 -2 -1 0 +1 +2 +3 +4 +5 +6 +7
(+/-)3.72 => p < 0.05 n(fg) = 52
=> fixed position n(bg) = 3102
http://plogo.uconn.edu
v1.2.0

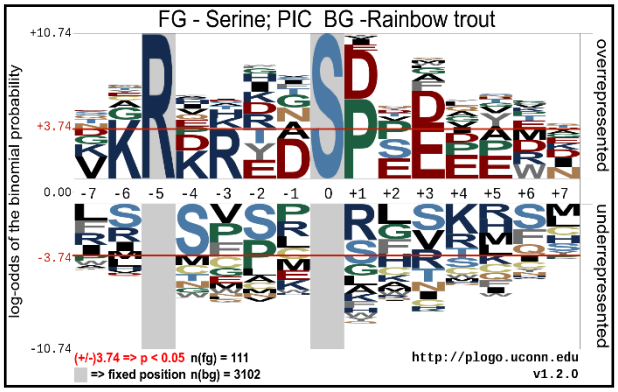
FG - Serine; PIC BG -Rainbow trout
log-odds of the binomial probability
overrepresented
underrepresented
+10.74
+3.74
0.00
-3.74
-10.74
-7 -6 -5 -4 -3 -2 -1 0 +1 +2 +3 +4 +5 +6 +7
(+/-)3.74 => p < 0.05 n(fg) = 111
=> fixed position n(bg) = 3102
http://plogo.uconn.edu
v1.2.0

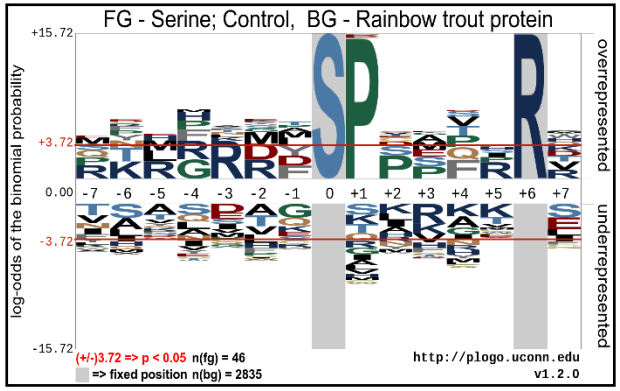
FG - Serine; Control, BG - Rainbow trout protein
log-odds of the binomial probability
overrepresented
underrepresented
+15.72
+3.72
0.00
-3.72
-15.72
-7 -6 -5 -4 -3 -2 -1 0 +1 +2 +3 +4 +5 +6 +7
(+/-)3.72 => p < 0.05 n(fg) = 46
=> fixed position n(bg) = 2835
http://plogo.uconn.edu
v1.2.0

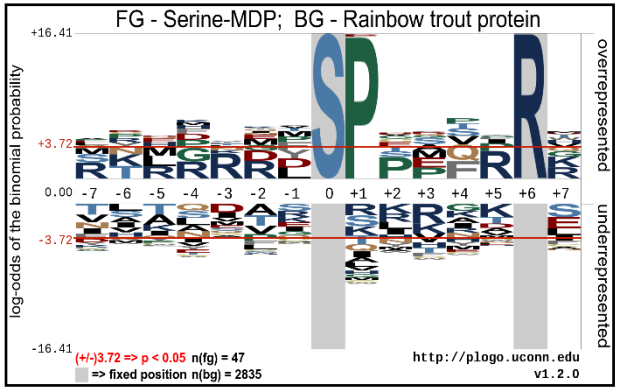
FG - Serine-MDP; BG - Rainbow trout protein
log-odds of the binomial probability
overrepresented
underrepresented
+16.41
+3.72
0.00
-3.72
-16.41
-7 -6 -5 -4 -3 -2 -1 0 +1 +2 +3 +4 +5 +6 +7
(+/-)3.72 => p < 0.05 n(fg) = 47
=> fixed position n(bg) = 2835
http://plogo.uconn.edu
v1.2.0

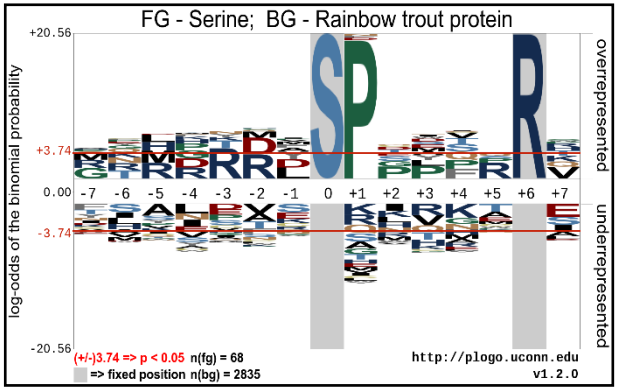
FG - Serine; BG - Rainbow trout protein
log-odds of the binomial probability
overrepresented
underrepresented
+20.56
+3.74
0.00
-3.74
-20.56
-7 -6 -5 -4 -3 -2 -1 0 +1 +2 +3 +4 +5 +6 +7
(+/-)3.74 => p < 0.05 n(fg) = 68
=> fixed position n(bg) = 2835
http://plogo.uconn.edu
v1.2.0

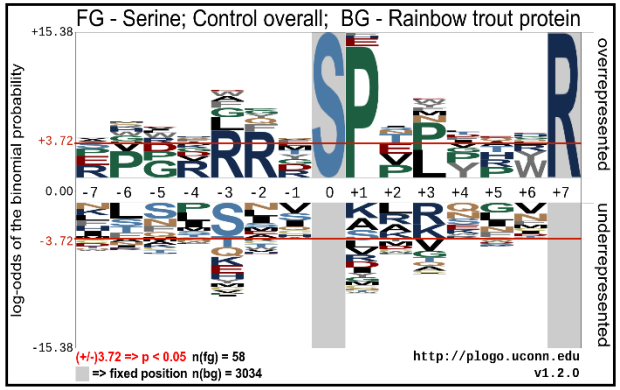
FG - Serine; Control overall; BG - Rainbow trout protein
log-odds of the binomial probability
overrepresented
underrepresented
+15.38
+3.72
0.00
-3.72
-15.38
-7 -6 -5 -4 -3 -2 -1 0 +1 +2 +3 +4 +5 +6 +7
(+/-)3.72 => p < 0.05 n(fg) = 58
=> fixed position n(bg) = 3034
http://plogo.uconn.edu
v1.2.0

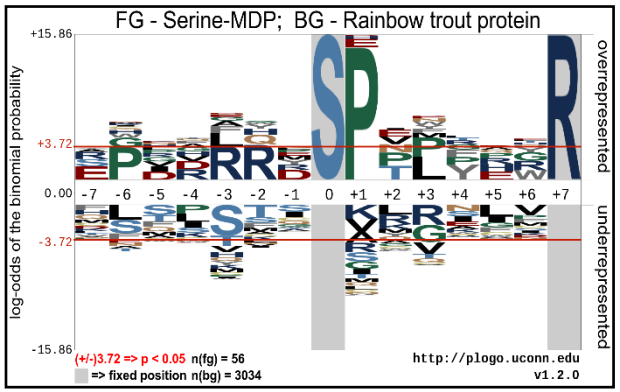
FG - Serine-MDP; BG - Rainbow trout protein
log-odds of the binomial probability
overrepresented
underrepresented
+15.86
+3.72
0.00
-3.72
-15.86
-7 -6 -5 -4 -3 -2 -1 0 +1 +2 +3 +4 +5 +6 +7
(+/-)3.72 => p < 0.05 n(fg) = 56
=> fixed position n(bg) = 3034
http://plogo.uconn.edu
v1.2.0

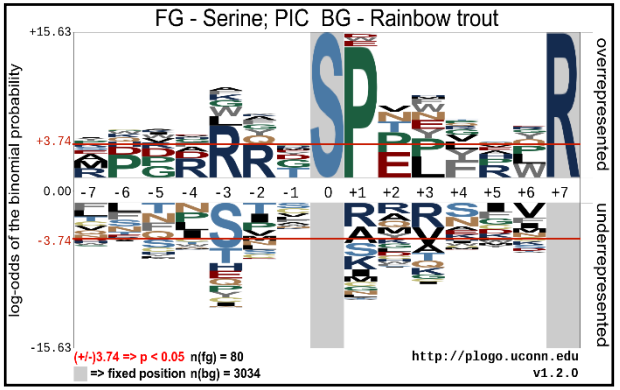
FG - Serine; PIC BG - Rainbow trout
log-odds of the binomial probability
overrepresented
underrepresented
+15.63
+3.74
0.00
-3.74
-15.63
-7 -6 -5 -4 -3 -2 -1 0 +1 +2 +3 +4 +5 +6 +7
(+/-)3.74 => p < 0.05 n(fg) = 80
=> fixed position n(bg) = 3034
http://plogo.uconn.edu
v1.2.0

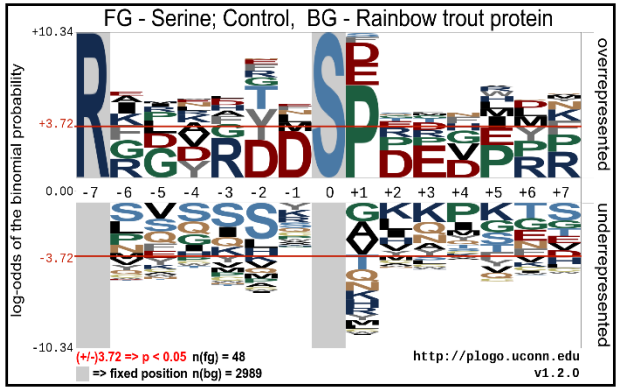
FG - Serine; Control, BG - Rainbow trout protein
log-odds of the binomial probability
overrepresented
underrepresented
+10.34
+3.72
0.00
-3.72
-10.34
-7 -6 -5 -4 -3 -2 -1 0 +1 +2 +3 +4 +5 +6 +7
(+/-)3.72 => p < 0.05 n(fg) = 48
=> fixed position n(bg) = 2989
http://plogo.uconn.edu
v1.2.0

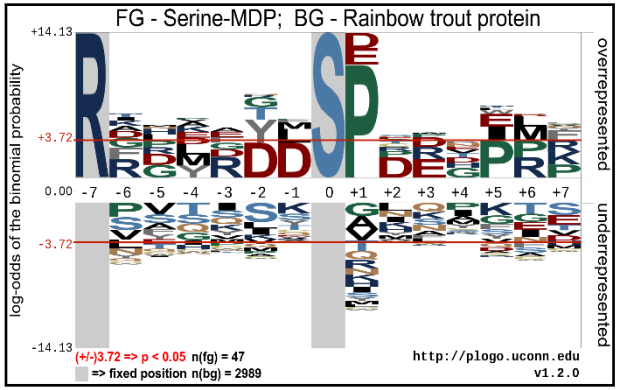
FG - Serine-MDP; BG - Rainbow trout protein
log-odds of the binomial probability
overrepresented
underrepresented
+14.13
+3.72
0.00
-3.72
-14.13
-7 -6 -5 -4 -3 -2 -1 0 +1 +2 +3 +4 +5 +6 +7
(+/-)3.72 => p < 0.05 n(fg) = 47
=> fixed position n(bg) = 2989
http://plogo.uconn.edu
v1.2.0

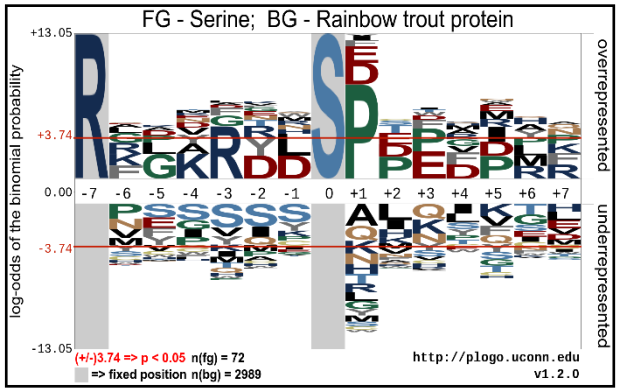
FG - Serine; BG - Rainbow trout protein
log-odds of the binomial probability
overrepresented
underrepresented
+13.05
+3.74
0.00
-3.74
-13.05
-7 -6 -5 -4 -3 -2 -1 0 +1 +2 +3 +4 +5 +6 +7
(+/-)3.74 => p < 0.05 n(fg) = 72
=> fixed position n(bg) = 2989
http://plogo.uconn.edu
v1.2.0

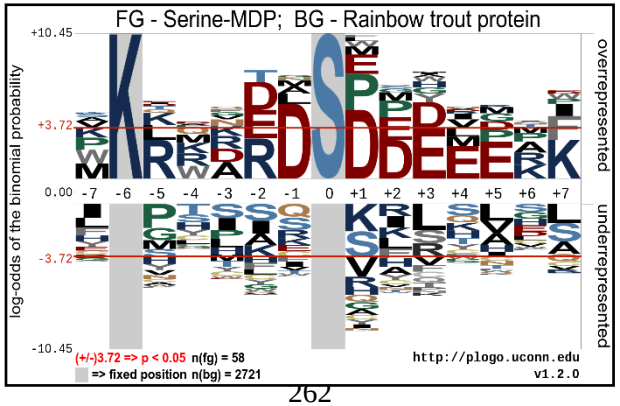
FG - Serine-MDP; BG - Rainbow trout protein
log-odds of the binomial probability
overrepresented
underrepresented
+10.45
+3.72
0.00
-3.72
-10.45
-7 -6 -5 -4 -3 -2 -1 0 +1 +2 +3 +4 +5 +6 +7
(+/-)3.72 => p < 0.05 n(fg) = 58
=> fixed position n(bg) = 2721
http://plogo.uconn.edu
v1.2.0

Table S3.5: List of kinases identified from the motifs at serine residue in RTgill-W1 cells in the study.

		Foreground matching			Background matching			Reference
Motif	Kinases	Control	MDP	Poly(I:C)	Control	MDP	Poly(:IC)	
.....sP.....	Proline directed MAPK	156	153	242	3910	3910	3910	(Schwartz & Gygi, 2005)
....R..s.....	CaMK II	121	96	210	3455	3455	3455	(Pearson & Kemp, 1991)
.K.....s.....		63	58	95	2721	2721	2721	
.....R.s.....	PKB	61	52	96	2653	2653	2653	(Pearson & Kemp, 1991)
..R....s.....	Casein II	64	52	111	3102	3102	3102	(Pinna & Ruzzene, 1996)
...R...s.....	cGMP dependent protein kinase	58	48	85	2900	2900	2900	(Pearson & Kemp, 1991)
.....sD.....	CK2	51	40	68	2464	2372	2372	(Villen et al., 2007)
.....s.....R		58	58	80	3034	3034	3034	
R.....s.....		48	47	72	2989	2989	2989	
.....s..E....	CK2	63	53	97	3476	3476	3476	(Villen et al., 2007)
.....s.D.....	CaMK II/CK2	49	43	77	2500	2500	2500	(Schwartz & Gygi, 2005)/ (Villen et al., 2007)
.....s.....R.		46	47	68	2835	2835	2835	
.....s.E.....	G-CK/CK2	49	48	79	3128	3128	3128	(Schwartz & Gygi, 2005)/ (Villen et al., 2007)
.....R.sP.....		29	27	38	270	270	270	
.....sP.....R		30	30	36	326	326	326	
....R..sP.....		35		51	430		430	
....R..s..P....		26		37	35		351	
.K....Ds.....		17			180			
.KR....s.....		16		22	242		242	
....RR.s.....	PKA kinase	22		32	320		320	(Pearson & Kemp, 1991)
..R....s..E....		19		21	231		231	
..R...Ds.....		12		14	152		152	

..R....sD.....		14	14		182	182		
.....DsD.....	CK-II like	18	17	23	256	2124	256	(Schwartz & Gygi, 2005)
.....Ds..E....		18	14	22	266	266	266	
....R..s.....R		21			403			
R.....sP.....		19	24	27	326	326	326	
.....s.D..E..	CK2	15			238			(Villen et al., 2007)
....R..sD.....		11		20	147		147	
.....sD.E....	CK2	21	20	33	297	297	297	(Schwartz & Gygi, 2005)
....R..s.....R.		16			351			
.K.....s.E.....		12	10		230	2999		
.....Ds.E.....		13	14	19	221	221	221	
.....sP..E...		14		26	232		232	
....R..s...E...		18		31	272		272	
.K.....s...E...		14			208			
..R....s...E...		12			230			
....R..s.....								
.....Ds.....			44	65		2464	2464	
.....sPE.....			16			267		
.....sDE.....	CK2		10	16		2292	213	(Schwartz & Gygi, 2005)
.....D.sD.....			10			1842		
.P..R..s.....	Protein kinase B		20			290		
.P..R..sP.....			11			380		
.K.....sD.....			14			170		
..RR...s.....			13			242		
...R...sD.....			14			182		
...R...s..E....			15			231		
...R...sP.....			16	22		294	294	
.....s..E.E..	CK2		18			451		(Villen et al., 2007)

......Ds.....	CK2		44	65		2464	2464	(Villen et al., 2007)
.....s.....R.		46	47	68	2835	2835	2835	
...K...s.....	PKA kinase substrate			77			2864	(Pearson & Kemp, 1991)
.....s.S.....				141			6531	
.....s...E...	CK2			82			3338	(Villen et al., 2007)
....K..s.....	PKA kinase			76			2824	(Pearson & Kemp, 1991)
.....s..P....				78			3403	
.....s.P.....				76			3278	
.....sP....R.				39			312	
....RT.s.....				24			168	
..R.R..s.....	p70 S6 kinase			35			535	(Leighton et al., 1995)
..R....sP.....				31			349	
K......sP.....				24			225	
K.....Ds.....				18			180	
K......s...E...				20			208	
.....sED.....				17			206	
.....s.D.E...	CK2			21			238	(Villen et al., 2007)
....R..s..E....				31			240	
...RR..s.....	ZIP kinase			29			393	(Burch et al., 2004)
...KR..s.....	PKA/PKC kinase			33			286	(Pearson & Kemp, 1991)
...K...sP.....				23			217	
....K..s.....R				27			403	
....R..s.S.....				56			746	
..R....s.S.....				29			582	
.....sPS.....				50			596	
.....s.SP....				35			690	
....R..s.SP....				20			150	
.....sPSP....				16			117	

....R..s.E.....		21	258	
.......sDEE....	CK2	12	58	(Villen et al., 2007)
.......s.EE....		18	466	
.......s...E..R		15	207	
.....DDs.....		14	156	
....K..sP.....		17	244	
R...R..s.....		24	409	
..K....sD.....		18	171	
.......s..R..R.		21	351	
.......s		35	346	
......Gs.....		72	3050	
......GsP.....		20	247	
....R.Gs.....		18	246	

Table S3.6: List of kinases identified from the motifs at threonine residue in RTgill-W1 cells in the study.

Motif	Kinase	Foreground	Background	% matching	Score	Reference
Control group						
.....tP.....	Proline directed MAPK	18	2252	34.62	7.07	(Schwartz & Gygi, 2005)
...R...t.....		11	1427	21.15	4.14	
MDP treated group						
.....tP.....		15	2252	30.61	5.24	
Poly(I:C) stimulated group						
...R...t.....	cGMP dependent protein kinase	21	1427	17.5	5.95	(Pearson & Kemp, 1991)
K.....t.....		21	1845	17.5	4.27	
.....tP.....		30	2252	25	7.51	
...R...tP.....		10	115			

References

Avella, M., Peter, P., & Ehrenfeld, J. (1999). Regulation of Cl- secretion in seawater fish (*Dicentrarchus labrax*) gill respiratory cells in primary culture. *Journal of Physiology*, *516*(2), 353—363.

Balbuena, P., Li, W., Magnin-Bissel, G., Meldrum, J. B., & Ehrich, M. (2010). Comparison of two blood-brain barrier in vitro systems: Cytotoxicity and transfer assessments of malathion/oxon and lead acetate. *Toxicological Sciences*, *114*(2), 260–271.

Bazes, A., Nollevaux, G., Coco, R., Joly, A., Sergent, T., & Schneider, Y.-J. (2011). Development of a triculture based system for improved benefit/risk assessment in pharmacology and human food. *BMC Proceedings*, *5*(Suppl 8), P67.

Béduneau, A., Tempesta, C., Fimbel, S., Pellequer, Y., Jannin, V., Demarne, F., & Lamprecht, A. (2014). A tunable Caco-2/HT29-MTX co-culture model mimicking variable permeabilities of the human intestine obtained by an original seeding procedure. *European Journal of Pharmaceutics and Biopharmaceutics*, *87*(2), 290–298.

Blank, F., Rothen-Rutishauser, B. M., Schurch, S., & Gehr, P. (2006). An Optimized *In Vitro* Model of the Respiratory Tract Wall to Study Particle Cell Interactions. *Journal of Aerosol Medicine*, *19*(3), 392–405.

Bui, P., & Kelly, S. P. (2015). Claudins in a primary cultured puffer fish (*Tetraodon nigroviridis*) gill epithelium model alter in response to acute seawater exposure. *Comparative Biochemistry and Physiology, Part A*, *189*, 91–101.

Burch, L. R., Scott, M., Pohler, E., Meek, D., & Hupp, T. (2004). Phage-peptide Display Identifies the Interferon-responsive, Death-activated Protein Kinase Family as a Novel Modifier of MDM2 and p21WAF1. *Journal of Molecular Biology*, *337*(1), 115–128.

Carlsson, C., & Pärt, P. (2001). 7-Ethoxyresorufin O-deethylase induction in rainbow trout gill epithelium cultured on permeable supports: asymmetrical distribution of substrate metabolites. *Aquatic Toxicology (Amsterdam, Netherlands)*, *54*(1–2), 29–38.

Chasiotis, H., & Kelly, S. P. (2011a). Effect of cortisol on permeability and tight junction protein transcript abundance in primary cultured gill epithelia from stenohaline goldfish and euryhaline trout. *General and Comparative Endocrinology*, *172*(3), 494–504.

Chasiotis, H., & Kelly, S. P. (2011b). Permeability properties and occludin expression in a primary cultured model gill epithelium from the stenohaline freshwater goldfish. *Journal of Comparative Physiology. B, Biochemical, Systemic, and Environmental Physiology*, *181*(4), 487–500.

Chasiotis, H., Kolosov, D., & Kelly, S. P. (2012). Permeability properties of the teleost gill epithelium under ion-poor conditions. *AJP: Regulatory, Integrative and Comparative Physiology*, *302*, R727–R739.

Chasiotis, H., Wood, C. M., & Kelly, S. P. (2010). Cortisol reduces paracellular permeability and increases occludin abundance in cultured trout gill epithelia. *Molecular and Cellular Endocrinology*, *323*(2), 232–8.

Da Violante, G., Zerrouk, N., Richard, I., Frendo, J.-L., Zhiri, A., Li-Khuan, R., et al. (2004). Short term Caco-2/TC7 cell culture: comparison between conventional 21-d and a commercially available 3-d system. *Biological & Pharmaceutical Bulletin*, *27*(12), 1986–92.

Damek-Poprawa, M., Korostoff, J., Gill, R., & DiRienzo, J. M. (2013). Cell junction remodeling in gingival tissue exposed to a microbial toxin. *Journal of Dental Research*, *92*(6), 518–23.

des Rieux, A., Fievez, V., IvanTh´eate, Mast, J., Pr´eat, V., & Schneider, Y. J. (2007). An improved in vitro model of human intestinal follicle-associated epithelium to study nanoparticle transport by M cells. *European Journal of Pharmaceutical Sciences*, *30*(5), 380–391.

Ferruzza, S., Rossi, C., Sambuy, Y., & Scarino, M. L. (2012). Serum-Reduced and Serum-Free Media for Differentiation of Caco-2 Cells. *Toxicology in Vitro : An International Journal Published in Association with BIBRA*, *26*(8), 1247–51.

Fletcher, M., Kelly, S. P., Pärt, P., O'Donnell, M. J., & Wood, C. M. (2000). Transport properties of cultured branchial epithelia from freshwater rainbow trout: a novel preparation with mitochondria-rich cells. *The Journal of Experimental Biology*, *203*, 1523–1537.

Kelly, S. P., & Wood, C. M. (2001a). Effect of cortisol on the physiology of cultured pavement cell epithelia from freshwater trout gills. *Am J Physiol Regulatory Integrative Comp Physiol*, *281*(3), 811–820.

Kelly, S. P., & Wood, C. M. (2001b). The Physiological Effects of 3,5′,3′-Triiodo-l-thyronine Alone or Combined with Cortisol on Cultured Pavement Cell Epithelia from Freshwater Rainbow Trout Gills. *General and Comparative Endocrinology*,

123(3), 280–294.

Kelly, S. P., & Wood, C. M. (2002). Cultured gill epithelia from freshwater tilapia (*Oreochromis niloticus*): Effect of cortisol and homologous serum supplements from stressed and unstressed fish. *Journal of Membrane Biology*, *190*(1), 29–42.

Kelly, S. P., & Wood, C. M. (2002). Prolactin effects on cultured pavement cell epithelia and pavement cell plus mitochondria-rich cell epithelia from freshwater rainbow trout gills. *General and Comparative Endocrinology*, *128*(1), 44–56.

Kelly, S. P., & Wood, C. M. (2003). Dilute culture media as an environmental or physiological simulant in cultured gill epithelia from freshwater rainbow trout. *In Vitro Cellular & Developmental Biology. Animal*, *39*(1–2), 21–8.

Kelly, S. P., & Wood, C. M. (2008). Cortisol stimulates calcium transport across cultured gill epithelia from freshwater rainbow trout. *In VItro Cell. Dev. Biol-Animal*, *44*, 96–104.

Kolosov, D., & Kelly, S. P. (2013). A role for tricellulin in the regulation of gill epithelium permeability. *AJP: Regulatory, Integrative and Comparative Physiology*, *304*(12), R1139–R1148.

Leguen, I., Peron, S., & Prunet, P. (2011). Effects of iron on rainbow trout gill cells in primary culture. *Cell Biology and Toxicology*, *27*(5), 311–9.

Lehmann, A. D., Daum, N., Bur, M., Lehr, C. M., Gehr, P., & Rothen-Rutishauser, B. M. (2011). An in vitro triple cell co-culture model with primary cells mimicking the human alveolar epithelial barrier. *European Journal of Pharmaceutics and Biopharmaceutics*, *77*(3), 398–406.

Leighton, I. A., Dalby, K. N., Barry Caudwell, F., Cohen, P. T. W., & Cohen, P. (1995). Comparison of the specificities of p70 S6 kinase and MAPKAP kinase-1 identifies a relatively specific substrate for p70 S6 kinase: the N-terminal kinase domain of MAPKAP kinase-1 is essential for peptide phosphorylation. *FEBS Letters*, *375*(3), 289–293.

Oshima, T., Gedda, K., Koseki, J., Chen, X., Husmark, J., Watari, J., et al. (2011). Establishment of esophageal-like non-keratinized stratified epithelium using normal human bronchial epithelial cells. *American Journal of Physiology. Cell Physiology*, *300*(6), C1422–C1429.

PÄRT, C. M. W. A. P. (1997). Cultured branchial epithelia from freshwater fish gills. *The Journal of Experimental Biology*, *200*(Pt 6), 1047–59.

Pearson, R. B., & Kemp, B. E. (1991). Protein Kinase Phosphorylation Site Sequences and

Consensus Specificity Motifs: Tabulations. *Methods in Enzymology*, *200*, 62–81.

Pinna, L. A., & Ruzzene, M. (1996). How do protein kinases recognize their substrates? *Biochimica et Biophysica Acta - Molecular Cell Research*, *1314*(3), 191–255.

Rothen-Rutishauser, B. M., Kiama, S. G., & Gehr, P. (2005). A three-dimensional cellular model of the human respiratory tract to study the interaction with particles. *American Journal of Respiratory Cell and Molecular Biology*, *32*(4), 281–289.

Sandbichler, A. M., Egg, M., Schwerte, T., & Pelster, B. (2011). Claudin 28b and F-actin are involved in rainbow trout gill pavement cell tight junction remodeling under osmotic stress. *The Journal of Experimental Biology*, *214*(Pt 9), 1473–1487.

Sandbichler, A. M., Farkas, J., Salvenmoser, W., & Pelster, B. (2011). Cortisol affects tight junction morphology between pavement cells of rainbow trout gills in single-seeded insert culture. *Journal of Comparative Physiology. B, Biochemical, Systemic, and Environmental Physiology*, *181*(8), 1023–34.

Schwartz, D., & Gygi, S. P. (2005). An iterative statistical approach to the identification of protein phosphorylation motifs from large-scale data sets. *Nature Biotechnology*, *23*(11), 1391–1398.

Shahsavarani, A., McNeill, B., Galvez, F., Wood, C. M., Goss, G. G., Hwang, P.-P., & Perry, S. F. (2006). Characterization of a branchial epithelial calcium channel (ECaC) in freshwater rainbow trout (*Oncorhynchus mykiss*). *The Journal of Experimental Biology*, *209*, 1928–1943.

Smith, R. W., Jonsson, M., Houlihan, D. F., & Part, P. (2001). Minimising aerobic respiratory demands could form the basis to sub-lethal copper tolerance by rainbow trout gill epithelial cells in vitro. *Fish Physiology and Biochemistry*, *24*(2), 157–169.

Steensma, A., Noteborn, H. P. J. M., & Kuiper, H. A. (2004). Comparison of Caco-2, IEC-18 and HCEC cell lines as a model for intestinal absorption of genistein, daidzein and their glycosides. *Environmental Toxicology and Pharmacology*, *16*(3), 131–139.

Stott, L. C., Schnell, S., Hogstrand, C., Owen, S. F., & Bury, N. R. (2014). A primary fish gill cell culture model to assess pharmaceutical uptake and efflux: Evidence for passive and facilitated transport. *Aquatic Toxicology*, *159*, 127–137.

Tavana, H., Zamankhan, P., Christensen, P. J., Grotberg, J. B., & Takayama, S. (2011). Epithelium damage and protection during reopening of occluded airways in a physiologic microfluidic pulmonary airway model. *Biomedical Microdevices*, *13*(4), 731–742.

Trubitt, R. T., Rabeneck, D. B., Bujak, J. K., Bossus, M. C., Madsen, S. S., & Tipsmark,

C. K. (2015). Transepithelial resistance and claudin expression in trout RTgill-W1 cell line: Effects of osmoregulatory hormones. *Comparative Biochemistry and Physiology Part A: Molecular & Integrative Physiology*, *182*, 45–52.

Villen, J., Beausoleil, S. A., Gerber, S. A., & Gygi, S. P. (2007). Large-scale phosphorylation analysis of mouse liver. *Proceedings of the National Academy of Sciences*, *104*(5), 1488–1493.

Wood, C. M., Eletti, B., & Pärt, P. (2002). New methods for the primary culture of gill epithelia from freshwater rainbow trout. *Fish Physiology and Biochemistry*, *26*(4), 329–344.

Zhou, B., Kelly, S. P., Ianowski, J. P., & Wood, C. M. (2003). Effects of cortisol and prolactin on Na+ and Cl- transport in cultured branchial epithelia from FW rainbow trout. *American Journal of Physiology. Regulatory, Integrative and Comparative Physiology*, *285*(6), R1305–R1316.

Zhou, B., Liu, C., Wang, J., Lam, P. K. S., & Wu, R. S. S. (2006). Primary cultured cells as sensitive in vitro model for assessment of toxicants-comparison to hepatocytes and gill epithelia. *Aquatic Toxicology*, *80*(2), 109–118. Available at:

Zhou, B., Nichols, J., Playle, R. C., & Wood, C. M. (2005). An *in vitro* biotic ligand model (BLM) for silver binding to cultured gill epithelia of freshwater rainbow trout (*Oncorhynchus mykiss*). *Toxicology and Applied Pharmacology*, *202*(1), 25–37.